CSIRO
Marine Laboratories

REPORT 90-HC3

ALIPHATIC AND AROMATIC HYDROCARBONS IN SOME BITUMENS AND SEDIMENTS

Prepared by: J. K. Volkman and T. O'Leary
CSIRO Division of Oceanography, Hobart

Mr Malcolm Bendall
Managing Director
Conga Oil Pty Ltd
84 Wells Parade
Blackmans Bay
Tasmania

September 17, 1990

CSIRO
AUSTRALIA

SAMPLES

This report documents the aliphatic and aromatic hydrocarbon compositions of two sediment samples from outcrops in Tasmania, two Tasmanian tar samples and two bitumen samples obtained from the Queen Victoria Museum in Launceston provided by Mr M. Bendall. These analyses were undertaken at the request of Conga Oil Pty Ltd. Details of the samples are provided in Table 1.

METHODS

Total Hydrocarbon Content

A portion of the solvent extract was analysed by Iatroscan thin-layer chromatography-flame ionisation detection (Volkman *et al.*, 1986), using hexane as the developing solvent to separate aliphatic from aromatic hydrocarbons: quantitative data are shown in Table 1.

Saturated and aromatic hydrocarbons were isolated by applying a portion of the total solvent extract to a column of 3 g of silicic acid (100–200 mesh) capped with 1 g of activated alumina (BDH). Aliphatics were eluted with hexane (20 mL), and a second fraction containing aromatic hydrocarbons was obtained by eluting with toluene:hexane (1:1; 20 mL). Resins and asphaltenes were eluted with chloroform (20 mL) and methanol (10 mL).

Aliphatic and aromatic hydrocarbon fractions were analysed by capillary gas chromatography on a 50 metre non-polar methyl silicone fused silica capillary column. The GC temperature program was 45 ^{o}C for 1 minute followed by a ramp of 30 ^{o}C/min. to 120 ^{o}C, then a ramp of 4 ^{o}C/min. to 320 ^{o}C. The oven was then held isothermally at 320 ^{o}C for 15 minutes. Peak areas were measured using DAPA software.

Aliphatic Biomarkers

To obtain more detailed information about the hydrocarbon compositions, each aliphatic hydrocarbon fraction was analysed by gas chromatography–mass spectrometry in selected ion monitoring mode (SIM). n–Alkanes were not removed beforehand since their concentration in the biomarker region were quite low and did not interfere with the analysis.

Ion chromatograms for ions m/z 217 and 218 (steranes), m/z 259 (diasteranes), m/z 231 (methyl steranes), m/z 191 (hopanes and other triterpanes), m/z 177 (demethylated hopanes), m/z 205 (methyl hopanes) were obtained. Representative structures of these aliphatic biomarkers are shown in Fig. 1.

(a) Steranes: Steranes are readily detectable constituents in most sediments and crude oils. These hydrocarbons provide information about the maturity and source of a crude oil. Their distribution is fingerprinted using mass fragmentograms for m/z 217 and m/z 218.

(b) Diasteranes: Diasteranes are rearranged steranes. They are commonly abundant in source rocks that contain significant amounts of clays which catalyse the steroid backbone rearrangement. Their distribution is usually determined from a m/z 259 mass fragmentogram, although peaks are also evident in the m/z 217 mass fragmentogram.

(c) Methyl steranes: Mass fragmentograms for m/z 231 are used to fingerprint steranes having an additional methyl group in the A–ring. These are usually much less abundant than desmethyl steranes, although some lacustrine source rocks are known to contain large quantities (e.g McKirdy *et al.*, 1986).

(d) Tricyclic alkanes: Tricyclic alkanes occur in most sediments and crude oils, although usually they are very much less abundant than hopanes. They are usually identified from

m/z 191 mass fragmentograms. Tricyclic alkanes are particularly abundant in the Tasmanite oil shale (Denwer, 1986; Simoneit *et al.*, 1986).

(e) Hopanes: Hopane distributions are fingerprinted using mass fragmentograms of the major fragment ion m/z 191. Hopane distributions can be used to ascertain the degree of thermal maturity from the relative proportions of key isomers. (i) In the extended hopanes (i.e. $>C_{30}$) the ratio of the 22S epimer to the 22R epimer (e.g. peaks H7 and H8) varies with maturity, but the two epimers isomerise to an equilibrium mixture (about 3:2) before the onset of the oil window. (ii) The ratio of moretanes (peaks H4, H6 and H9) to 17α(H),21β(H)–hopanes of the same chain–length (H3, H5 and H7+8) decreases with increasing thermal maturity. (iii) The ratio of the two C_{27} hopanes Ts (peak H1) and Tm (peak H2) is a sensitive indicator of thermal maturity. Ts is more abundant than Tm in oils generated at high levels of thermal maturity.

(f) C–10 Demethylated hopanes: These compounds are conventional hopanes which lack a C–10 methyl group. It is believed that these are formed from hopanes by microbial removal of the methyl group during biodegradation. These compounds can be present in relatively high amounts in extremely biodegraded crude oils (Volkman *et al.*, 1983).

Aromatic hydrocarbons

Peak areas for phenanthrene and methylphenanthrenes in the capillary gas chromatograms of the total aromatic hydrocarbons were used to calculate methyl phenanthrene indices (MPI; Radke and Welte, 1983). Values are given in Table 1. These values were converted into calculated equivalent vitrinite reflectances according to the following equations:

$$MPI = \frac{1.5\ (2\text{–}MP + 3\text{–}MP)}{P + 1\text{–}MP + 9\text{–}MP}$$

$$MPR = \frac{2\text{-}MP}{1\text{-}MP}$$

$VR_{CALCa} = 0.6\ MPI + 0.4$ (Radke and Welte, 1983)

$VR_{CALCb} = 0.99\ Log_{10}\ MPR + 0.94$ (Radke *et al.*, 1984)

$VR_{CALCc} = 0.7\ MPI + 0.22$ (Boreham *et al.*, 1988).

Aromatic Steroid Biomarkers

Each aromatic hydrocarbon fraction was analysed by gas chromatography–mass spectrometry in selected ion monitoring mode (SIM) to determine the distribution of mono- and triaromatic hydrocarbons. These distributions provide information about the maturity of a crude oil, although some information on source affinities can sometimes be obtained from the relative proportions of C_{26}–C_{29} components.

At least 7 types of aromatic steroid hydrocarbons are commonly found in oils as summarised in Fig. 2 (Mackenzie *et al.*, 1981). Monoaromatic components may have one, two or three methyl groups distributed on the A, B and C rings. These give characteristic cleavage ions at m/z 239, 253 and 267 respectively. Triaromatic steroids may also have one, two or three methyl groups distributed on the A, B and C rings. These give characteristic cleavage ions at m/z 217, 231 and 245 respectively (Fig. 2).

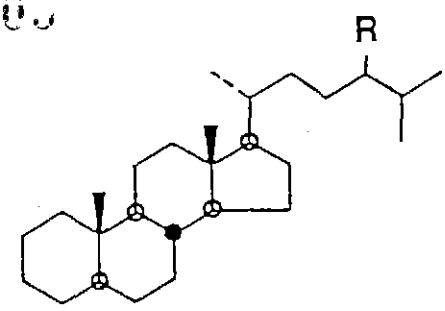

5α(H)-sterane

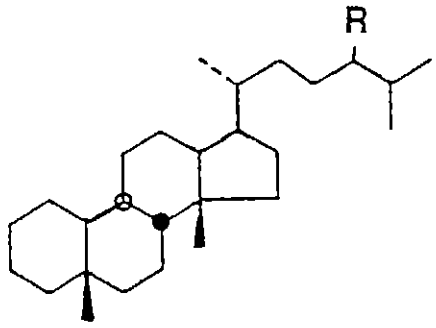

diasterane

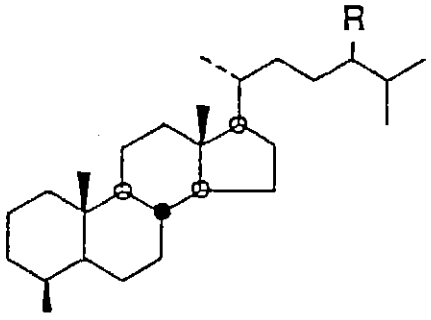

4–methyl sterane

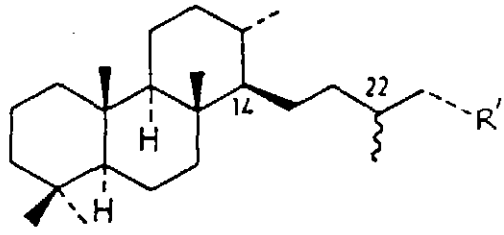

tricyclic alkane

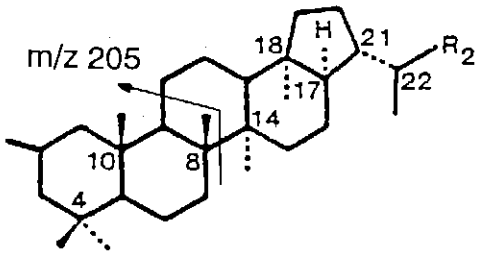

2–methyl hopane

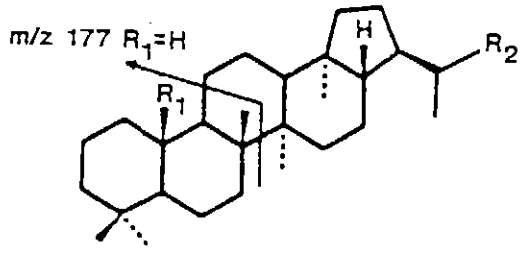

25–norhopane

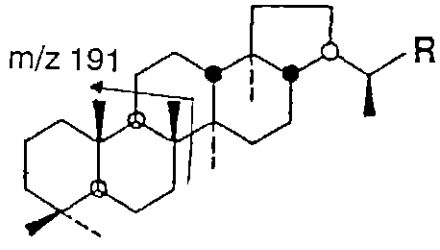

17β(H),21α(H)-hopanes
(moretanes)

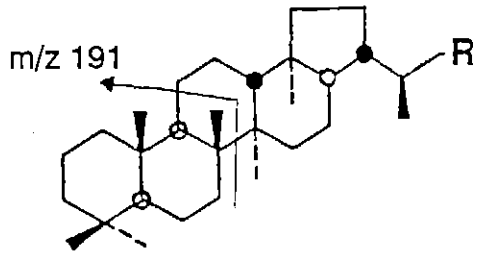

17α(H),21β(H)-hopanes

Figure 1. Structures of some of the commonly encountered aliphatic biomarkers found in crude oils.

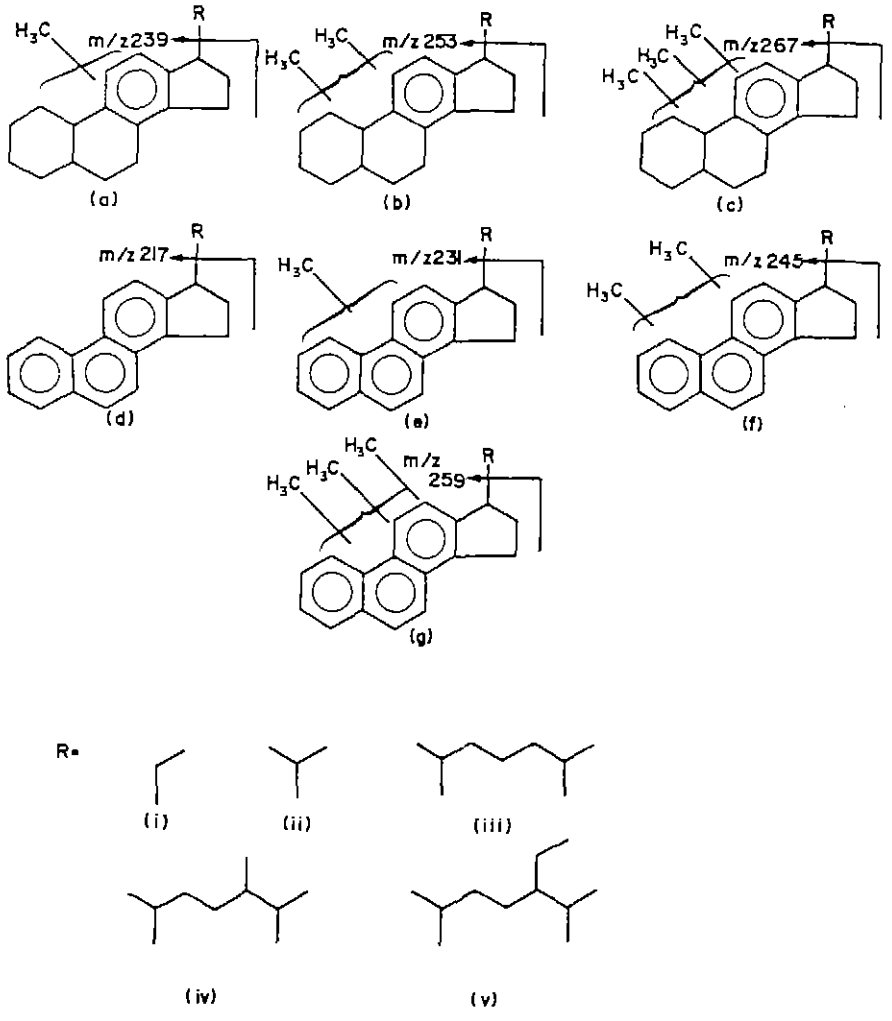

Figure 2. Structures of aromatic steroid hydrocarbons commonly found in crude oils. The major fragment ions are show, plus structures of the common side-chains (R).

007

Key 1. Identifications of peaks in sterane and diasterane (m/z 217, 218 and 259) mass fragmentograms.

PEAK	COMPOUND
	STERANES:
S1	C_{27} (20S)–5α(H),14α(H),17α(H)–cholestane
S2	C_{27} (20R)–5α(H),14β(H),17β(H)–cholestane
S3	C_{27} (20S)–5α(H),14β(H),17β(H)–cholestane
S4	C_{27} (20R)–5α(H),14α(H),17α(H)–cholestane
S5	C_{28} (20S)–5α(H),14α(H),17α(H)–24–methylcholestane
S6	C_{28} (20R)–5α(H),14β(H),17β(H)–24–methylcholestane
S7	C_{28} (20S)–5α(H),14β(H),17β(H)–24–methylcholestane
S8	C_{28} (20R)–5α(H),14α(H),17α(H)–24–methylcholestane
S9	C_{29} (20S)–5α(H),14α(H),17α(H)–24–ethylcholestane
S10	C_{29} (20R)–5α(H),14β(H),17β(H)–24–ethylcholestane
S11	C_{29} (20S)–5α(H),14β(H),17β(H)–24–ethylcholestane
S12	C_{29} (20R)–5α(H),14α(H),17α(H)–24–ethylcholestane
	DIASTERANES:
D1	C_{27} (20S)–13β(H),17α(H)–diasterane
D2	C_{27} (20R)–13β(H),17α(H)–diasterane
D3	C_{28} (20S)–13β(H),17α(H)–diasterane
D4	C_{28} (20R)–13β(H),17α(H)–diasterane
D5	C_{29} (20S)–13β(H),17α(H)–diasterane
D6	C_{29} (20R)–13β(H),17α(H)–diasterane

Key 2. Identifications of peaks in hopane (m/z 191) and methyl hopane (m/z 205) mass fragmentograms

PEAK		COMPOUND
H1	C_{27}	18α(H)–22,29,30–trisnorneohopane (Ts)
H2	C_{27}	17α(H)–22,29,30–trisnorhopane (Tm)
H3	C_{29}	17α(H),21β(H)–30–norhopane
H4	C_{29}	17β(H),21α(H)–30–normoretane
H5	C_{30}	17α(H),21β(H)–hopane
H6	C_{30}	17β(H),21α(H)–moretane
H7	C_{31}	(22S)–17α(H),21β(H)–homohopane
H8	C_{31}	(22R)–17α(H),21β(H)–homohopane
H9	C_{31}	(22R+S)–17β(H),21α(H)–bishomomoretane
H10	C_{32}	(22S)–17α(H),21β(H)–bishomohopane
H11	C_{32}	(22R)–17α(H),21β(H)–bishomohopane
H12	C_{33}	(22S)–17α(H),21β(H)–trishomohopane
H13	C_{33}	(22R)–17α(H),21β(H)–trishomohopane
H14	C_{34}	(22S)–17α(H),21β(H)–tetrakishomohopane
H15	C_{34}	(22R)–17α(H),21β(H)–tetrakishomohopane
H16	C_{35}	(22S)–17α(H),21β(H)–pentakishomohopane
H17	C_{35}	(22R)–17α(H),21β(H)–pentakishomohopane

Key 3. Identifications of peaks in methyl hopane (m/z 205) mass fragmentograms

PEAK		COMPOUND
M1	C_{28}	18α(H)–22,29,30–trisnorneo–2–methylhopane (Ts)
M2	C_{28}	17α(H)–22,29,30–trisnor–2–methylhopane (Tm)
M3	C_{30}	17α(H),21β(H)–30–nor–2–methylhopane
M4	C_{30}	17β(H),21α(H)–30–nor–2–methylmoretane
M5	C_{31}	17α(H),21β(H)–2–methylhopane
M6	C_{31}	17β(H),21α(H)–2–methylmoretane
M7	C_{32}	(22S)–17α(H),21β(H)–2–methylhomohopane
M8	C_{32}	(22R)–17α(H),21β(H)–2–methylhomohopane
M9	C_{32}	(22R+S)–17β(H),21α(H)–2–methylbishomomoretane
M10	C_{33}	(22S)–17α(H),21β(H)–2–methylbishomohopane
M11	C_{33}	(22R)–17α(H),21β(H)–2–methylbishomohopane
M12	C_{34}	(22S)–17α(H),21β(H)–2–methyltrishomohopane
M13	C_{34}	(22R)–17α(H),21β(H)–2–methyltrishomohopane
M14	C_{35}	(22S)–17α(H),21β(H)–2–methyltetrakishomohopane
M15	C_{35}	(22R)–17α(H),21β(H)–2–methyltetrakishomohopane
M16	C_{36}	(22S)–17α(H),21β(H)–2–methylpentakishomohopane
M17	C_{36}	(22R)–17α(H),21β(H)–2–methylpentakishomohopane

ABLE 1. Hydrocarbon and asphaltene contents of bitumens and Tasmanian outcrop samples.

Sample Location	Sample description	EOM ppm	Aliphatics %	Aromatics %	Asphaltenes %	MPI	MPR	$VR_{(CALCa)}$	$VR_{(CALCb)}$
Benders Quarry, Tas.	Dark grey shale	2.4	12.8	43.6	43.6	1.1	4.1	1.1	1.5
Florentine Valley, Tas.	Light brown–yellow fossil bearing mudstone.	19.4	50.5	2.7	46.8	1.0	2.4	1.0	1.3
Bruny Island South, Tas.	Black brittle tar on weathered sandstone	–	0.2	38.5	61.1	0.2	1.3	0.5	1.1
Tunnack, Tas.	Medium–coarse grained sandstone with bituminous matrix	85420	0.4	40.7	58.9	0.2	1.1	0.5	1.0
Cape Jaffa, S.A.	Black, shiny bitumen with conchoidal fracture	–	13.8	10.6	75.6	0.6	0.8	0.7	0.8
South Coast, W.A.	Black, shiny bitumen with conchoidal fracture	–	17.3	5.8	76.9	0.7	0.9	0.8	0.9

RESULTS

1. Benders Quarry "Shale"

This dark grey shale–carbonate of probable Ordovician age was collected by M. Bendall from a fault zone in the carbonates at Benders Quarry at Lune River, Tasmania. It appeared to have been metamorphosed, and contained very low concentrations of extractable hydrocarbons (2.4 ppm, Table 1). Aliphatic hydrocarbons represented 12% of the total extract, whereas aromatic hydrocarbons were much more abundant (43% of the extract), with the remaining 43% consisting of polar resins and asphaltenes.

Aliphatic Hydrocarbons

The aliphatic C_{15+} hydrocarbons (Fig. 3a) showed a predominance of n–alkanes in the C_{16}–C_{20} range, with an unusual predominance of C_{18} and C_{16} over C_{17}. Pristane was only slightly more abundant than phytane. High molecular weight n–alkanes (i.e $>C_{25}$) were very minor constituents.

(a) Steranes: Mass fragmentograms for m/z 217 and m/z 218 (Figs. 3b) show a distribution typical of a moderately mature crude oil. C_{29} steranes were slightly more abundant than C_{27} steranes, which in turn were about twice as abundant as C_{28} steranes. The distribution of shorter–chain steranes is shown in Fig. 3c.

Diasteranes were significant constituents (m/z 259; Fig. 3d) of the aliphatic biomarkers. These constituents are not common in pure carbonates, and thus are not found or are of low abundance in most Middle East crude oils. They are very abundant in Gippsland Basin crudes. A complex mixture of methyl steranes (m/z 231; Fig 3d) was also present, although at much lower concentrations.

Sterane maturity parameters are consistent with a moderately mature oil. C_{29} sterane $\alpha\beta\beta$ isomers (peaks S10 and S11) are slightly more abundant in the m/z 217 mass fragmentograms compared with $\alpha\alpha\alpha$ isomers (peaks S9 and S12), and the ratio of 20S to 20R isomers is slightly less than 1.

Hopanes: Hopane distributions as represented by mass fragmentograms of the major fragment ion m/z 191 over the C_{27}–C_{36} carbon number ranges are shown in Fig. 3e. A chromatogram showing C_{27}–C_{32} hopanes is shown in Fig. 3f. Comparable data from the hydrocarbons isolated from the Ordovician limestones from Ida Bay are shown in Fig. 5.

The hopane distribution is quite distinctive with a high predominance of the C_{29} hopane (peak H3; Figs. 3e and 3f). No hopenes or hopanes having an "immature" 17β(H),21β(H)–stereochemistry were detected indicating that the hydrocarbons were not derived from thermally immature source rocks. Moretanes were very minor constituents, which is consistent with moderately mature oil.

These biomarker distributions are similar to those previously reported from Ordovician limestones obtained from Ida Bay and Queenstown (Volkman, 1988), although the biomarker parameters suggest a slightly higher maturity level. For comparison, GC–MS data for the Ida Bay limestone are shown in Figs. 4 and 5. Further details are given in Volkman (1988).

The hopane biomarker parameters are all consistent with moderately mature organic matter:

(i) In the extended hopanes (i.e. >C_{30}), the 22S epimer is more abundant than the 22R epimer (e.g. peaks H7 and H8). (ii) The moretanes (peaks H4, H6 and H9) are very minor components compared with 17α(H),21β(H)–hopanes of the same chain–length (peaks H3, H5 and H7/H8). (iii) The C_{27} hopane Ts (peak H1) is less abundant than Tm (peak H2).

Tricyclic alkanes: These were very minor constituents.

Methyl hopanes: The shale contains a similar distribution of 2–methyl hopanes (m/z 205 mass fragmentogram; Fig. 3e) to that found in the Ordovician limestones (Volkman, 1988 and Fig. 5). High abundances are commonly associated with carbonate source rocks although they are not restricted to this source facies.

Demethylated hopanes: The m/z 177 mass fragmentogram (Fig. 3f) indicated that C–10 demethylated hopanes are not present in this sediment.

Aromatic Hydrocarbons

A gas chromatogram of the aromatic hydrocarbons in the Benders Quarry shale is shown in Fig. 3g.

Phenanthrene and alkylated phenanthrenes: Phenanthrene was the major constituent of the total aromatic hydrocarbon fraction, followed by 3– and 2–methylphenanthrenes. Mass fragmentograms for m/z 178 (phenanthrene) and 192 (methylphenanthrenes) are shown in Fig. 3h. The 2– and 3–methylphenanthrene isomers greatly predominate over the 1– and 9–methylphenanthrene isomers which is a common characteristic of mature oils (Radke and Welte, 1983). This distribution is very different from that found in the Tasmanian bitumens analysed by Volkman and O'Leary (1990b).

The equivalent vitrinite reflectance calculated from the MPI and MPR values according to the equations of Radke and Welte (1983) was 1.1 and 1.5 (Table 1). The distributions of dimethylphenanthrenes and trimethylphenanthrenes determined from mass fragmentograms for m/z 206 and 220 respectively are shown in Fig. 3i. These compounds

were very much less abundant than the methylphenanthrenes and individual isomers were not assigned.

A GC–MS search for monoaromatic steroids was made using these characteristic ions, but only trace amounts could be detected in the samples. Triaromatic steroid hydrocarbons were also difficult to detect (Fig. 3j).

Figure 3. GC and GC–MS data for the Benders Quarry shale sample.

(3a) Capillary gas chromatogram of the total aliphatic hydrocarbons in the Benders Quarry shale sample. Pr: pristane; Ph: phytane. n–Alkanes are denoted by n–C_X where "x" is the number of carbon atoms.

(3b). Mass fragmentograms for m/z 217 and 218 showing distribution of C_{26}–C_{30} steranes (labelled S) and diasteranes (labelled D) in the Benders Quarry shale sample. See Key 1 for peak identifications.

(3c) Mass fragmentograms for m/z 217 and 218 showing distribution of C_{21}–C_{23} steranes in the Benders Quarry shale sample.

(3d) Mass fragmentograms for m/z 259 showing distribution of C_{27}–C_{30} diasteranes (labelled D), and m/z 231 showing distribution of C_{28}–C_{30} 4–methyl steranes in the Benders Quarry shale sample.

(3e) Mass fragmentograms for m/z 191 showing distribution of C_{27}–C_{35} hopanes and m/z 205 showing distribution of methyl hopanes in the Benders Quarry shale sample. See Keys 2 and 3 for peak identifications.

(3f) Mass fragmentograms for m/z 191 showing distribution of C_{27}–C_{32} hopanes and m/z 177 showing distribution of demethylated hopanes (none present) in the Benders Quarry shale sample.

(3g) Capillary gas chromatogram of the total aromatic hydrocarbons in the Benders Quarry shale sample.

(3h) Mass fragmentograms for m/z 178 and 192 showing the presence of phenanthrene and distribution of methylphenanthrenes respectively in the Benders Quarry shale sample.

(3i) Mass fragmentograms for m/z 206 and 220 showing the distribution of di– and trimethylphenanthrenes in the Benders Quarry shale sample.

(3j) Mass fragmentograms for m/z 231 and 245 showing the distribution of triaromatic steroidal hydrocarbons (with one and two methyl groups in the ABC ring system respectively) in the Benders Quarry shale sample.

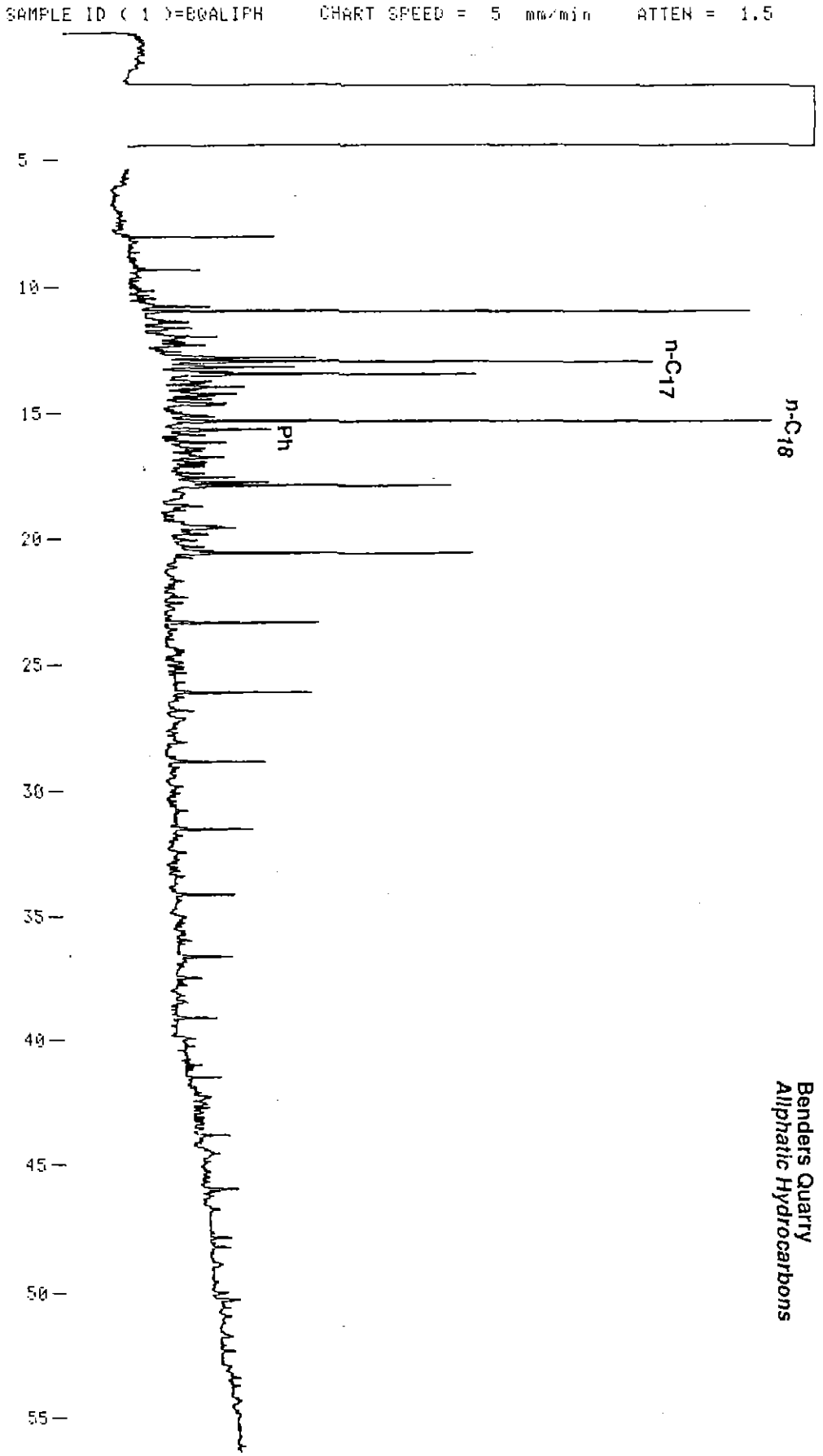

Fig. 3(a)

Fig. 3(b)

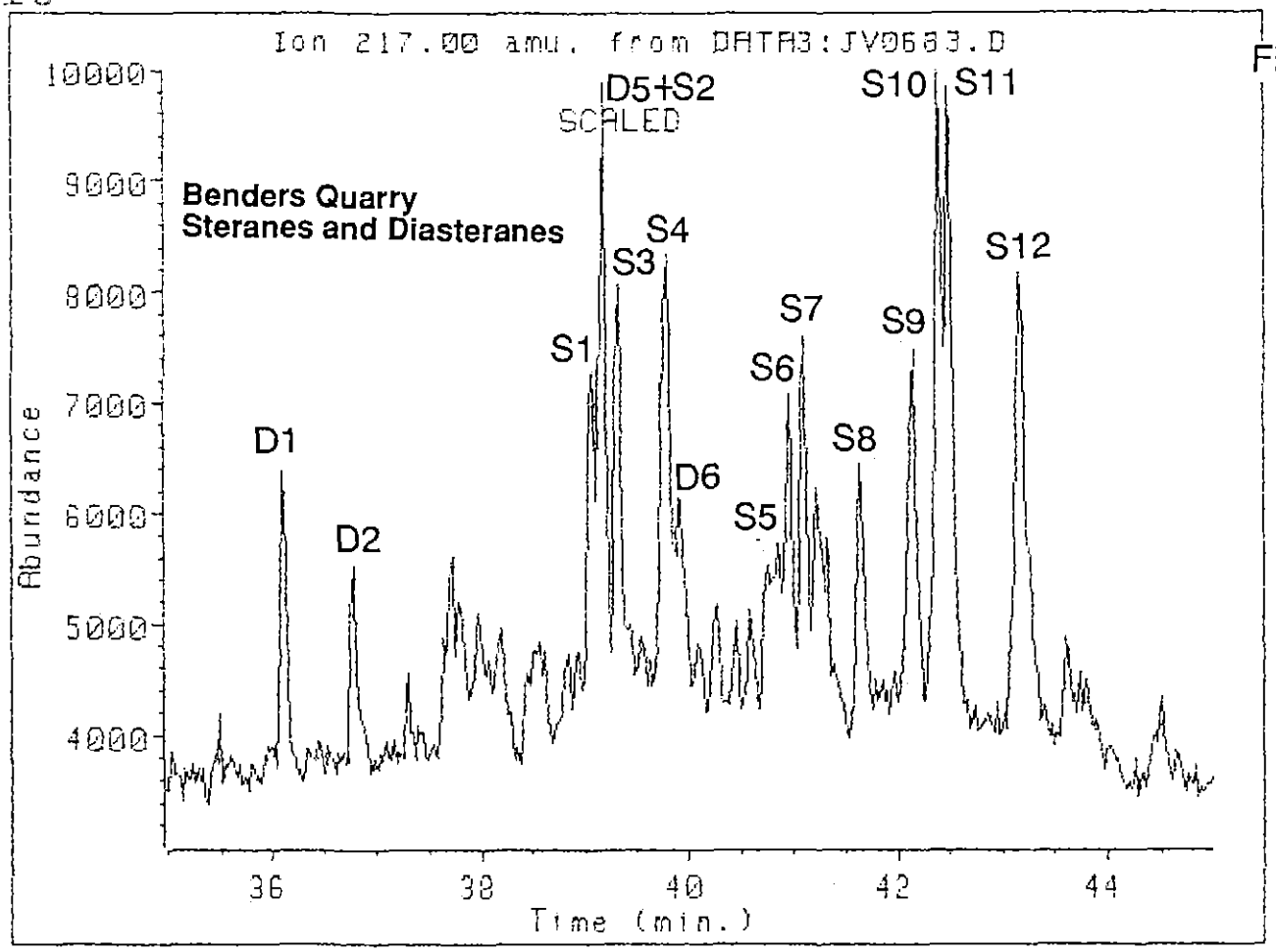
Ion 217.00 amu. from DATA3:JV0683.D
Benders Quarry
Steranes and Diasteranes
SCALED
D5+S2
S10
S11
S4
S3
S12
S7
S9
S1
S6
D1
S8
D6
S5
D2
Abundance
10000
9000
8000
7000
6000
5000
4000
36
38
40
42
44
Time (min.)

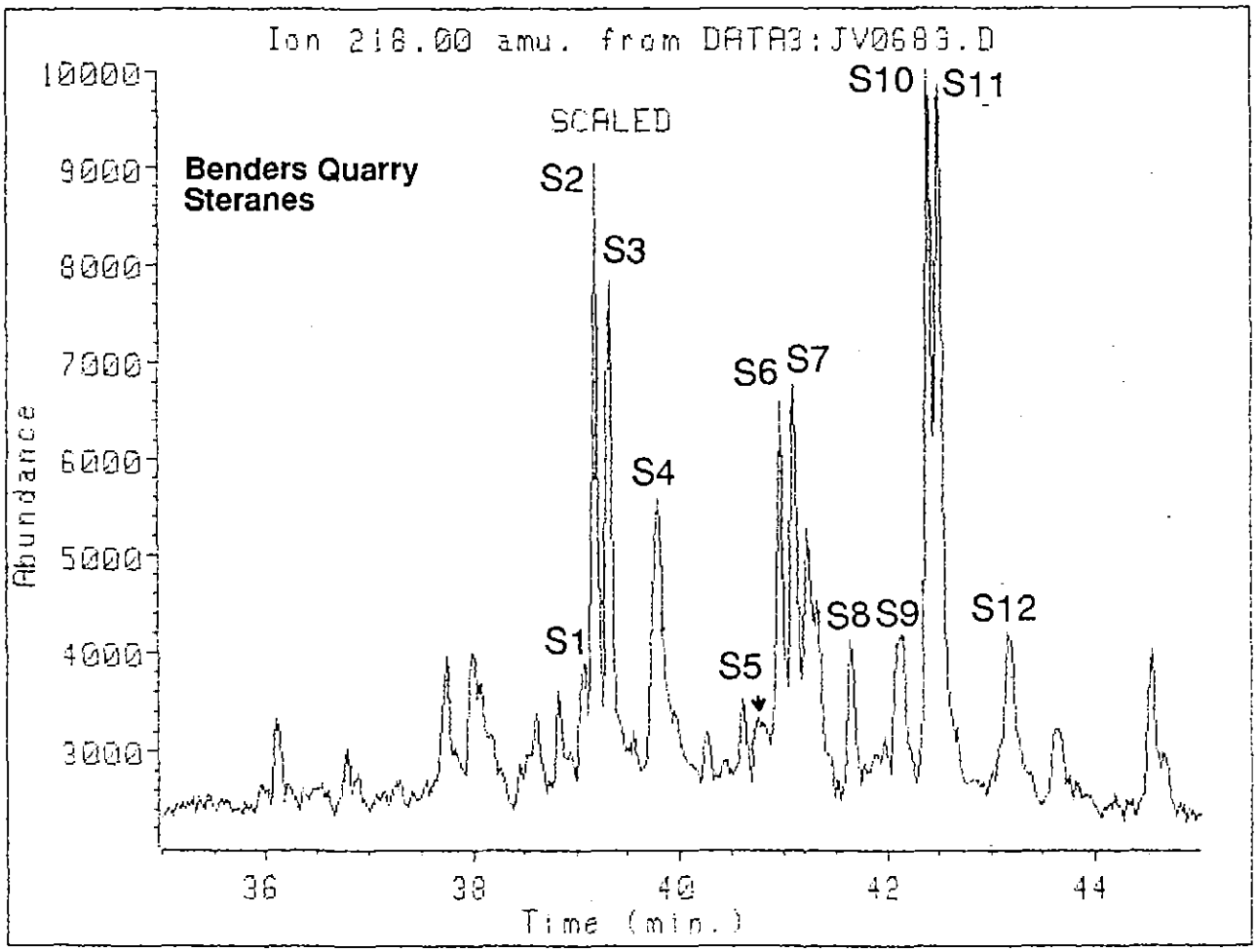
Ion 218.00 amu. from DATA3:JV0683.D
Benders Quarry
Steranes
SCALED
S10
S11
S2
S3
S6
S7
S4
S1
S8
S9
S12
S5
Abundance
10000
9000
8000
7000
6000
5000
4000
3000
36
38
40
42
44
Time (min.)

5 cm

Fig. 3(c)

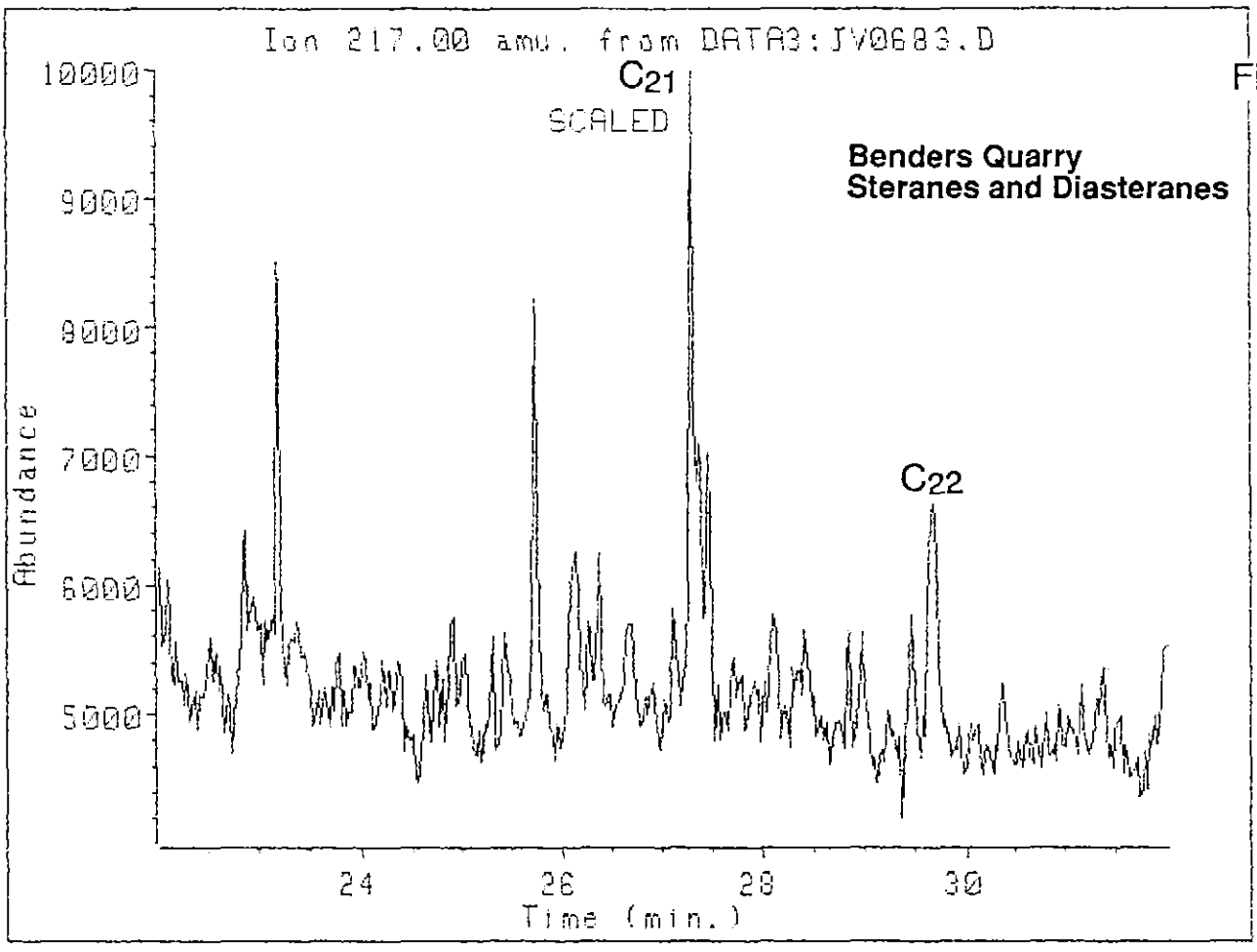
Ion 217.00 amu. from DATA3:JV0683.D
C21
SCALED
Benders Quarry
Steranes and Diasteranes
C22
Abundance
10000
9000
8000
7000
6000
5000
24
26
28
30
Time (min.)

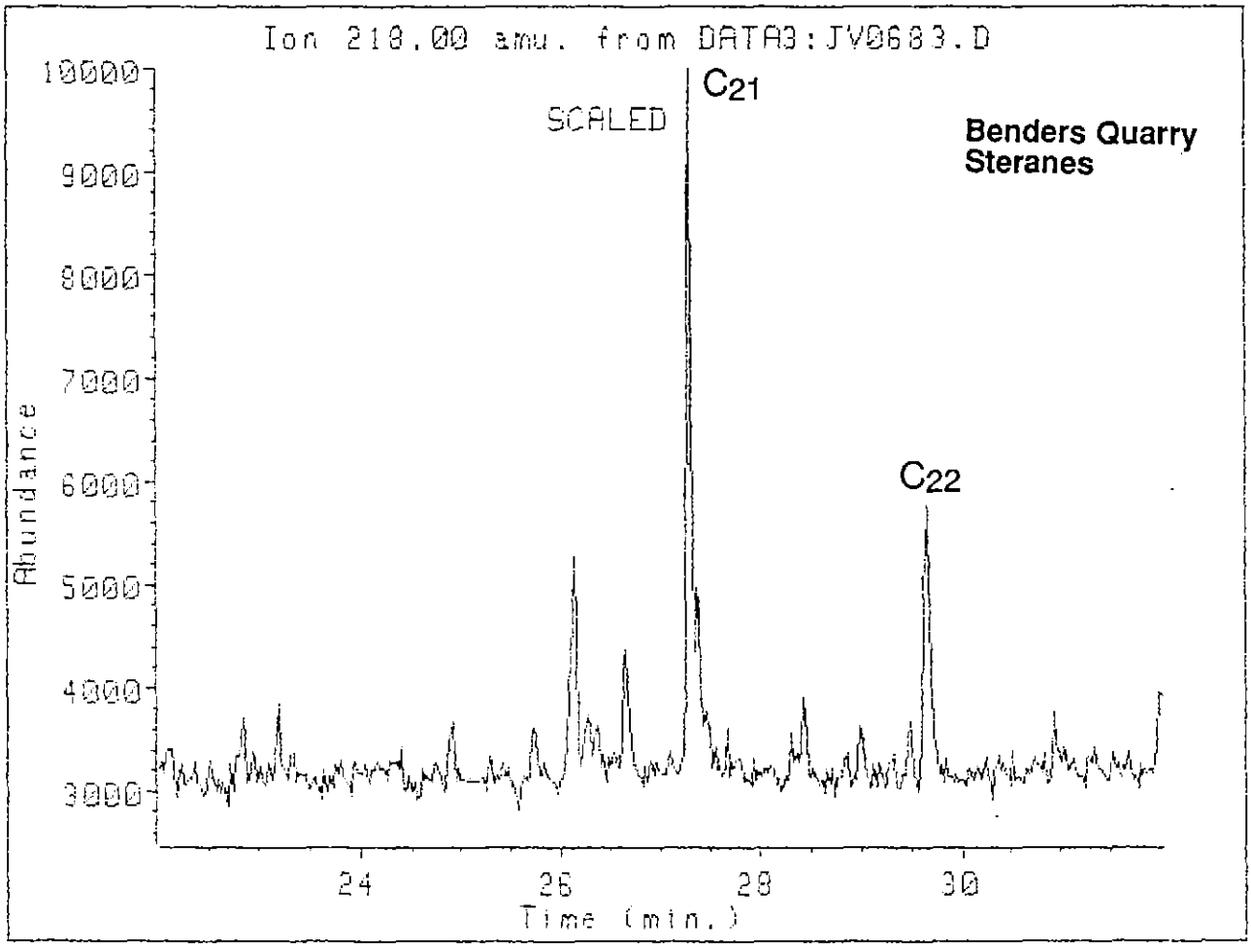
Ion 218.00 amu. from DATA3:JV0683.D
C21
SCALED
Benders Quarry
Steranes
C22
Abundance
10000
9000
8000
7000
6000
5000
4000
3000
24
26
28
30
Time (min.)

5 cm

Fig. 3(d)

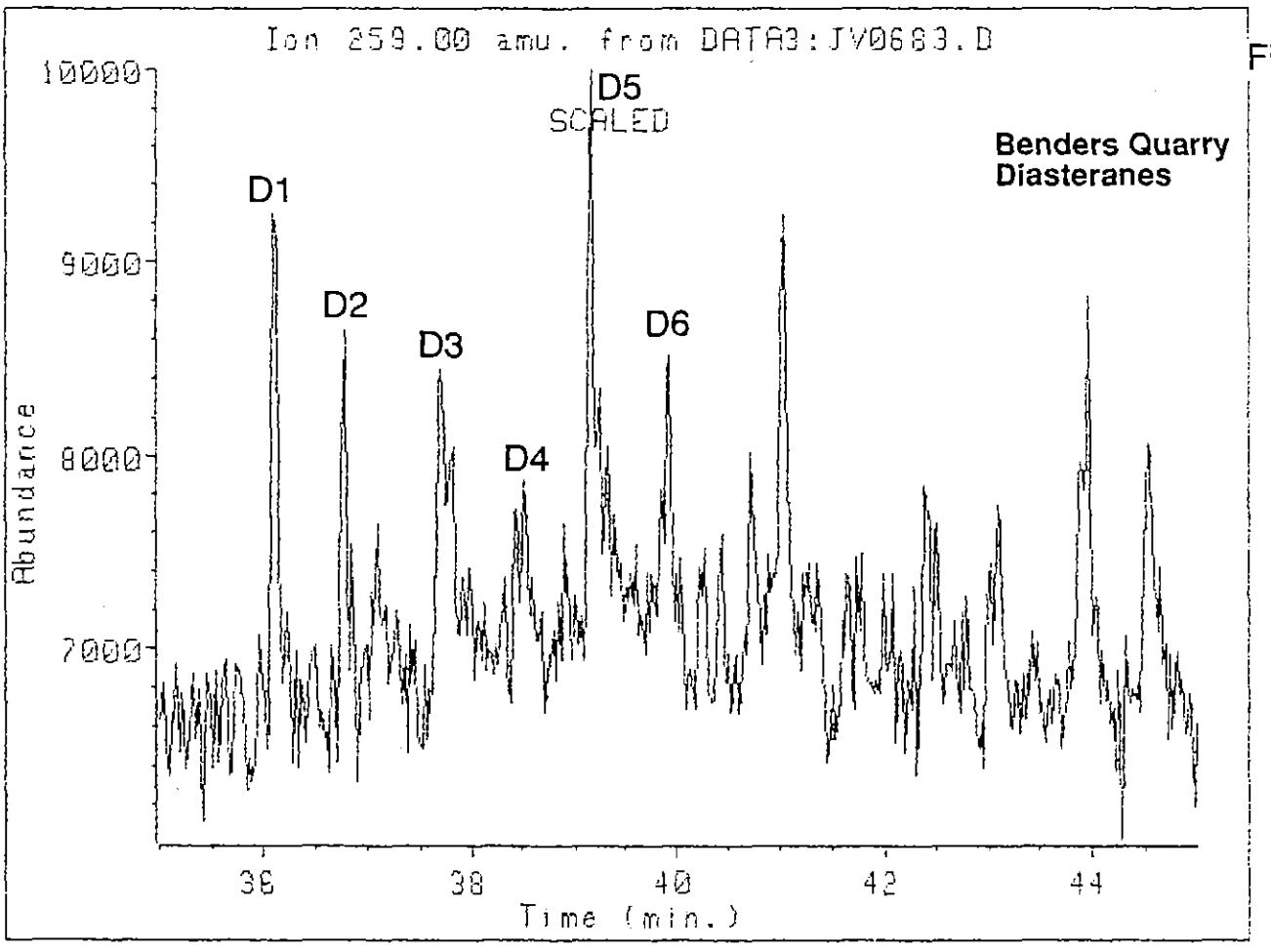
Ion 259.00 amu. from DATA3:JV0683.D
10000
9000
8000
7000
Abundance
SCALED
D1
D2
D3
D4
D5
D6
Benders Quarry
Diasteranes
36
38
40
42
44
Time (min.)

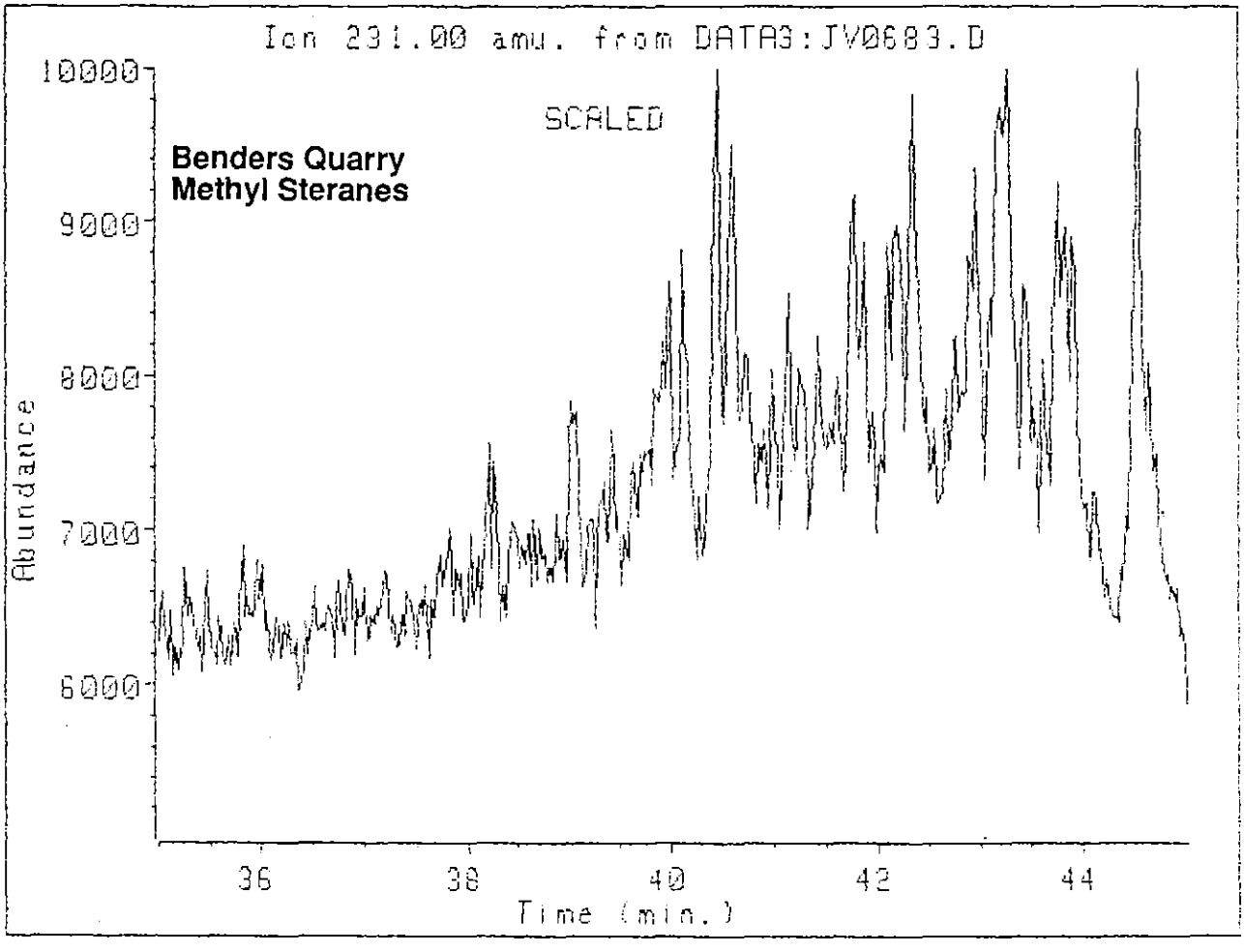
Ion 231.00 amu. from DATA3:JV0683.D
10000
9000
8000
7000
6000
Abundance
SCALED
Benders Quarry
Methyl Steranes
36
38
40
42
44
Time (min.)

5 cm

Fig. 3(e)

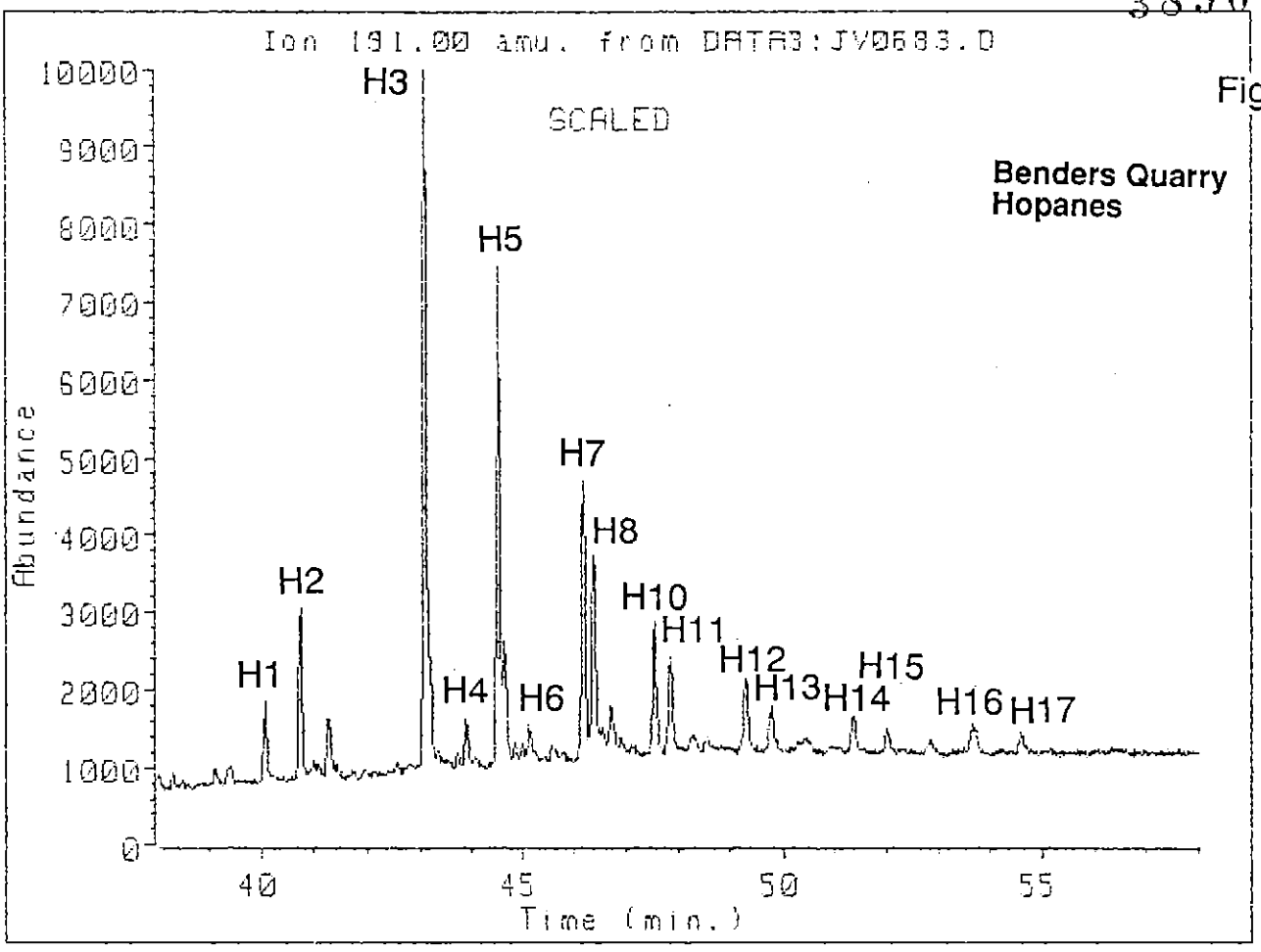
Ion 191.00 amu. from DATA3:JV0683.D
SCALED
Benders Quarry
Hopanes
H1
H2
H3
H4
H5
H6
H7
H8
H10
H11
H12
H13
H14
H15
H16
H17
Abundance
Time (min.)

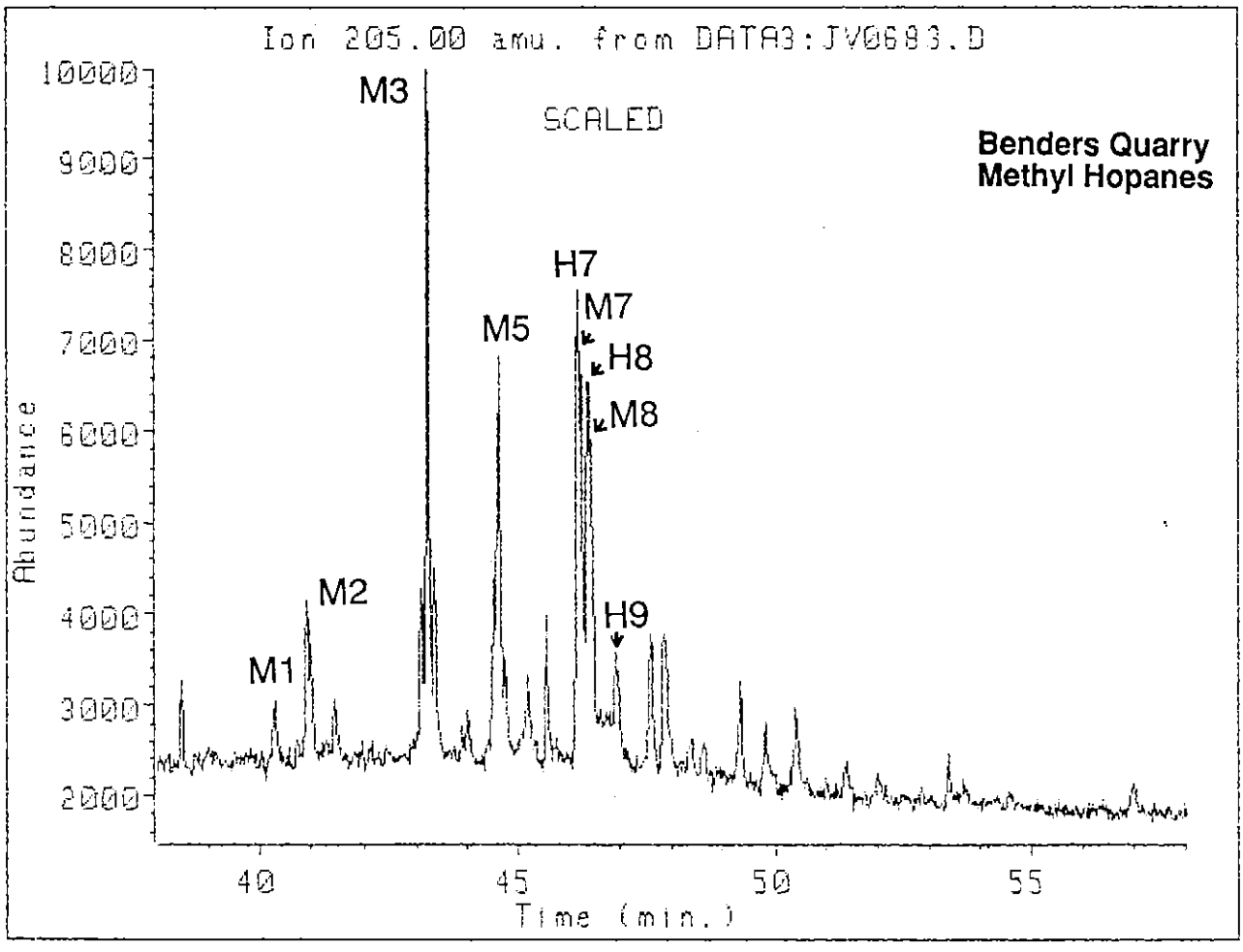
Ion 205.00 amu. from DATA3:JV0683.D
SCALED
Benders Quarry
Methyl Hopanes
M1
M2
M3
M5
H7
M7
H8
M8
H9
Abundance
Time (min.)

5 cm

Fig. 3(f)

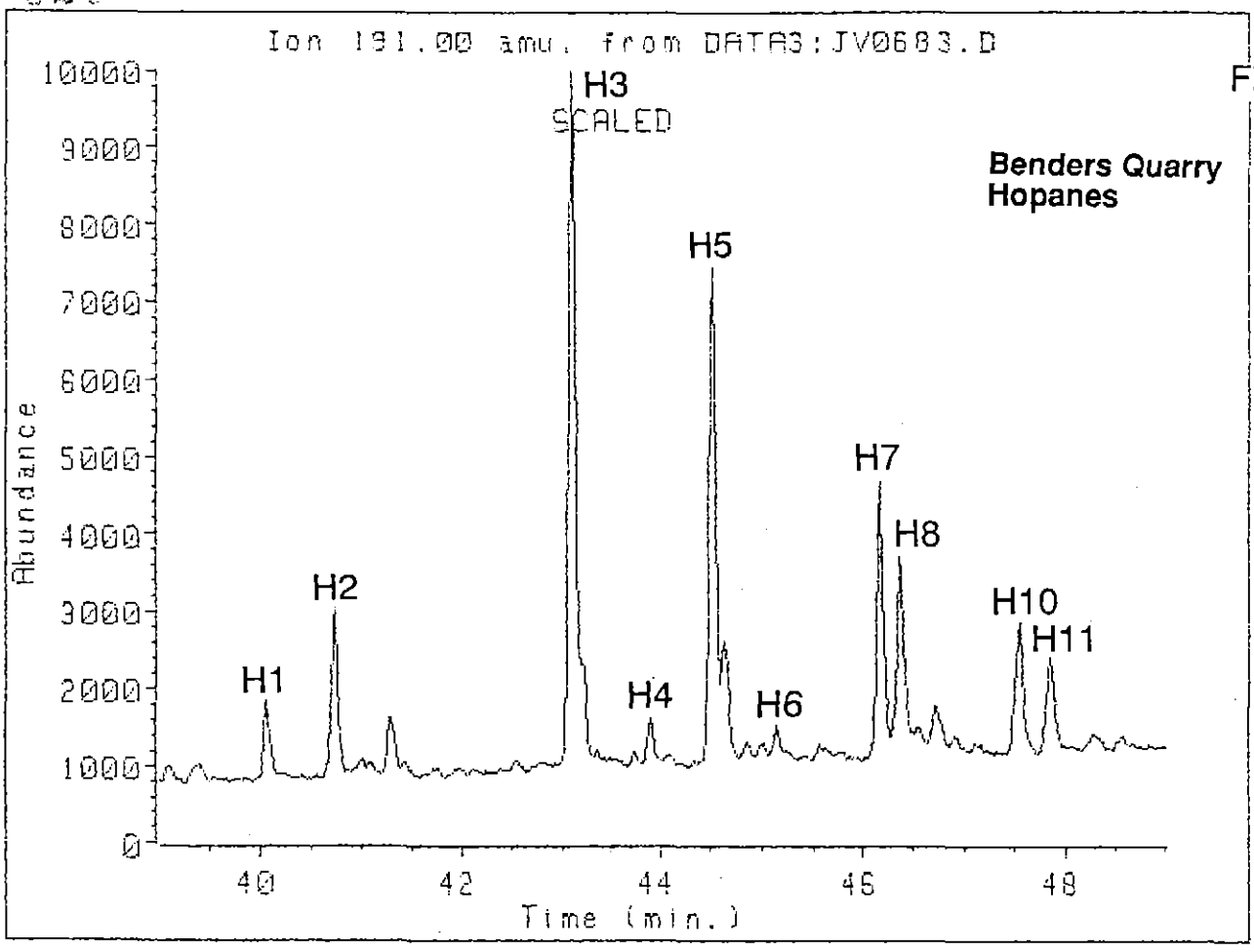
Ion 191.00 amu. from DATA3:JV0683.D
10000
9000
8000
7000
6000
5000
4000
3000
2000
1000
0
Abundance
H3
SCALED
Benders Quarry
Hopanes
H5
H7
H8
H2
H10
H11
H1
H4
H6
40
42
44
46
48
Time (min.)

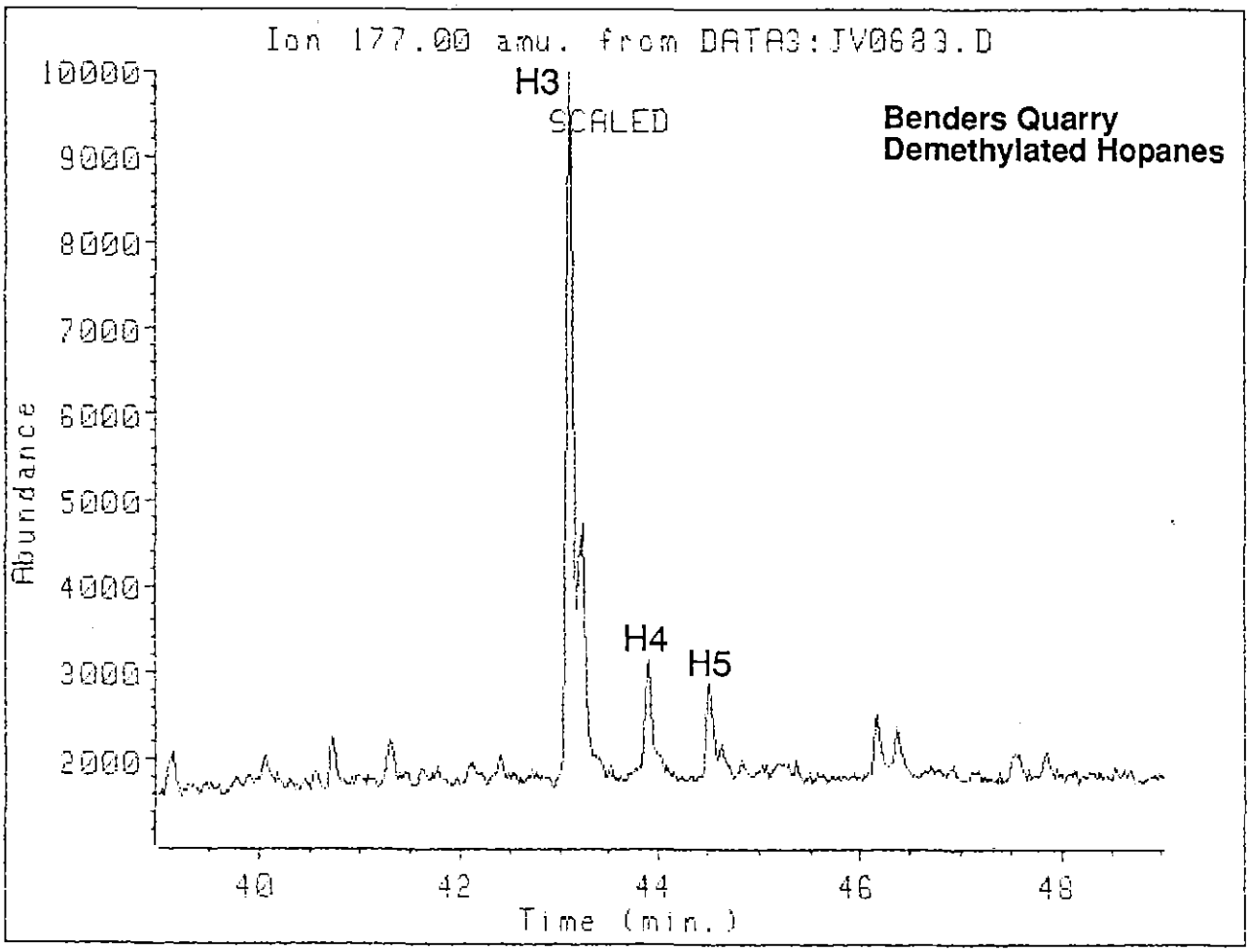
Ion 177.00 amu. from DATA3:JV0683.D
10000
9000
8000
7000
6000
5000
4000
3000
2000
Abundance
H3
SCALED
Benders Quarry
Demethylated Hopanes
H4
H5
40
42
44
46
48
Time (min.)

5 cm

Fig. 3(g)

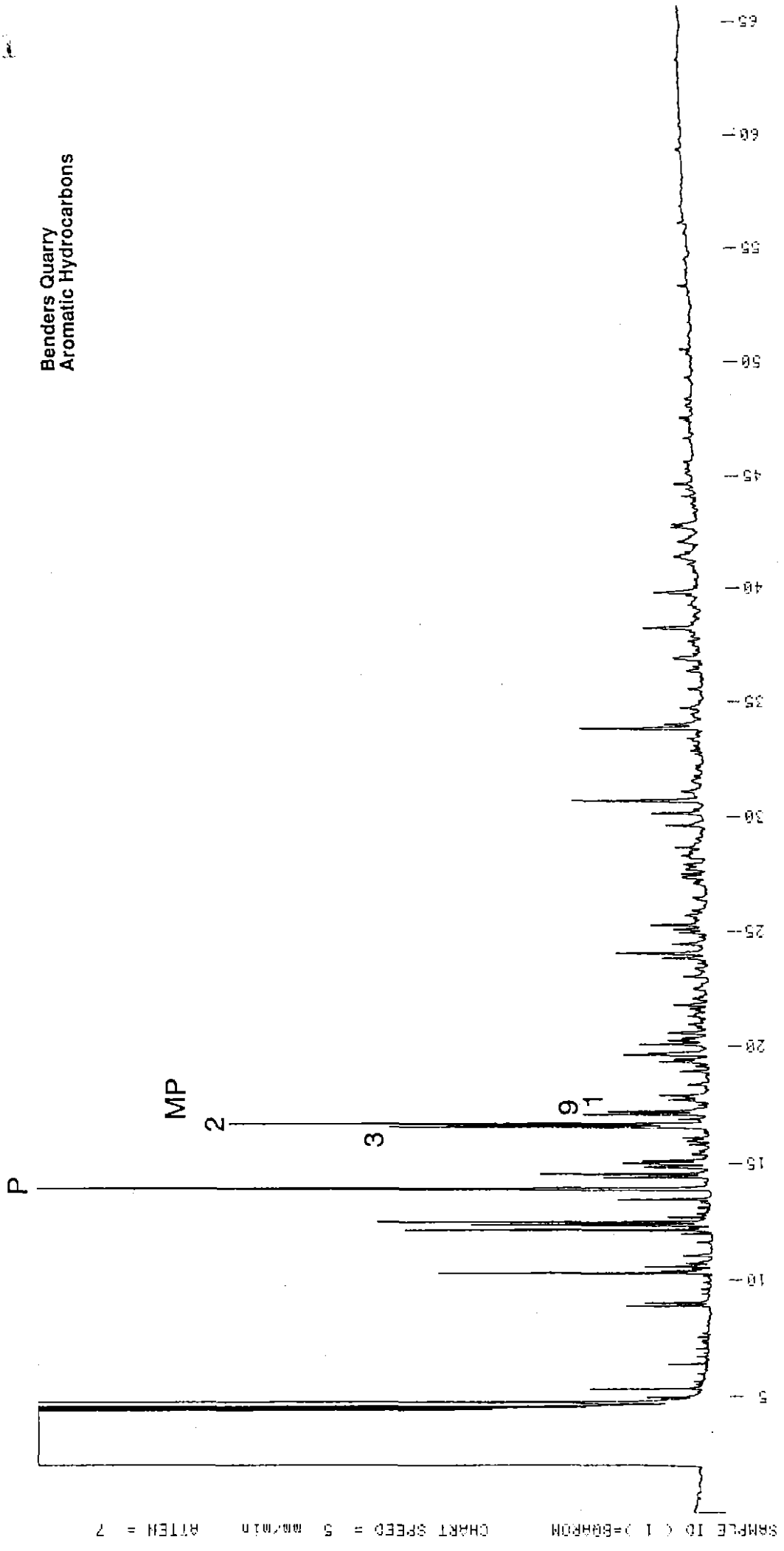
Benders Quarry
Aromatic Hydrocarbons
P
MP
2
3
9
1
65
60
55
50
45
40
35
30
25
20
15
10
5
SAMPLE ID (1)=BOHROM
CHART SPEED = 5 mm/min
ATTEN = 7

Fig. 3(h)

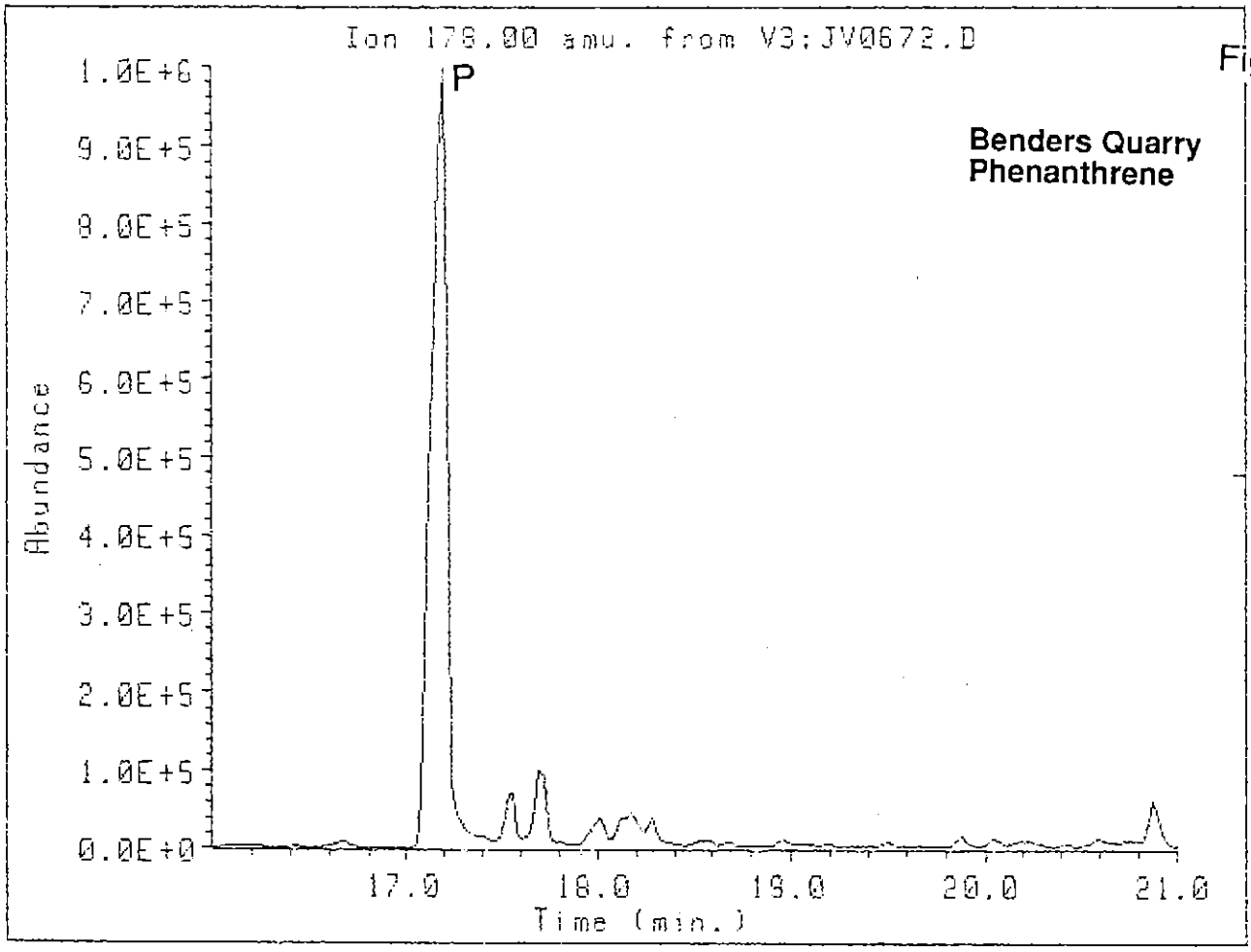
Ion 178.00 amu. from V3:JV0672.D
P
Benders Quarry
Phenanthrene
Abundance
1.0E+6
9.0E+5
8.0E+5
7.0E+5
6.0E+5
5.0E+5
4.0E+5
3.0E+5
2.0E+5
1.0E+5
0.0E+0
17.0
18.0
19.0
20.0
21.0
Time (min.)

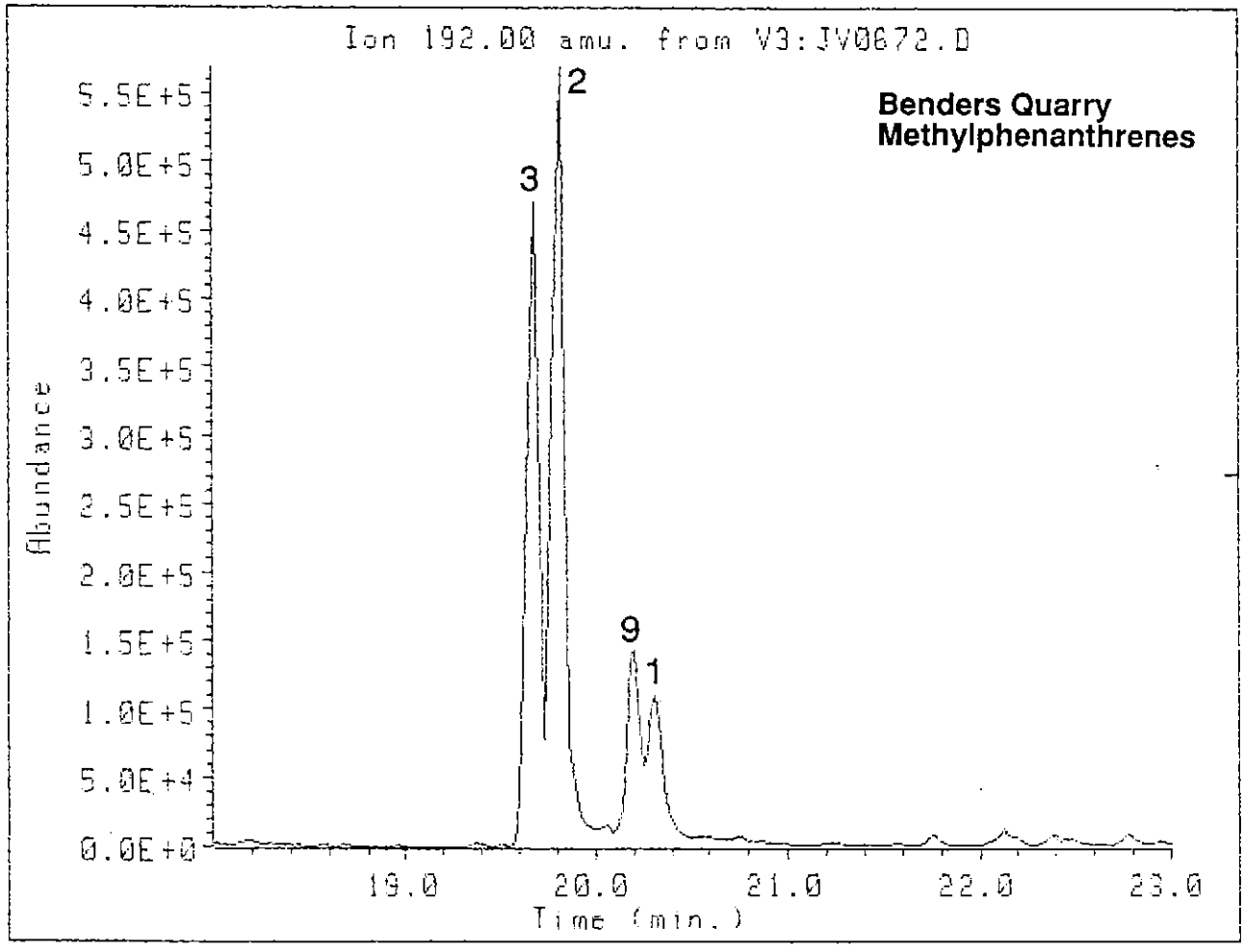
Ion 192.00 amu. from V3:JV0672.D
2
3
9
1
Benders Quarry
Methylphenanthrenes
Abundance
5.5E+5
5.0E+5
4.5E+5
4.0E+5
3.5E+5
3.0E+5
2.5E+5
2.0E+5
1.5E+5
1.0E+5
5.0E+4
0.0E+0
19.0
20.0
21.0
22.0
23.0
Time (min.)

Fig. 3(i)

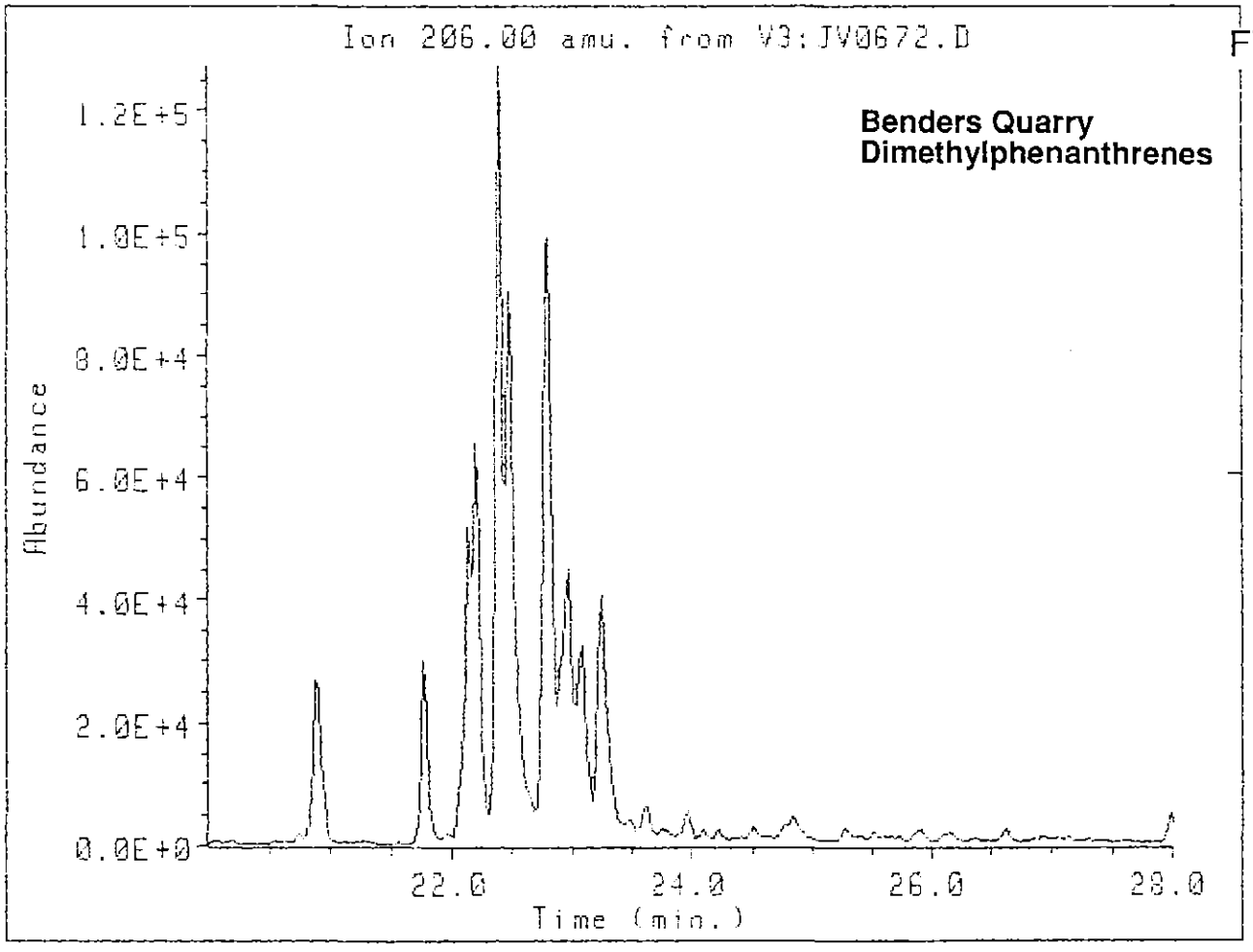
Ion 206.00 amu. from V3:JV0672.D
Benders Quarry
Dimethylphenanthrenes
Abundance
1.2E+5
1.0E+5
8.0E+4
6.0E+4
4.0E+4
2.0E+4
0.0E+0
22.0
24.0
26.0
28.0
Time (min.)

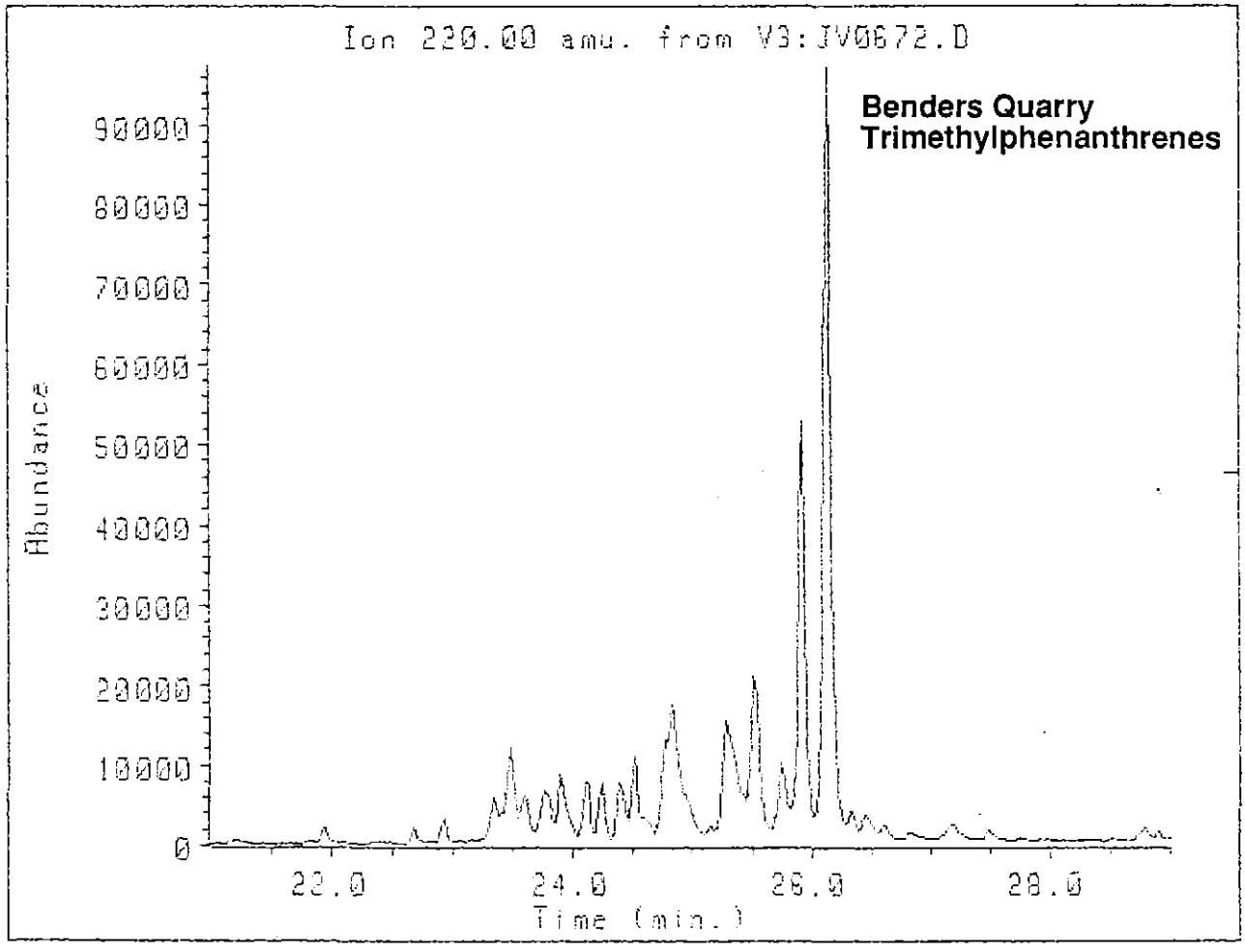
Ion 220.00 amu. from V3:JV0672.D
Benders Quarry
Trimethylphenanthrenes
Abundance
90000
80000
70000
60000
50000
40000
30000
20000
10000
0
22.0
24.0
26.0
28.0
Time (min.)

Fig. 3(j)

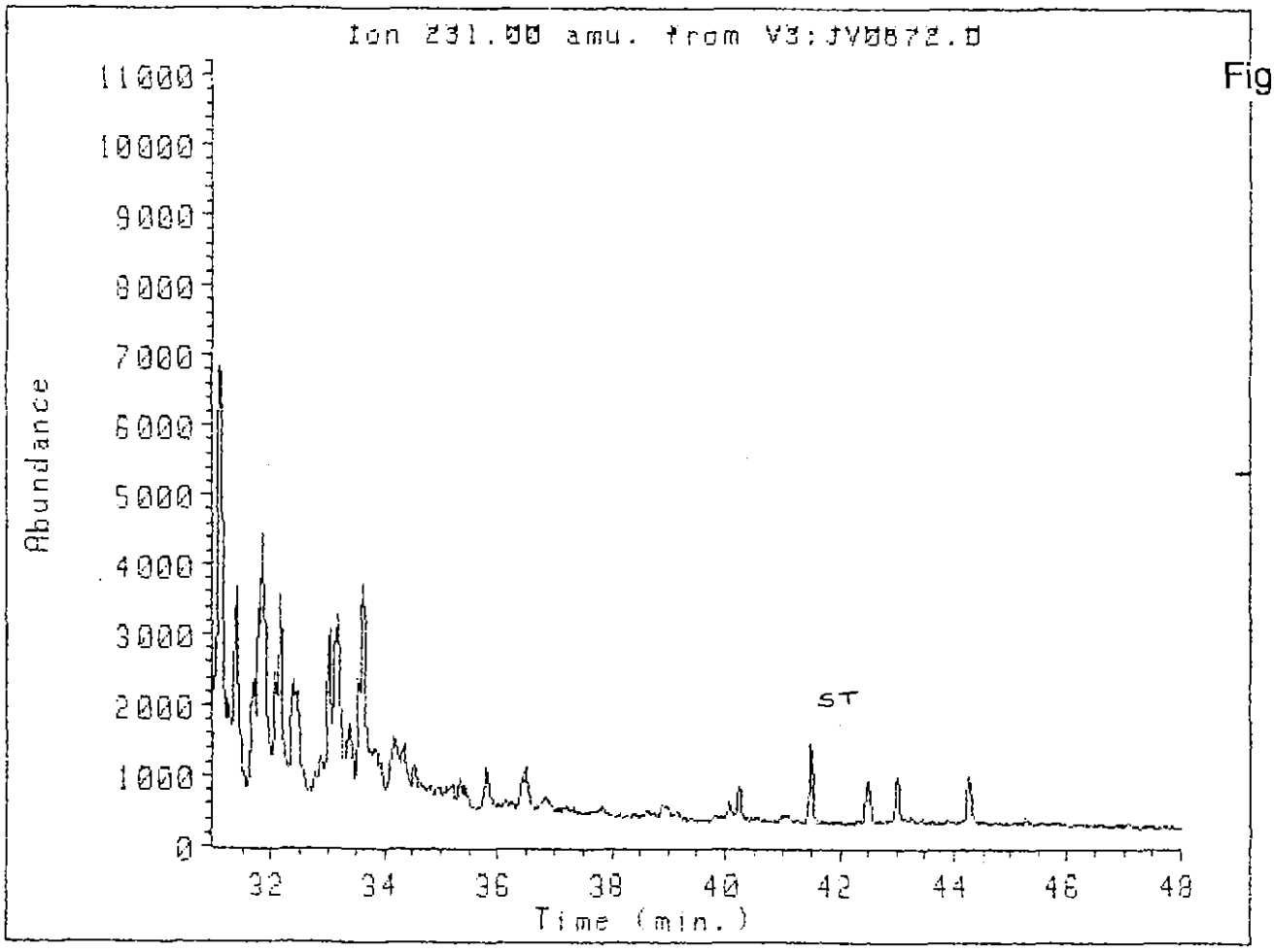
Ion 231.00 amu. from V3:JV0672.D
Abundance
11000
10000
9000
8000
7000
6000
5000
4000
3000
2000
1000
0
ST
32
34
36
38
40
42
44
46
48
Time (min.)

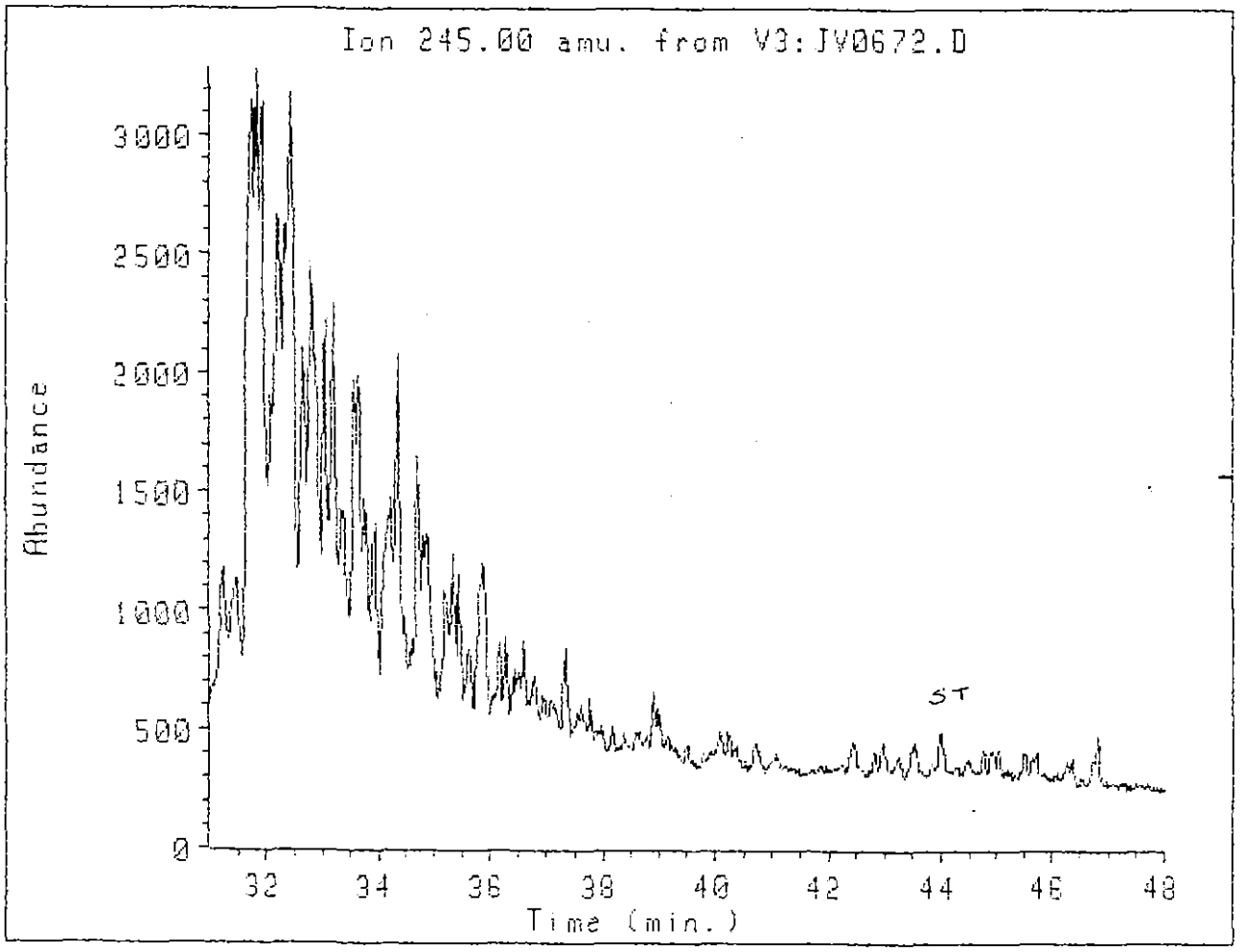
Ion 245.00 amu. from V3:JV0672.D
Abundance
3000
2500
2000
1500
1000
500
0
ST
32
34
36
38
40
42
44
46
48
Time (min.)

5 cm

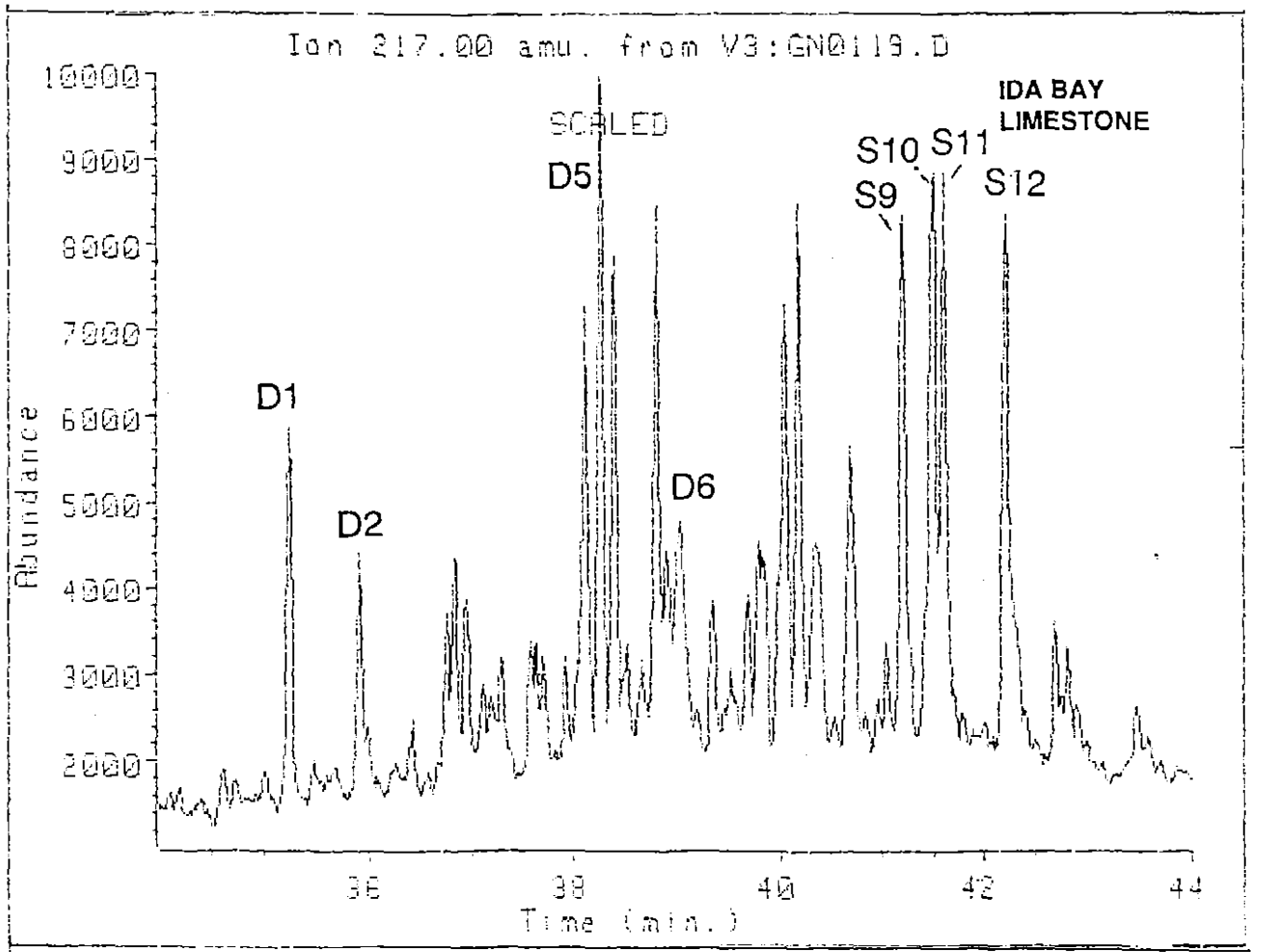

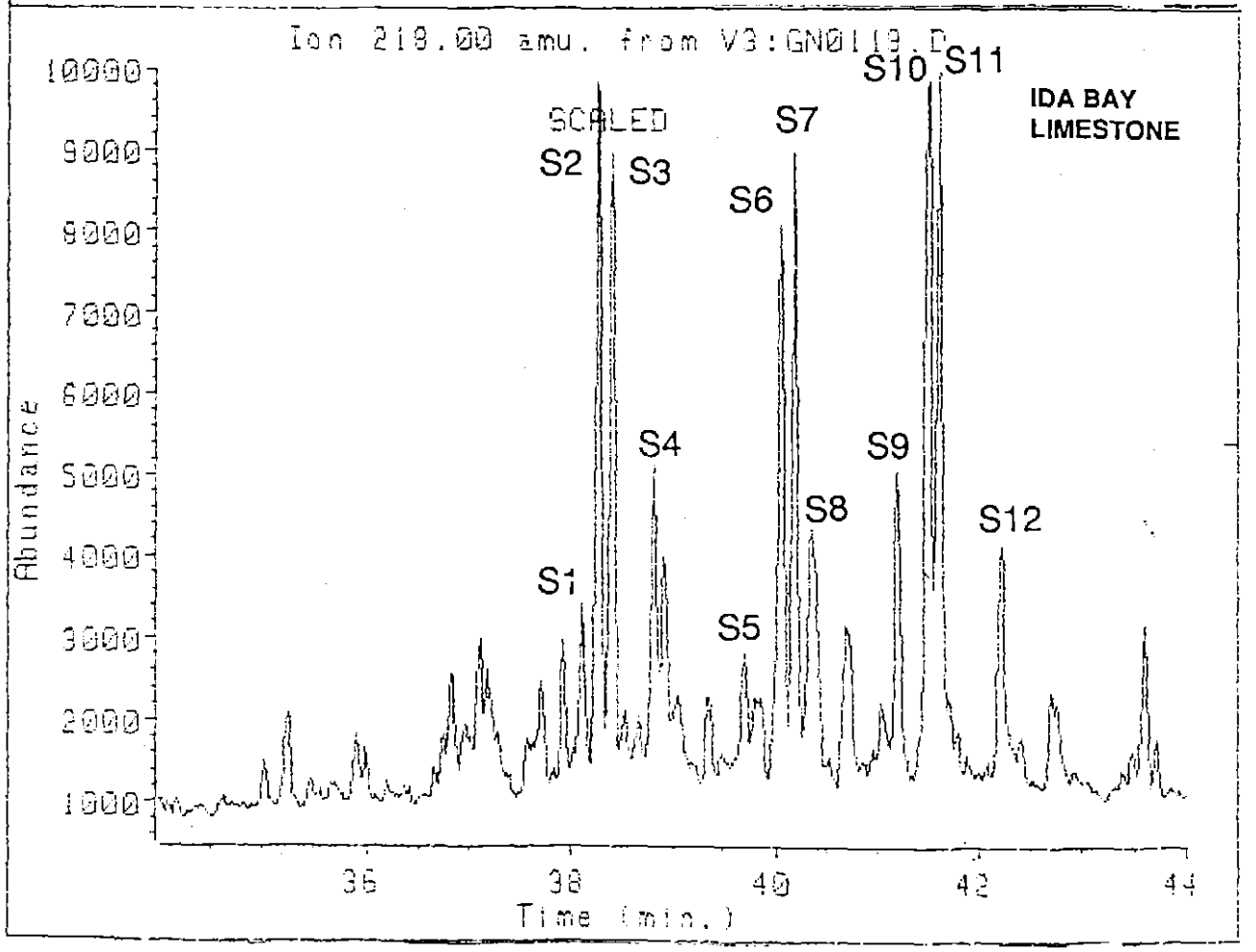

Figure 4. Mass fragmentograms for m/z 217 and m/z 218 showing distribution of C26–C30 steranes (labelled S) and diasteranes (labelled D) in a limestone from Ida Bay (Volkman, 1988). See Key 1 for peak identifications.

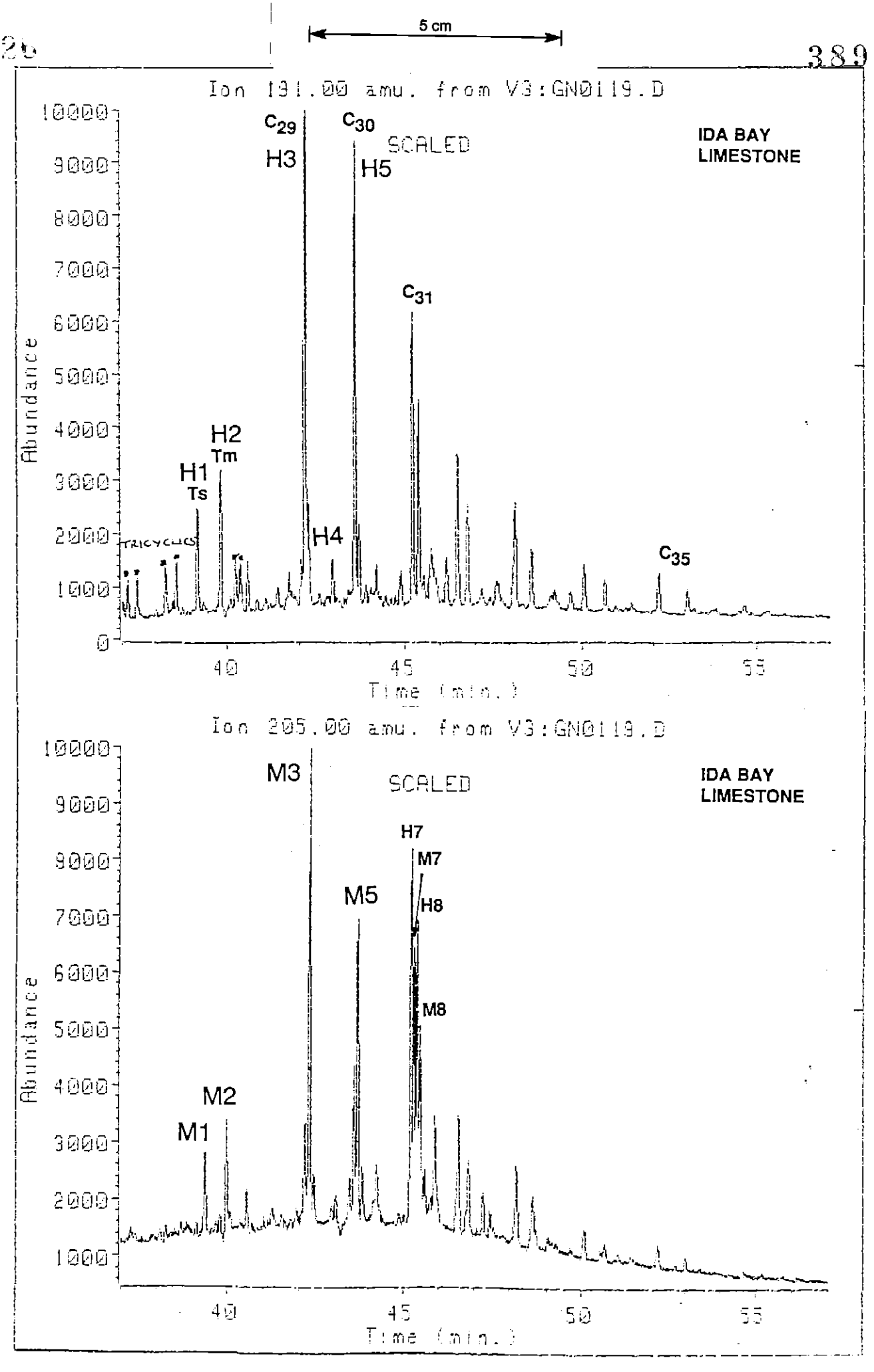

Figure 5. Mass fragmentograms for m/z 191 showing distribution of C_{27}–C_{35} hopanes and m/z 205 showing distribution of methyl hopanes a limestone from Ida Bay (Volkman, 1988). See Key 2 for peak identifications.

2. *Florentine Valley Mudstone*

This sediment was a light brown–yellow mudstone which contained abundant fossils. It dates from the early Ordovician and is both deeper and older than the carbonates previously analysed from Ida Bay. The concentration of organic–soluble material was 19.4 μg/g dry wt. of rock. Aliphatic hydrocarbons comprised 50% of the total extract. Aromatic hydrocarbons represented only 2.8% of the extract, and asphaltenes 46.8%.

Aliphatic Hydrocarbons

The aliphatic C_{15+} hydrocarbons (Fig. 6a) showed a very strong predominance of n–alkanes in the C_{16}–C_{20} range, with the major component being n–C_{17} and no odd–even predominance. High molecular weight n–alkanes (i.e >C_{25}) were barely detectable. The pristane/phytane ratio was 2.6, which is consistent with an oxic depositional environment, and the n–C_{17}/pristane ratio was 2.9.

(a) Steranes: Mass fragmentograms for m/z 217 and m/z 218 (Figs. 3b) show a distribution typical of a moderately mature crude oil. C_{27} and C_{29} steranes were present in approximately equal proportions, and these were about 50% more abundant then the C_{28} steranes. The distribution of C_{21}–C_{23} steranes is shown in Fig. 6c.

Diasteranes were significant constituents (m/z 259; Fig. 6d), as might be expected for a mudstone. C_{27} diasteranes were more abundant than C_{29}. A complex mixture of methyl steranes (m/z 231; Fig 6d) was also present. GC–MS MRM studies are needed to fully identify the methyl steranes present.

Sterane maturity parameters are consistent with a moderately mature oil. C_{29} $\alpha\beta\beta$ sterane isomers (peaks S10 and S11) are slightly more abundant in the m/z 217 mass fragmentograms than $\alpha\alpha\alpha$ isomers (peaks S9 and S12), and the ratio of 20S and 20R

isomers is slightly less than 1. Note that the peak due to the C_{29} $\alpha\alpha\alpha$-sterane is enhanced by the presence of a co-eluting compound (methyl sterane?).

These biomarker distributions are similar to those previously reported from Ordovician limestones obtained from Ida Bay and Queenstown (Volkman, 1988), and the maturity level is very similar (Fig. 4).

Hopanes: Hopane distributions as represented by mass fragmentograms of the major fragment ion m/z 191 over the C_{27}-C_{32} and C_{27}-C_{35} carbon number ranges are shown in Fig. 6e and 6f. Comparable data from the hydrocarbons isolated from the Ordovician limestones from Ida Bay are shown in Fig. 5.

The hopane distribution exhibits a high predominance of the C_{29} hopane (peak H3; Figs. 6e,f), due to the presence of a series of 29-nor hopanes. The C_{29}/C_{30} hopane ratio is greater in the mudstone than in the Ida Bay carbonates (Figs. 5 and 6e). Moretanes (peaks H4, H6 and H9) were very minor constituents, which is typical of mature oils. All of the hopane maturity parameters are very similar to those obtained from Ida Bay Ordovician limestone analysed previously (Volkman, 1988).

(i) In the extended hopanes (i.e. $>C_{30}$), the 22S epimer is more abundant than the 22R epimer (e.g. peaks H7 and H8). (ii) The moretanes were very minor components compared with 17α(H),21β(H)-hopanes of the same chain-length. (iii) The Ts/Tm ratio is 0.4.

Tricyclic alkanes: Although very minor constituents, small peaks can be discerned in the m/z 191 mass fragmentogram (Fig. 6e; labelled *).

Methyl hopanes: The mudstone contains significant amounts of 2-methyl hopanes as shown by the m/z 205 mass fragmentogram (Fig 6e). The distribution is very similar to that found in the Ordovician limestones (Volkman, 1988 and Fig. 5). High abundances are

more commonly associated with carbonate source rocks, so it is rather surprising to find such high concentrations in this mudstone.

Demethylated hopanes: The m/z 177 mass fragmentogram indicated that C–10 demethylated hopanes are not present in the mudstone (Fig. 6f).

Aromatic Hydrocarbons

A gas chromatogram of the aromatic hydrocarbons in the mudstone is shown in Fig. 6g.

Phenanthrene and alkylated phenanthrenes: Phenanthrene was the major constituent of the total aromatic hydrocarbon fraction. Alkyl naphthalenes and methyl phenanthrenes were only slightly less abundant. Mass fragmentograms for m/z 178 (phenanthrene) and 192 (methylphenanthrenes) are shown in Fig. 6h. The 2– and 3–methylphenanthrene isomers are more abundant than the 1– and 9–methylphenanthrene isomers, and their distribution is similar to that found in mature oils (Radke and Welte, 1983). It is quite different from that found in the Tasmanian bitumens where the 9–methyl phenanthrene is much more abundant than the other isomers Volkman and O'Leary (1990b).

The equivalent vitrinite reflectance calculated from the MPI and MPR values were 1.0 and 1.3 (Table 1). The distributions of dimethylphenanthrenes and trimethylphenanthrenes determined from mass fragmentograms for m/z 206 and 220 respectively are shown in Fig. 6i.

Monomethyl triaromatic steroids (m/z 231) and dimethyl triaromatic steroids (m/z 245 were detected (Fig. 6j). The distributions were generally similar to those found in the museum bitumen samples (Volkman and O'Leary, 1990b), except that the relative abundance of C_{20}–C_{22} constituents (i.e. those with short side–chains) was higher, consistent with a higher level of thermal maturity.

Figure 6. GC and GC–MS data for the Florentine Valley mudstone.

(6a) Capillary gas chromatogram of the total aliphatic hydrocarbons in the Florentine Valley mudstone. Pr: pristane; Ph: phytane. n–Alkanes are denoted by n–C_X where "x" is the number of carbon atoms.

(6b). Mass fragmentograms for m/z 217 and 218 showing distribution of C_{26}–C_{30} steranes (labelled S) and diasteranes (labelled D) in Florentine Valley mudstone. See Key 1 for peak identifications.

(6c) Mass fragmentograms for m/z 217 and 218 showing distribution of C_{21}–C_{23} steranes in Florentine Valley mudstone.

(6d) Mass fragmentograms for m/z 259 showing distribution of C_{27}–C_{30} diasteranes (labelled D), and m/z 231 showing distribution of C_{28}–C_{30} 4–methyl steranes in Florentine Valley mudstone.

(6e) Mass fragmentograms for m/z 191 showing distribution of C_{27}–C_{35} hopanes and m/z 205 showing distribution of methyl hopanes in Florentine Valley mudstone. See Keys 2 and 3 for peak identifications.

(6f) Mass fragmentograms for m/z 191 showing distribution of C_{27}–C_{32} hopanes and m/z 177 showing distribution of demethylated hopanes (none present) in Florentine Valley mudstone.

(6g) Capillary gas chromatogram of the total aromatic hydrocarbons in the Florentine Valley mudstone.

(6h) Mass fragmentograms for m/z 178 and 192 showing the presence of phenanthrene and distribution of methylphenanthrenes respectively in the Florentine Valley mudstone.

(6i) Mass fragmentograms for m/z 206 and 220 showing the distribution of di– and trimethylphenanthrenes in the Florentine Valley mudstone.

(6j) Mass fragmentograms for m/z 231 and 245 showing the distribution of triaromatic steroidal hydrocarbons (with one and two methyl groups in the ABC ring system respectively) in the Florentine Valley mudstone.

Fig. 6(a)

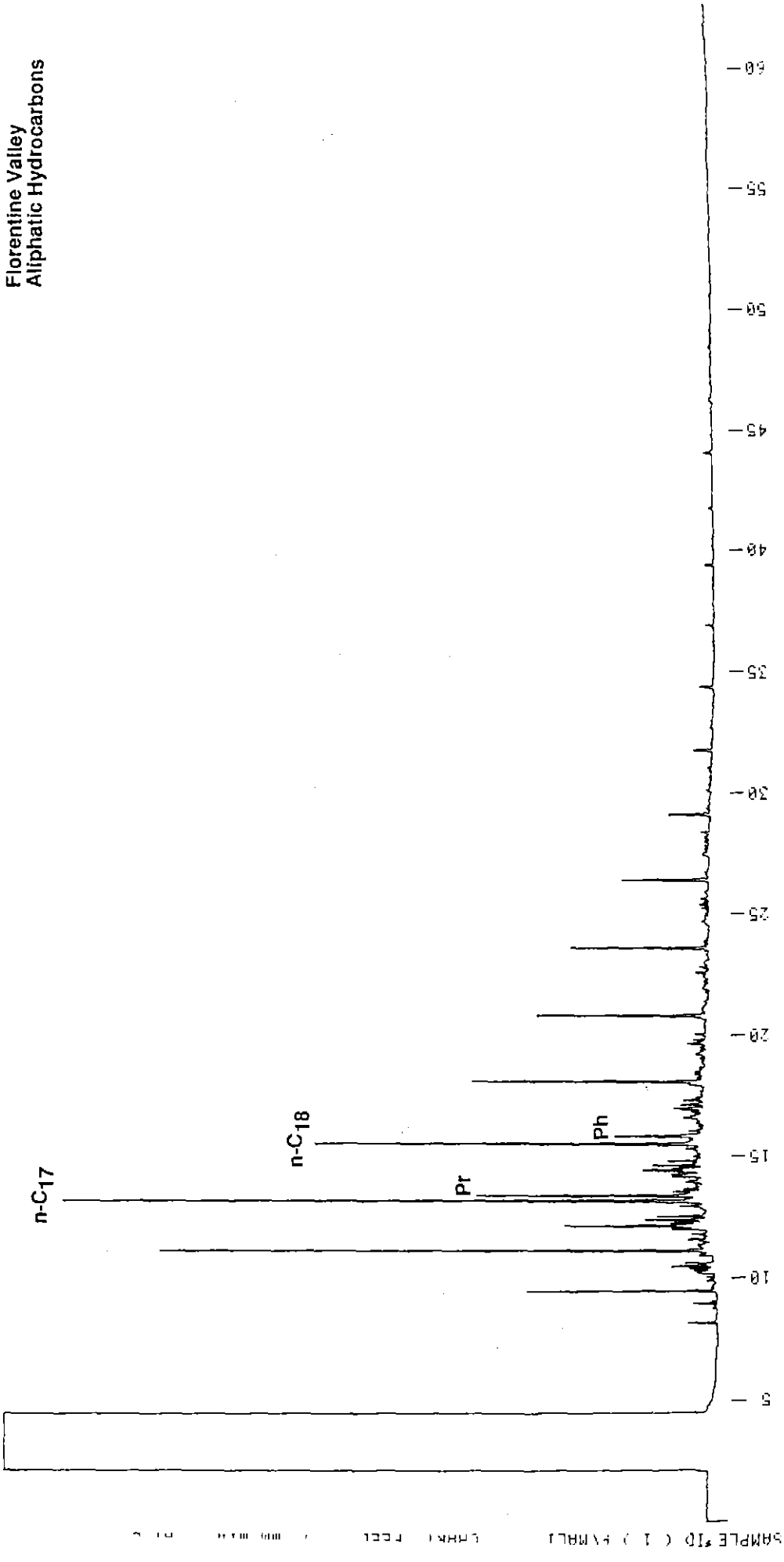

U3A

5 cm

389033

Fig. 6(b)

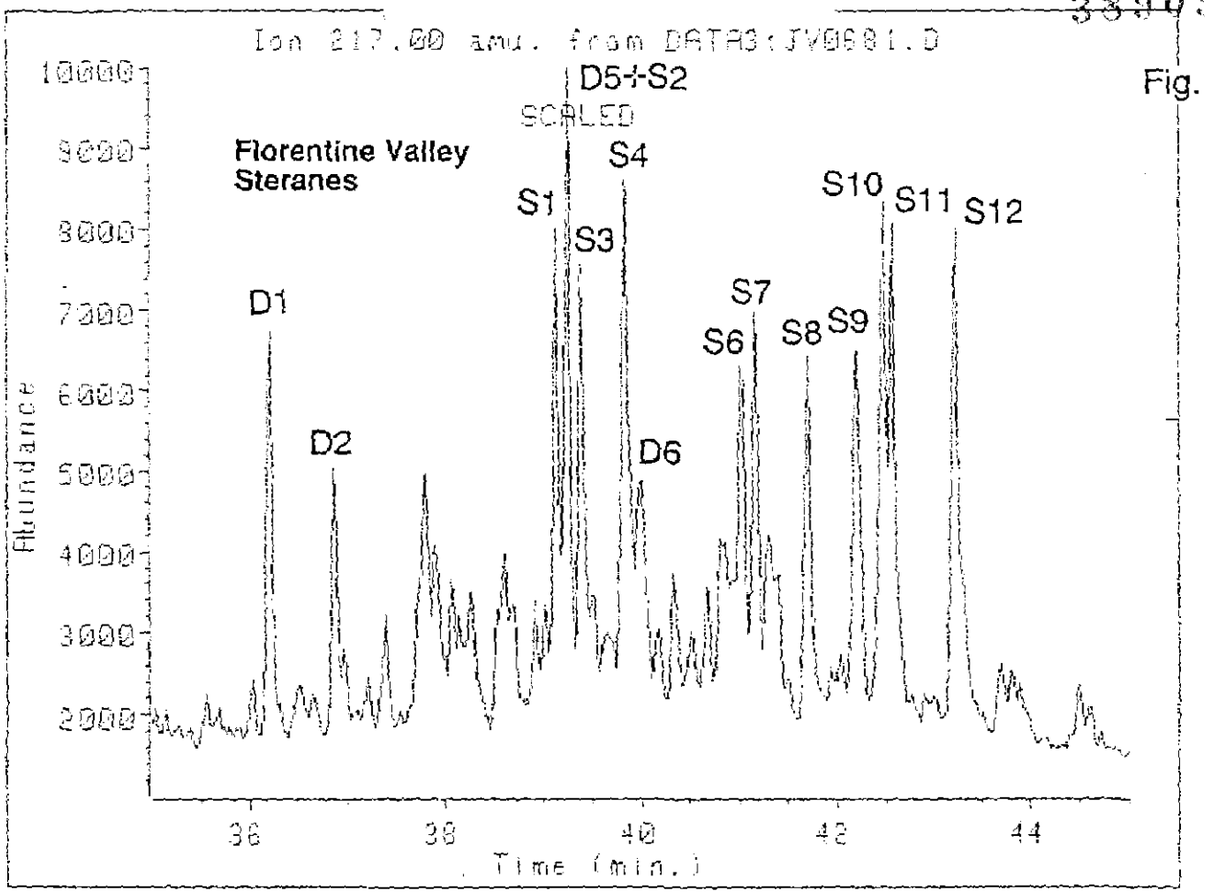

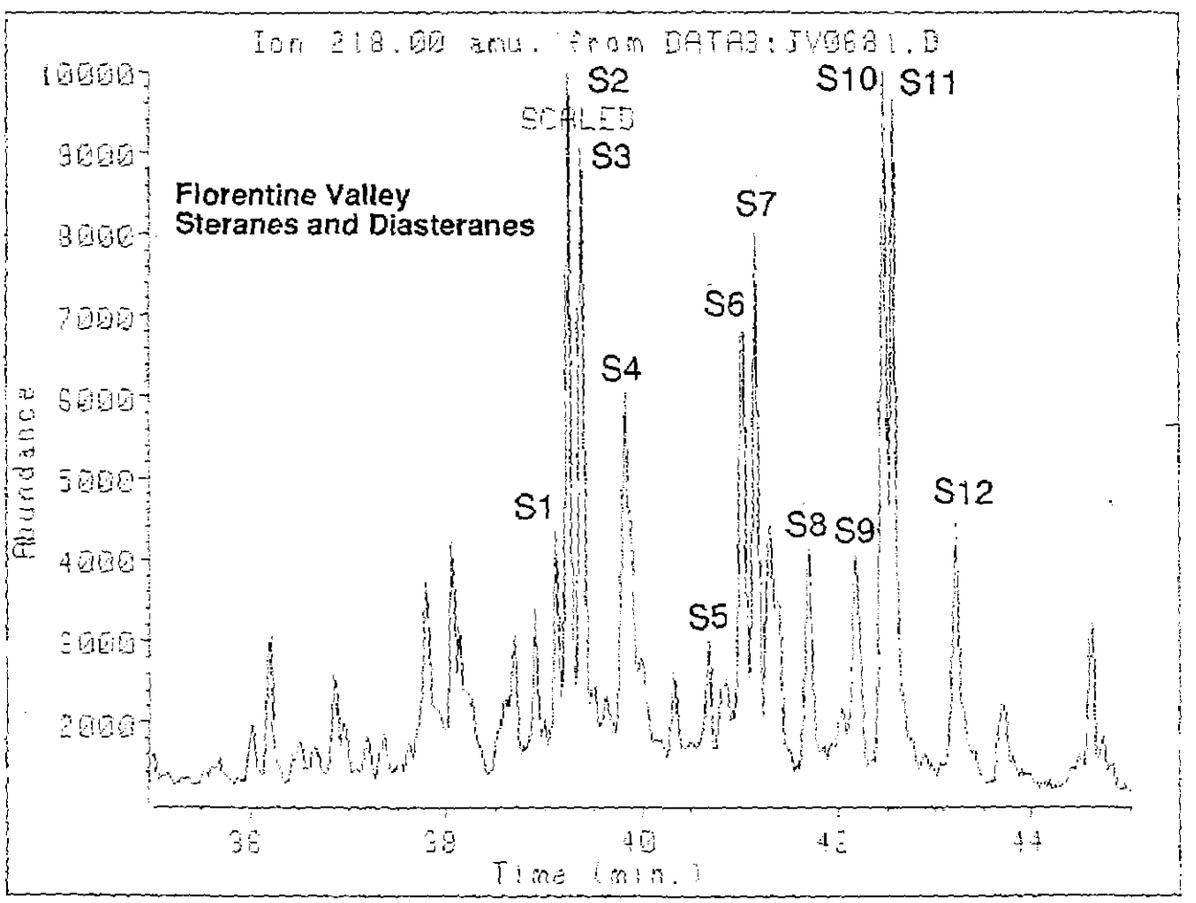

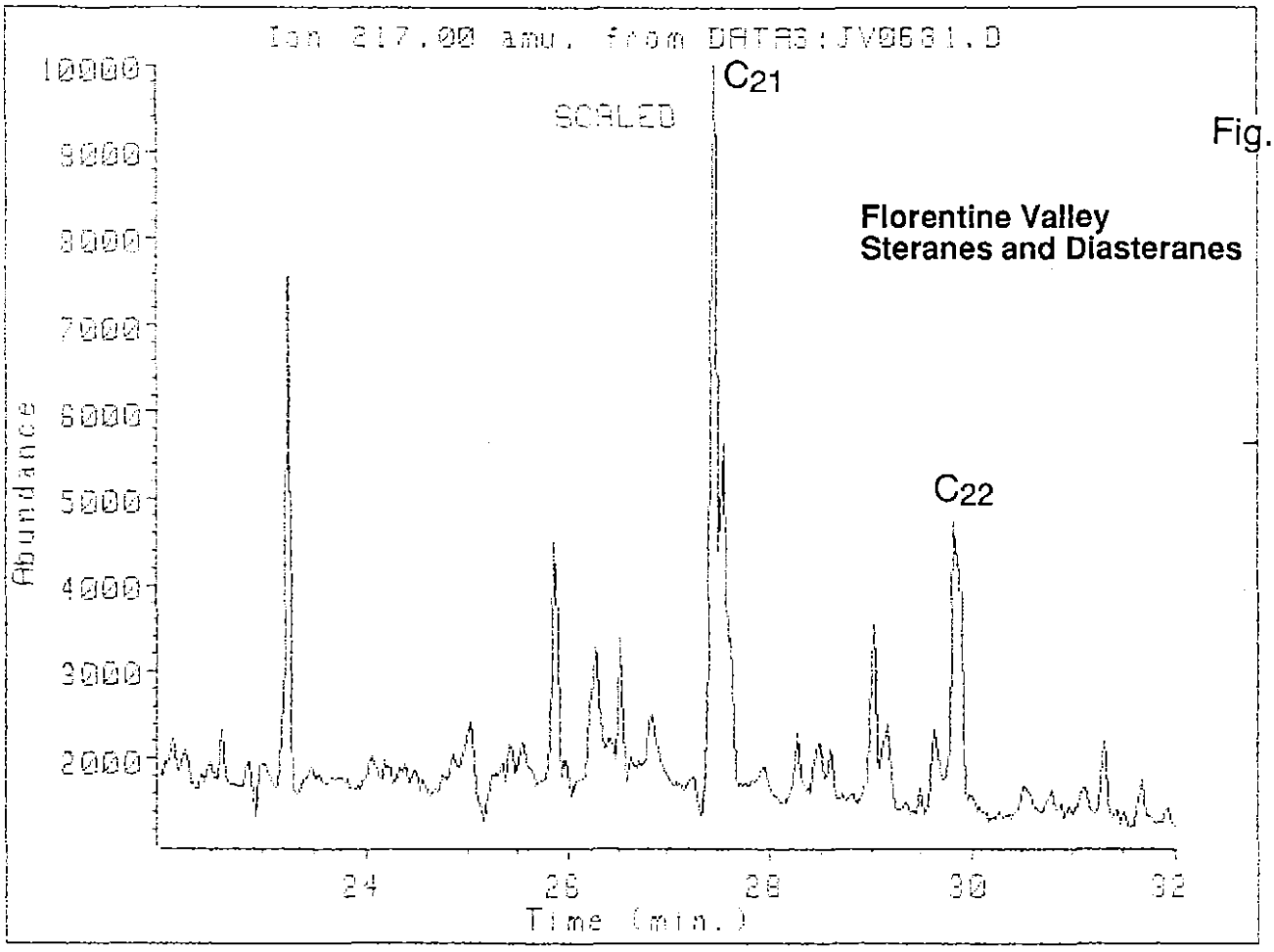
Ion 217.00 amu, from DATA3:JV0661.D
SCALED
C21
C22
Florentine Valley
Steranes and Diasteranes
Abundance
Time (min.)

Fig. 6(c)

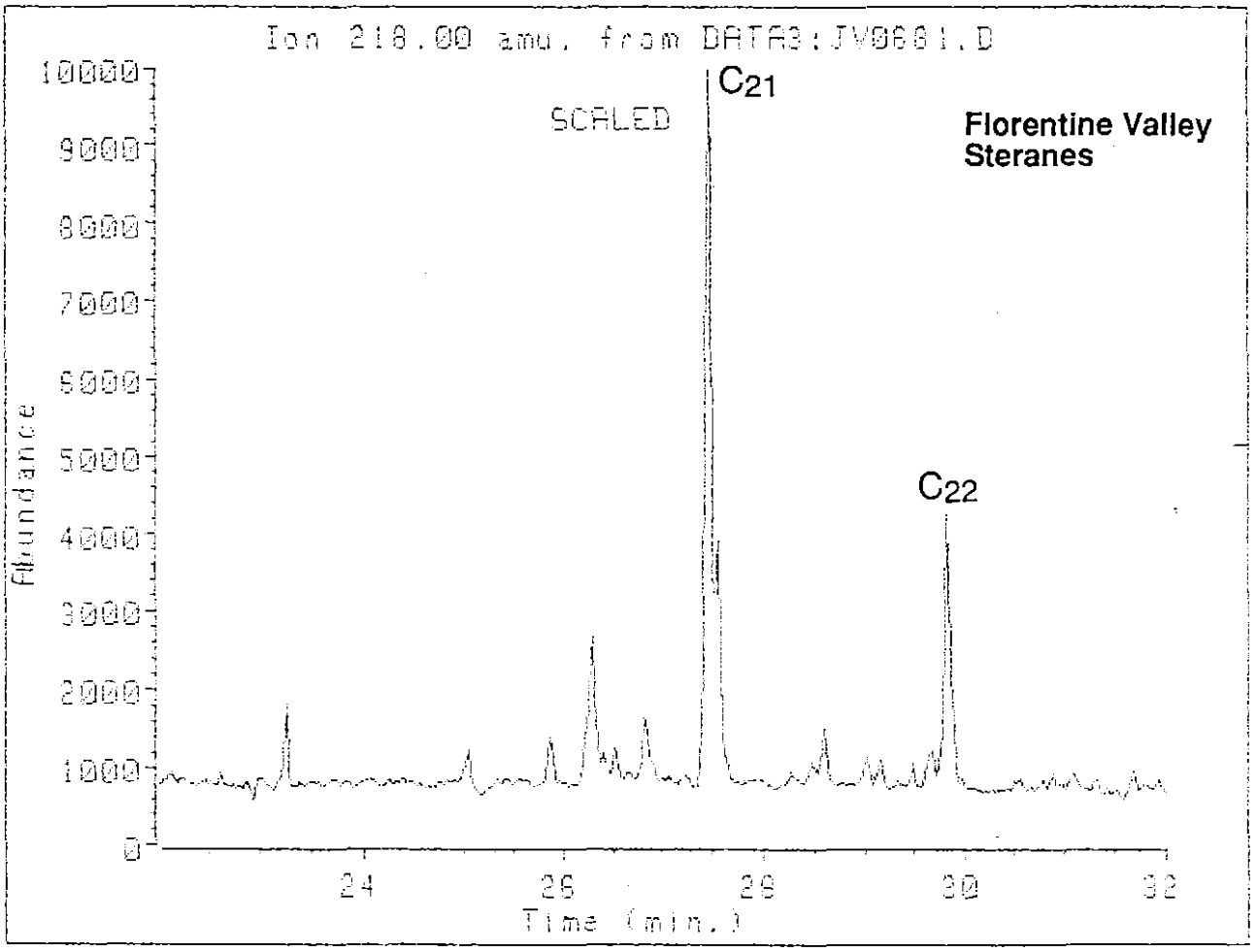
Ion 218.00 amu, from DATA3:JV0661.D
SCALED
C21
C22
Florentine Valley
Steranes
Abundance
Time (min.)

5 cm

5 cm

Fig. 6(d)

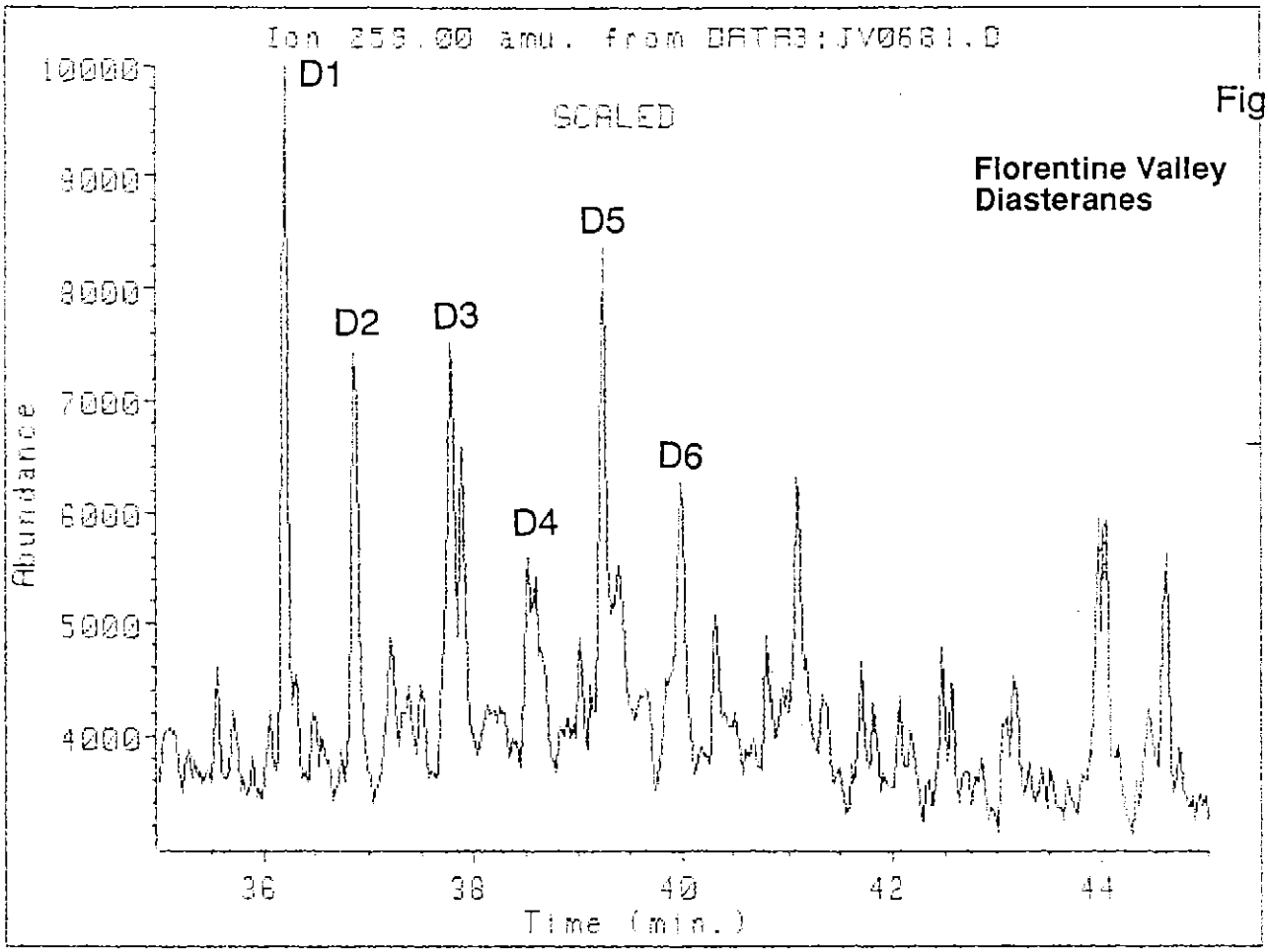
Ion 259.00 amu. from DATA3:JV0681.D
SCALED
Florentine Valley
Diasteranes
D1
D2
D3
D4
D5
D6
Abundance
10000
9000
8000
7000
6000
5000
4000
36
38
40
42
44
Time (min.)

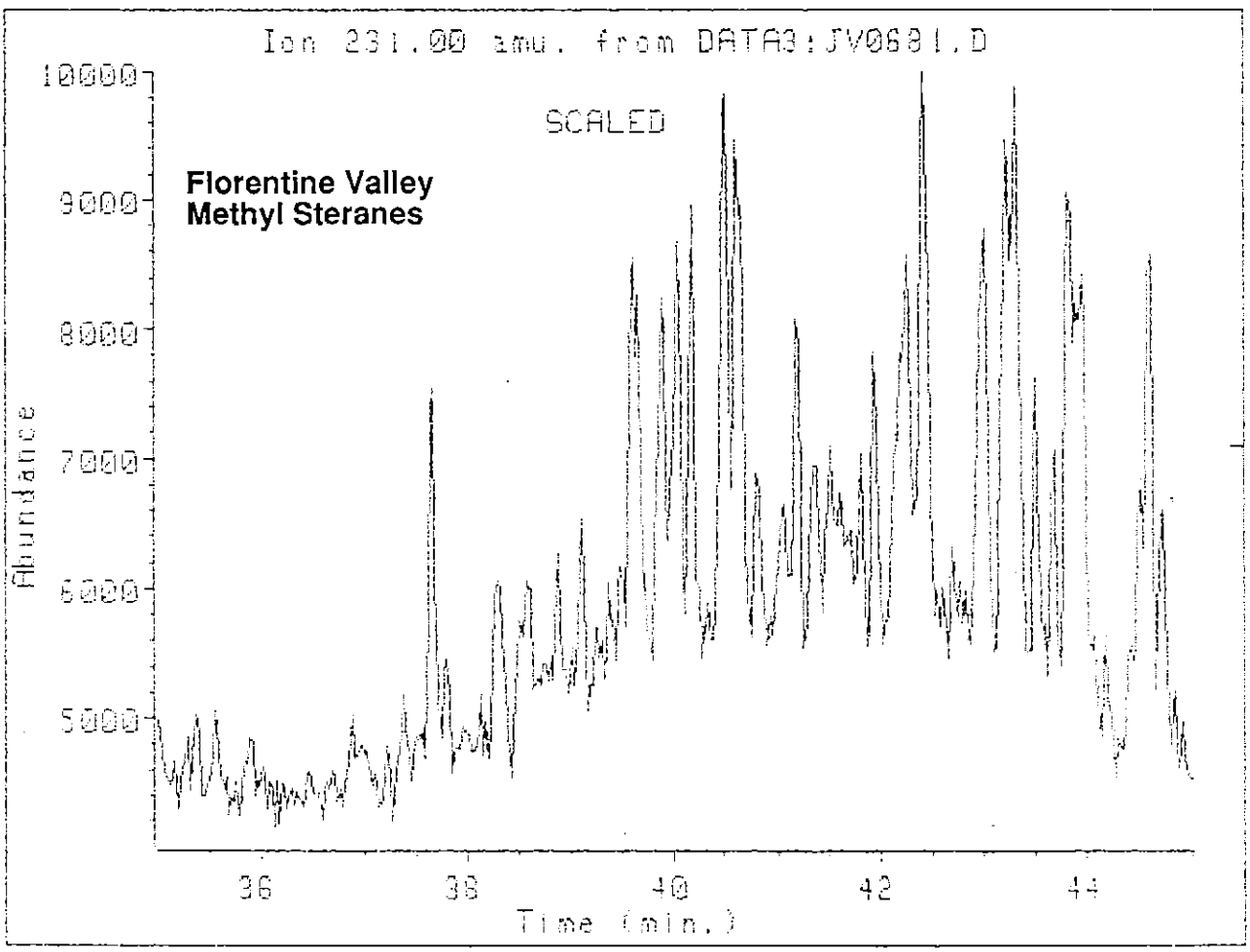
Ion 231.00 amu. from DATA3:JV0681.D
SCALED
Florentine Valley
Methyl Steranes
Abundance
10000
9000
8000
7000
6000
5000
36
38
40
42
44
Time (min.)

5 cm

Fig. 6(e)

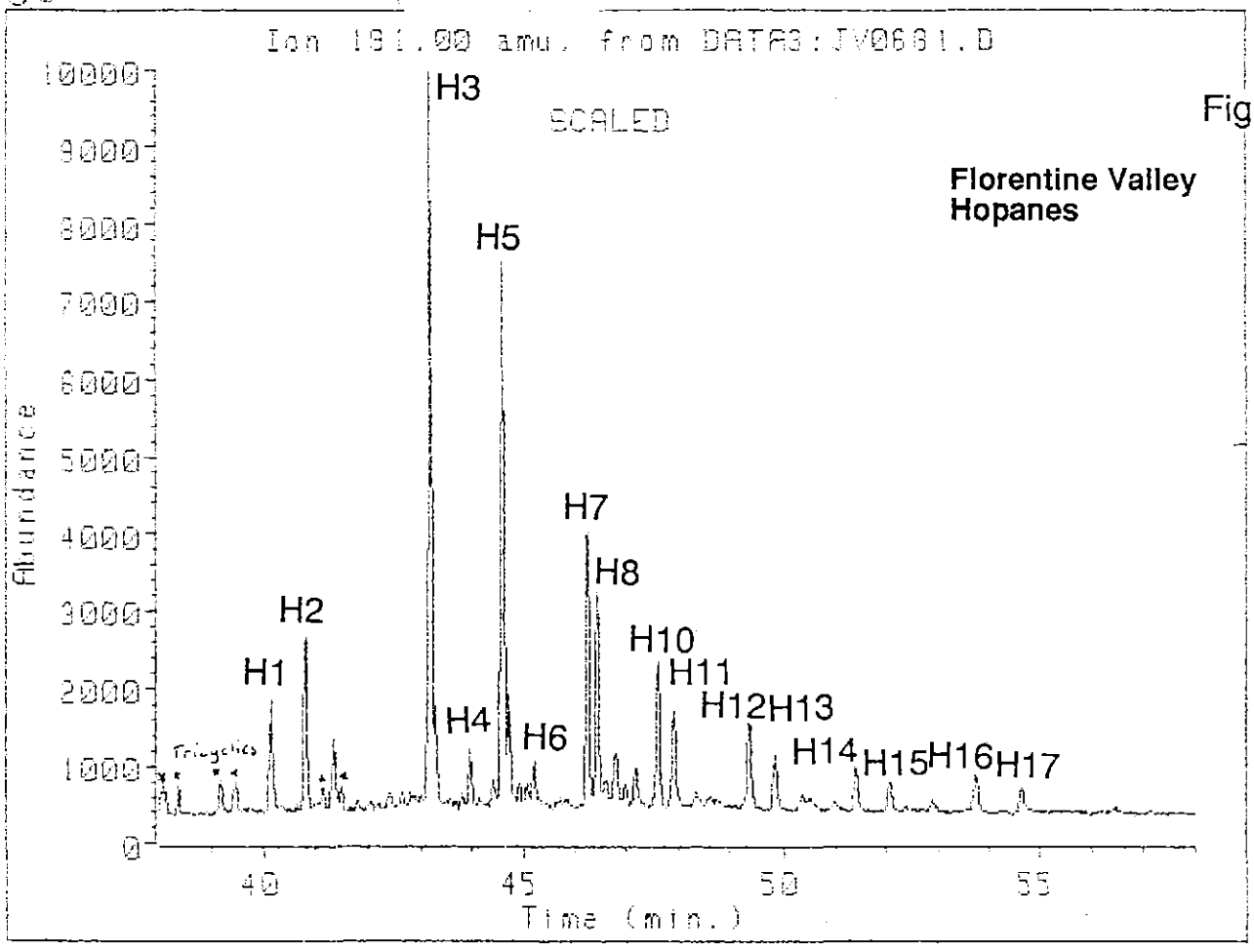
Ion 191.00 amu. from DATA3:JV0681.D
SCALED
Florentine Valley
Hopanes
H1
H2
H3
H4
H5
H6
H7
H8
H10
H11
H12
H13
H14
H15
H16
H17
Abundance
Time (min.)

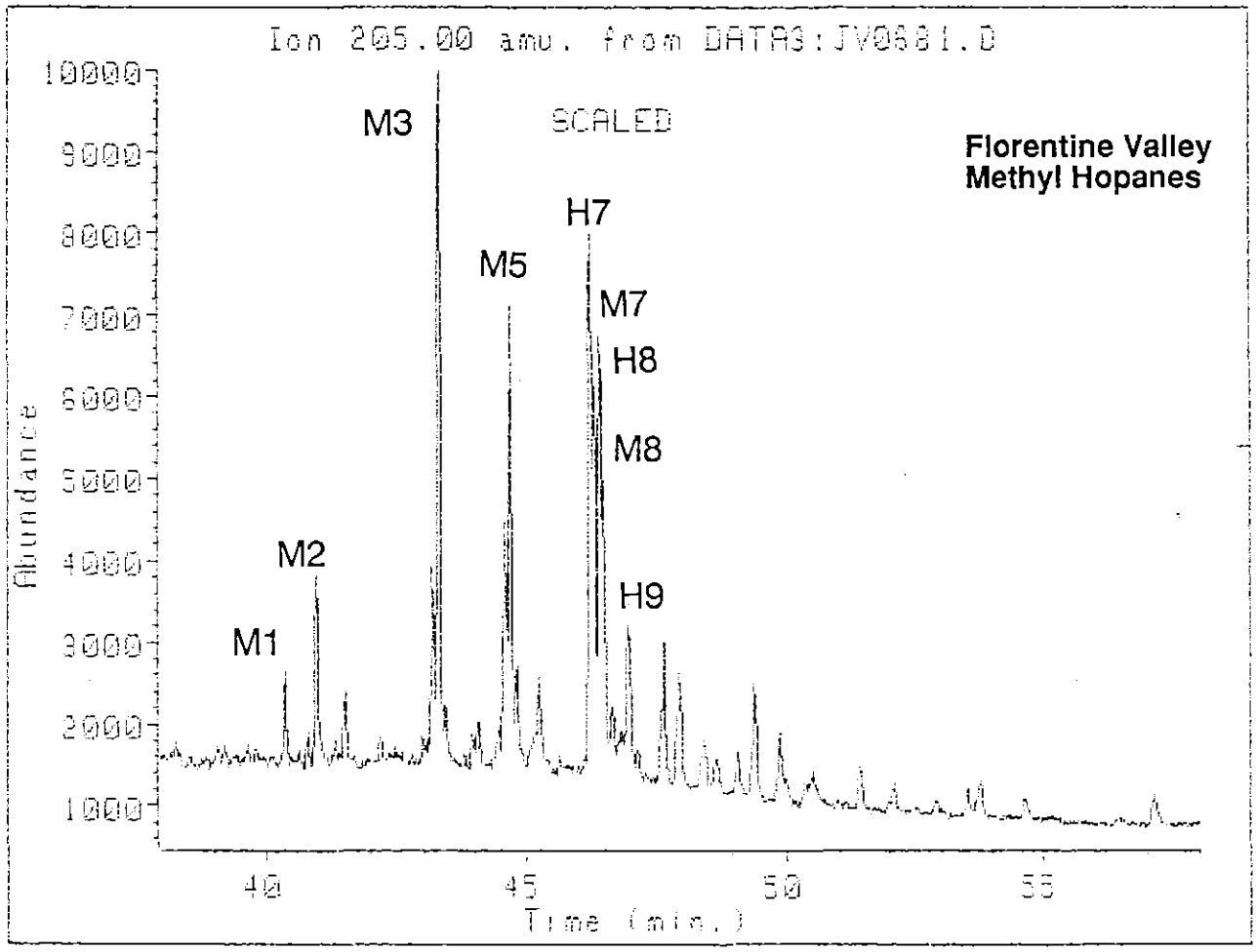
Ion 205.00 amu. from DATA3:JV0681.D
SCALED
Florentine Valley
Methyl Hopanes
M1
M2
M3
M5
H7
M7
H8
M8
H9
Abundance
Time (min.)

5 cm

Fig. 6(f)

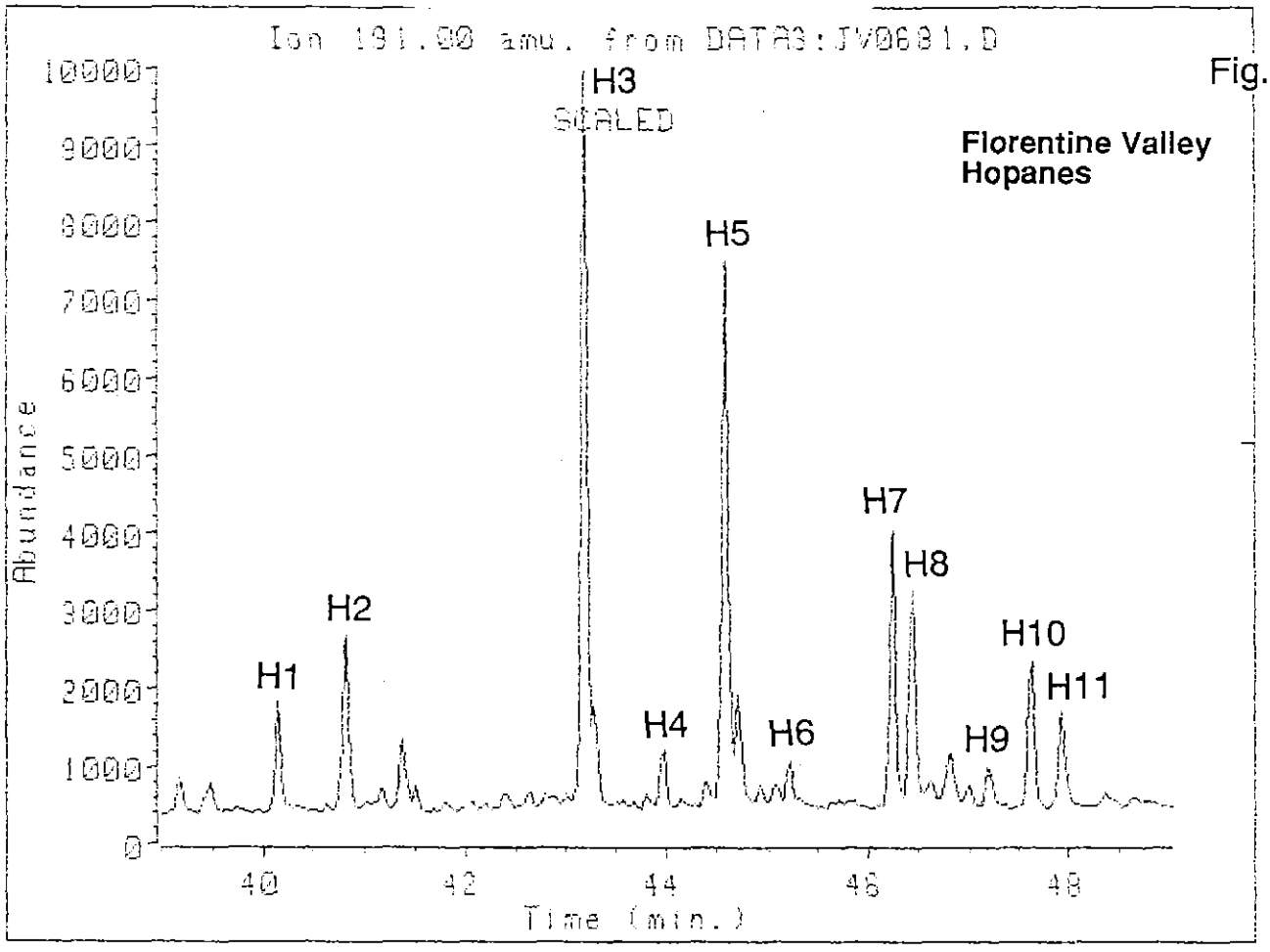
Ion 191.00 amu. from DATA3:JV0681.D
H3
SCALED
Florentine Valley
Hopanes
H5
H7
H8
H10
H11
H2
H1
H4
H6
H9
Abundance
10000
9000
8000
7000
6000
5000
4000
3000
2000
1000
0
40
42
44
46
48
Time (min.)

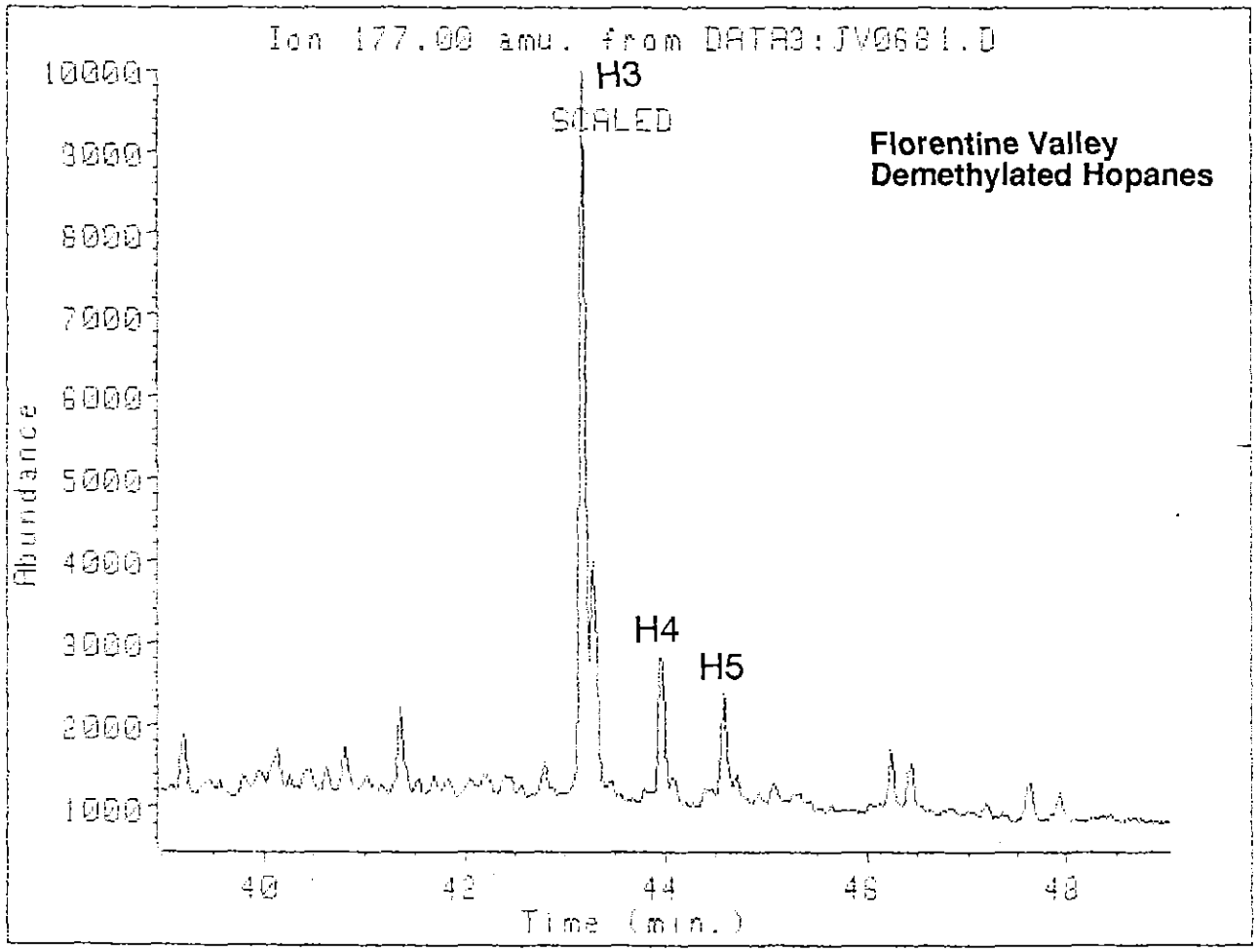
Ion 177.00 amu. from DATA3:JV0681.D
H3
SCALED
Florentine Valley
Demethylated Hopanes
H4
H5
Abundance
10000
9000
8000
7000
6000
5000
4000
3000
2000
1000
40
42
44
46
48
Time (min.)

Fig. 6(g)

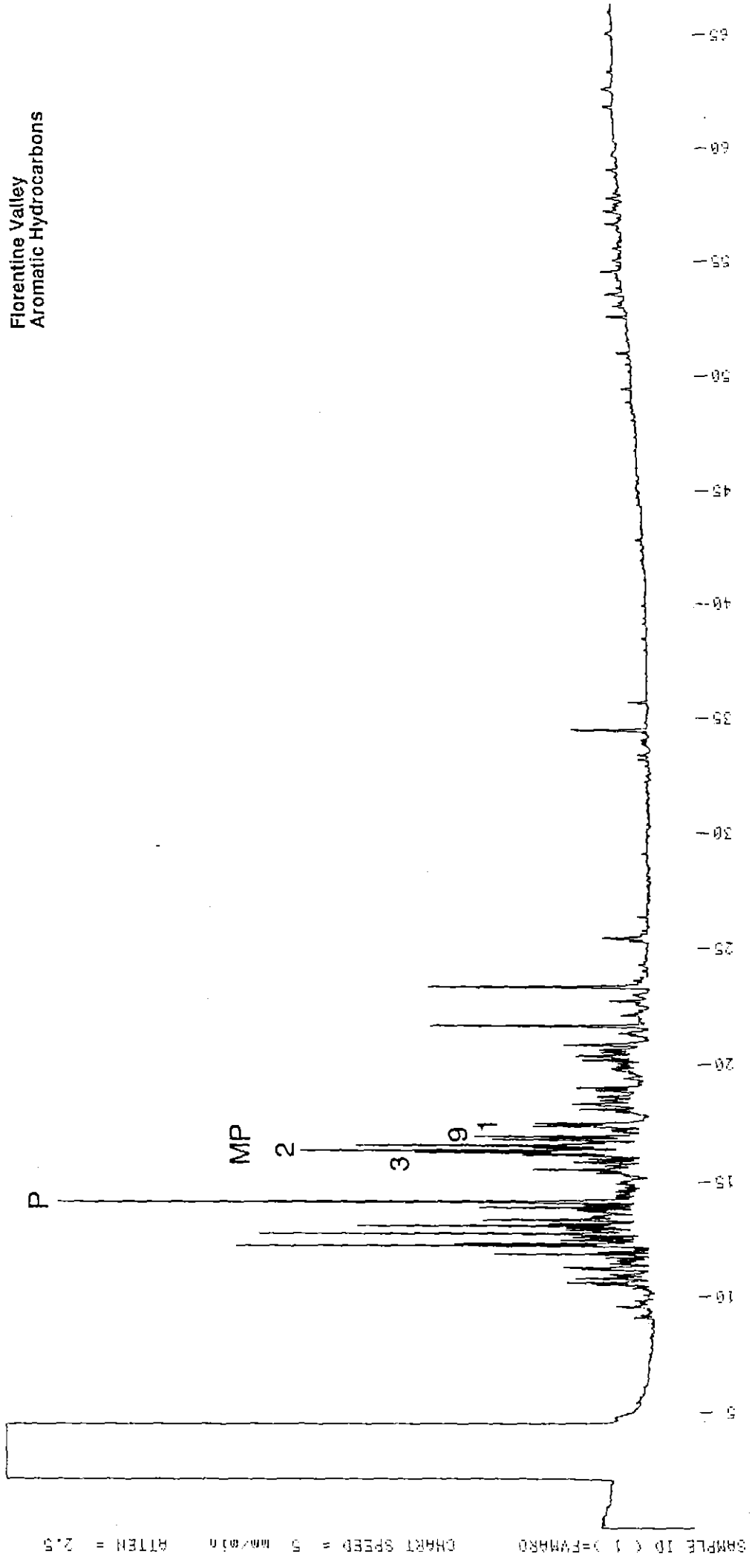
Florentine Valley
Aromatic Hydrocarbons
P
MP
2
3
9
1
65
60
55
50
45
40
35
30
25
20
15
10
5
SAMPLE ID (1)=FVAHRO
CHART SPEED = 5 mm/min
ATTEN = 2.5

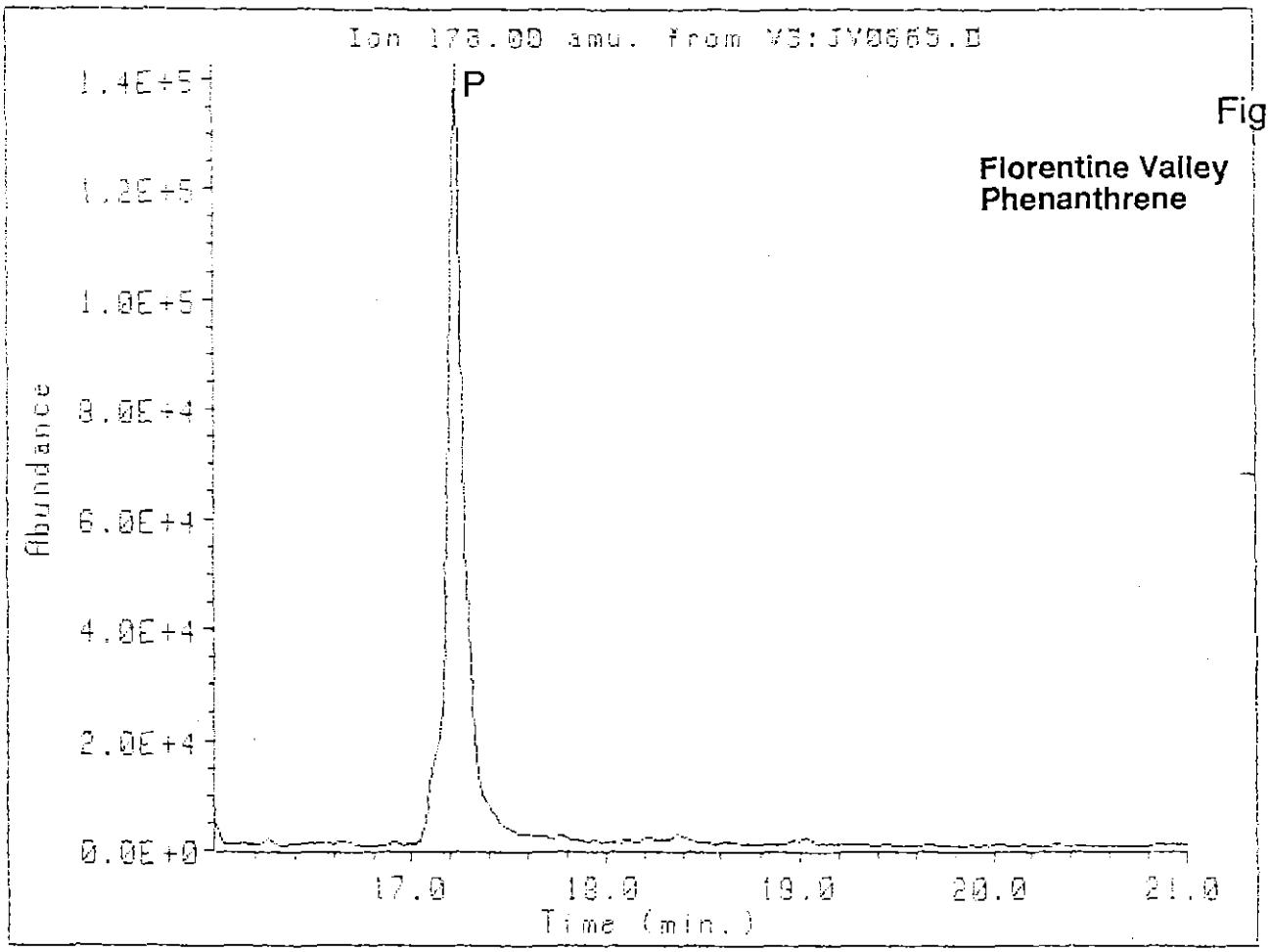
Ion 178.00 amu. from V3:JV0665.D
P
Florentine Valley
Phenanthrene
Abundance
1.4E+5
1.2E+5
1.0E+5
8.0E+4
6.0E+4
4.0E+4
2.0E+4
0.0E+0
17.0
18.0
19.0
20.0
21.0
Time (min.)

Fig. 6(h)

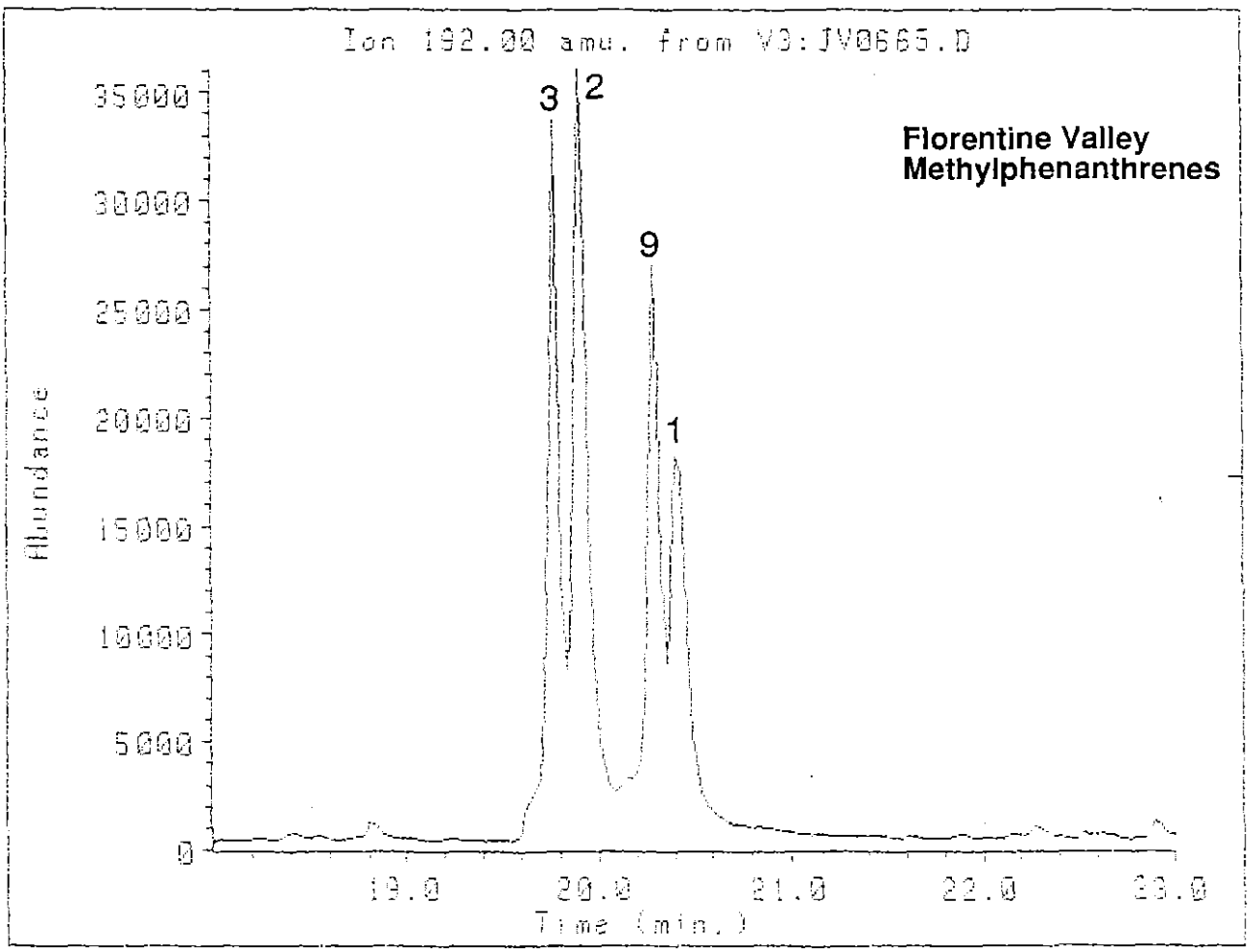
Ion 192.00 amu. from V3:JV0665.D
3
2
9
1
Florentine Valley
Methylphenanthrenes
Abundance
35000
30000
25000
20000
15000
10000
5000
0
19.0
20.0
21.0
22.0
23.0
Time (min.)

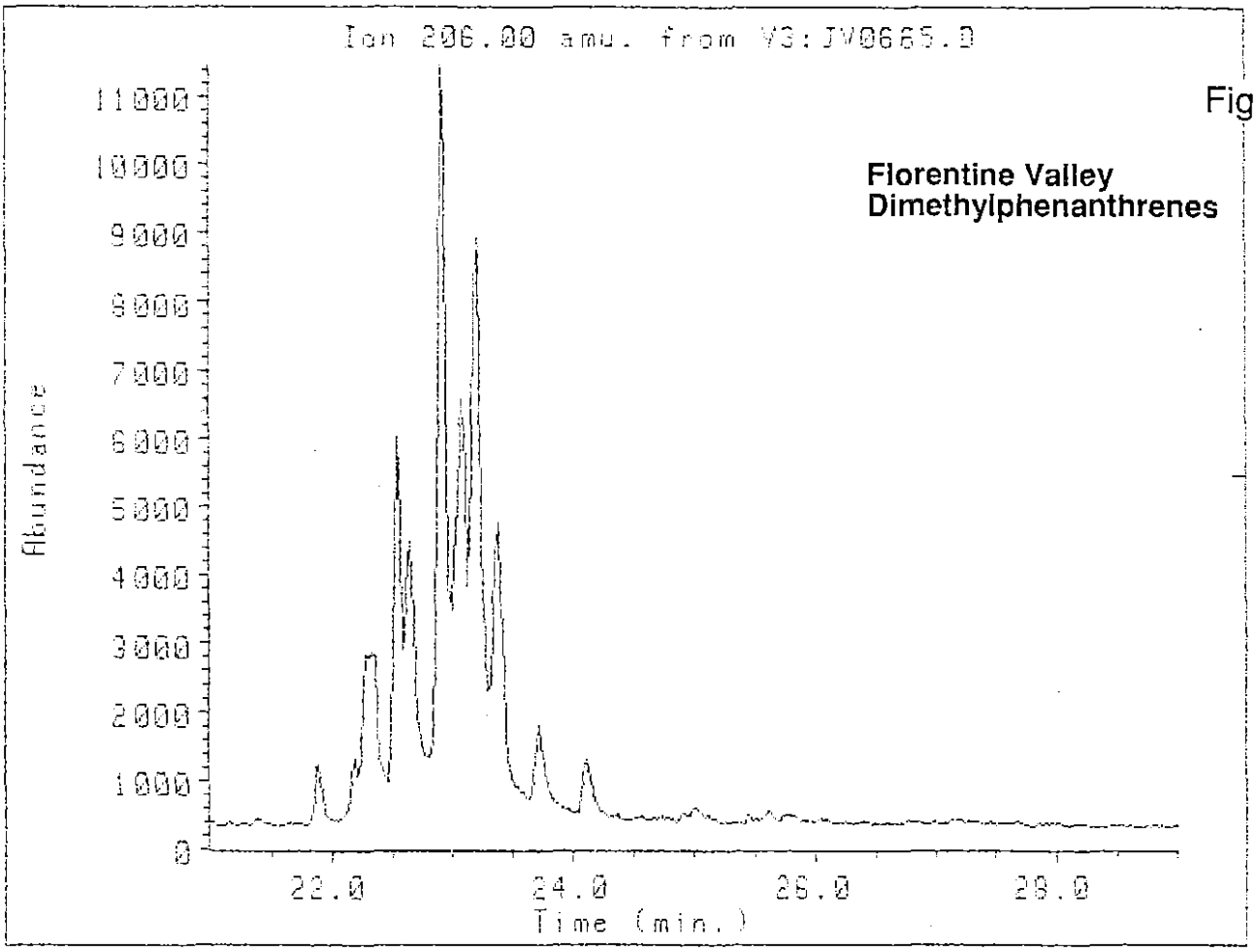
Ion 206.00 amu. from V3:JV0665.D
Florentine Valley
Dimethylphenanthrenes
Abundance
11000
10000
9000
8000
7000
6000
5000
4000
3000
2000
1000
0
22.0
24.0
26.0
28.0
Time (min.)

Fig. 6(i)

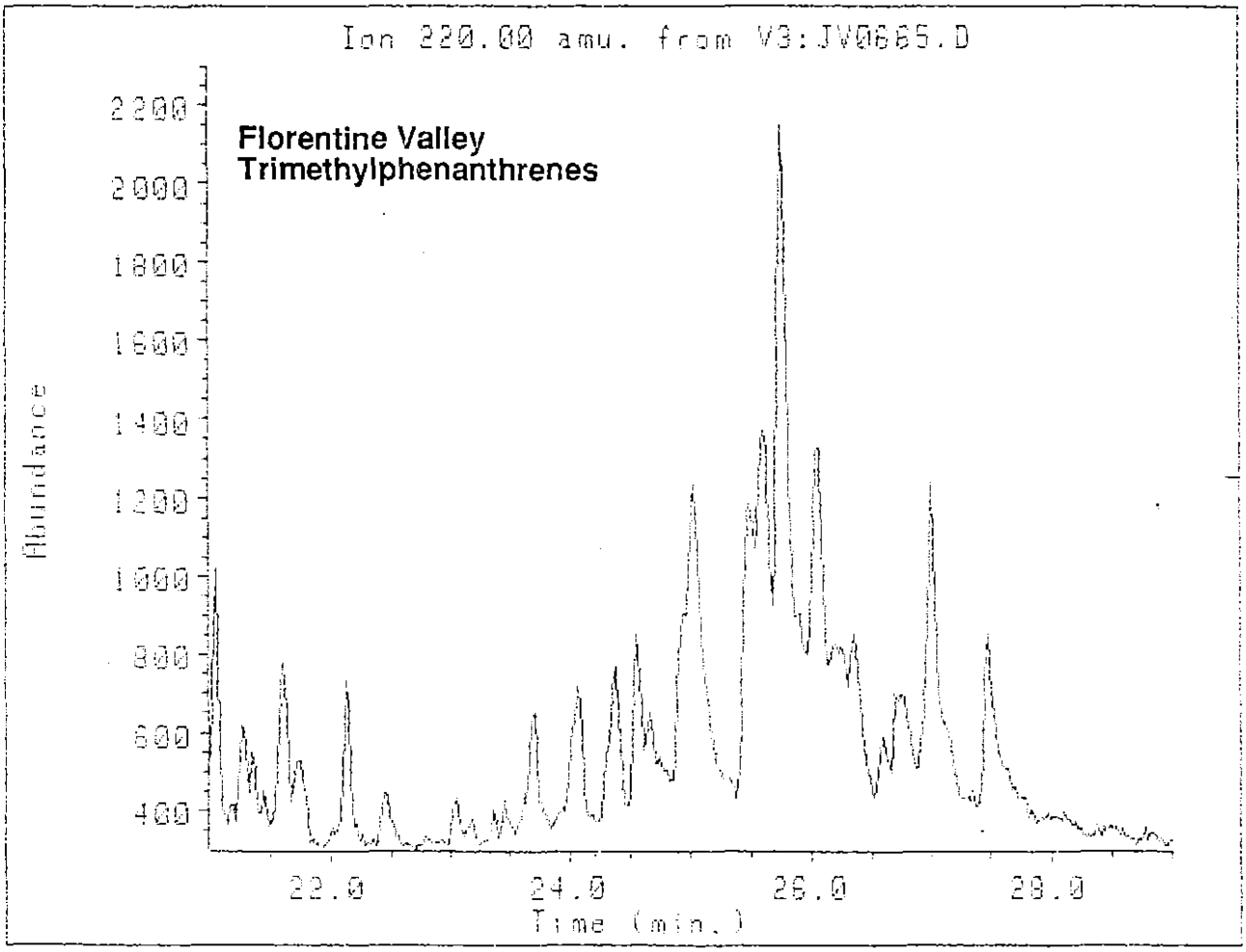
Ion 220.00 amu. from V3:JV0665.D
Florentine Valley
Trimethylphenanthrenes
Abundance
2200
2000
1800
1600
1400
1200
1000
800
600
400
22.0
24.0
26.0
28.0
Time (min.)

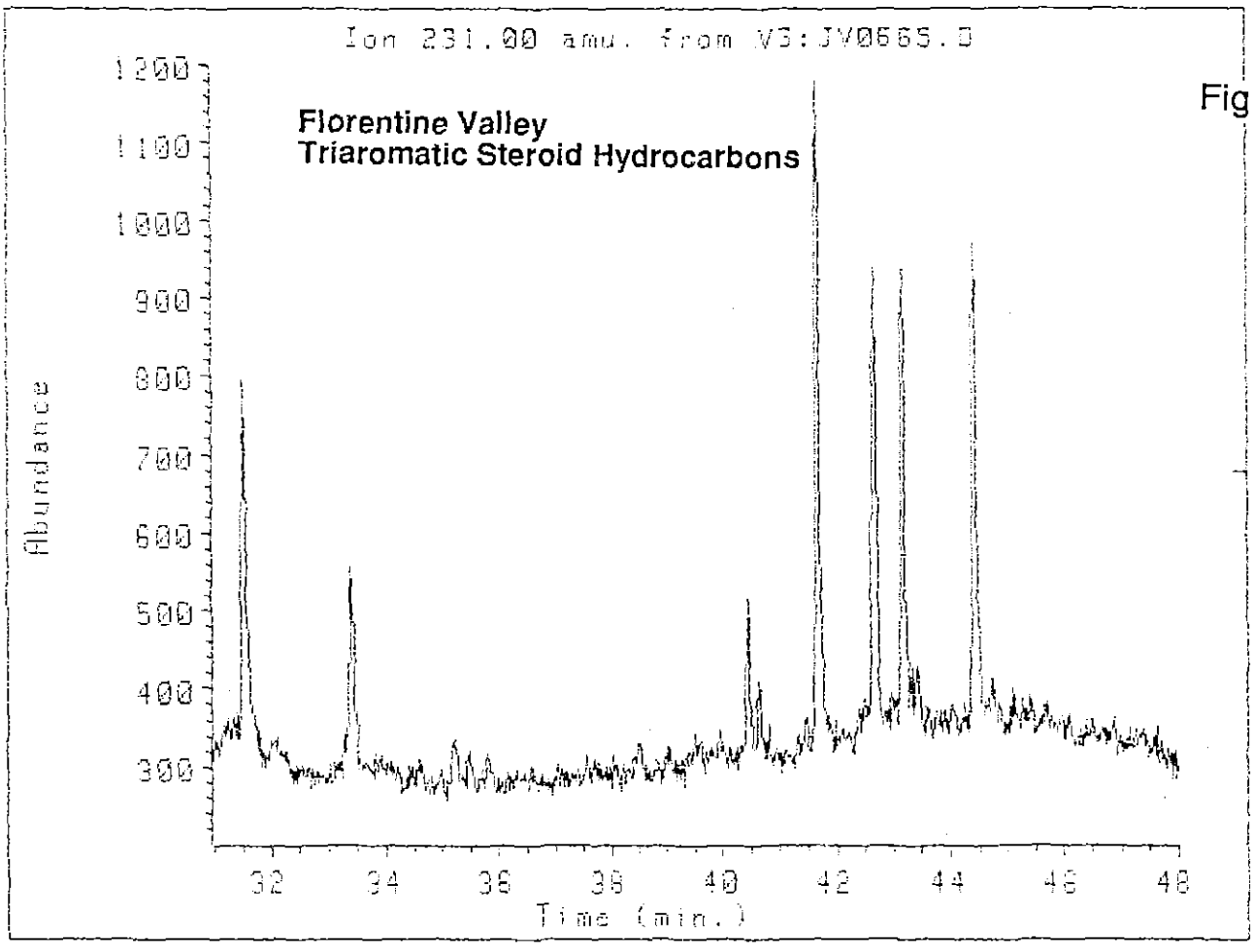
Ion 231.00 amu. from V3:JV0665.D
Florentine Valley
Triaromatic Steroid Hydrocarbons
Abundance
1200
1100
1000
900
800
700
600
500
400
300
32
34
36
38
40
42
44
46
48
Time (min.)

Fig. 6(j)

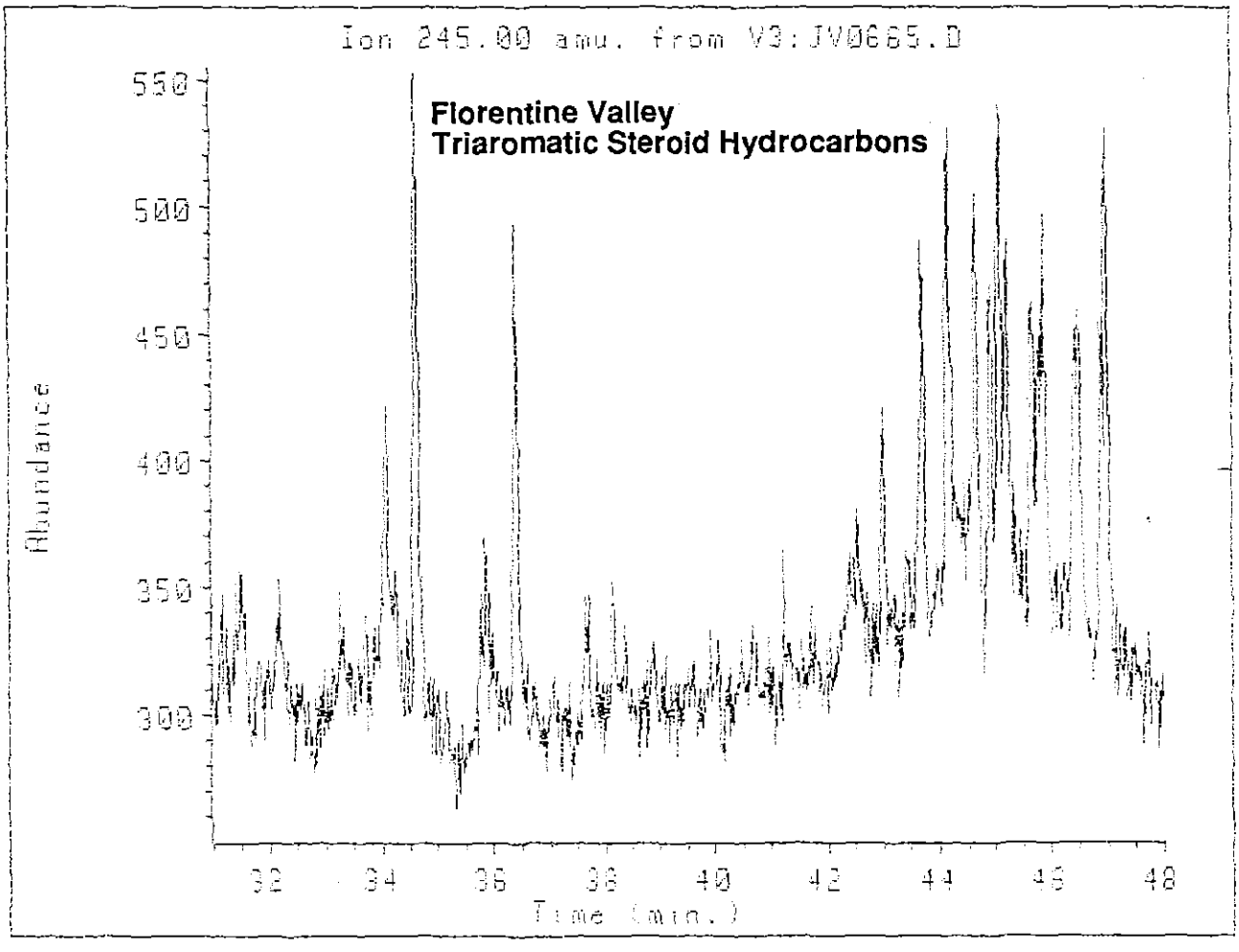
Ion 245.00 amu. from V3:JV0665.D
Florentine Valley
Triaromatic Steroid Hydrocarbons
Abundance
550
500
450
400
350
300
32
34
36
38
40
42
44
46
48
Time (min.)

3. *Tars from South Bruny Island and Tunnack, Tasmania.*

The Bruny Island sample was a black, brittle tar found on weathered sandstone on South Bruny Island. Aliphatic hydrocarbons were very minor constituents of the solvent extract and represented only 0.23% of the total extract. Aromatic hydrocarbons comprised 38.6% of the extract with asphaltenes and resins comprising the bulk of the samples (61.1%).

The sample from Tunnack consisted of black bituminous organic matter dispersed throughout a medium-grained sandstone. Solvent extractable material represented 8.5% of the sediment. Aliphatic hydrocarbons comprised only 0.42% of the total extract, aromatic hydrocarbons 40.7% with most of the extractable material being resins and asphaltenes (58.8%). The sand grains fell apart once the tar had been extracted, suggesting that the oil had seeped into unconsolidated sand.

Aliphatic hydrocarbons

The aliphatic C_{15+} hydrocarbons (Fig. 7a) of the Bruny Island sample showed a very strong predominance of n-alkanes extending to about n-C_{35}. The major constituents were n-C_{16} and n-C_{18}. There was a strong predominance of even chain-lengths below n-C_{20}, but there was no odd or even predominance above n-C_{22}. A series of n-alkenes from n-C_{14} to n-C_{26} was also present. This distribution is most unlike that found in crude oils or mature sediments. Alkenes are commonly found when organic matter is pyrolysed at high temperatures. Pristane and phytane were relatively minor components; the pristane/phytane ratio was 2.8, which is suggestive of an oxic depositional environment for the source rock, and the n-C_{17}/pristane ratio was 4.1.

The distribution of aliphatic hydrocarbons in the Tunnack sample was remarkably similar (Fig. 8a) to those in the Bruny Island tar, as were the aliphatic and aromatic biomarker distributions. The descriptions provided below apply to both samples.

(a) Steranes: The sterane distributions (m/z 217 and m/z 218; Figs. 7b and 8b) were quite unusual. C_{29} steranes were in greatest abundant, with C_{27} and C_{28} steranes present in approximately equal amounts. Diasteranes were significant constituents (m/z 259; Fig. 7d and 8d), with C_{29} components predominating as in the steranes.

Sterane maturity parameters suggest that the organic matter was much less mature than hydrocarbons found in the Ordovician limestones. C_{29} $\alpha\beta\beta$ sterane isomers (peaks S10 and S11) are less than half as intense in the m/z 217 mass fragmentograms as $\alpha\alpha\alpha$ isomers (peaks S9 and S12), and the ratio of 20S and 20R isomers is still slightly in favour of the 20R biological isomer.

Hopanes: Hopane distributions as represented by mass fragmentograms of the major fragment ion m/z 191 from C_{27} to C_{35} are shown in Fig. 7e and 8e. The distributions from C_{27}–C_{32} are shown in Fig. 7f and 8f..

The major peak in the hopane distribution is that due to C_{30}, with the C_{29} hopane peak only slightly less abundant. Moretanes (peaks H4, H6 and H9) were fairly significant constituents, which is typical of the hydrocarbons found in immature sediments. Extended hopanes were quite minor constituents, with C_{35} hopanes only present in trace amounts.

(i) In the extended hopanes (i.e. >C_{30}), the 22S/22R epimer ratio (peaks H7 and H8) indicates that the two isomers have reached equilibrium, but note that this can occur well before the oil window. (ii) The moretane (peaks H4, H6 and H9) abundances are still high compared with 17α(H),21β(H)–hopanes of the same chain–length (peaks H3, H5 and H7/H8). (iii) The ratio of the two C_{27} hopanes Ts (peak H1) and Tm (peak H2) is a sensitive indicator of thermal maturity. The Ts/Tm ratio is 0.06, which indicates quite an immature sample.

Tricyclic alkanes: Although very minor constituents, peaks can be discerned in the m/z 191 mass fragmentogram (Figs. 7e and 8e). These samples are clearly unrelated to the Tasmanite oil shale.

Methyl hopanes: Both tars contain small amounts of 2-methyl hopanes as shown by the m/z 205 mass fragmentogram (Figs. 7e and 8e). Methyl hopanes are slightly more abundant relative to hopanes in the Tunnack sample than in the tar from Bruny Island. The methyl hopane to hopane ratio is about half that found in the Ordovician carbonates (Fig. 5). Extended methyl hopanes were barely detectable, in common with the hopane distributions.

Demethylated hopanes: The m/z 177 mass fragmentogram (Figs. 7f and 8f) indicated that C-10 demethylated hopanes are not present.

These aliphatic biomarker distributions match very closely data reported for two tars collected near Bridgewater (Volkman and Holdsworth, 1989). These tars were considered not to have been derived from *in-situ* seepage.

Aromatic Hydrocarbons

The aromatic hydrocarbon distributions in both samples were most unusual and quite unlike those commonly found in crude oils. TLC-FID analyses suggested that the aromatic compounds were mostly more polar than naphthalenes and phenanthrenes. A very strong red band was noted during column chromatography, and so the aromatic hydrocarbon fraction was split into several sub-fractions. Fraction 1 corresponded to aromatics less polar than the red band (e.g. phenanthrenes) and was eluted with 10 mL of hexane:toluene (1:1); Fraction 2 which was more orange in colour was eluted with a further 10 mL of hexane:toluene (1:3) ; Fraction 3 was eluted with 5 mL of chloroform and included the red band itself. More polar material was then eluted with chloroform and

methanol. In the Tunnack sample, Fraction 1 was collected in two halves; Fraction 1A consisted of simple aromatics while Fraction 1B was enriched in more polar compounds. Gas chromatograms of the various fractions are shown in Figs. 7g and 8g.

The distribution in Fraction 1 from Bruny Island is most unusual and shows a remarkably strong predominance of phenanthrene, and two major compounds eluting after 20 minutes which were identified as the polycyclic aromatic hydrocarbons fluoranthene and pyrene.

Fraction 2 was found to consist of more polar polycyclic aromatic hydrocarbons. A very similar distribution of compounds was reported for two tars from Bridgewater (Volkman and Holdsworth, 1989). Such distributions are commonly found in street dust and road bitumens.

Phenanthrene and alkylated phenanthrenes: Phenanthrene was the major constituent of the total aromatic hydrocarbon fraction. Alkyl naphthalenes and methyl phenanthrenes were considerably less abundant. Mass fragmentograms for m/z 178 (phenanthrene) and 192 (methylphenanthrenes) are shown in Figs. 7h and 8h. The peak immediately after phenanthrene was tentatively identified as anthracene. The 2- and 3-methylphenanthrene isomers were more abundant than the 1- and 9-methylphenanthrene isomers. This is the reverse of that found in the museum bitumens (Volkman and O'Leary, 1990b), and rather similar to that found in mature oils (Radke and Welte, 1983). Similar distributions (although with isomer ratios reversed in each pair), were found in carbonates from Surprise Bay and Ida Bay analysed by AMDEL (1987).

The equivalent vitrinite reflectance calculated from the MPI values was 0.5 for both samples. However, this low value is due to the high strong predominance of phenanthrene. The MPR values suggest an equivalent vitrinite reflectance of about 1.0 for both tars (Table 1). The distributions of dimethylphenanthrenes and trimethylphenanthrenes determined from mass fragmentograms for m/z 206 and 220 respectively are shown in Fig. 7i. The

apparently high maturity indicated by the MPR ratio seems at odds with the consistently lower maturities inferred from the aliphatic biomarkers.

A limited GC–MS search was made for aromatic steroids in both samples. Peaks were detected in the m/z 231 and m/z 245 mass fragmentograms used to fingerprint monomethyl triaromatic steroids (m/z 231) and dimethyl triaromatic steroids (m/z 245), but the distributions bore no resemblance to those commonly found in sediments or oils. No peaks were found corresponding to authentic triaromatic steroids (Figs. 7j and 8j).

Figure 7. GC and GC–MS data for the South Bruny Island tar.

(7a) Capillary gas chromatogram of the total aliphatic hydrocarbons in the South Bruny Island tar. Pr: pristane; Ph: phytane. n–Alkanes are denoted by n–C_X where "x" is the number of carbon atoms.

(7b). Mass fragmentograms for m/z 217 and 218 showing distribution of C_{26}–C_{30} steranes (labelled S) and diasteranes (labelled D) in the South Bruny Island tar. See Key 1 for peak identifications.

(7c) Mass fragmentograms for m/z 217 and 218 showing distribution of C_{21}–C_{23} steranes in the South Bruny Island tar.

(7d) Mass fragmentograms for m/z 259 showing distribution of C_{27}–C_{30} diasteranes (labelled D), and m/z 231 showing distribution of C_{28}–C_{30} 4–methyl steranes in the South Bruny Island tar.

(7e) Mass fragmentograms for m/z 191 showing distribution of C_{27}–C_{35} hopanes and m/z 205 showing distribution of methyl hopanes in the South Bruny Island tar. See Keys 2 and 3 for peak identifications.

(7f) Mass fragmentograms for m/z 191 showing distribution of C_{27}–C_{32} hopanes and m/z 177 showing distribution of demethylated hopanes (none present) in the South Bruny Island tar.

(7g) Capillary gas chromatogram of the aromatic hydrocarbon subfractions in the South Bruny Island tar (see text).

(7h) Mass fragmentograms for m/z 178 and 192 showing the presence of phenanthrene and distribution of methylphenanthrenes respectively in the South Bruny Island tar.

(7i) Mass fragmentograms for m/z 206 and 220 showing the distribution of di– and trimethylphenanthrenes in the South Bruny Island tar.

(7j) Mass fragmentograms for m/z 231 and 245 showing the distribution of triaromatic steroidal hydrocarbons (with one and two methyl groups in the ABC ring system respectively) in the South Bruny Island tar.

Fig. 7(a)

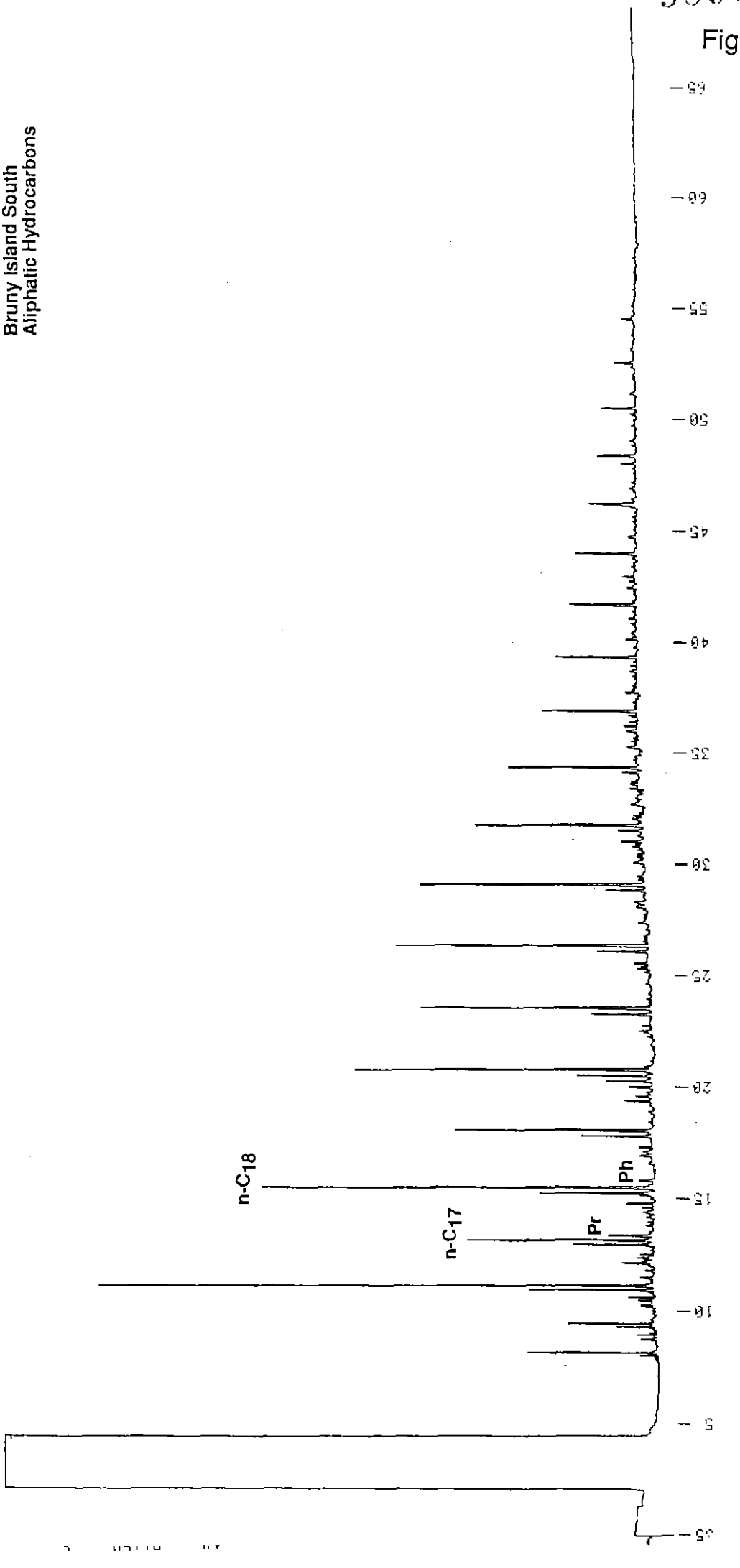

5 cm

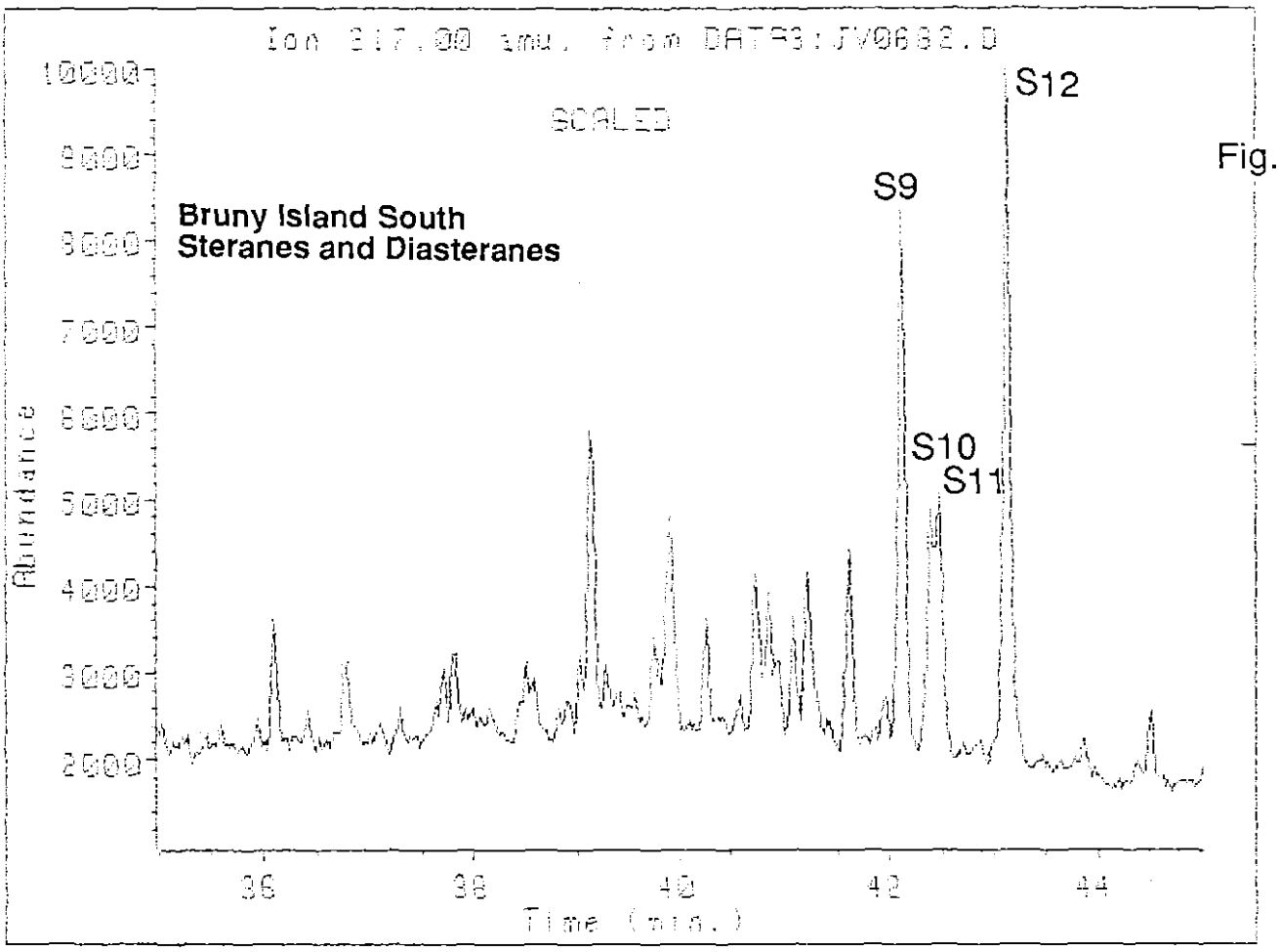
Ion 217.00 amu. from DATA3:JV0682.D
SCALED
Bruny Island South
Steranes and Diasteranes
S9
S12
S10
S11
Abundance
Time (min.)

Fig. 7(b)

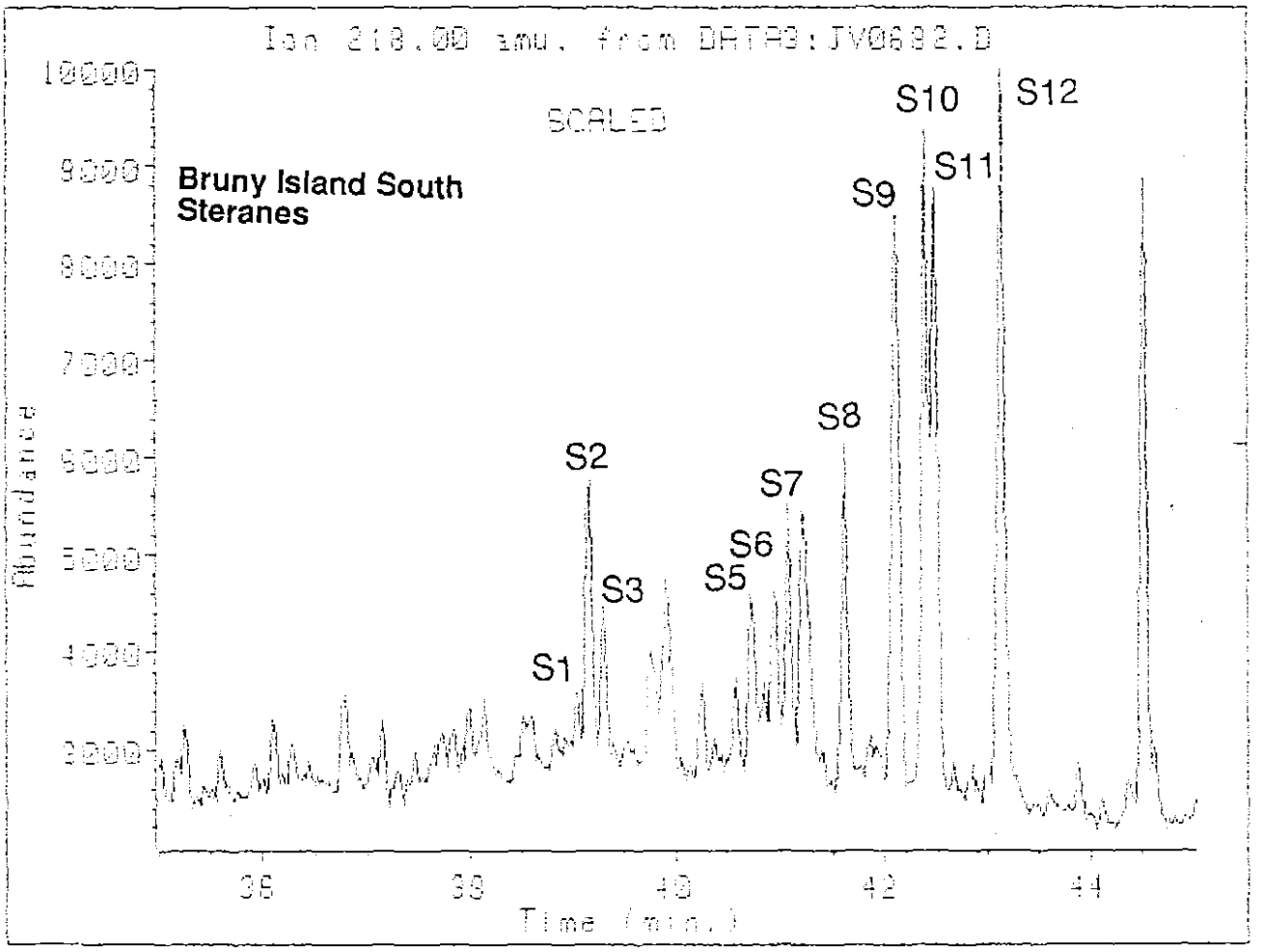
Ion 218.00 amu. from DATA3:JV0682.D
SCALED
Bruny Island South
Steranes
S1
S2
S3
S5
S6
S7
S8
S9
S10
S11
S12
Abundance
Time (min.)

5 cm

Fig. 7(c)

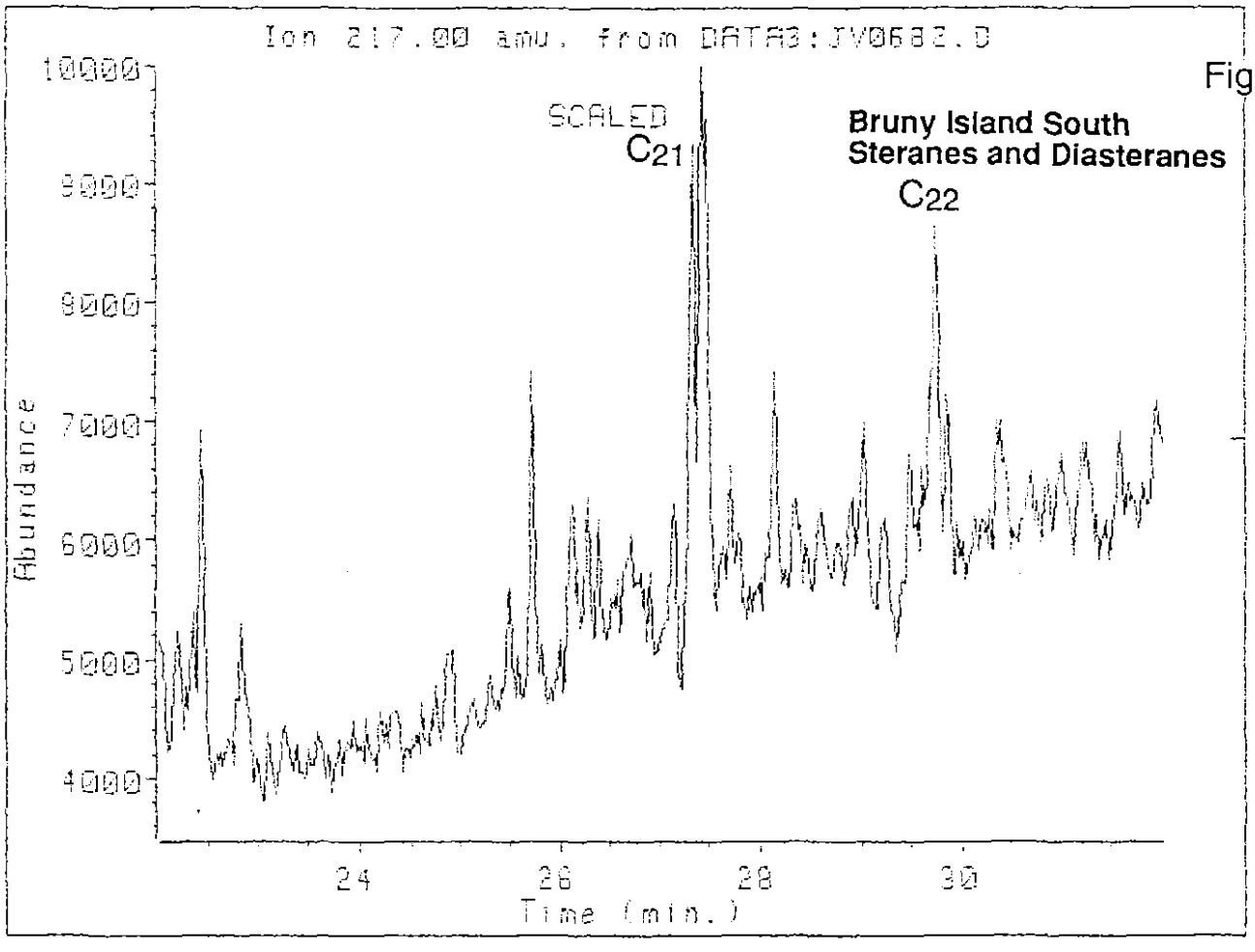
Ion 217.00 amu. from DATA3:JV0582.D
SCALED
C21
Bruny Island South
Steranes and Diasteranes
C22
Abundance
10000
9000
8000
7000
6000
5000
4000
24
26
28
30
Time (min.)

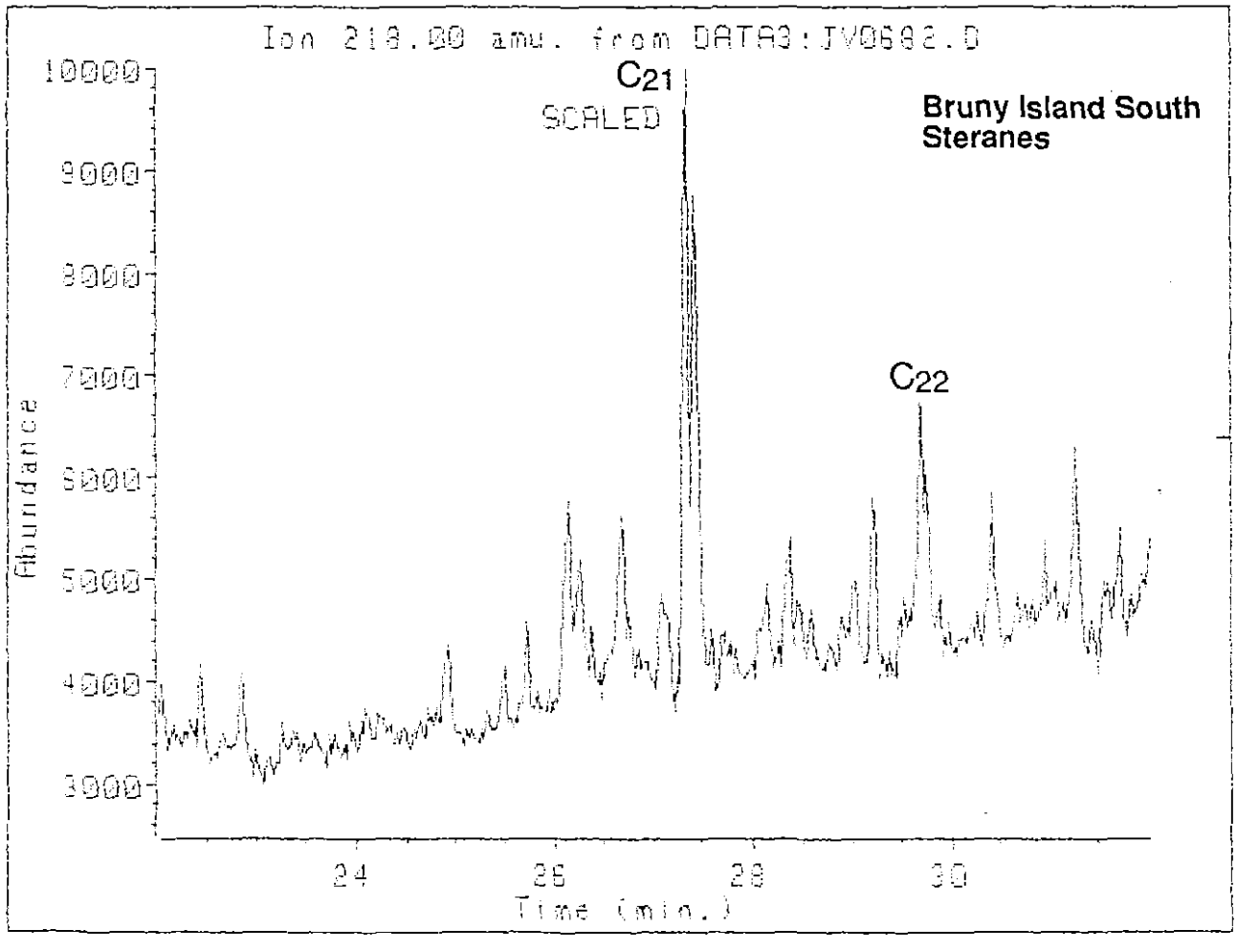
Ion 218.00 amu. from DATA3:JV0582.D
C21
SCALED
Bruny Island South
Steranes
C22
Abundance
10000
9000
8000
7000
6000
5000
4000
3000
24
26
28
30
Time (min.)

5 cm

Fig. 7(d)

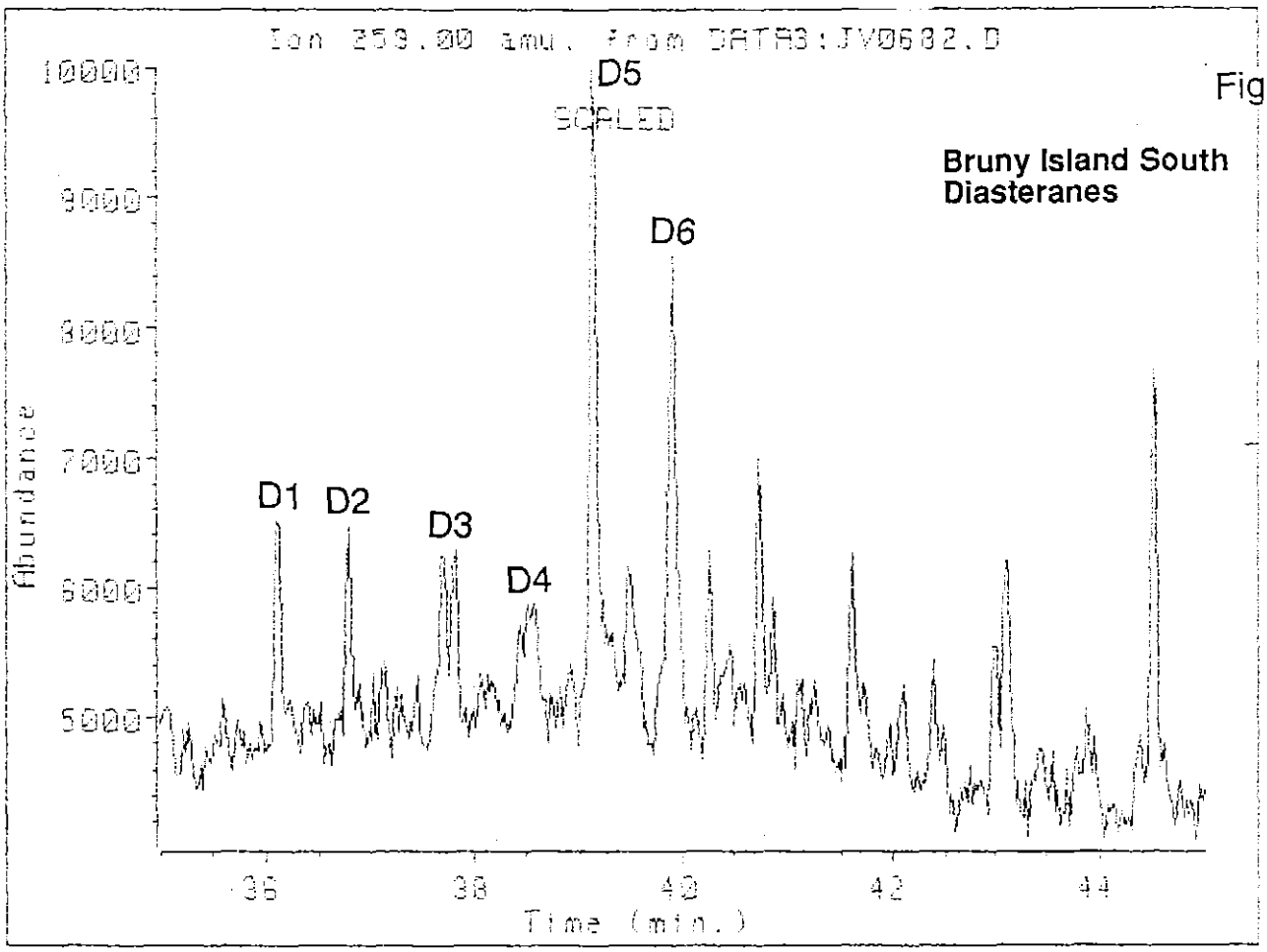
Ion 259.00 amu. from DATA3:JV0682.D
SCALED
Bruny Island South
Diasteranes
D1
D2
D3
D4
D5
D6
Abundance
10000
9000
8000
7000
6000
5000
36
38
40
42
44
Time (min.)

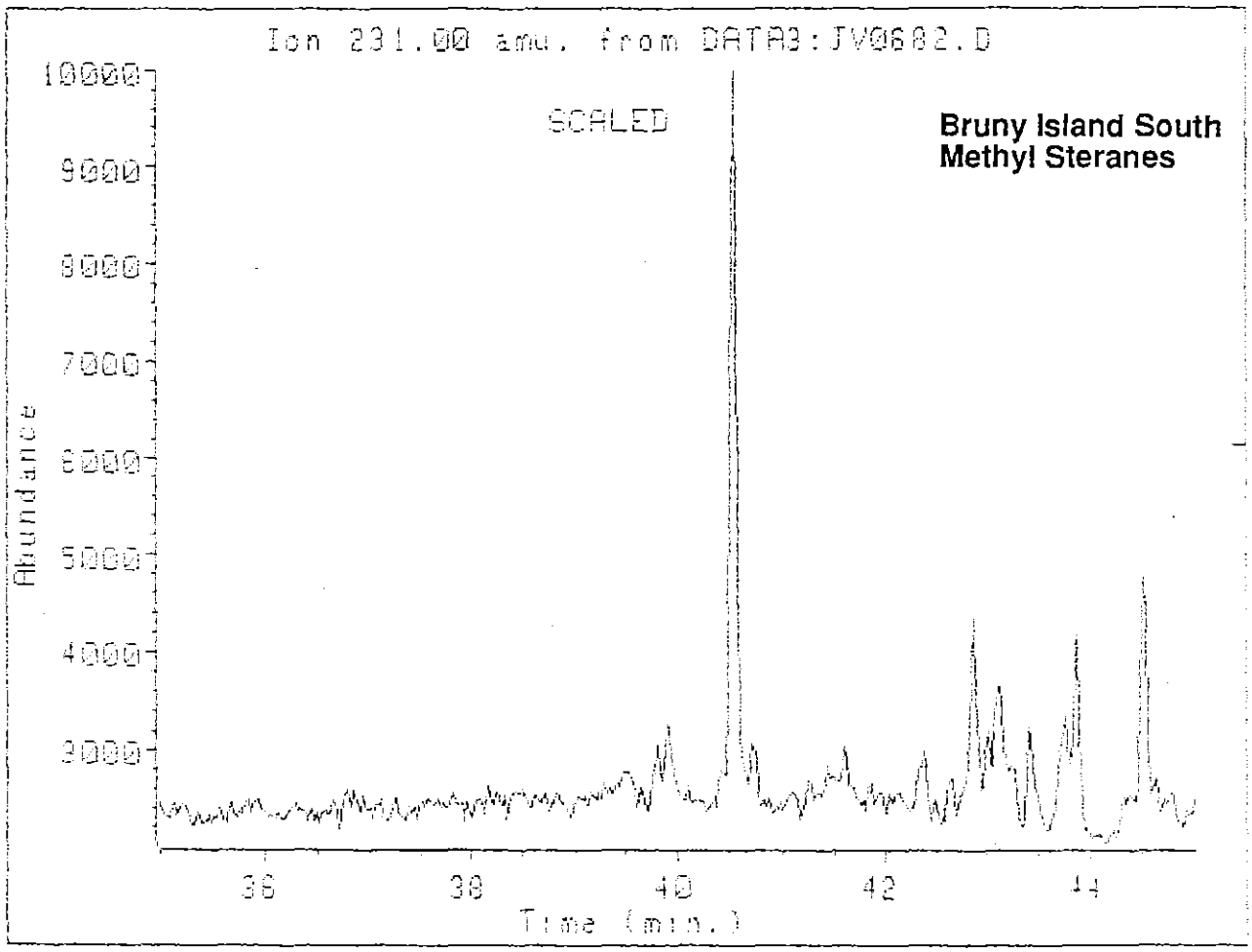
Ion 231.00 amu. from DATA3:JV0682.D
SCALED
Bruny Island South
Methyl Steranes
Abundance
10000
9000
8000
7000
6000
5000
4000
3000
36
38
40
42
44
Time (min.)

5 cm

Fig. 7(e)

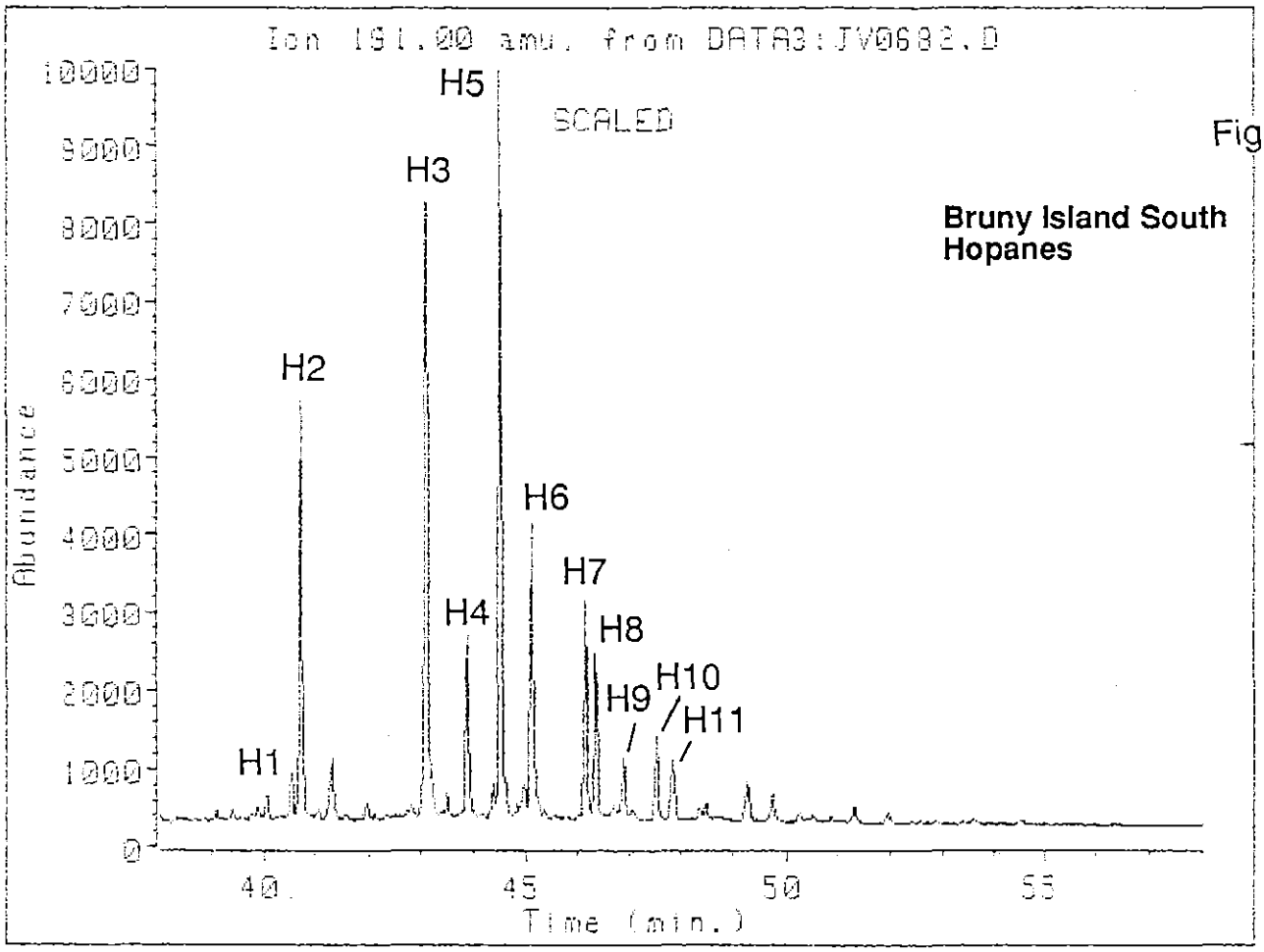
Ion 191.00 amu. from DATA3:JV0682.D
SCALED
Bruny Island South
Hopanes
H1
H2
H3
H4
H5
H6
H7
H8
H9
H10
H11
Abundance
Time (min.)

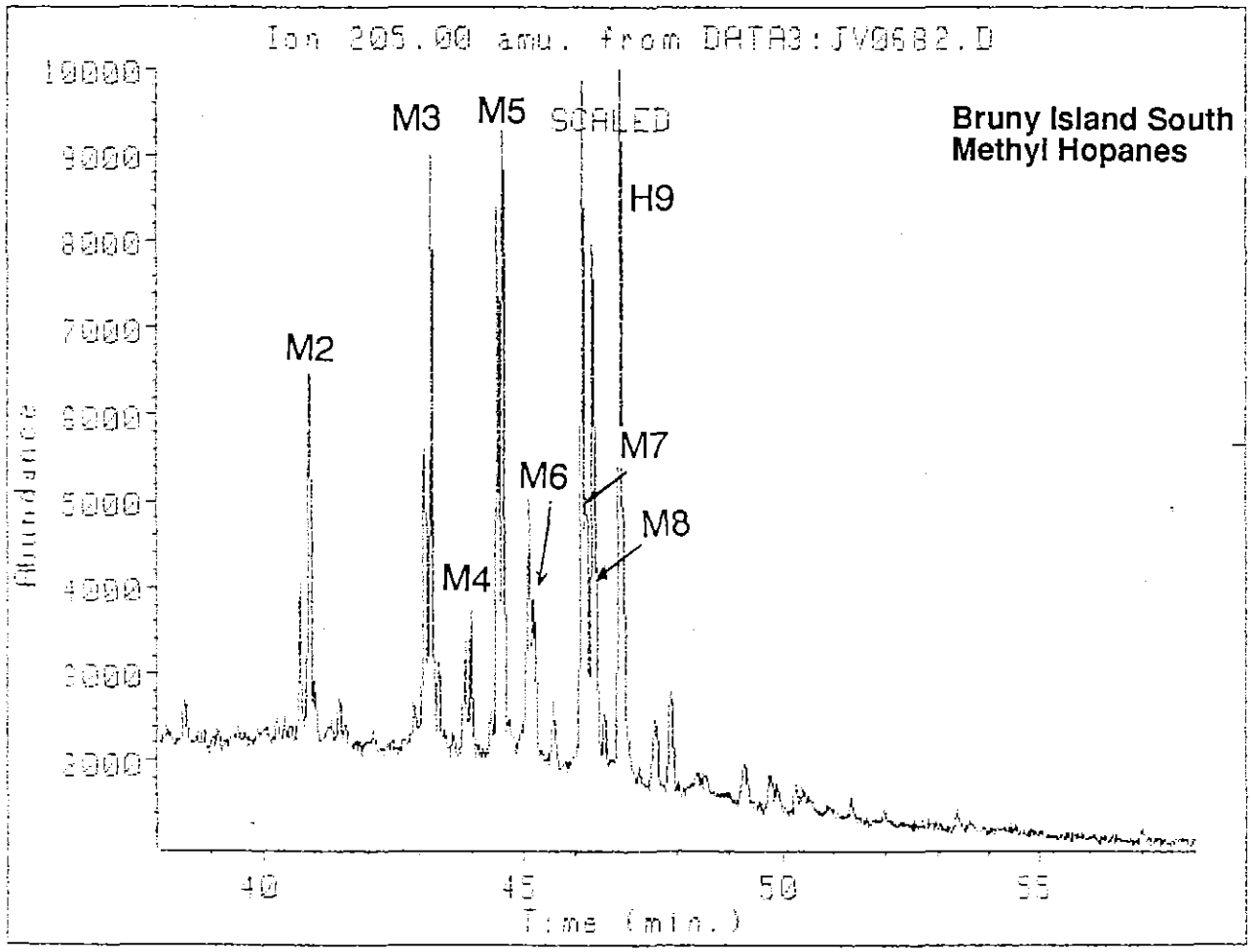
Ion 205.00 amu. from DATA3:JV0682.D
SCALED
Bruny Island South
Methyl Hopanes
M2
M3
M4
M5
M6
M7
M8
H9
Abundance
Time (min.)

5 cm

Fig. 7(f)

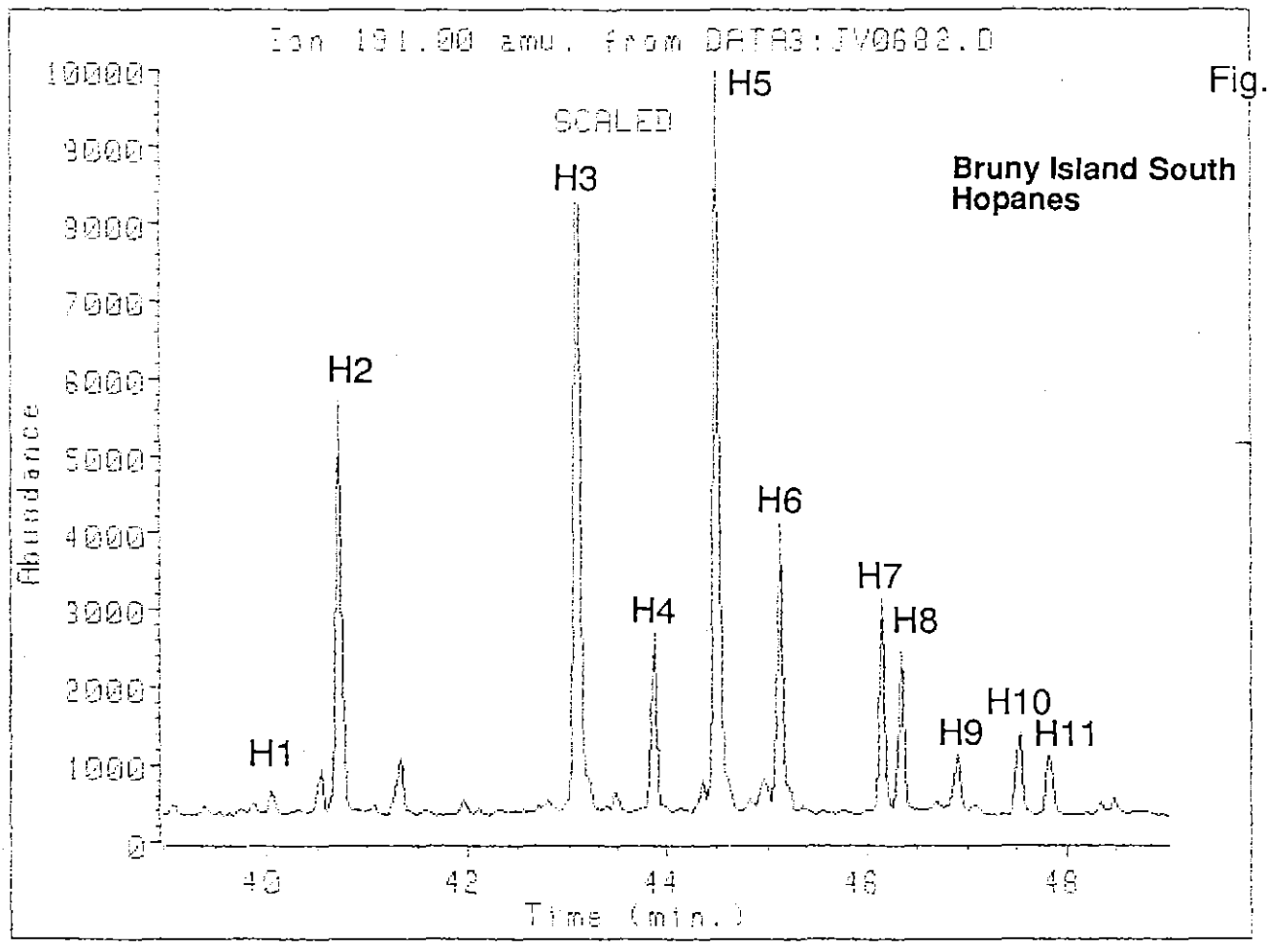
Ion 191.00 amu. from DATA3:JV0682.D
SCALED
H1
H2
H3
H4
H5
H6
H7
H8
H9
H10
H11
Bruny Island South
Hopanes
Abundance
Time (min.)

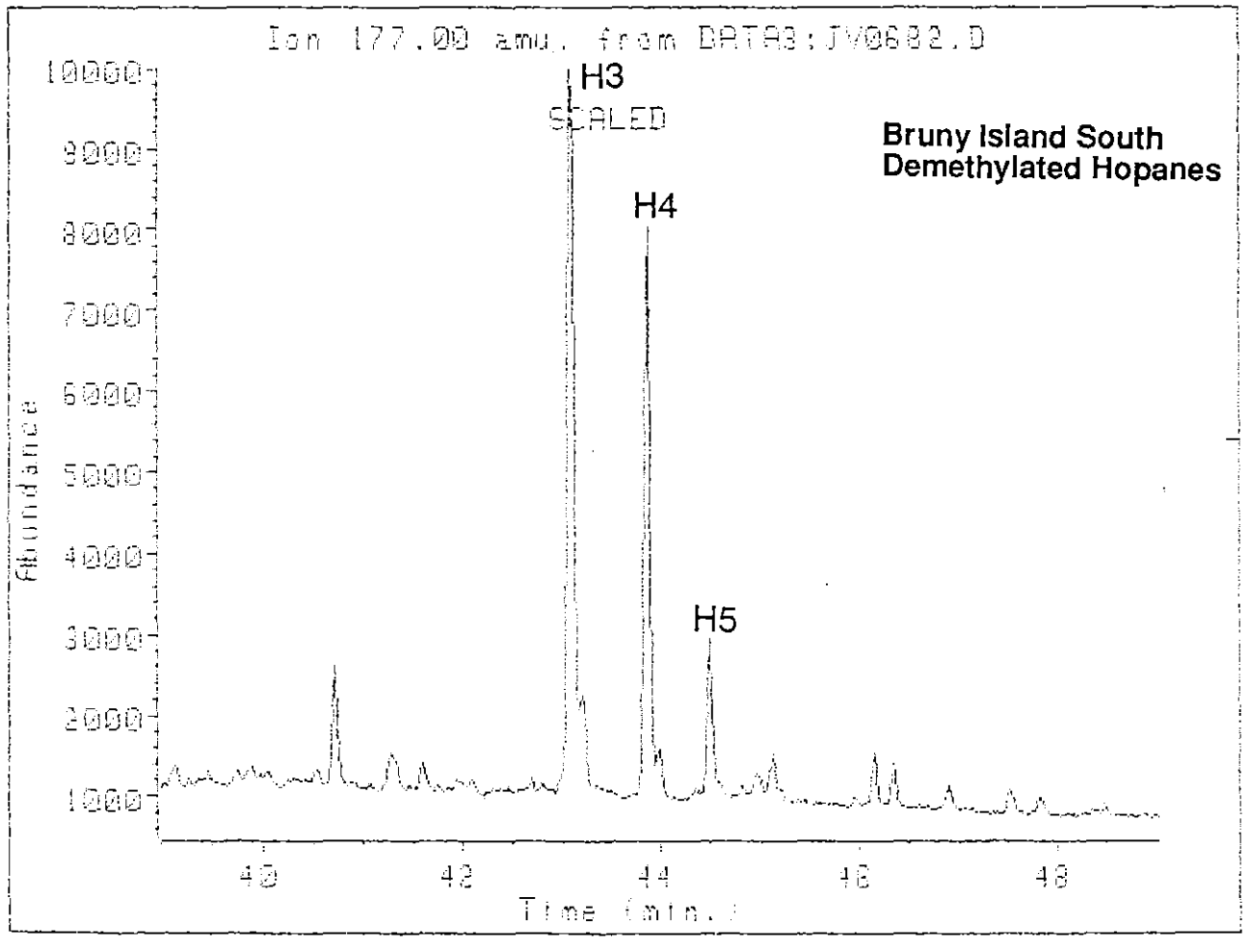
Ion 177.00 amu. from DATA3:JV0682.D
SCALED
H3
H4
H5
Bruny Island South
Demethylated Hopanes
Abundance
Time (min.)

Fig. 7(g)

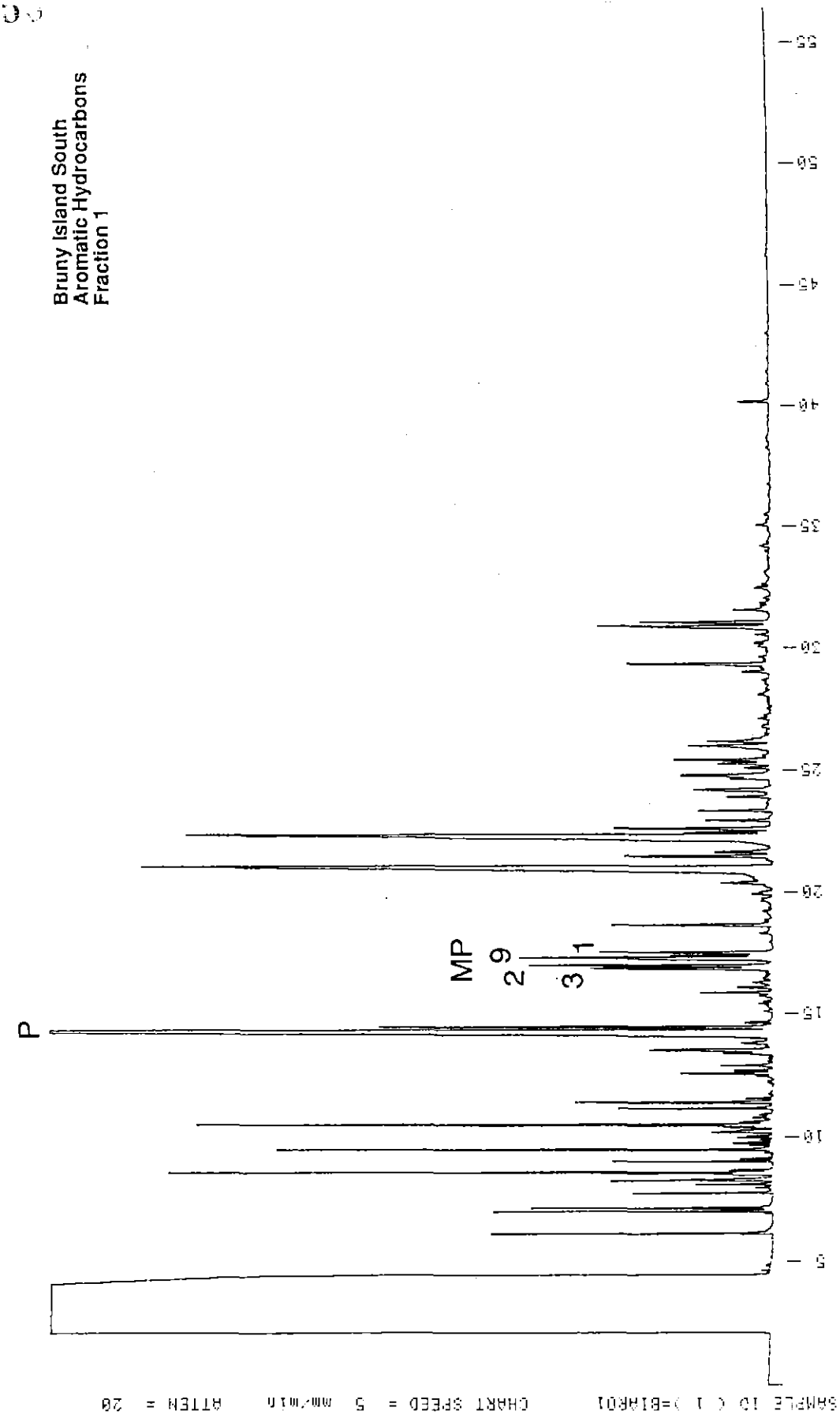
Bruny Island South
Aromatic Hydrocarbons
Fraction 1
P
MP
2 9
3 1
55
50
45
40
35
30
25
20
15
10
5
SAMPLE ID (1)=BIAR01 CHART SPEED = 5 MM/MIN ATTEN = 20

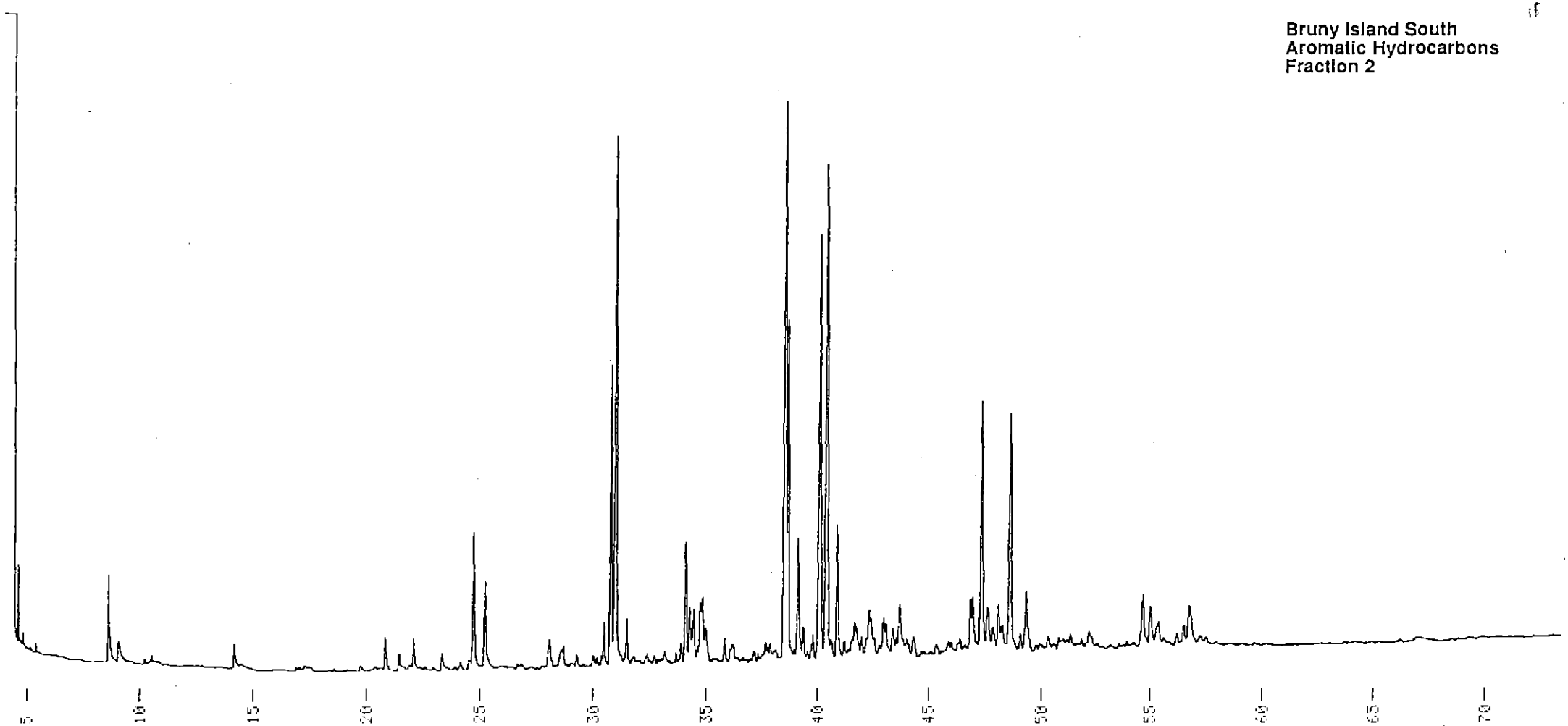
Bruny Island South
Aromatic Hydrocarbons
Fraction 2
5
10
15
20
25
30
35
40
45
50
55
60
65
70

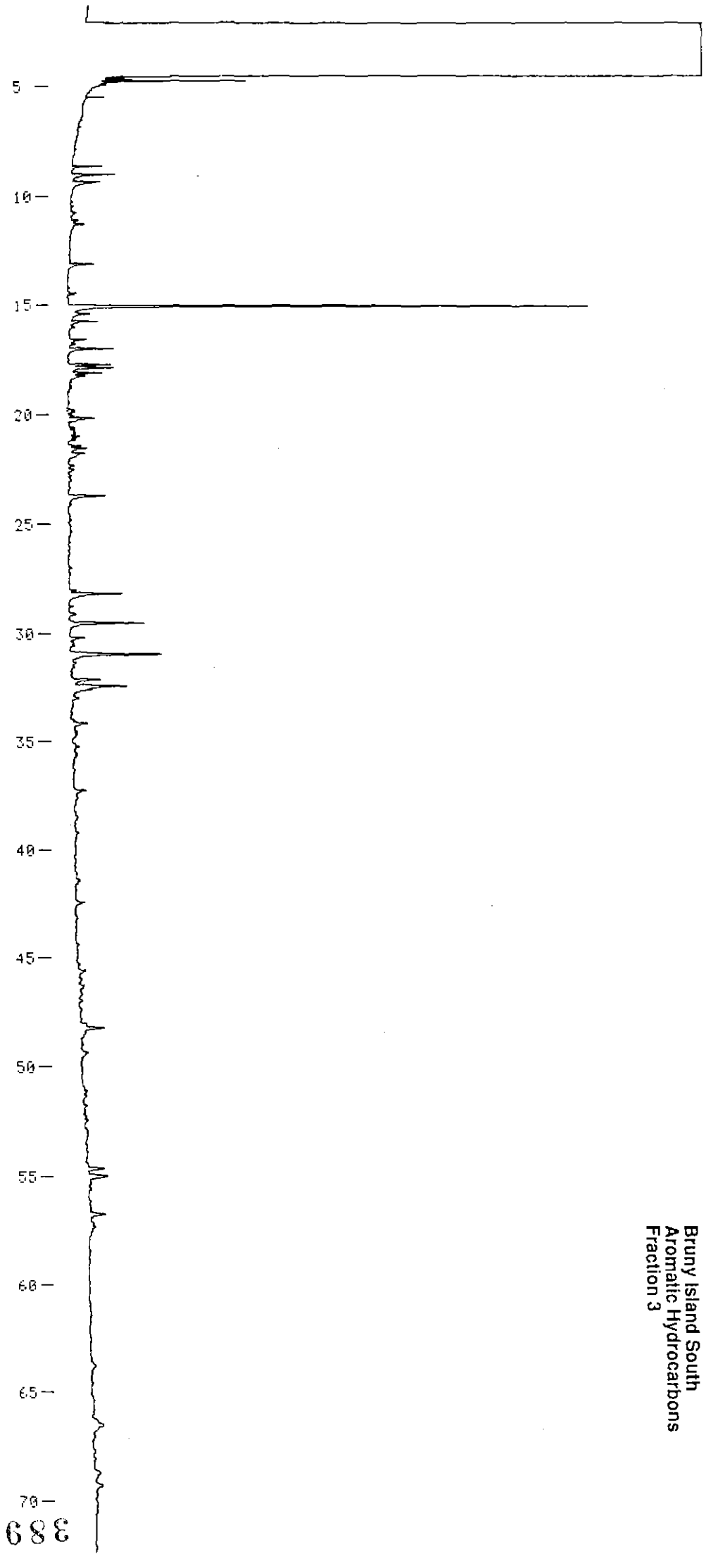

Bruny Island South
Aromatic Hydrocarbons
Fraction 3

Fig. 7(h)

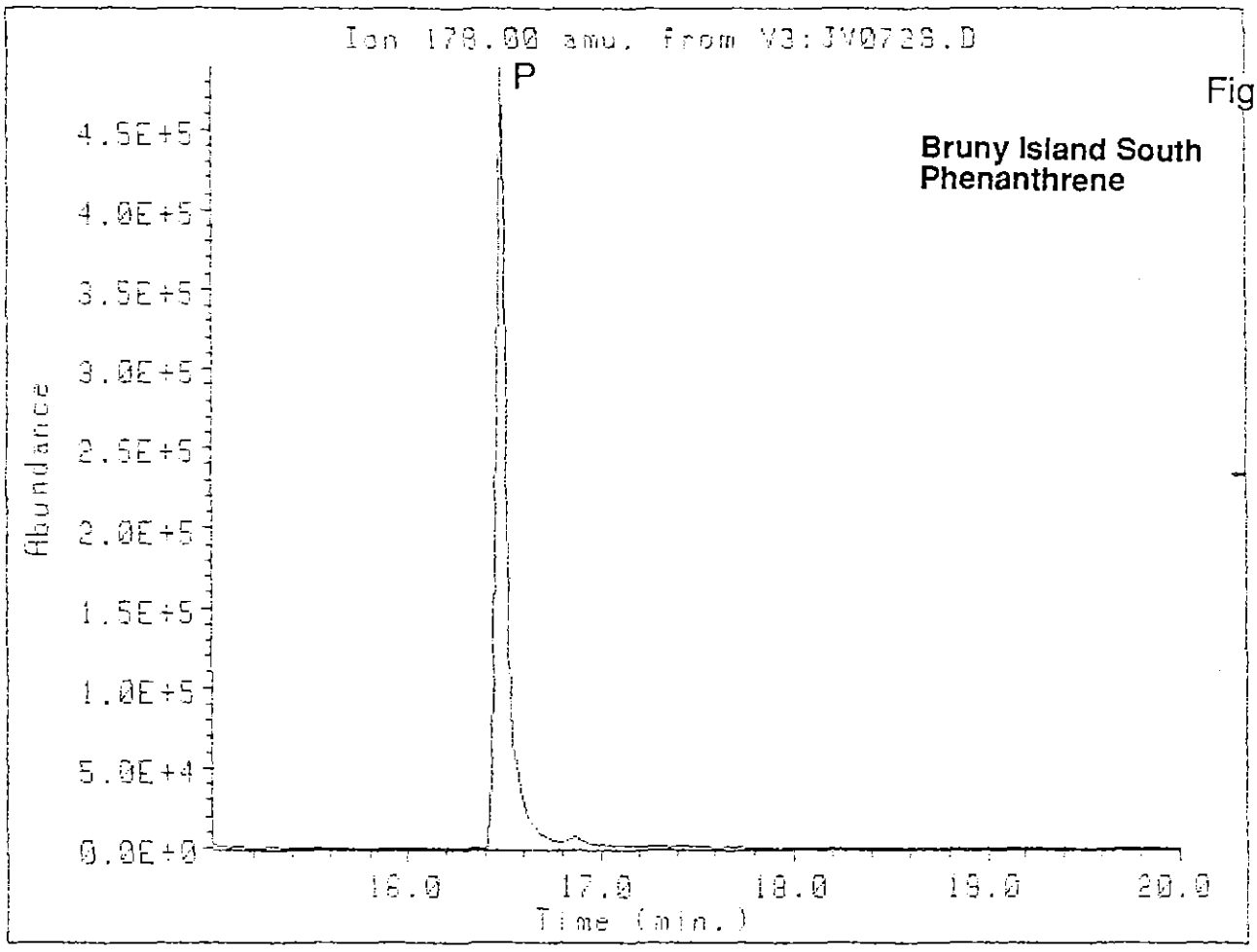
Ion 178.00 amu. from V3:JV0728.D
P
Bruny Island South
Phenanthrene
Abundance
4.5E+5
4.0E+5
3.5E+5
3.0E+5
2.5E+5
2.0E+5
1.5E+5
1.0E+5
5.0E+4
0.0E+0
16.0
17.0
18.0
19.0
20.0
Time (min.)

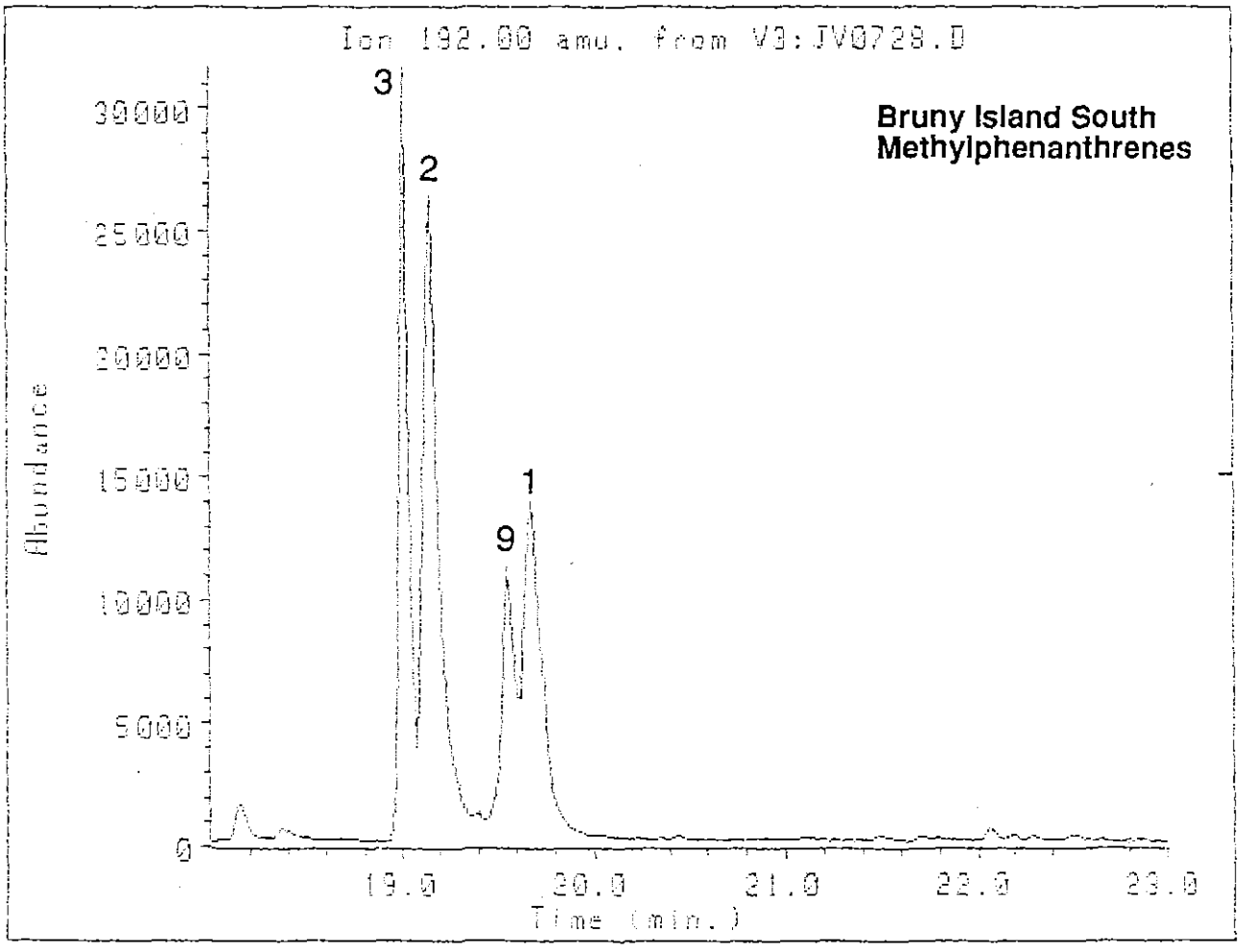
Ion 192.00 amu. from V3:JV0728.D
3
2
1
9
Bruny Island South
Methylphenanthrenes
Abundance
30000
25000
20000
15000
10000
5000
0
19.0
20.0
21.0
22.0
23.0
Time (min.)

Fig. 7(i)

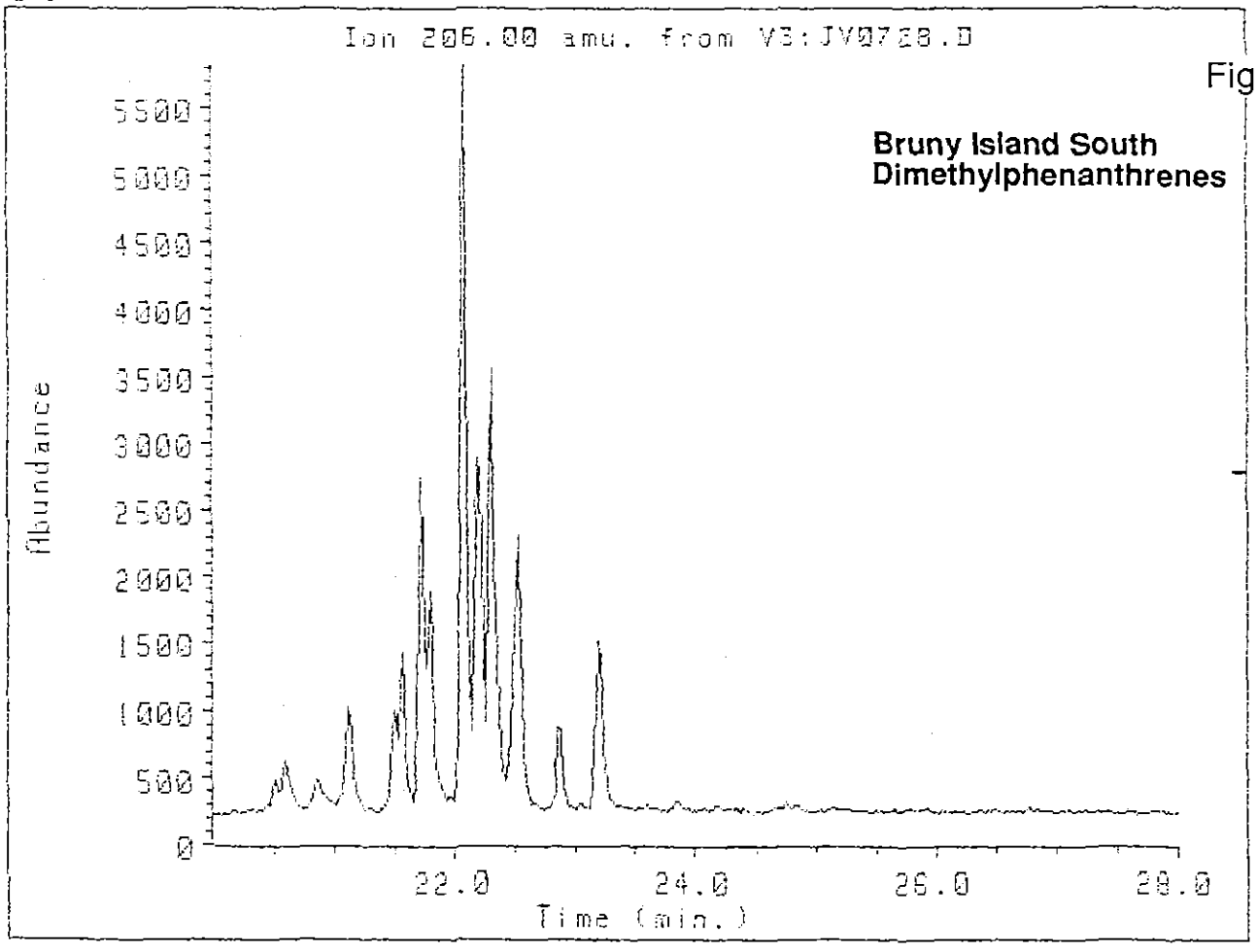
Ion 206.00 amu. from V3:JV0728.D
Bruny Island South
Dimethylphenanthrenes
Abundance
5500
5000
4500
4000
3500
3000
2500
2000
1500
1000
500
0
22.0
24.0
26.0
28.0
Time (min.)

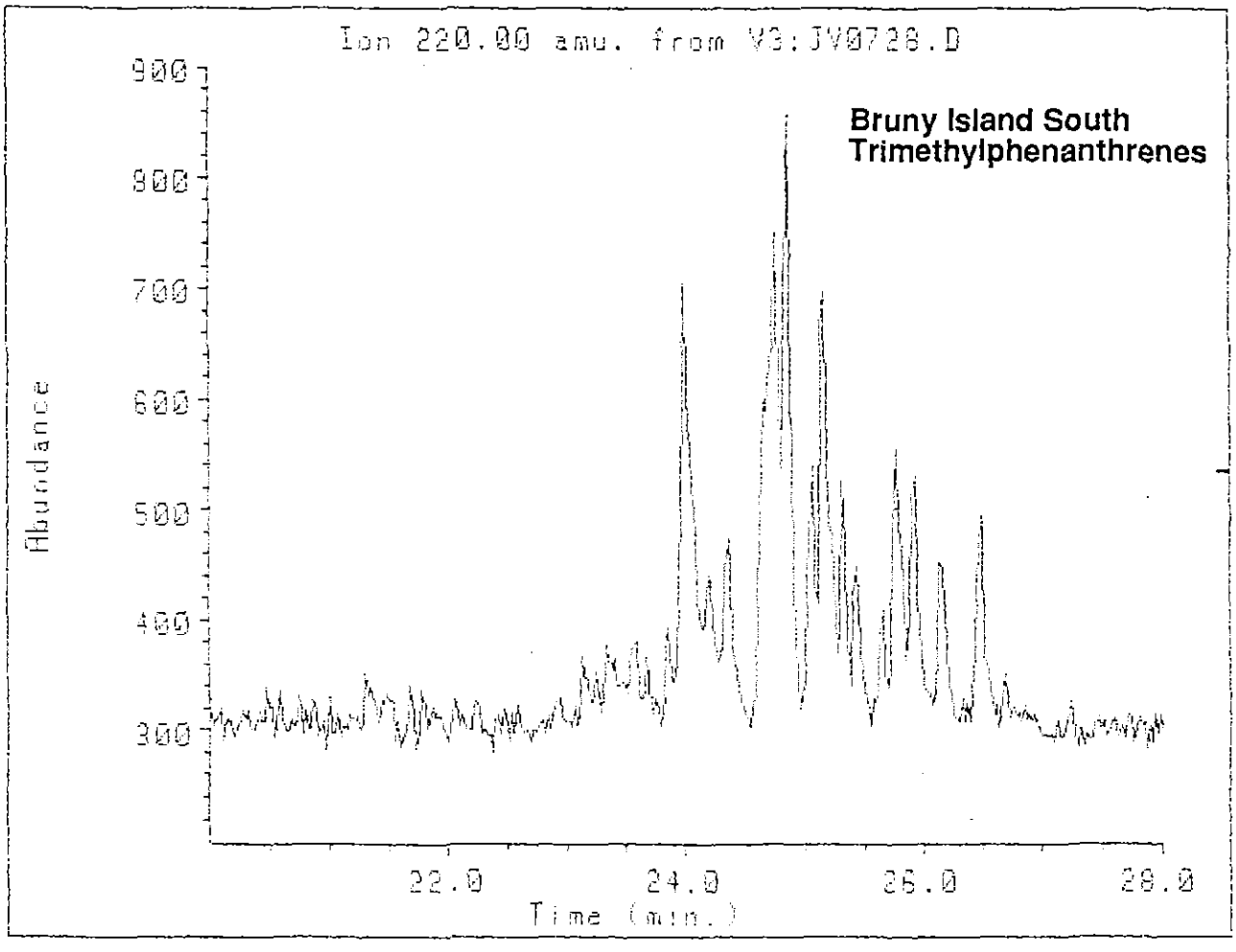
Ion 220.00 amu. from V3:JV0728.D
Bruny Island South
Trimethylphenanthrenes
Abundance
900
800
700
600
500
400
300
22.0
24.0
26.0
28.0
Time (min.)

Fig. 7(j)

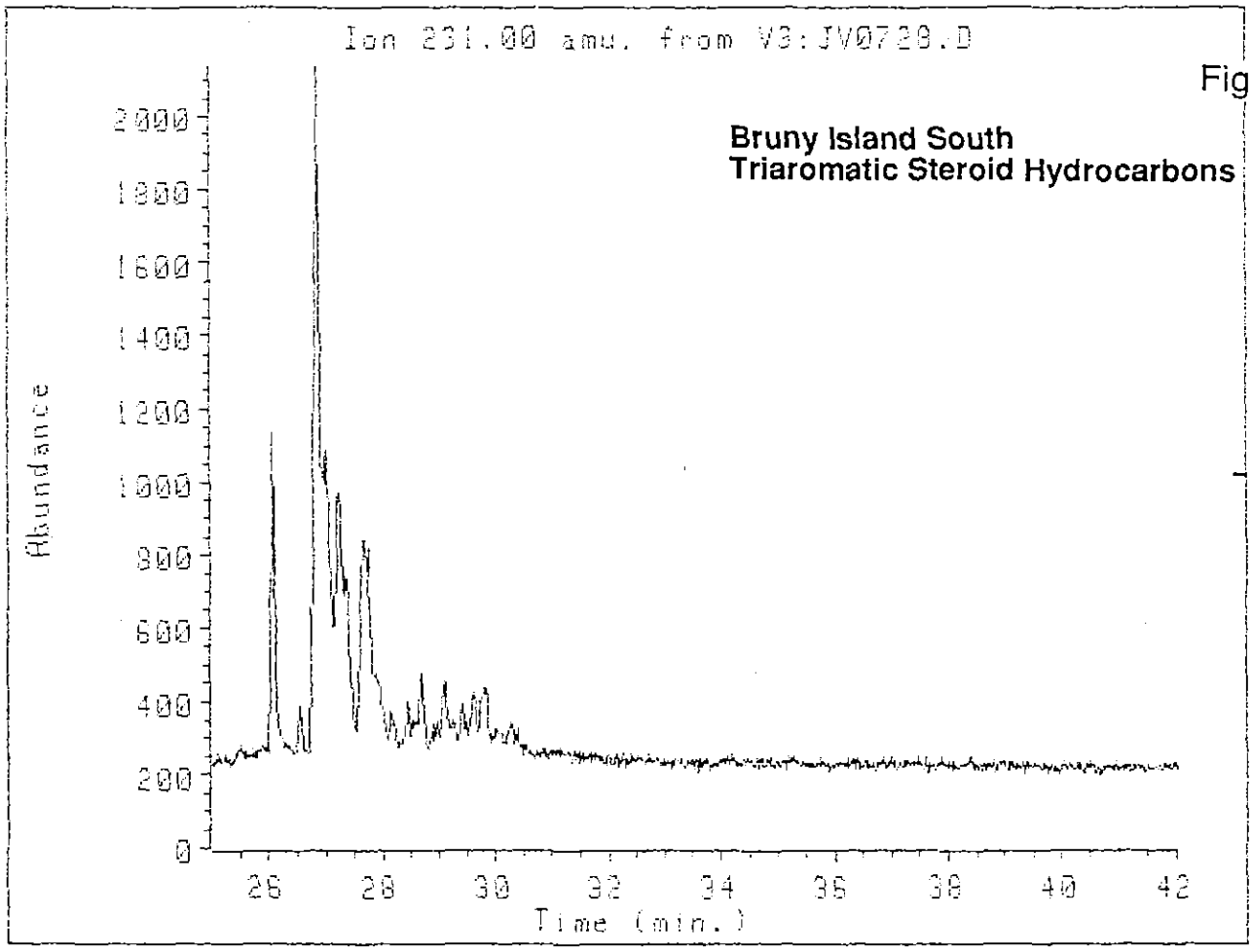
Ion 231.00 amu. from V3:JV0728.D
Bruny Island South
Triaromatic Steroid Hydrocarbons
Abundance
2000
1800
1600
1400
1200
1000
800
600
400
200
0
26
28
30
32
34
36
38
40
42
Time (min.)

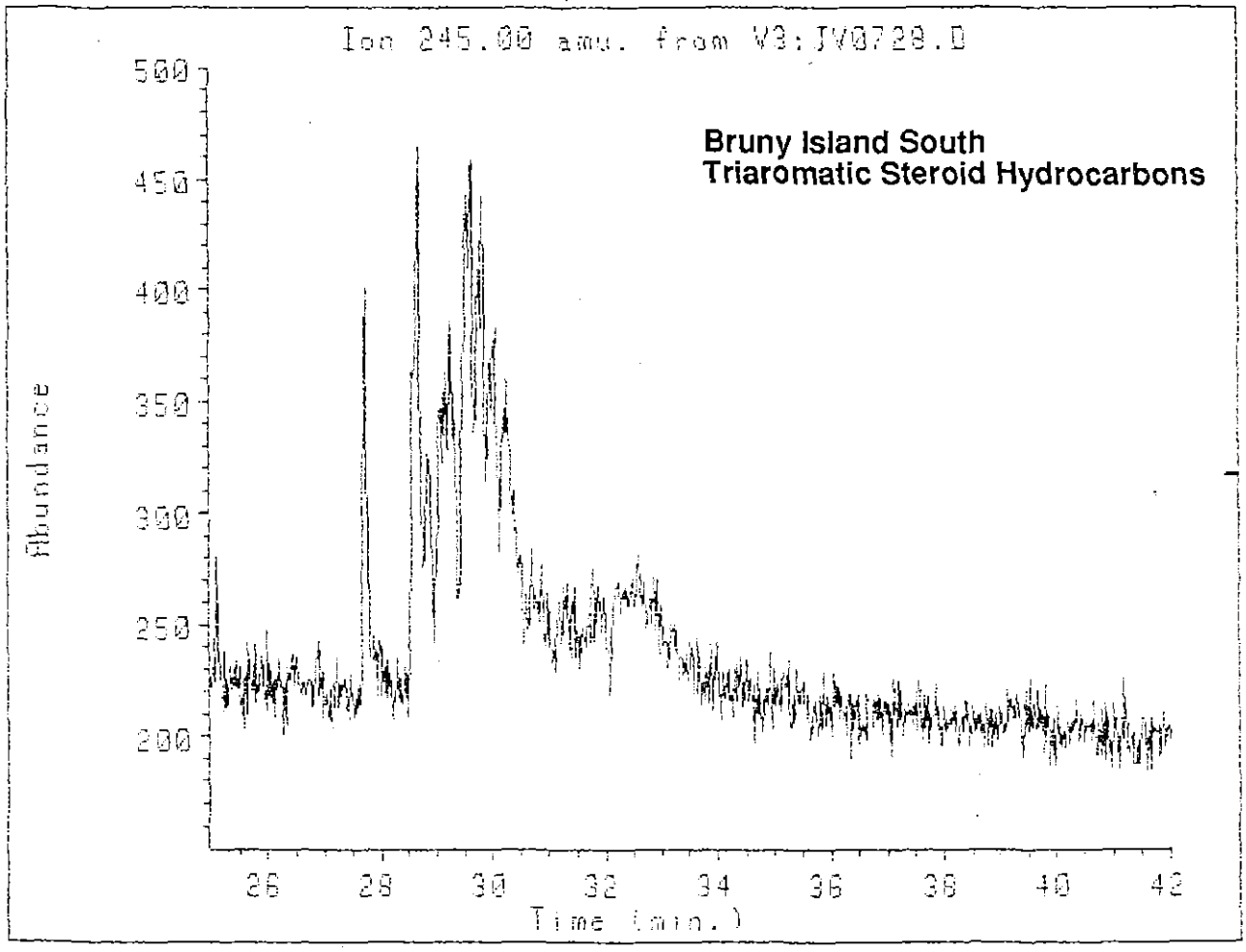
Ion 245.00 amu. from V3:JV0728.D
Bruny Island South
Triaromatic Steroid Hydrocarbons
Abundance
500
450
400
350
300
250
200
26
28
30
32
34
36
38
40
42
Time (min.)

Figure 8. GC and GC–MS data for the Tunnack bitumen.

(8a) Capillary gas chromatogram of the total aliphatic hydrocarbons in the Tunnack bitumen. Pr: pristane; Ph: phytane. n–Alkanes are denoted by n–C_X where "x" is the number of carbon atoms.

(8b). Mass fragmentograms for m/z 217 and 218 showing distribution of C_{26}–C_{30} steranes (labelled S) and diasteranes (labelled D) in the Tunnack bitumen. See Key 1 for peak identifications.

(8c) Mass fragmentograms for m/z 217 and 218 showing distribution of C_{21}–C_{23} steranes in the Tunnack bitumen.

(8d) Mass fragmentograms for m/z 259 showing distribution of C_{27}–C_{30} diasteranes (labelled D), and m/z 231 showing distribution of C_{28}–C_{30} 4–methyl steranes in the Tunnack bitumen.

(8e) Mass fragmentograms for m/z 191 showing distribution of C_{27}–C_{35} hopanes and m/z 205 showing distribution of methyl hopanes in the Tunnack bitumen. See Keys 2 and 3 for peak identifications.

(8f) Mass fragmentograms for m/z 191 showing distribution of C_{27}–C_{32} hopanes and m/z 177 showing distribution of demethylated hopanes (none detected) in the Tunnack bitumen.

(8g) Capillary gas chromatogram of the aromatic hydrocarbon subfractions in the Tunnack bitumen (see text).

(8h) Mass fragmentograms for m/z 178 and 192 showing the presence of phenanthrene and distribution of methylphenanthrenes respectively in the Tunnack bitumen.

(8i) Mass fragmentograms for m/z 206 and 220 showing the distribution of di– and trimethylphenanthrenes in the Tunnack bitumen.

Fig. 8(a)

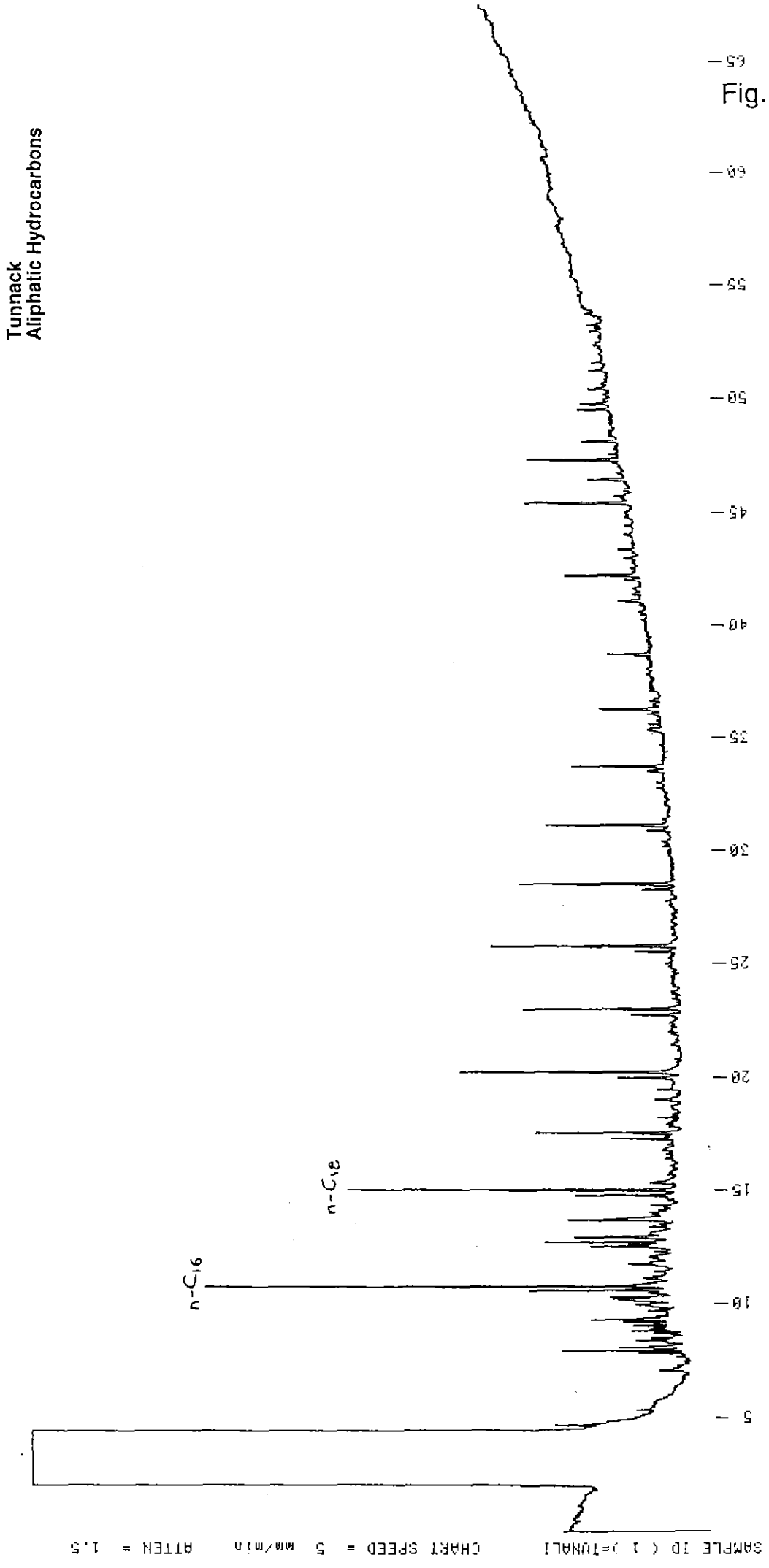

For Chart No. T 00729

5 cm

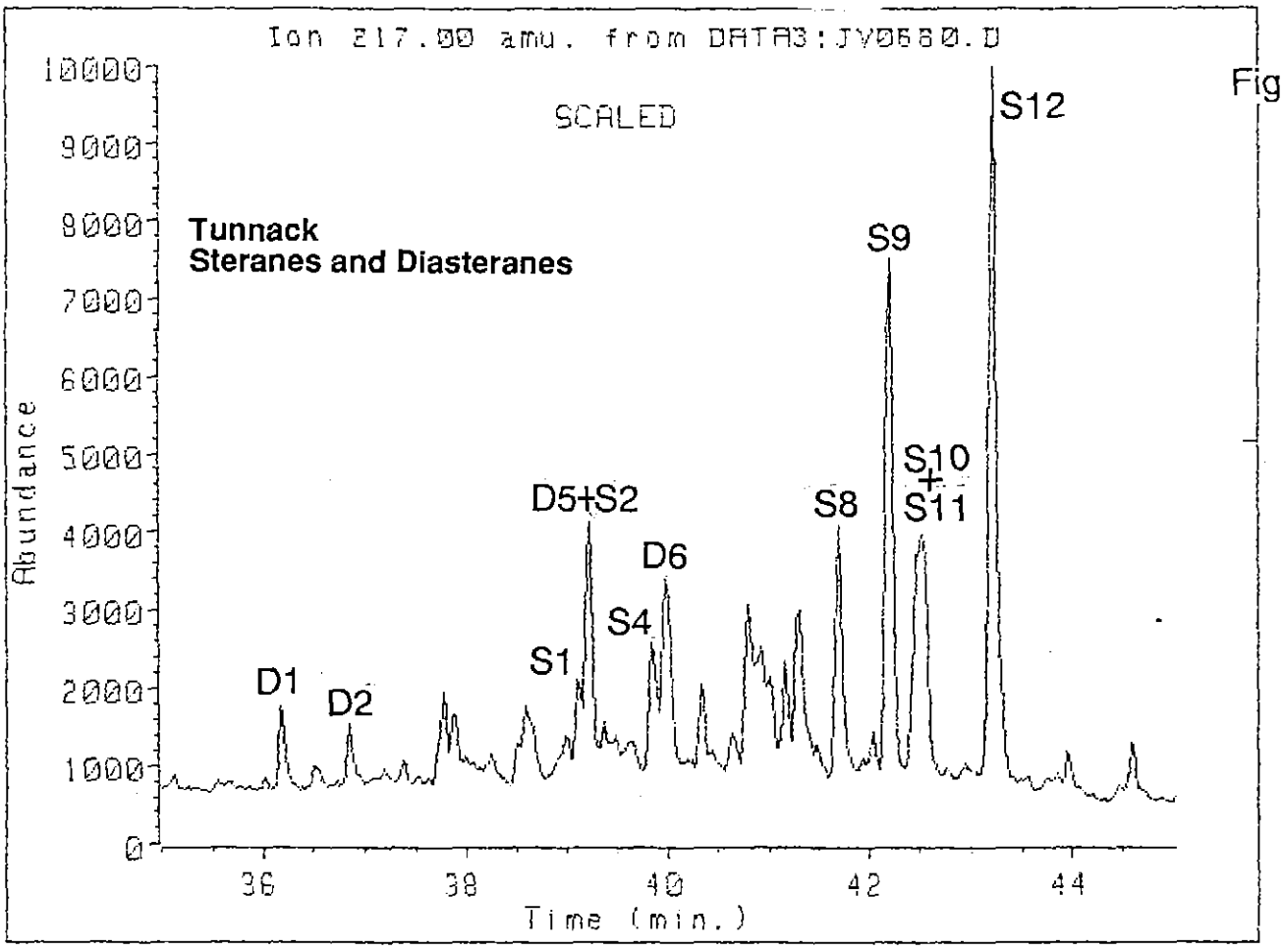
Ion 217.00 amu. from DATA3:JV0680.D
SCALED
Tunnack
Steranes and Diasteranes
Abundance
Time (min.)
D1
D2
S1
D5+S2
S4
D6
S8
S9
S10
+
S11
S12

Fig. 8(b)

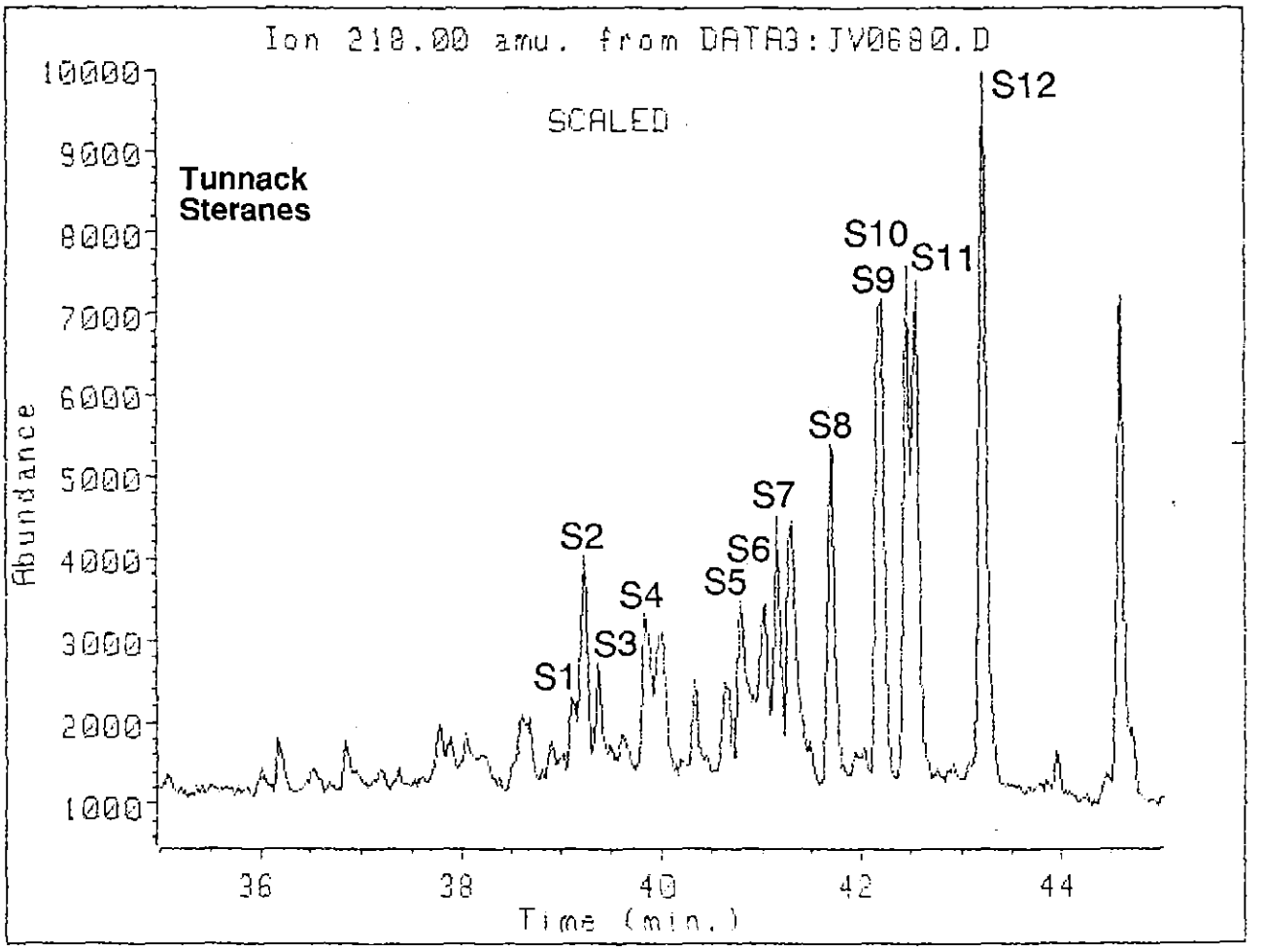
Ion 218.00 amu. from DATA3:JV0680.D
SCALED
Tunnack
Steranes
Abundance
Time (min.)
S1
S2
S3
S4
S5
S6
S7
S8
S9
S10
S11
S12

5 cm

Fig. 8(c)

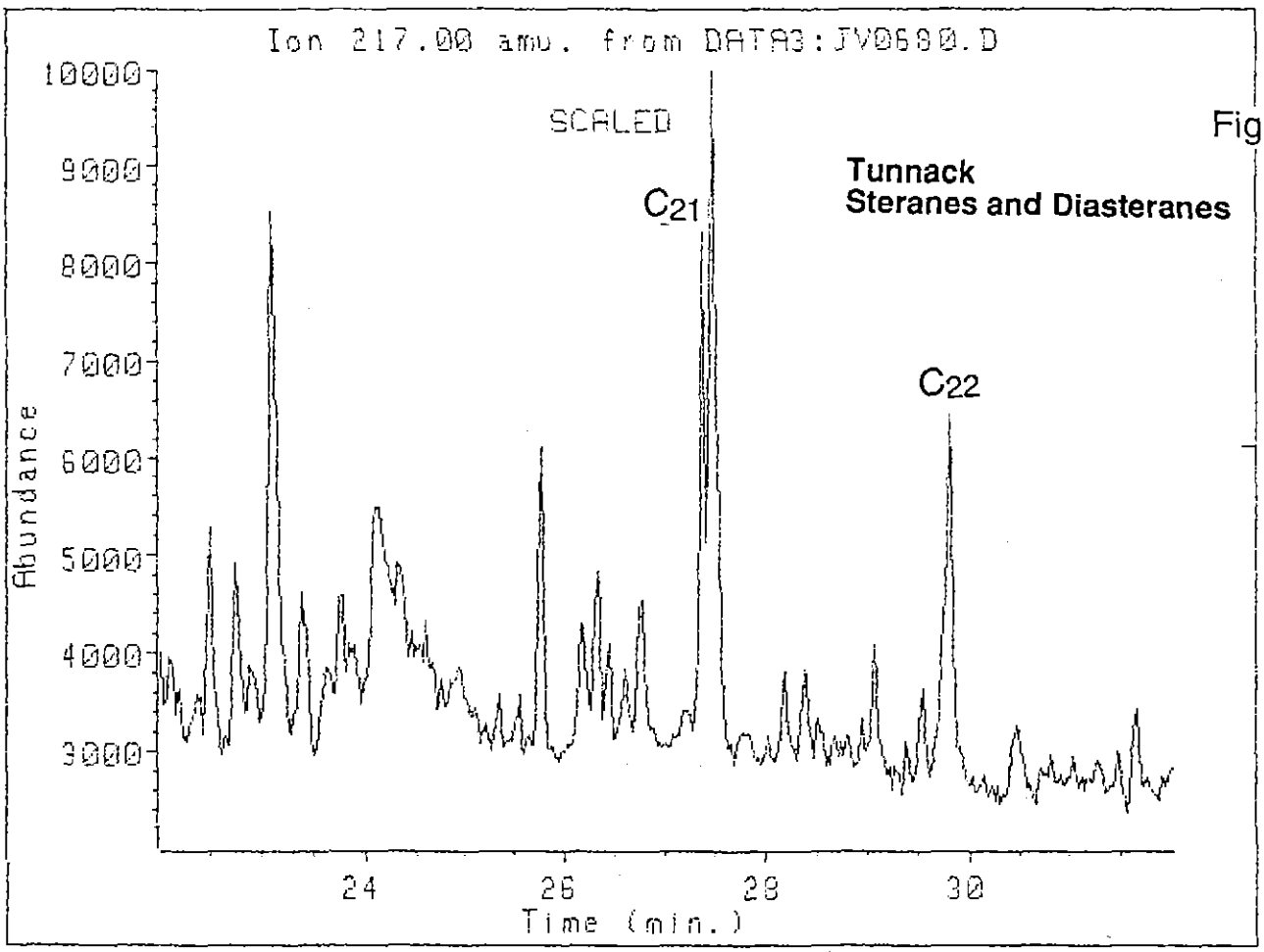
Ion 217.00 amu. from DATA3:JV0680.D
SCALED
C21
C22
Tunnack
Steranes and Diasteranes
Abundance
10000
9000
8000
7000
6000
5000
4000
3000
24
26
28
30
Time (min.)

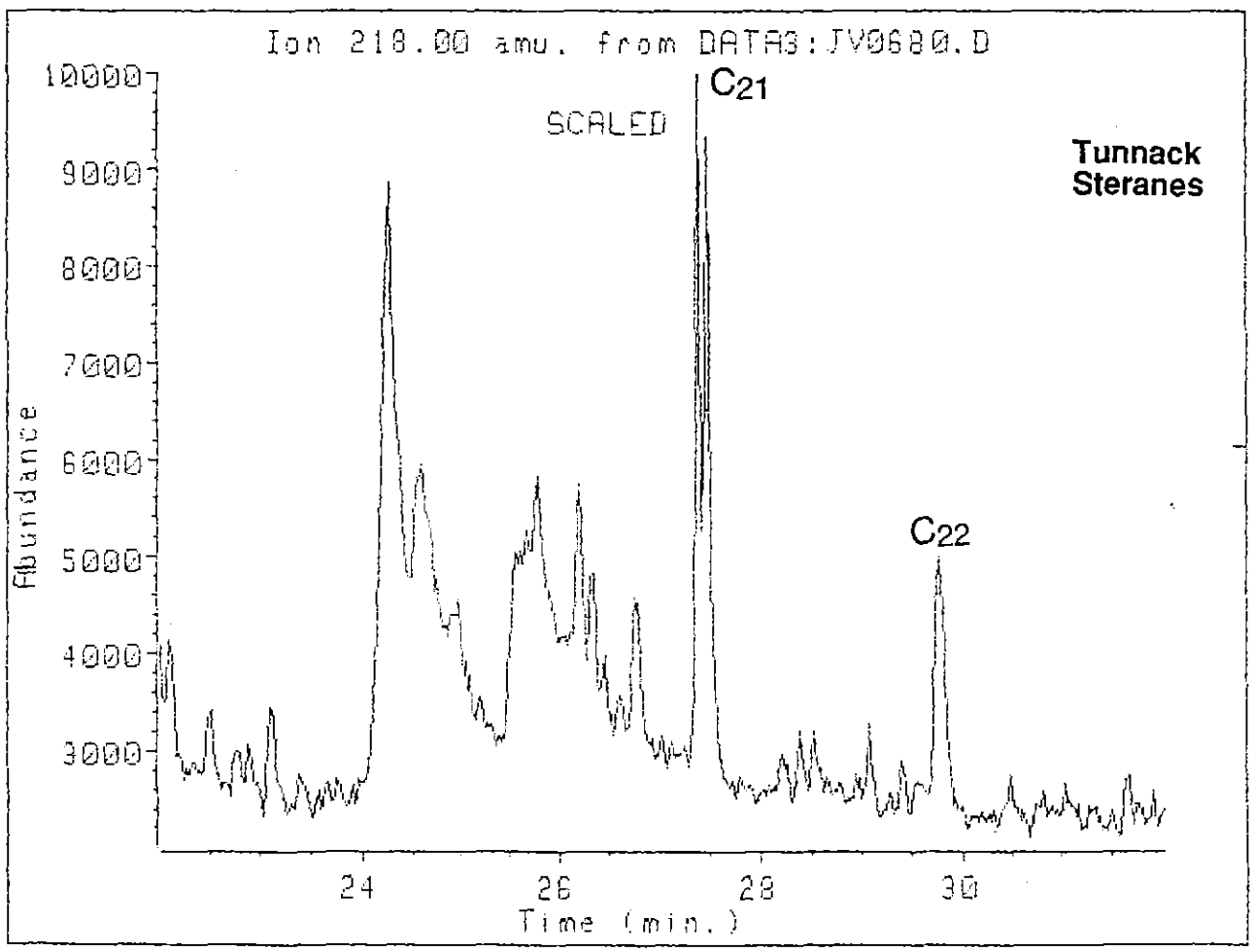
Ion 218.00 amu. from DATA3:JV0680.D
SCALED
C21
C22
Tunnack
Steranes
Abundance
10000
9000
8000
7000
6000
5000
4000
3000
24
26
28
30
Time (min.)

5 cm

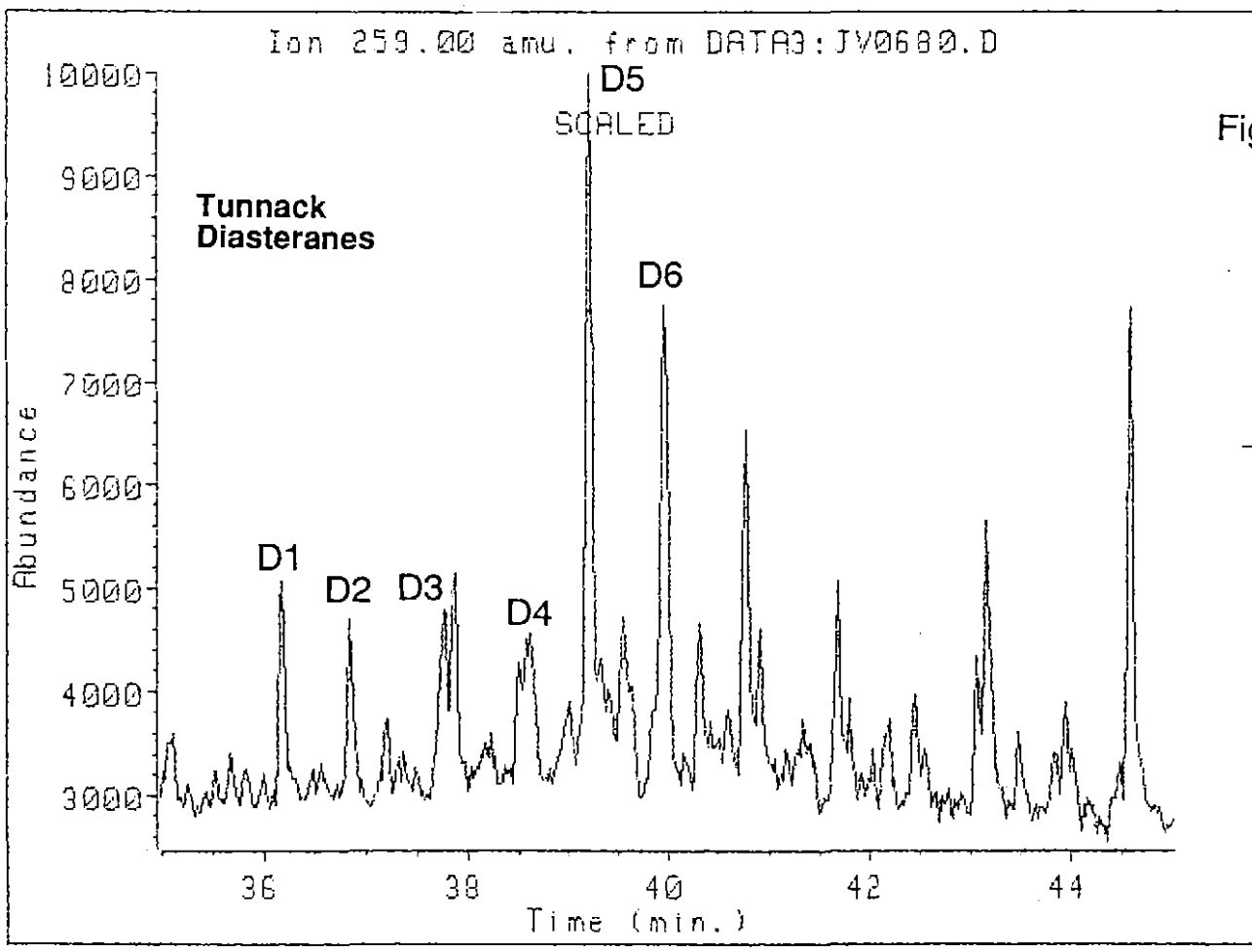
Ion 259.00 amu. from DATA3:JV0680.D
SCALED
Tunnack
Diasteranes
D1
D2
D3
D4
D5
D6
Abundance
Time (min.)

Fig. 8(d)

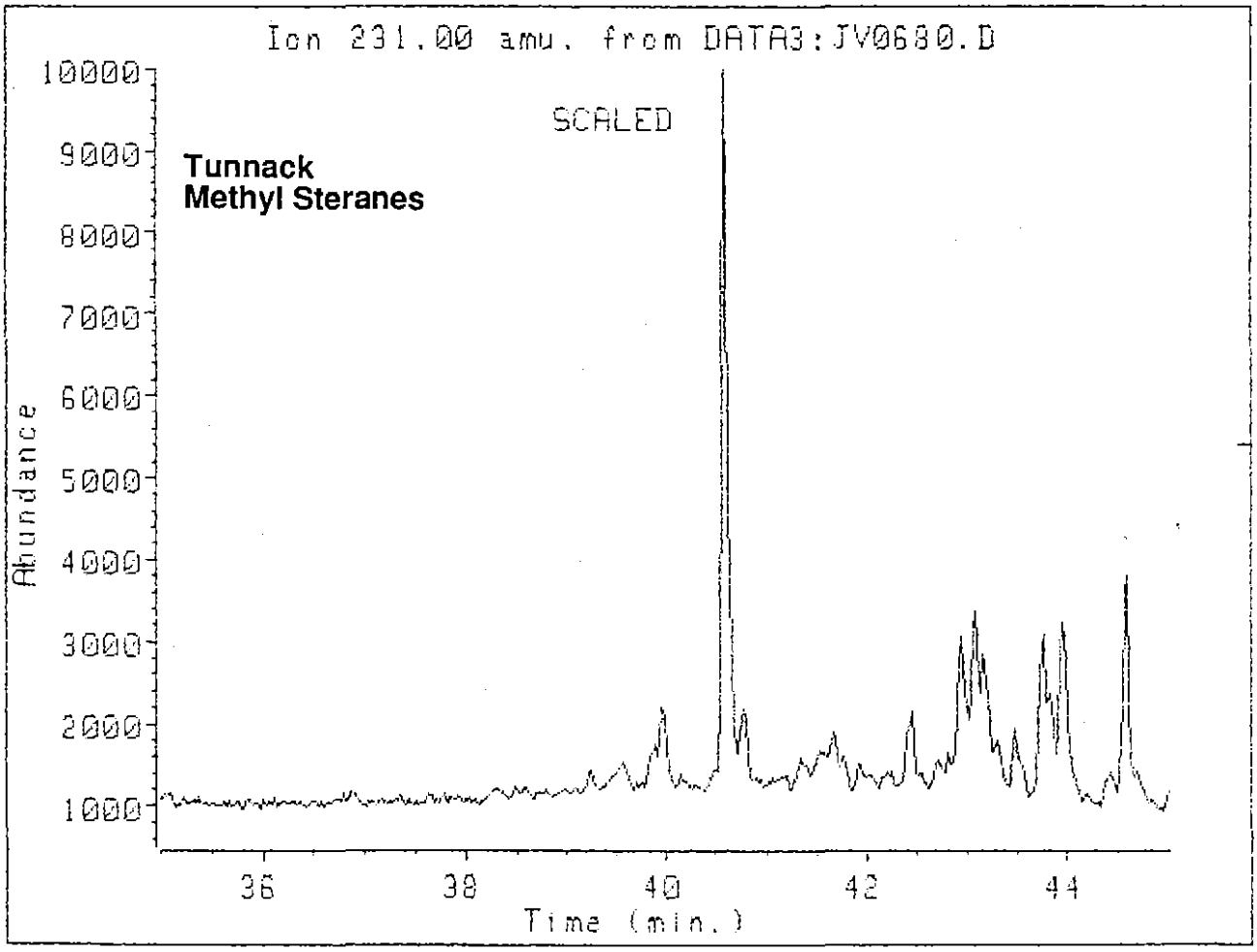
Ion 231.00 amu. from DATA3:JV0680.D
SCALED
Tunnack
Methyl Steranes
Abundance
Time (min.)

5 cm

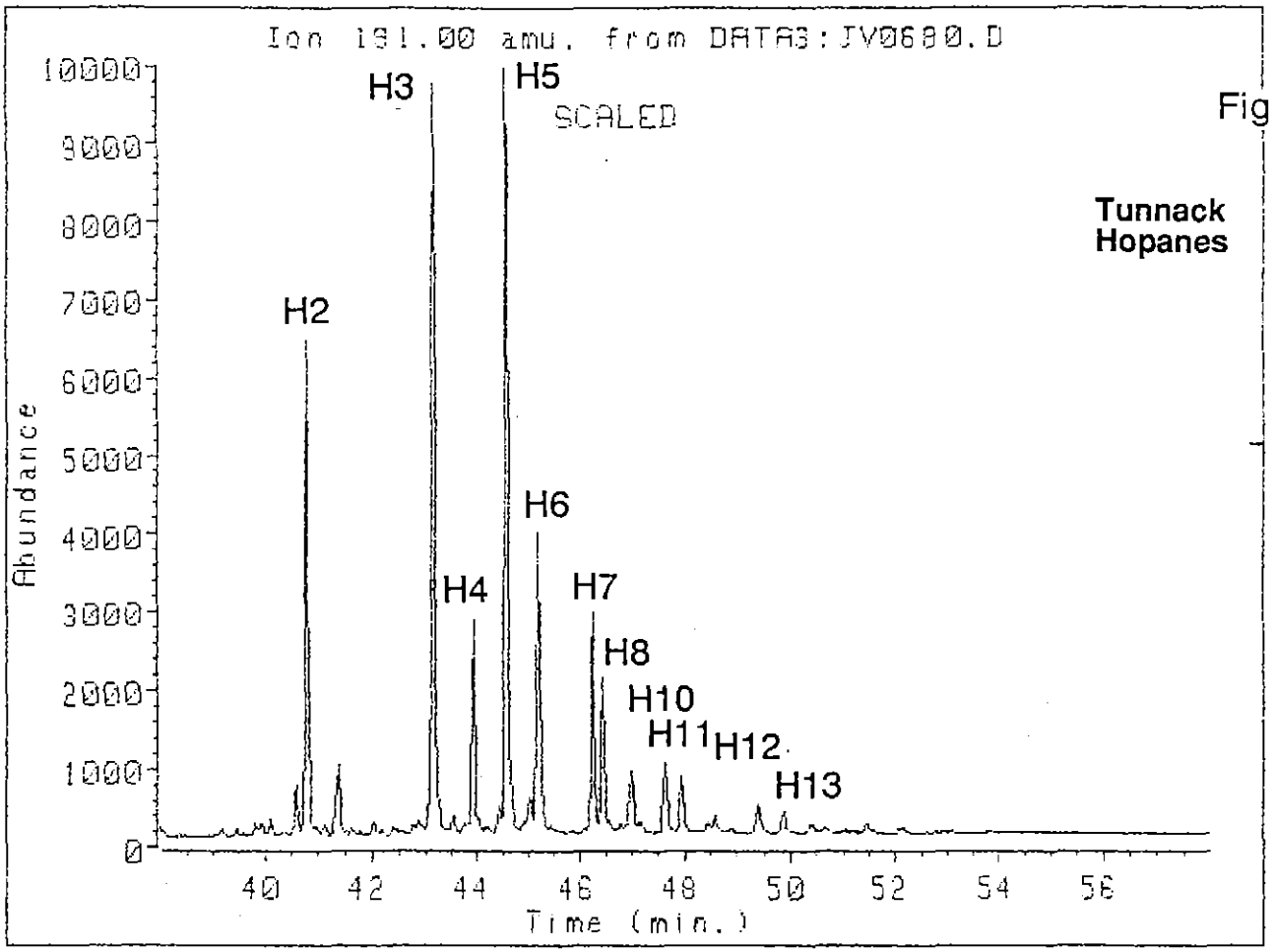
Ion 191.00 amu. from DATA3:JV0680.D
SCALED
H2
H3
H4
H5
H6
H7
H8
H10
H11
H12
H13
Tunnack
Hopanes
Abundance
Time (min.)

Fig. 8(e)

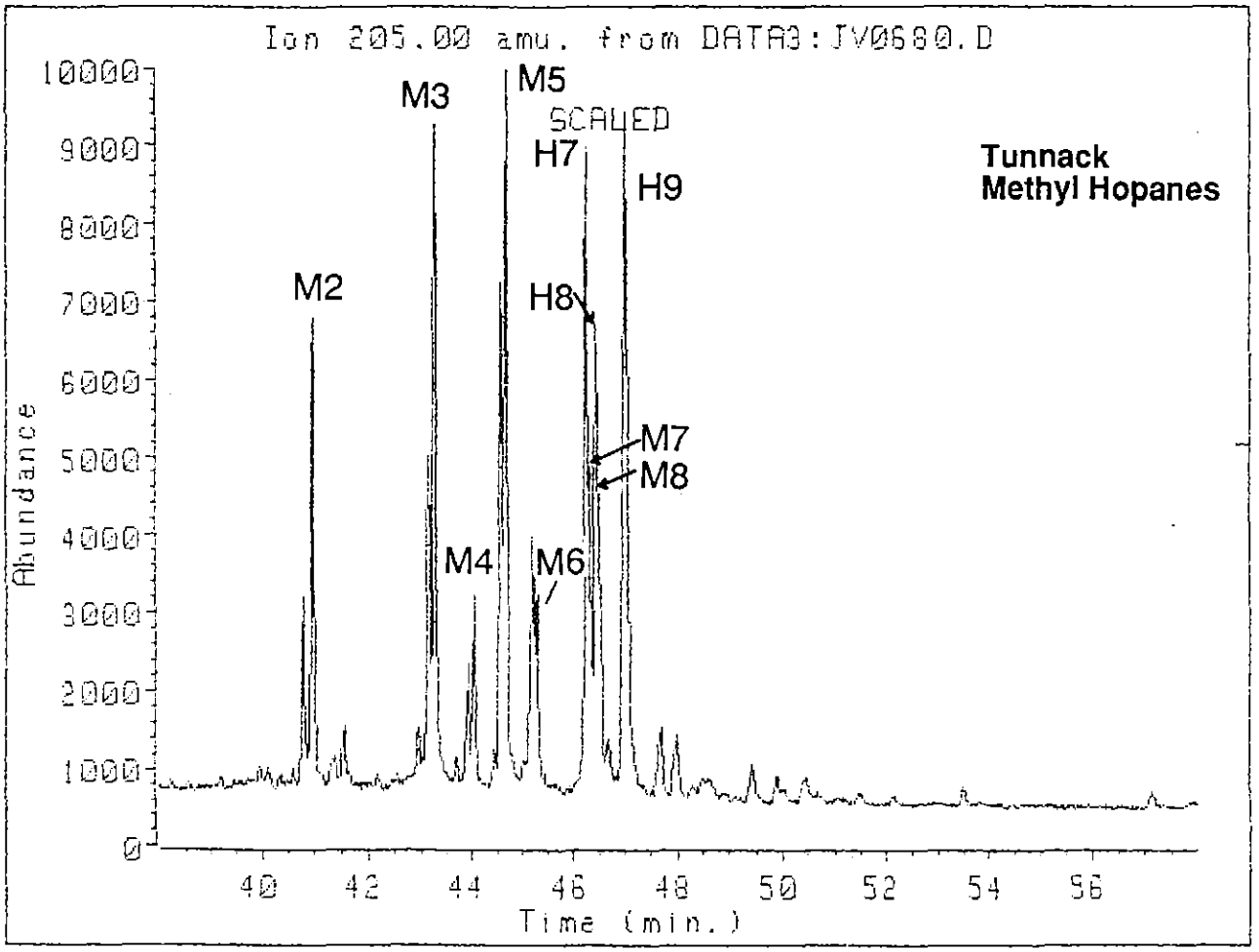
Ion 205.00 amu. from DATA3:JV0680.D
SCALED
M2
M3
M4
M5
M6
M7
M8
H7
H8
H9
Tunnack
Methyl Hopanes
Abundance
Time (min.)

5 cm

Fig. 8(f)

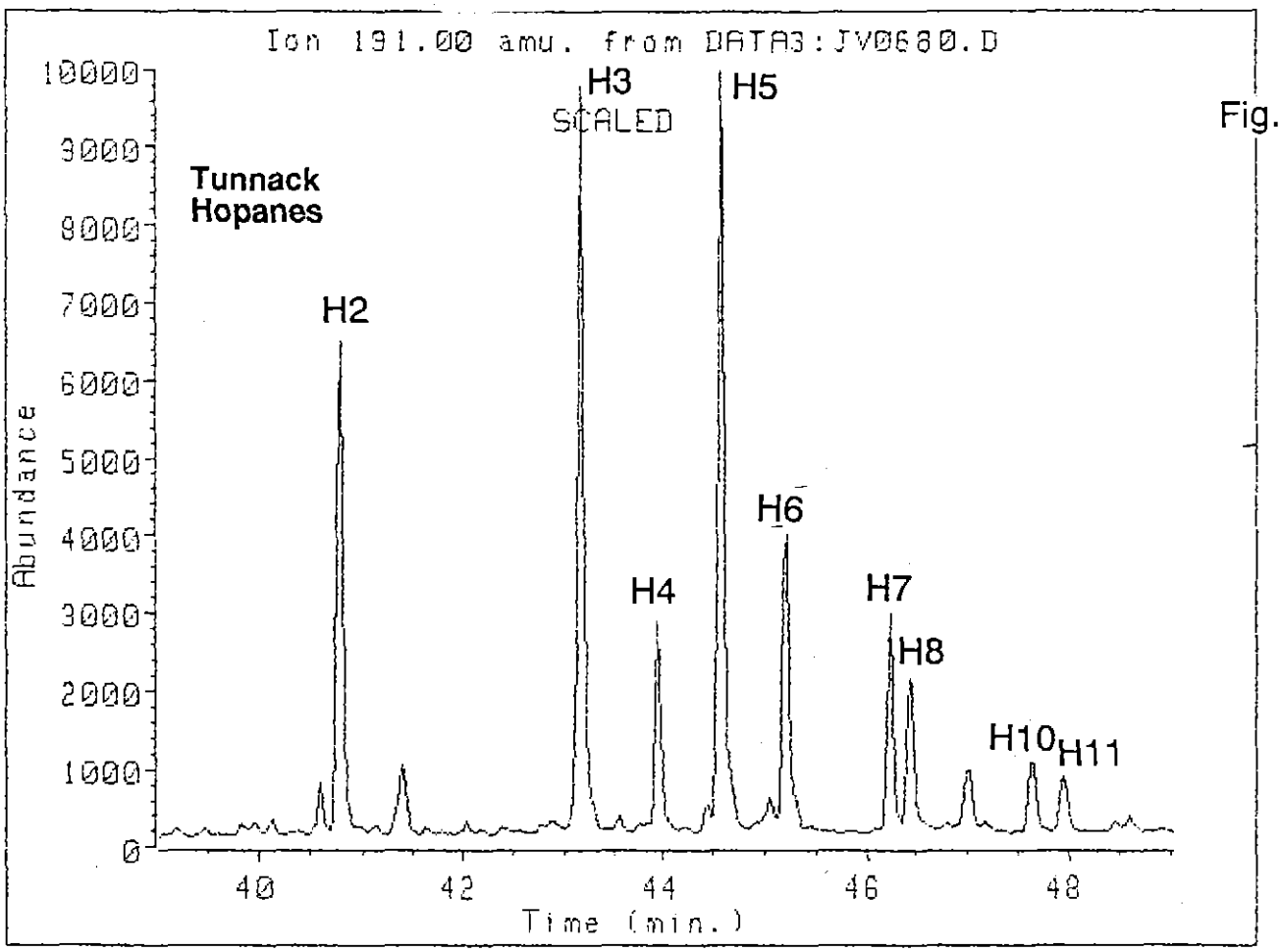
Ion 191.00 amu. from DATA3:JV0680.D
Tunnack
Hopanes
H2
H3
SCALED
H4
H5
H6
H7
H8
H10
H11
Abundance
Time (min.)

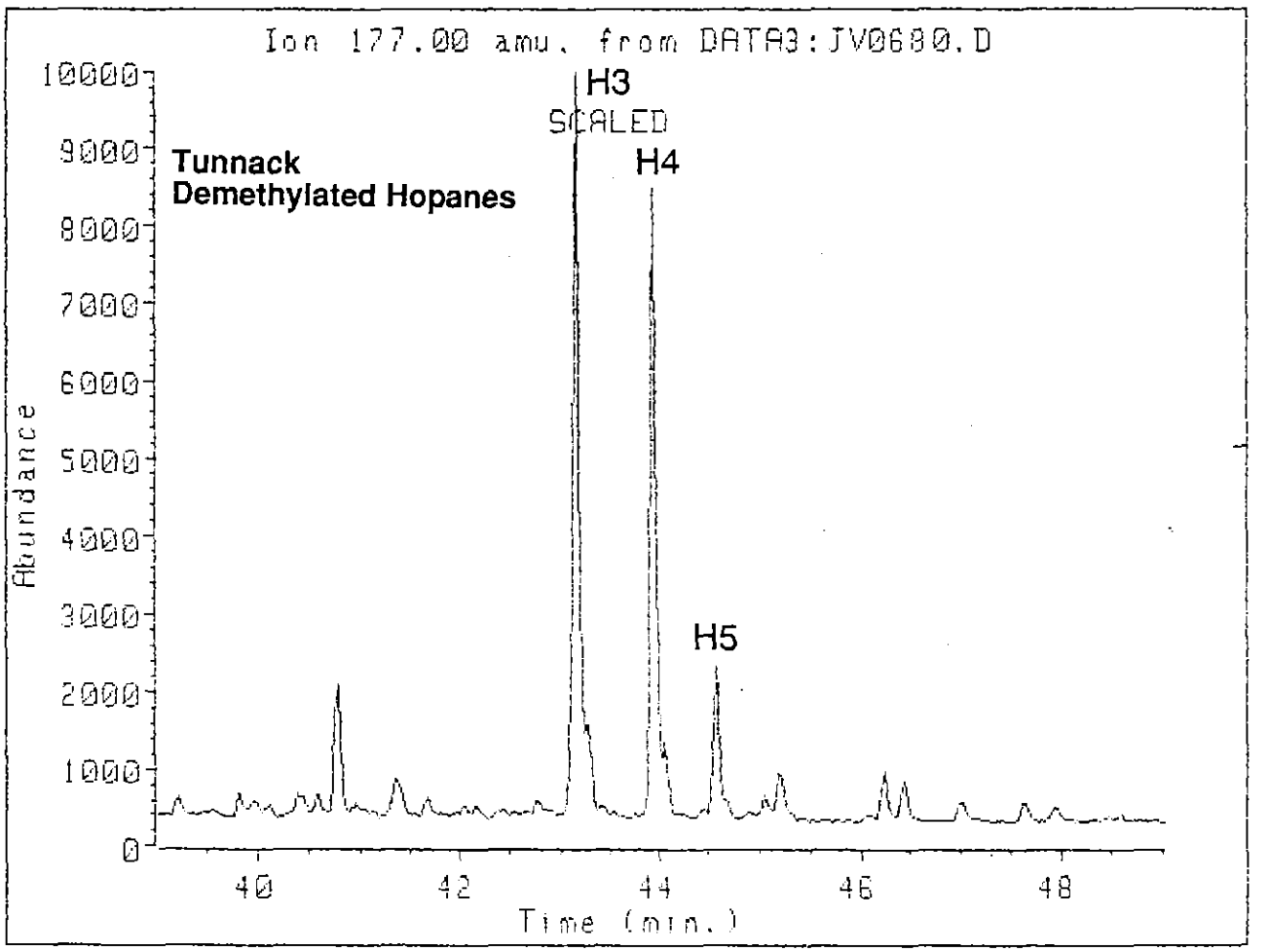
Ion 177.00 amu. from DATA3:JV0680.D
Tunnack
Demethylated Hopanes
H3
SCALED
H4
H5
Abundance
Time (min.)

Fig. 8(g)

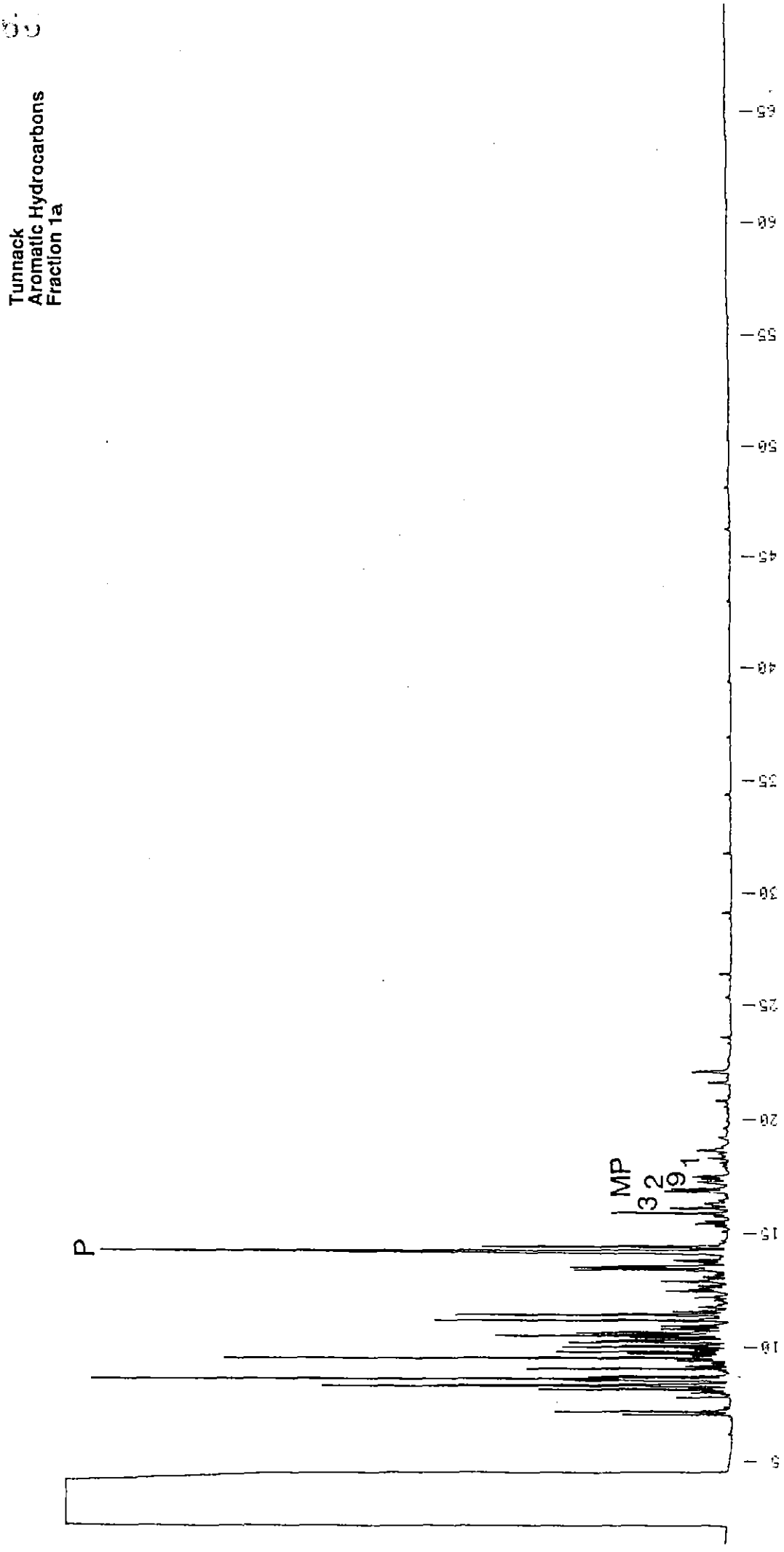
Tunnack
Aromatic Hydrocarbons
Fraction 1a
65
60
55
50
45
40
35
30
25
20
15
10
5
P
MP
3
2
9
1

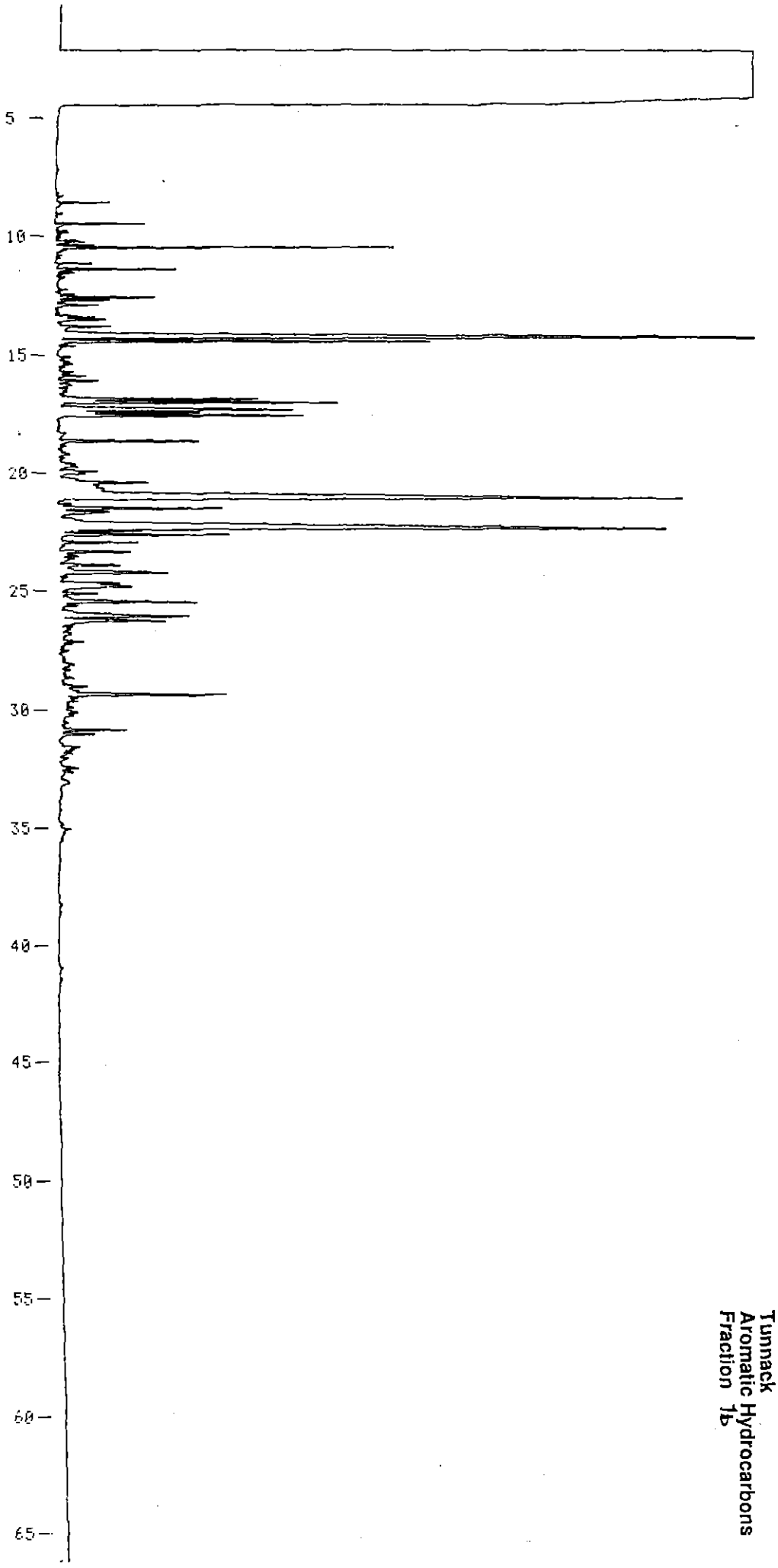

Tunnack
Aromatic Hydrocarbons
Fraction 1b

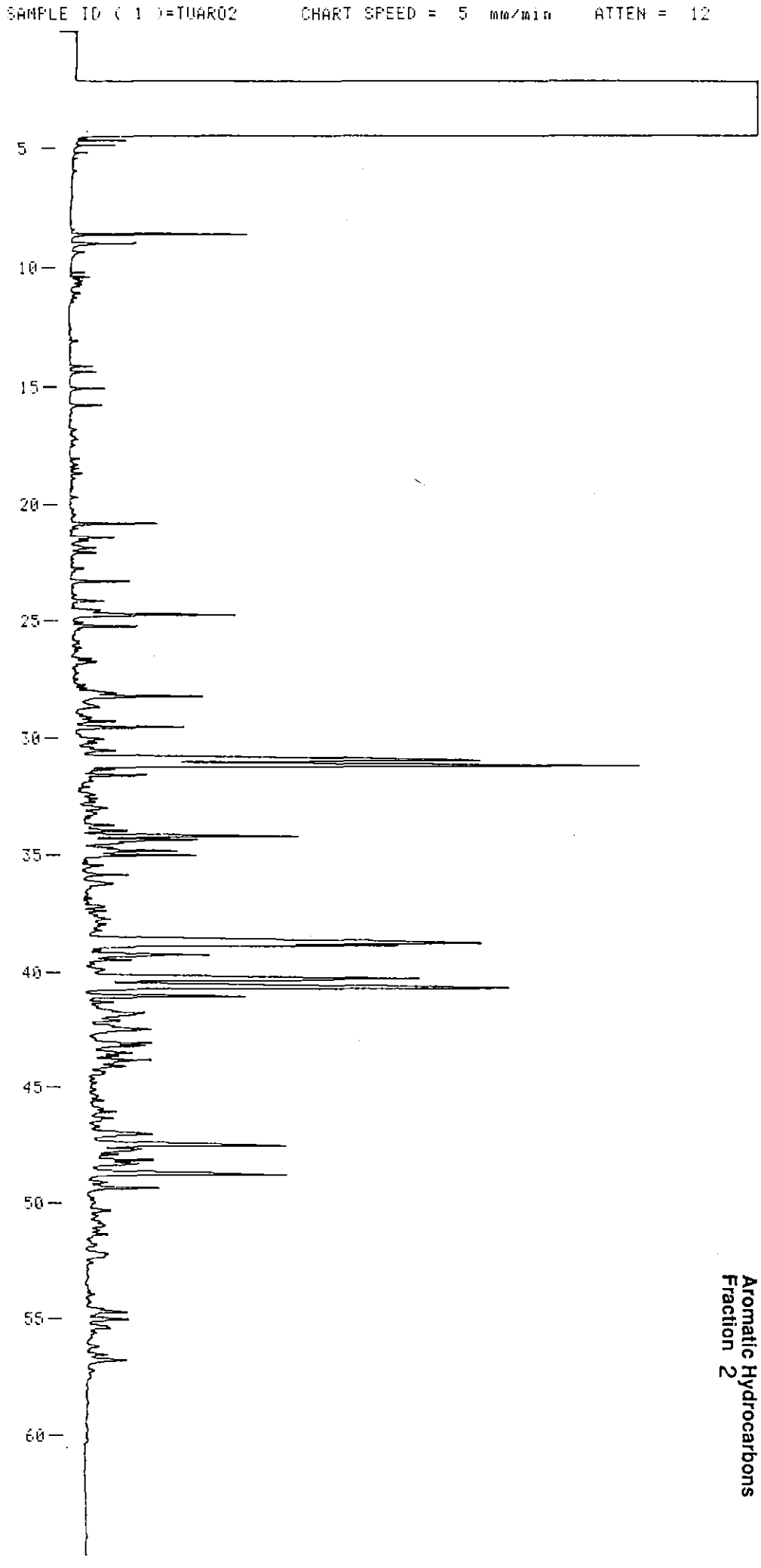

Tunnack
Aromatic Hydrocarbons
Fraction 2

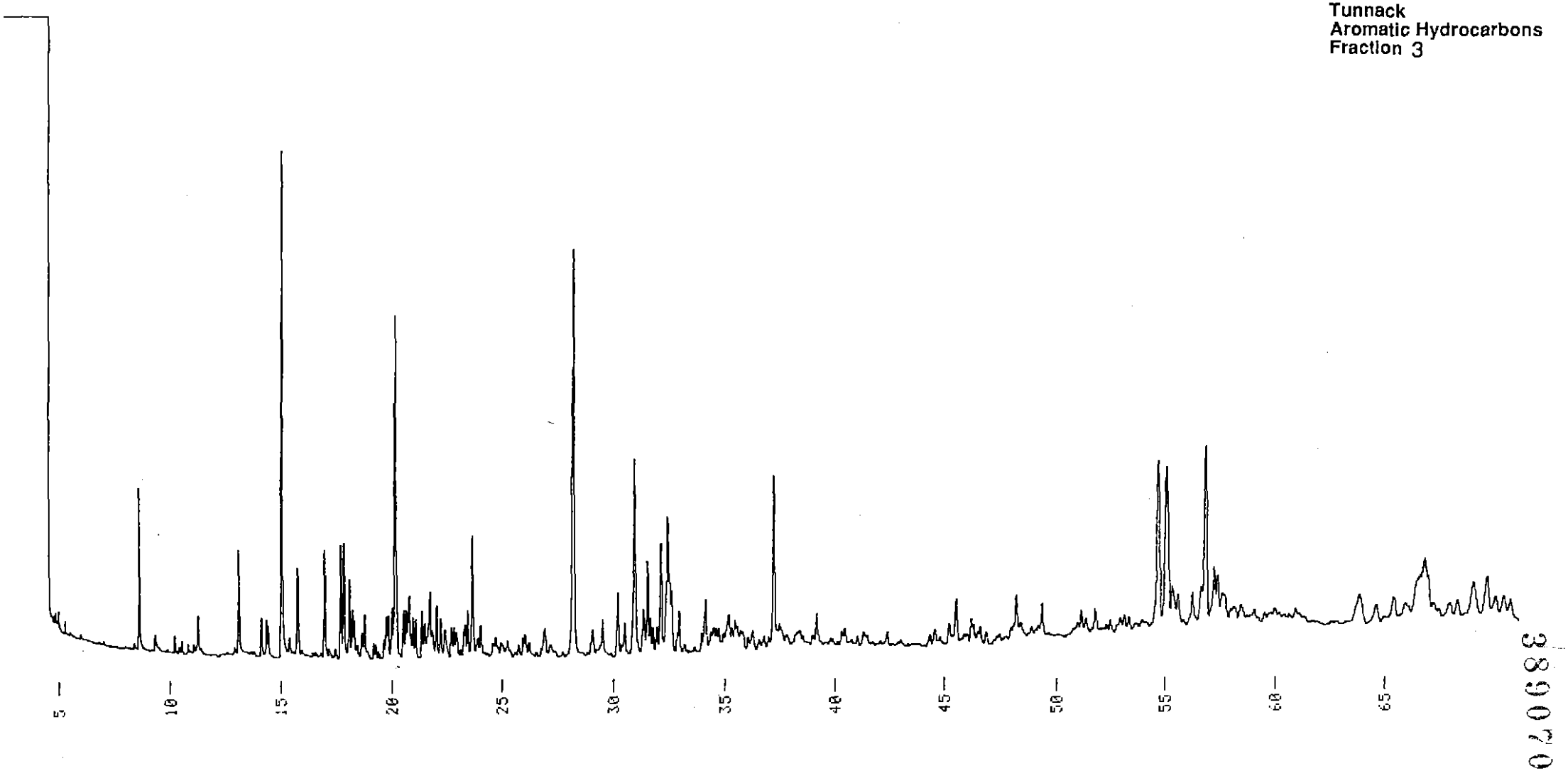
Tunnack
Aromatic Hydrocarbons
Fraction 3
5
10
15
20
25
30
35
40
45
50
55
60
65

Fig. 8(h)

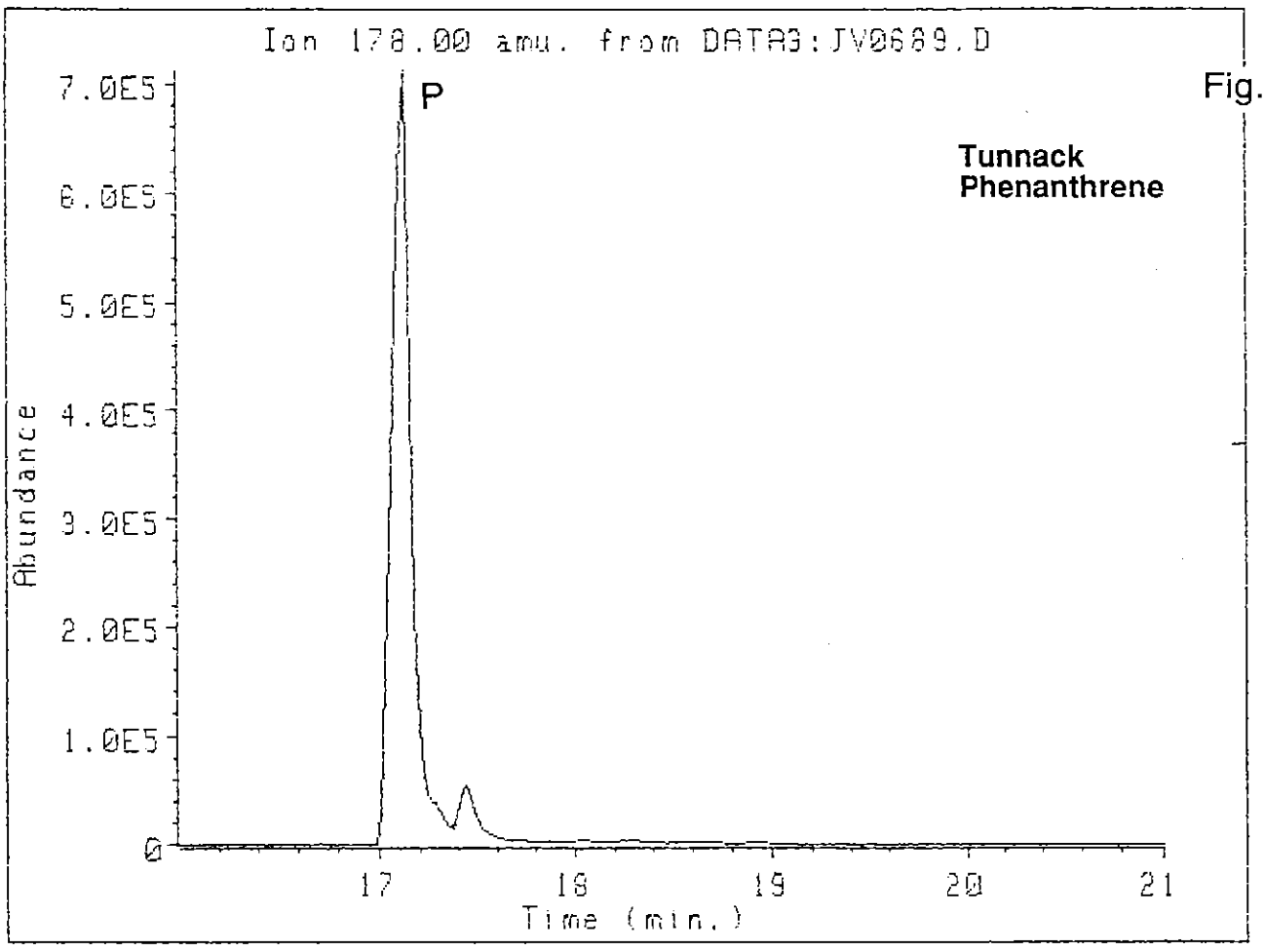
Ion 178.00 amu. from DATA3:JV0689.D
P
Tunnack
Phenanthrene
7.0E5
6.0E5
5.0E5
4.0E5
3.0E5
2.0E5
1.0E5
0
Abundance
17
18
19
20
21
Time (min.)

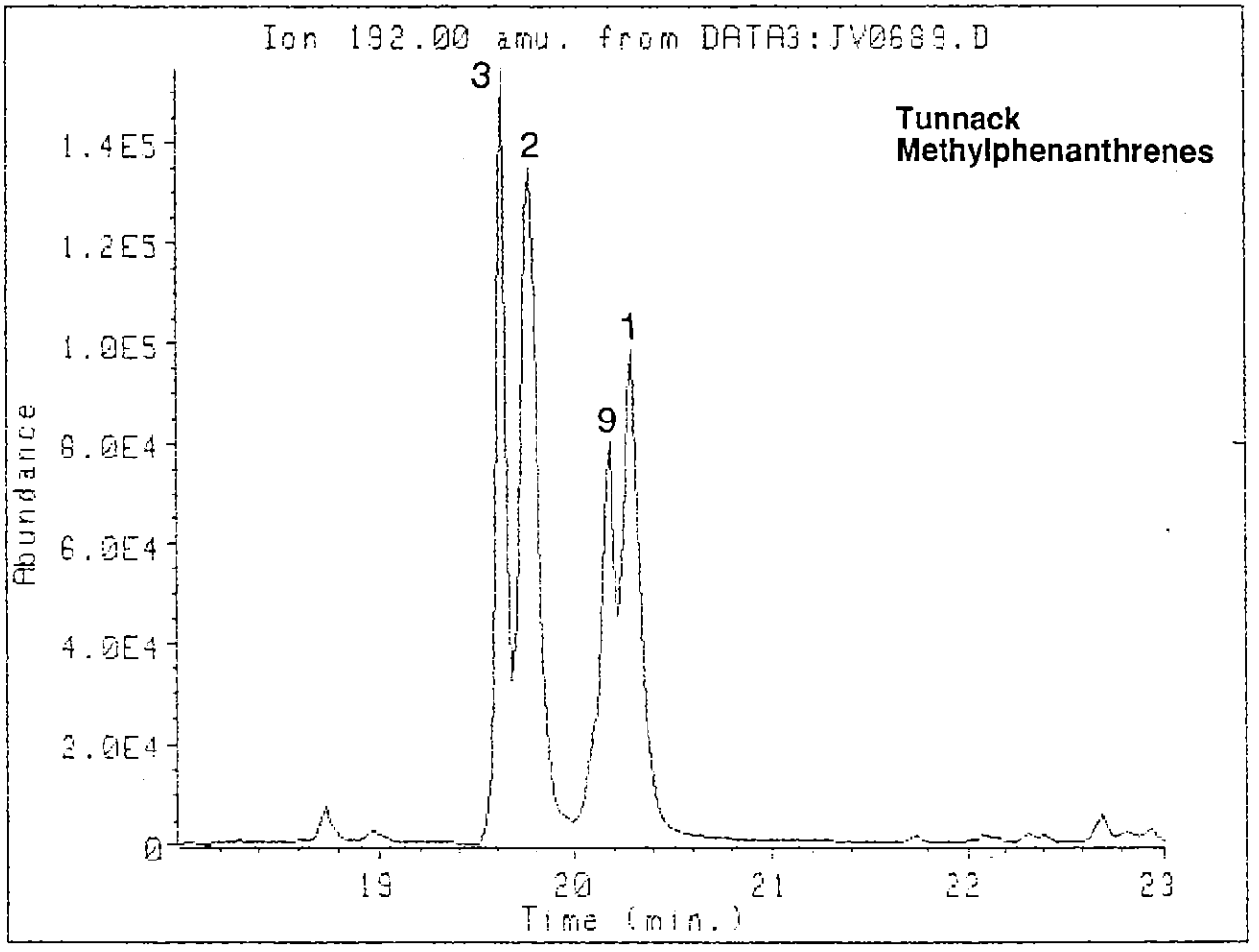
Ion 192.00 amu. from DATA3:JV0689.D
3
2
1
9
Tunnack
Methylphenanthrenes
1.4E5
1.2E5
1.0E5
8.0E4
6.0E4
4.0E4
2.0E4
0
Abundance
19
20
21
22
23
Time (min.)

Fig. 8(i)

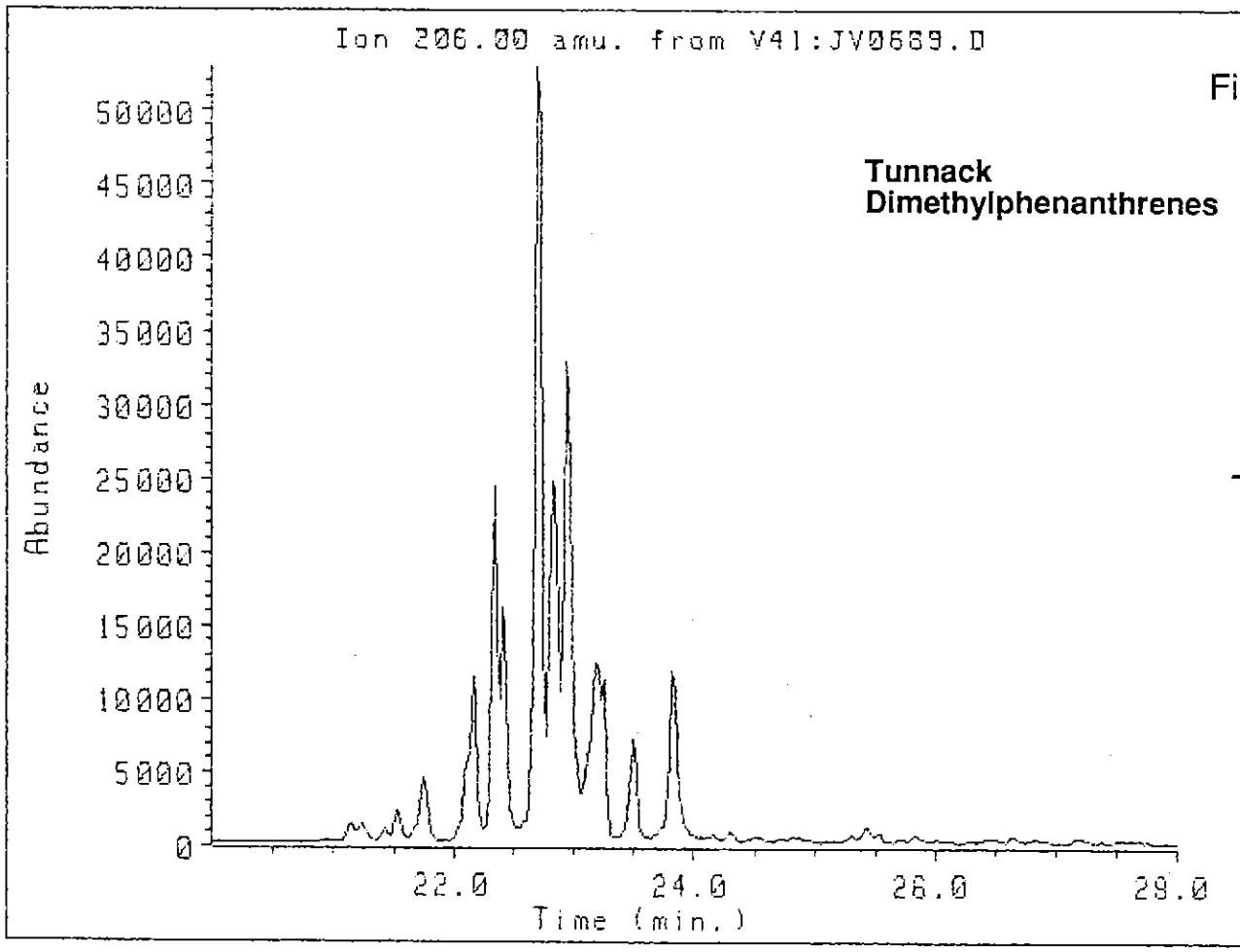
Ion 206.00 amu. from V41:JV0669.D
Tunnack
Dimethylphenanthrenes
Abundance
50000
45000
40000
35000
30000
25000
20000
15000
10000
5000
0
22.0
24.0
26.0
28.0
Time (min.)

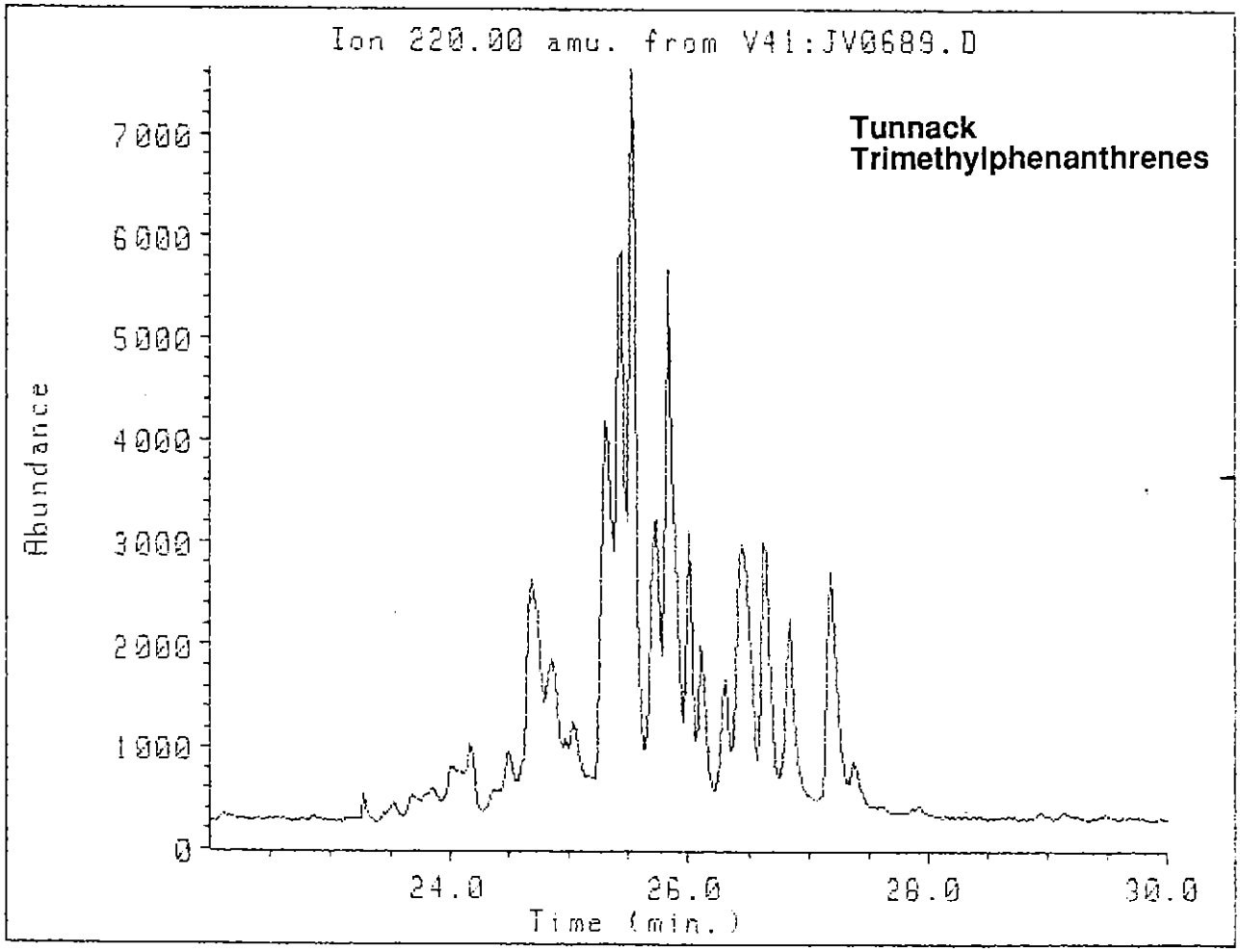
Ion 220.00 amu. from V41:JV0689.D
Tunnack
Trimethylphenanthrenes
Abundance
7000
6000
5000
4000
3000
2000
1000
0
24.0
26.0
28.0
30.0
Time (min.)

4. Tars from Cape Jaffa, South Australia and the south coast of Western Australia.

These two tars, although from very different locations, had similar geochemical compositions and so are discussed together. Both samples were obtained from the Queen Victoria Museum in Launceston by Mr M. Bendall. They are black shiny tars which break with conchoidal fracture.

Aliphatic hydrocarbons in the Cape Jaffa sample comprised 13.8% of the total extract, aromatic hydrocarbons 10.6% with most of the extractable material being resins and asphaltenes (75.6%). The corresponding values for the Western Australia sample were 17.3, 5.8 and 76.9% (Table 1).

Aliphatic Hydrocarbons

The aliphatic C_{15+} hydrocarbons (Figs. 9a and 10a) in both samples were similar and extended from about n-C_{14} to about n-C_{40} with no odd or even preference. Pristane was only slightly more abundant than phytane in the Cape Jaffa sample, and of similar abundance in the Western Australia sample. Pristane/phytane ratios were 1.21 and 1.04, and n-C_{17}/pristane ratios were 2.56 and 2.72 in the Cape Jaffa and Western Australian samples respectively. These distributions are quite similar to those isolated previously from the Tasmanian bitumen samples obtained from the Launceston museum (Volkman and O'Leary, 1990a).

(a) Steranes: Sterane distributions in the two samples are very similar as shown by mass fragmentograms for m/z 217 and m/z 218 (Figs. 9b and 10b). These distributions are also very similar to those from the Tasmanian bitumens. They are typical of a moderately mature crude oil. C_{27} steranes were slightly more abundant than C_{29} steranes, which in turn were slightly more abundant than C_{28} steranes.

Diasteranes were significant constituents (m/z 259; Fig. 9d and 10d) in both tar samples. The relative amounts of steranes to diasteranes was very comparable and the ratios of C_{27}, C_{28} and C_{29} components in the diasteranes were only slightly different to the sterane ratios. The m/z 259 mass fragmentograms were remarkably close to many of those obtained from the Tasmanian bitumens, even to the presence of minor unidentified components.

A complex mixture of methyl steranes (m/z 231; Figs. 9d and 10d) was also present in both samples, although at much lower concentrations, and again the patterns matched those obtained from the Tasmanian bitumens (Volkman and O'Leary, 1990a). However, there were small differences between the two fingerprints. The Cape Jaffa sample contains a few extra peaks which are minor constituents in the Western Australian sample. These are due to small amounts of triaromatic steroids which had bled into the aliphatic hydrocarbon fraction during column chromatography. This effect can also be seen in a few of the Tasmanian bitumens, particularly the samples from Deep Creek and Albina B (Volkman and O'Leary, 1990a). When this fact is taken into account, all the distributions match very closely.

Sterane maturity parameters are consistent with a moderately mature oil. C_{29} sterane $\alpha\beta\beta$ isomers (peaks S10 and S11) are very slightly less abundant in the m/z 217 mass fragmentograms than the $\alpha\alpha\alpha$ isomers (peaks S9 and S12), and the ratio of 20S and 20R isomers is slightly less than 1.

The sterane biomarker distributions are similar to those previously reported from Ordovician limestones obtained from Ida Bay and Queenstown (Volkman, 1988 and Fig. 4), although the maturity levels in the latter are slightly higher. A large number of bitumens have been collected on South Austrlian beaches, and a few ot these also have similar sterane biomarker fingerprints (McKirdy *et al.*, 1986).

Hopanes: Hopane distributions as represented by mass fragmentograms of the major fragment ion m/z 191 over the C_{27}–C_{32} carbon number ranges are shown in Figs. 9e,f and 10e,f.

The two hopane distributions are almost superimposable, except that the C_{29} hopane is slightly enhanced in the Western Australian sample and its Ts/Tm ratio suggest a very slightly greater maturity. Moretanes were very minor constituents, which is consistent with moderately mature oil.

All of the hopane maturity parameters are very similar to those obtained from Ida Bay Ordovician limestone analysed previously (Volkman, 1988 and Fig. 5).

Tricyclic alkanes: A series of tricyclic alkanes is present in both tars, at approximately the same low abundance relative to hopanes.

Methyl hopanes: Methyl hopanes were not detected. The m/z 205 mass fragmentograms (Figs. 9e and 10e) show only peaks due to hopanes. Methyl hopanes were not detected in the Tasmanian bitumens and the m/z 205 mass fragmentograms were very similar to those reported here (Fig. 5).

Demethylated hopanes: The m/z 177 mass fragmentogram indicated that C–10 demethylated hopanes were not present in either tar sample (Figs. 9f and 10f). Comparable m/z 177 mass fragmentograms were obtained from the Tasmanian bitumens.

Aromatic Hydrocarbons

Gas chromatograms of the aromatic hydrocarbons in the two tars were fairly similar (Figs. 9g and 10g), except for additional peaks in the chromatogram for the Western Australian sample due to the presence of small amounts of incompletely separated n–alkanes.

Phenanthrene and alkylated phenanthrenes: Mass fragmentograms for m/z 178 (phenanthrene) and 192 (methylphenanthrenes) for the two samples are almost identical (Figs. 9h and 10h). The 2– and 3–methylphenanthrene isomers are much less abundant than the 9–methylphenanthrene isomer, as found in the Tasmanian tars (Volkman and O'Leary, 1990b).

The equivalent vitrinite reflectances calculated from the MPI values was 0.7 for the Cape Jaffa sample and 0.8 for the Western Australian sample. Note the slightly higher maturity for the latter which is in accord with other biomarker parameters. The distributions of dimethylphenanthrenes and trimethylphenanthrenes determined from mass fragmentograms for m/z 206 and 220 respectively are the same in both samples (Figs. 9i and 10i).

A GC–MS search for aromatic steroids revealed significant amounts of monomethyl and dimethyl triaromatic steroids (m/z 231 and 245 respectively, Figs. 9j and 10j), in both tars. The m/z 231 mass fragmentograms are very similar, but there was an enhanced abundance of C_{21} and C_{22} dimethyl triaromatic steroids in the Western Australian sample. This is suggestive of a slightly higher level of thermal maturity, which is consistent with inferences drawn from the Ts/Tm hopane ratios.

Figure 9. GC and GC–MS data for the Cape Jaffa bitumen.

(9a) Capillary gas chromatogram of the total aliphatic hydrocarbons in the Cape Jaffa bitumen. Pr: pristane; Ph: phytane. n–Alkanes are denoted by n–C_X where "x" is the number of carbon atoms.

(9b). Mass fragmentograms for m/z 217 and 218 showing distribution of C_{26}–C_{30} steranes (labelled S) and diasteranes (labelled D) in the Cape Jaffa bitumen. See Key 1 for peak identifications.

(9c) Mass fragmentograms for m/z 217 and 218 showing distribution of C_{21}–C_{23} steranes in the Cape Jaffa bitumen.

(9d) Mass fragmentograms for m/z 259 showing distribution of C_{27}–C_{30} diasteranes (labelled D), and m/z 231 showing distribution of C_{28}–C_{30} 4–methyl steranes in the Cape Jaffa bitumen.

(9e) Mass fragmentograms for m/z 191 showing distribution of C_{27}–C_{35} hopanes and m/z 205 showing distribution of methyl hopanes in the Cape Jaffa bitumen. See Keys 2 and 3 for peak identifications.

(9f) Mass fragmentograms for m/z 191 showing distribution of C_{27}–C_{32} hopanes and m/z 177 showing distribution of demethylated hopanes (none found) in the Cape Jaffa bitumen.

(9g) Capillary gas chromatogram of the total aromatic hydrocarbons in the Cape Jaffa bitumen.

(9h) Mass fragmentograms for m/z 178 and 192 showing the presence of phenanthrene and distribution of methylphenanthrenes respectively in the Cape Jaffa bitumen.

(9i) Mass fragmentograms for m/z 206 and 220 showing the distribution of di– and trimethylphenanthrenes in the Cape Jaffa bitumen.

(9j) Mass fragmentograms for m/z 231 and 245 showing the distribution of triaromatic steroidal hydrocarbons (with one and two methyl groups in the ABC ring system respectively) in the Cape Jaffa bitumen.

Fig. 9(a)

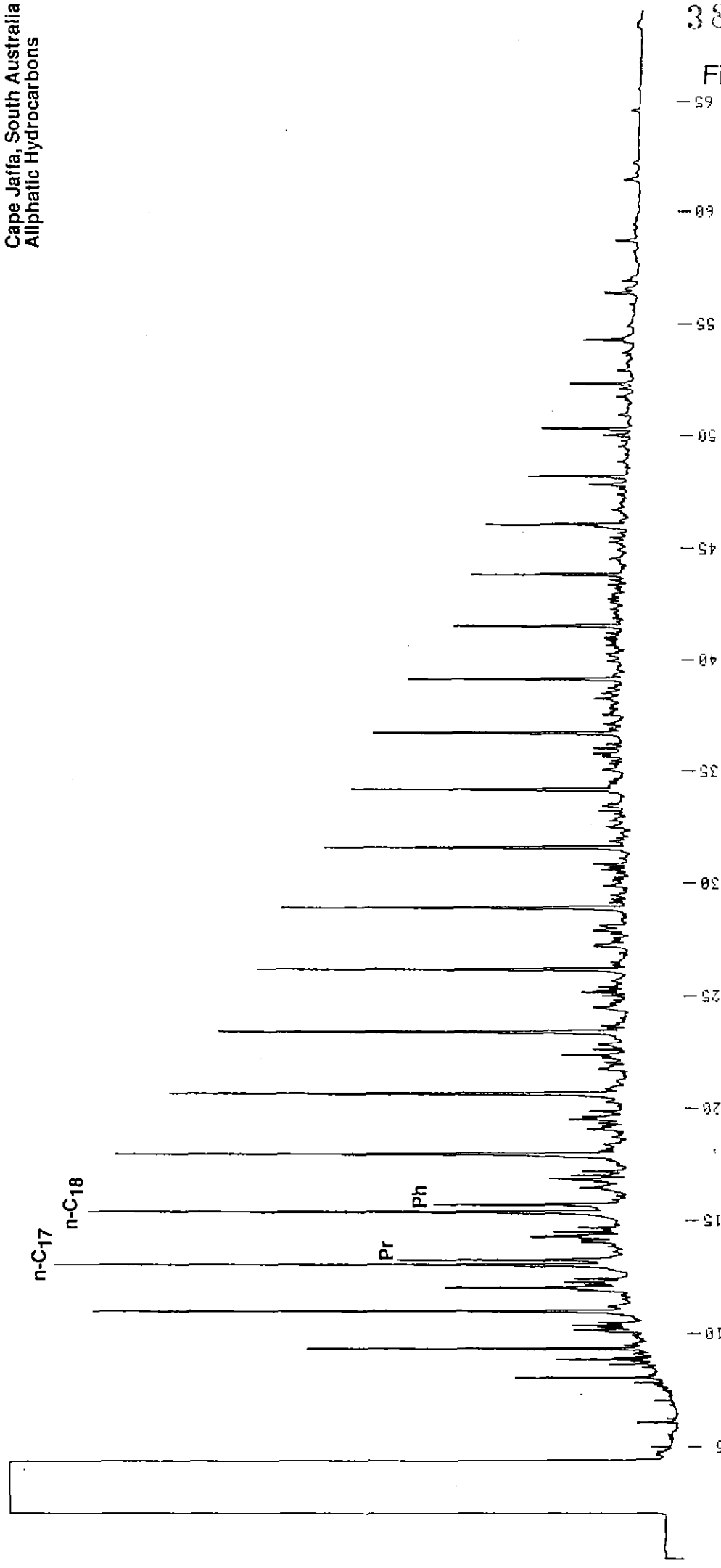
Cape Jaffa, South Australia
Allphatic Hydrocarbons
n-C17
n-C18
Pr
Ph
65
60
55
50
45
40
35
30
25
20
15
10
5

5 cm

Fig. 9(b)

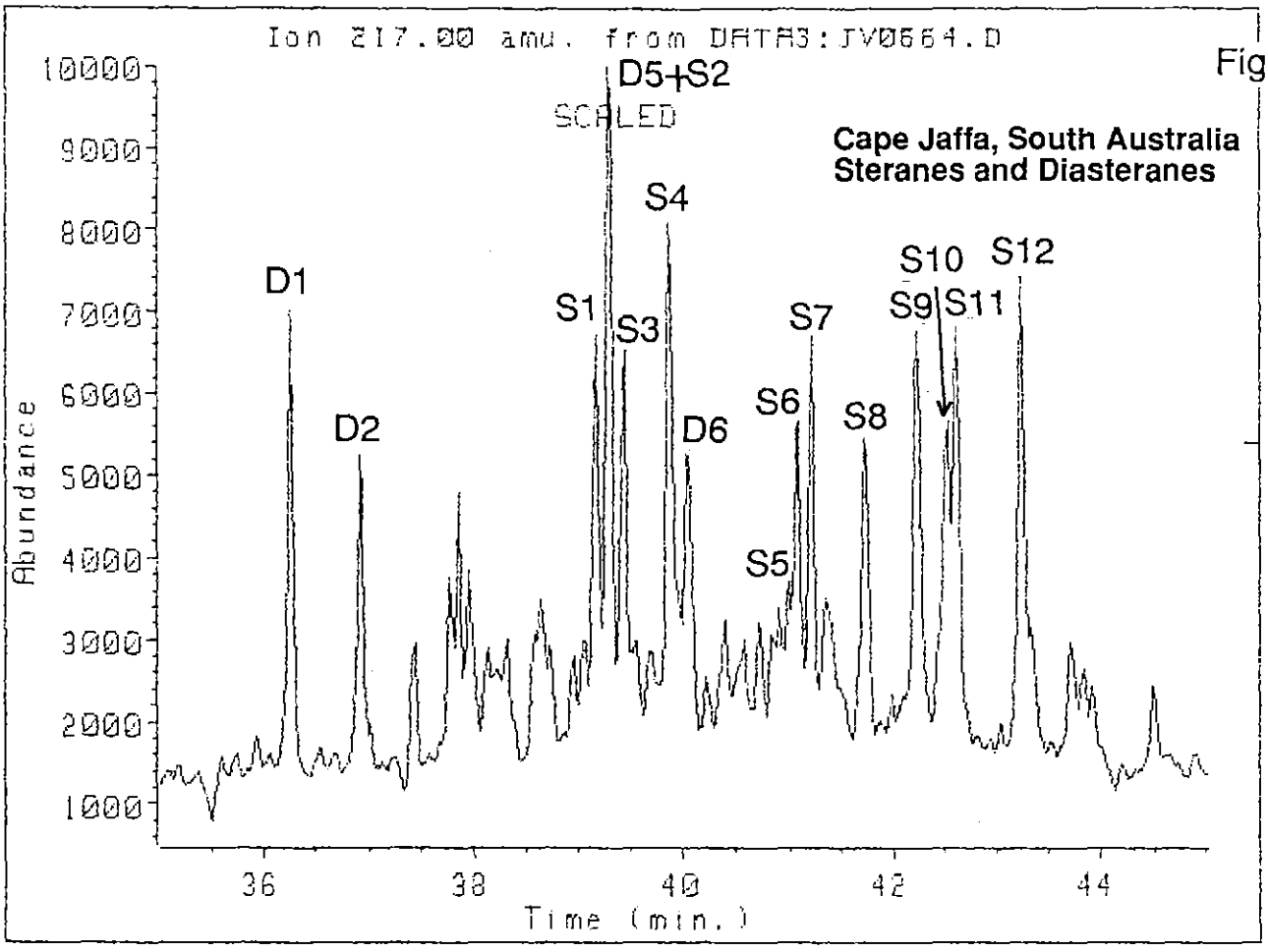
Ion 217.00 amu. from DATA3:JV0664.D
SCALED
Cape Jaffa, South Australia
Steranes and Diasteranes
D1
D2
D5+S2
S1
S3
S4
D6
S5
S6
S7
S8
S9
S10
S11
S12
Abundance
Time (min.)

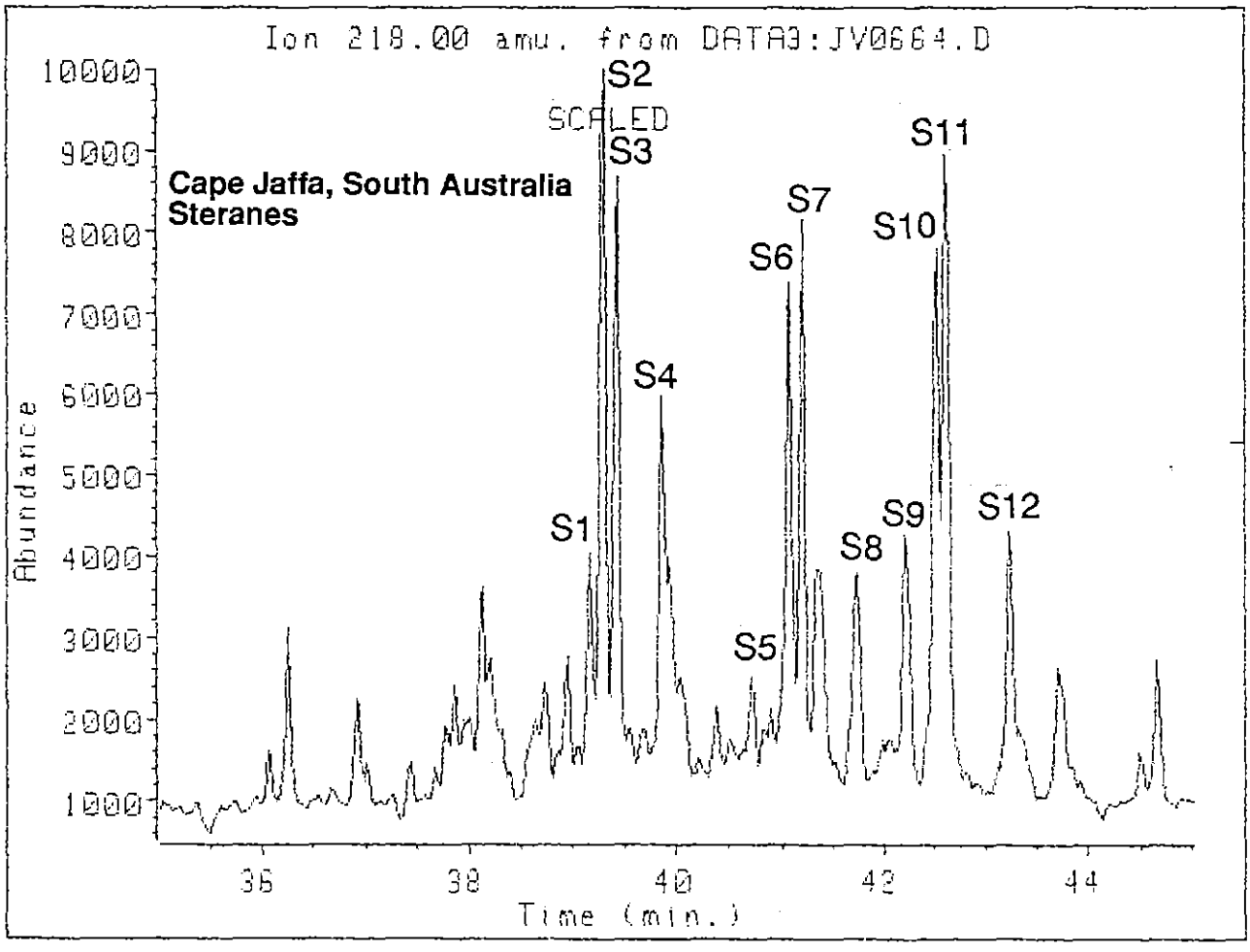
Ion 218.00 amu. from DATA3:JV0664.D
SCALED
Cape Jaffa, South Australia
Steranes
S1
S2
S3
S4
S5
S6
S7
S8
S9
S10
S11
S12
Abundance
Time (min.)

5 cm

Fig. 9(c)

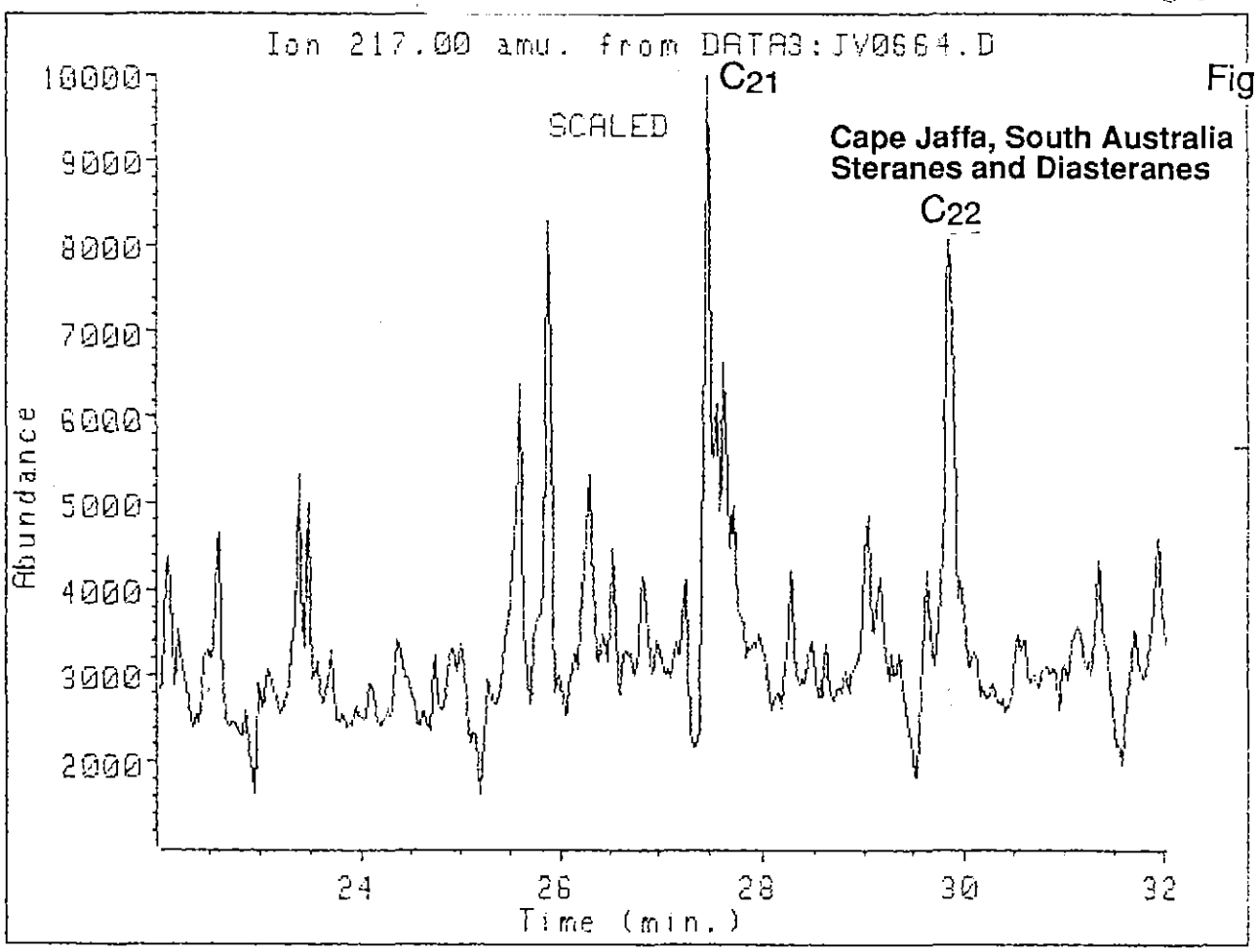
Ion 217.00 amu. from DATA3:JV0664.D
SCALED
C21
C22
Cape Jaffa, South Australia
Steranes and Diasteranes
Abundance
10000
9000
8000
7000
6000
5000
4000
3000
2000
24
26
28
30
32
Time (min.)

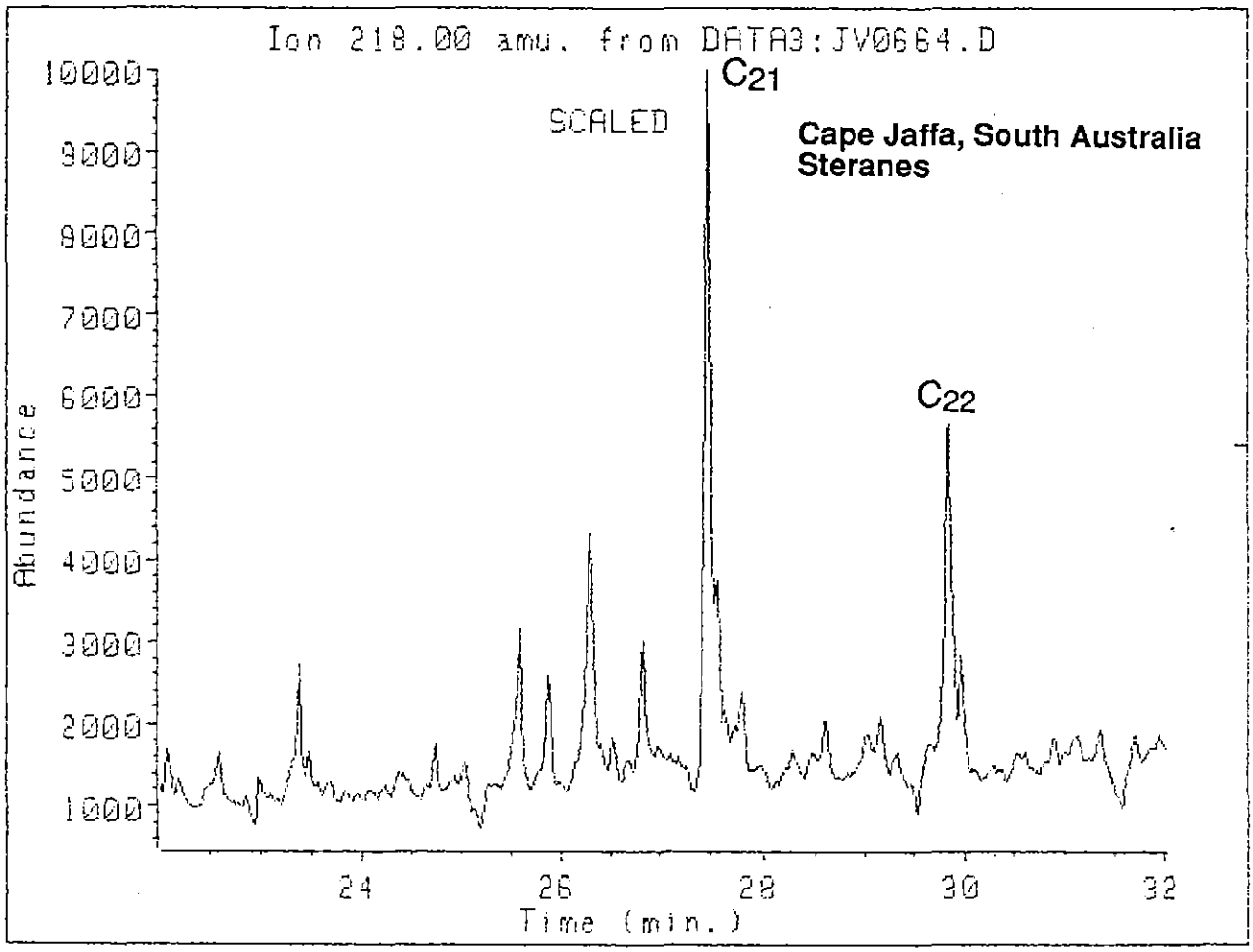
Ion 218.00 amu. from DATA3:JV0664.D
SCALED
C21
C22
Cape Jaffa, South Australia
Steranes
Abundance
10000
9000
8000
7000
6000
5000
4000
3000
2000
1000
24
26
28
30
32
Time (min.)

5 cm

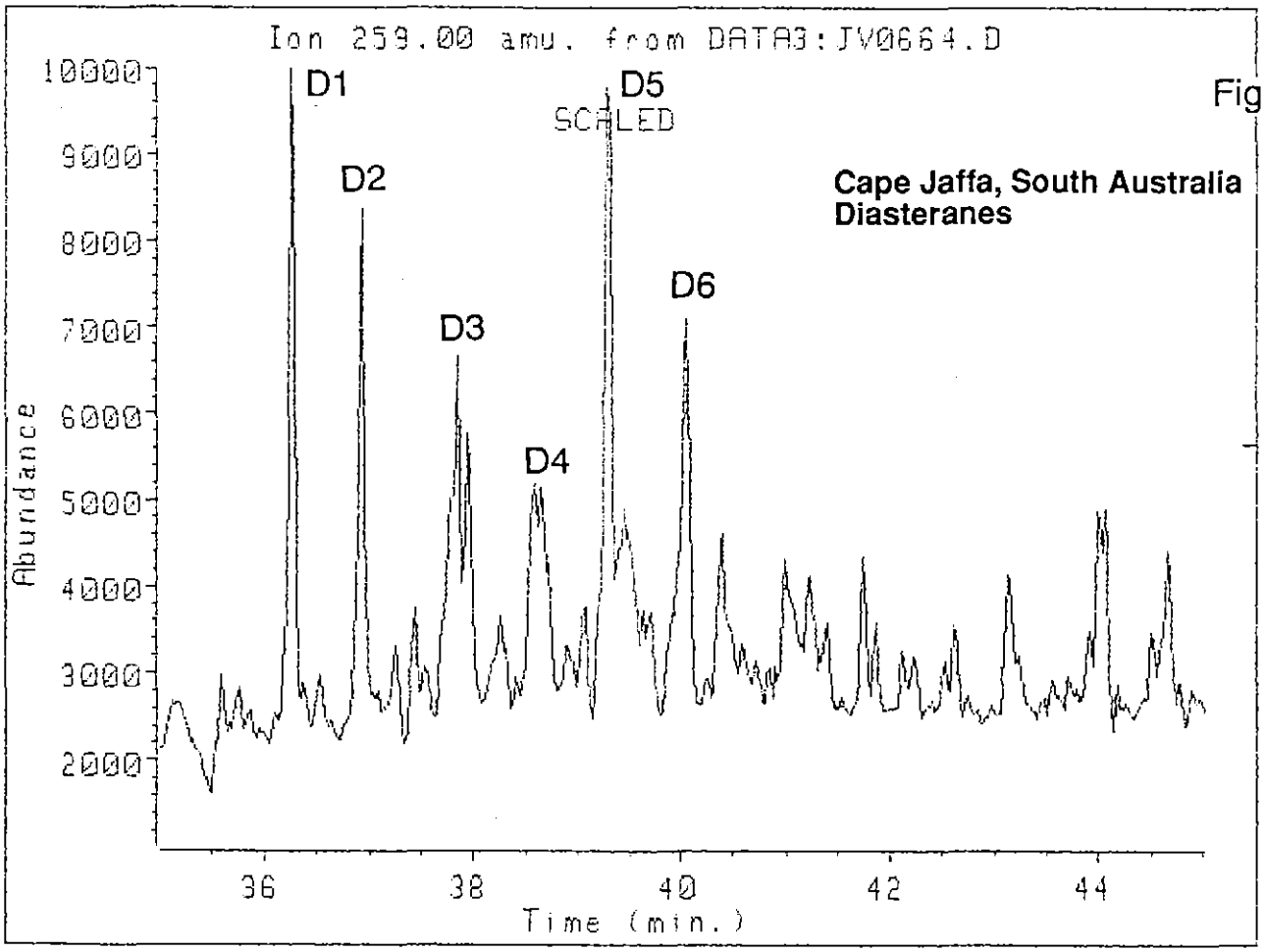
Ion 259.00 amu. from DATA3:JV0664.D
SCALED
D1
D2
D3
D4
D5
D6
Cape Jaffa, South Australia
Diasteranes
Abundance
Time (min.)

Fig. 9(d)

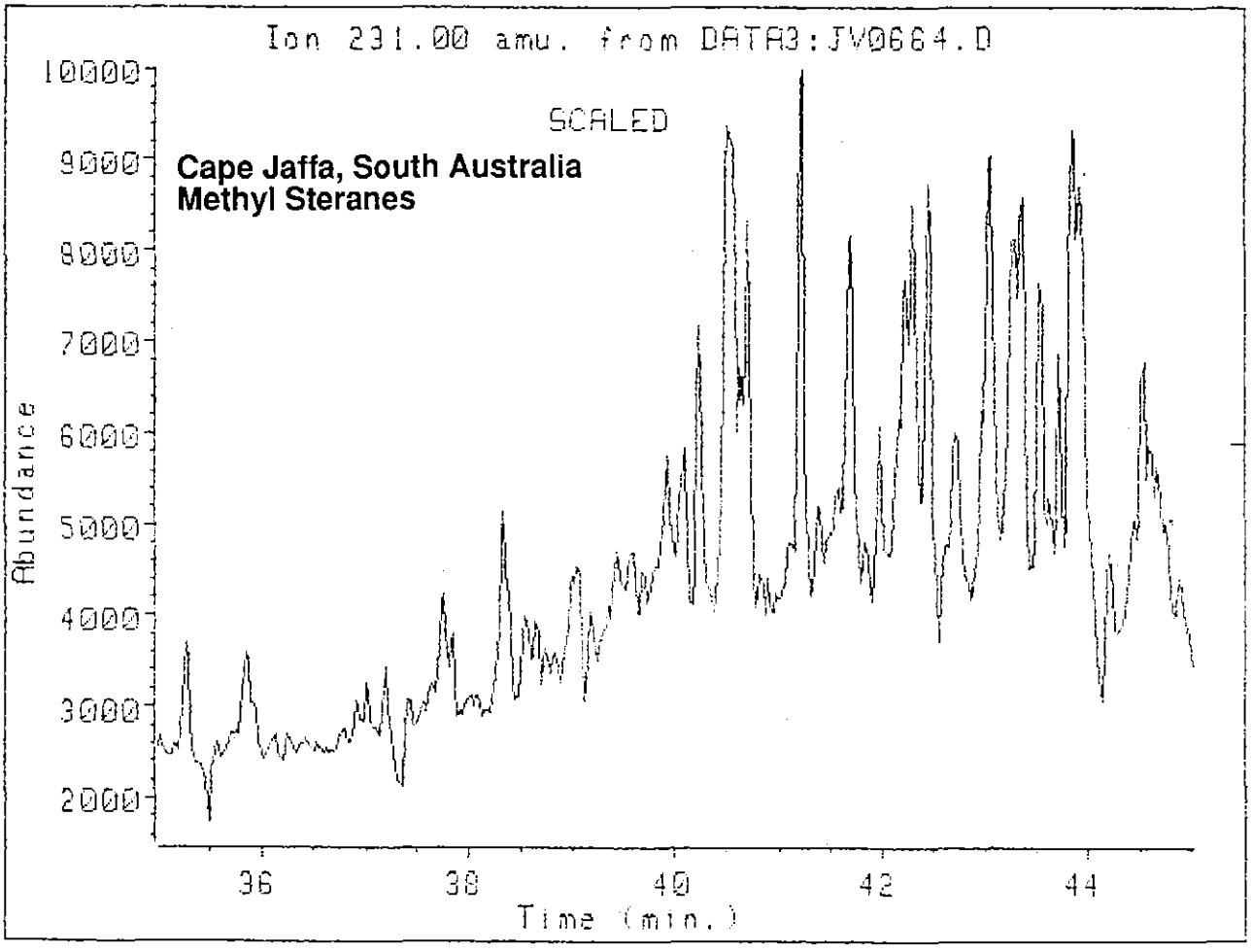
Ion 231.00 amu. from DATA3:JV0664.D
SCALED
Cape Jaffa, South Australia
Methyl Steranes
Abundance
Time (min.)

5 cm

Fig. 9(e)

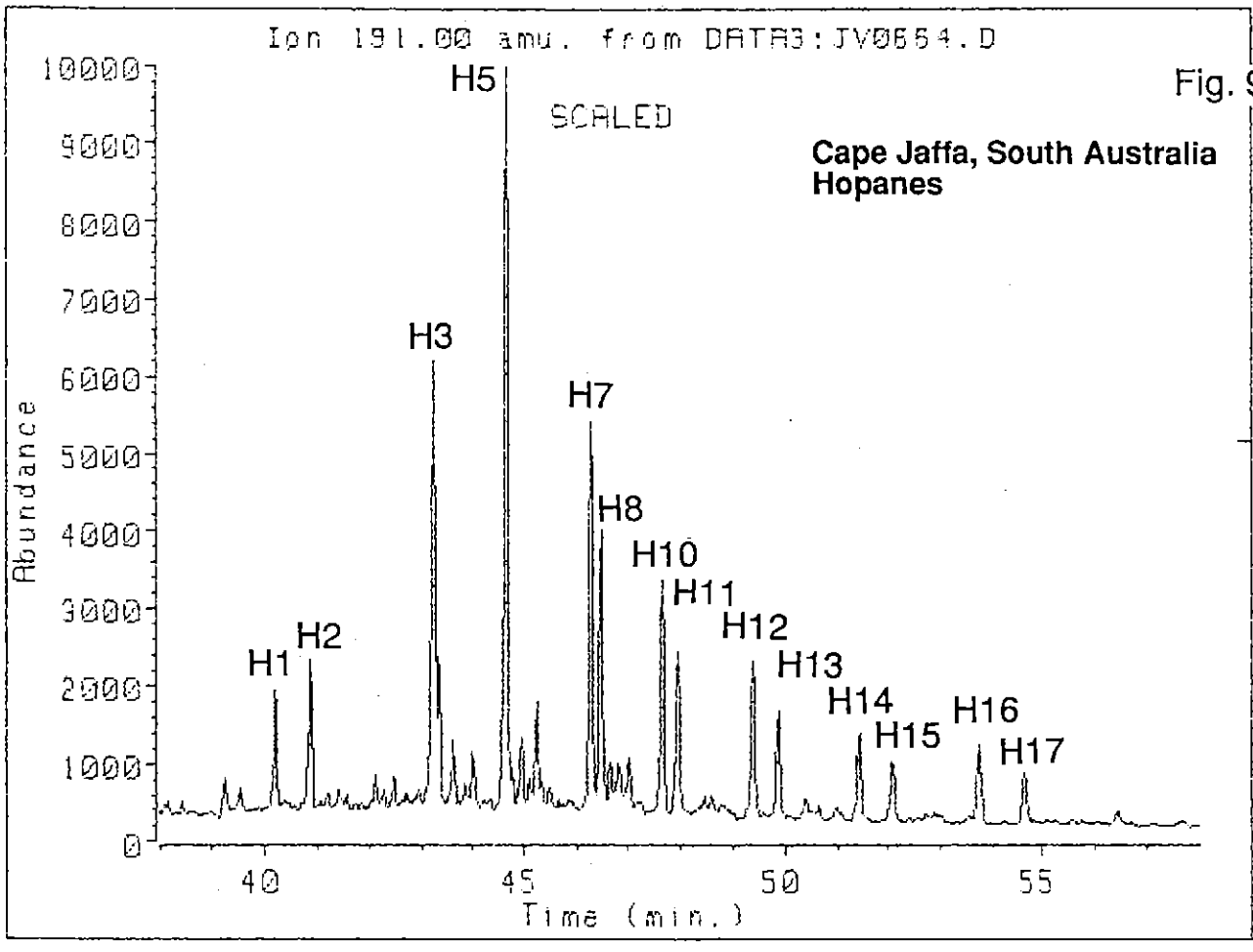
Ion 191.00 amu. from DATA3:JV0654.D
SCALED
Cape Jaffa, South Australia
Hopanes
H1
H2
H3
H5
H7
H8
H10
H11
H12
H13
H14
H15
H16
H17
Abundance
Time (min.)

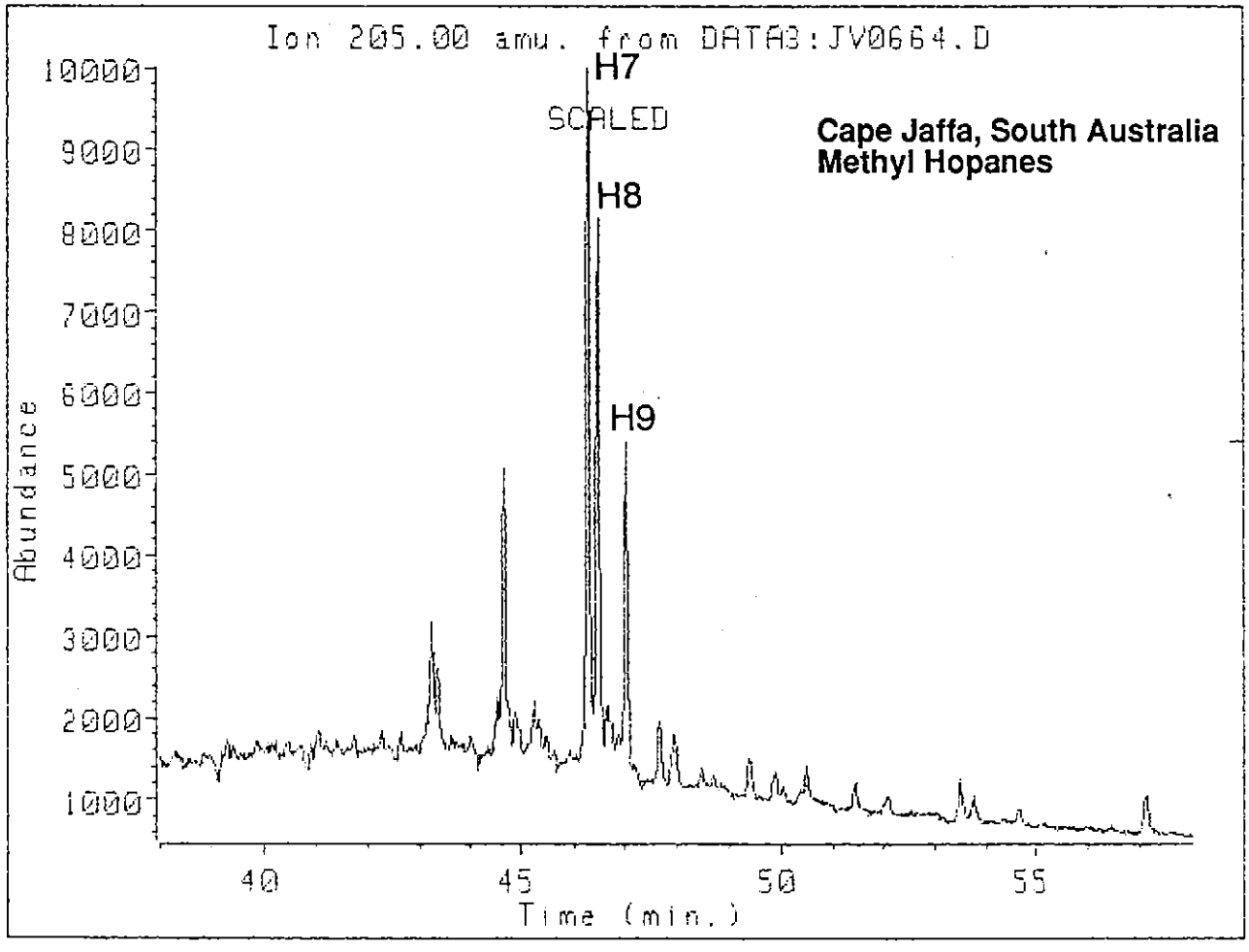
Ion 205.00 amu. from DATA3:JV0664.D
SCALED
Cape Jaffa, South Australia
Methyl Hopanes
H7
H8
H9
Abundance
Time (min.)

5 cm

Fig. 9(f)

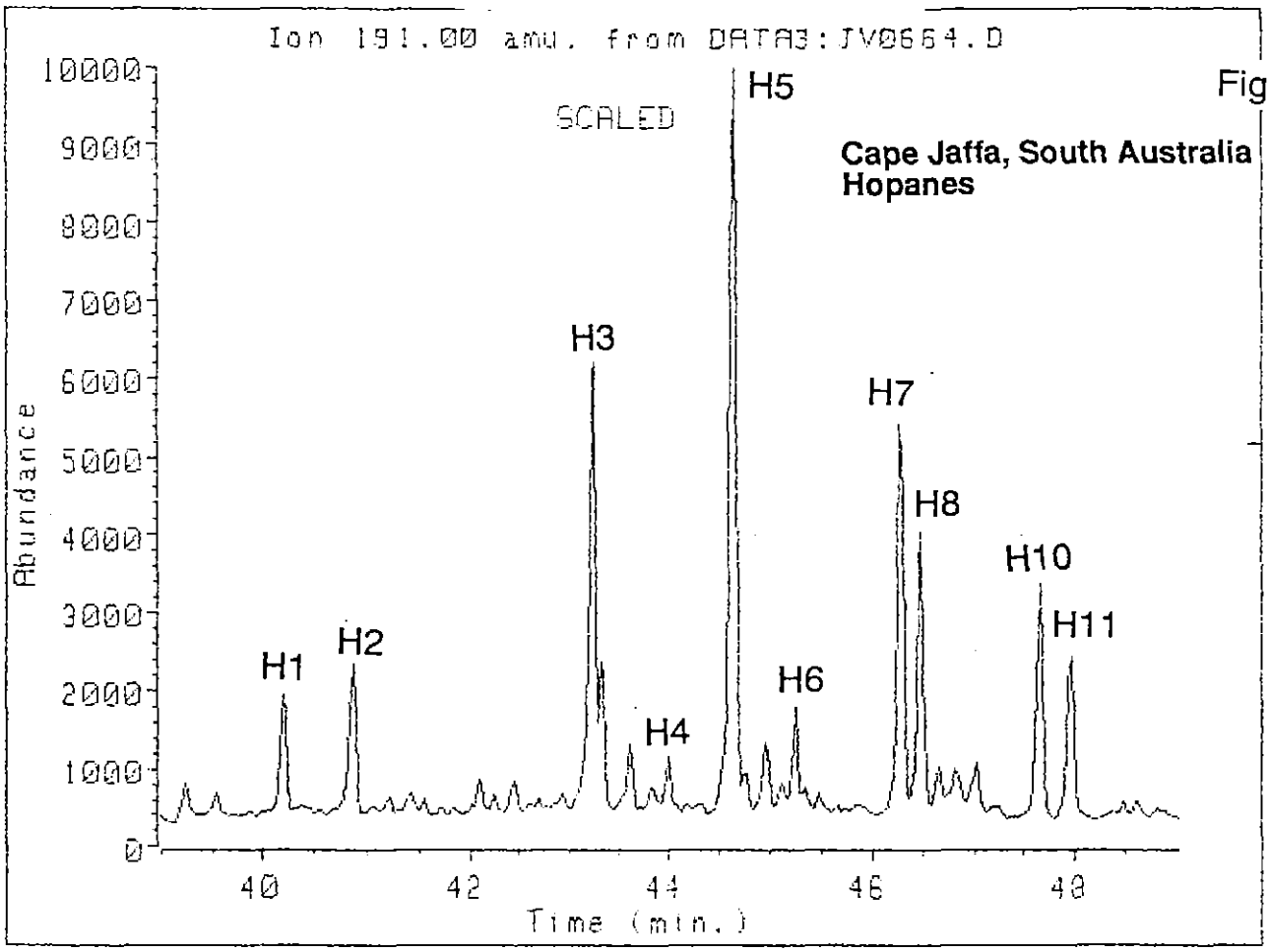
Ion 191.00 amu. from DATA3:JV0664.D
SCALED
Cape Jaffa, South Australia
Hopanes
H1
H2
H3
H4
H5
H6
H7
H8
H10
H11
Abundance
Time (min.)

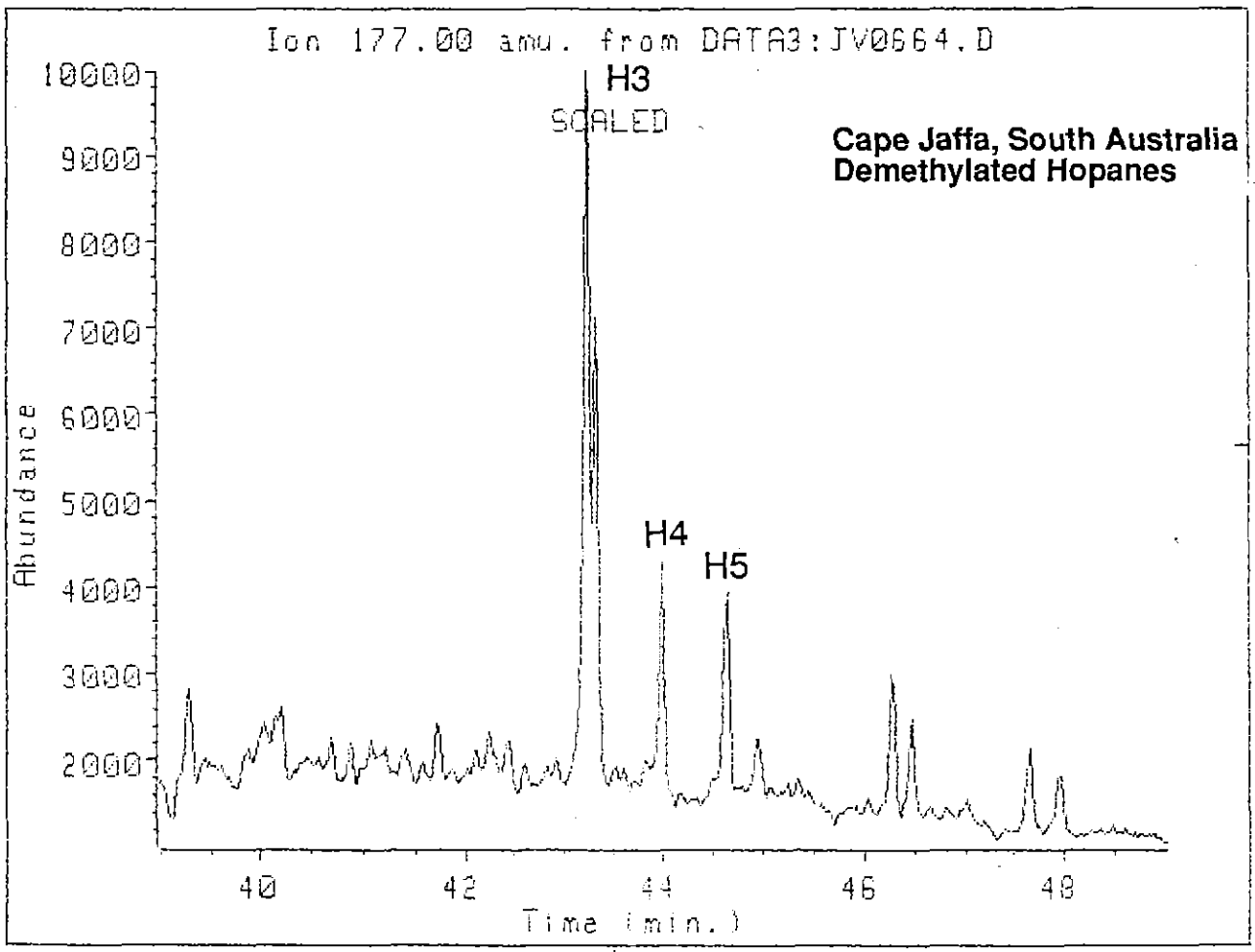
Ion 177.00 amu. from DATA3:JV0664.D
SCALED
Cape Jaffa, South Australia
Demethylated Hopanes
H3
H4
H5
Abundance
Time (min.)

Fig. 9(g)

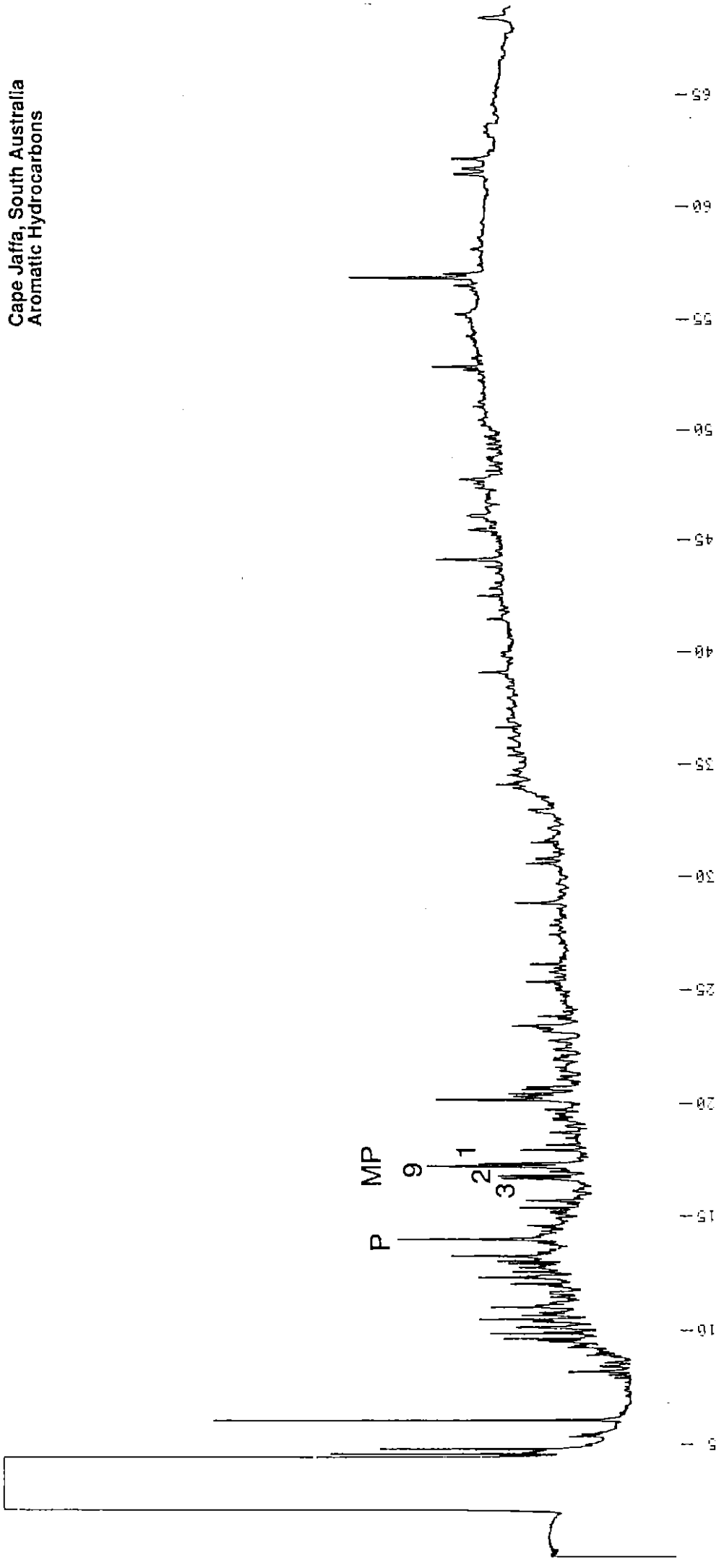
Cape Jaffa, South Australia
Aromatic Hydrocarbons
P
MP
9
1
2
3
65
60
55
50
45
40
35
30
25
20
15
10
5

Fig. 9(h)

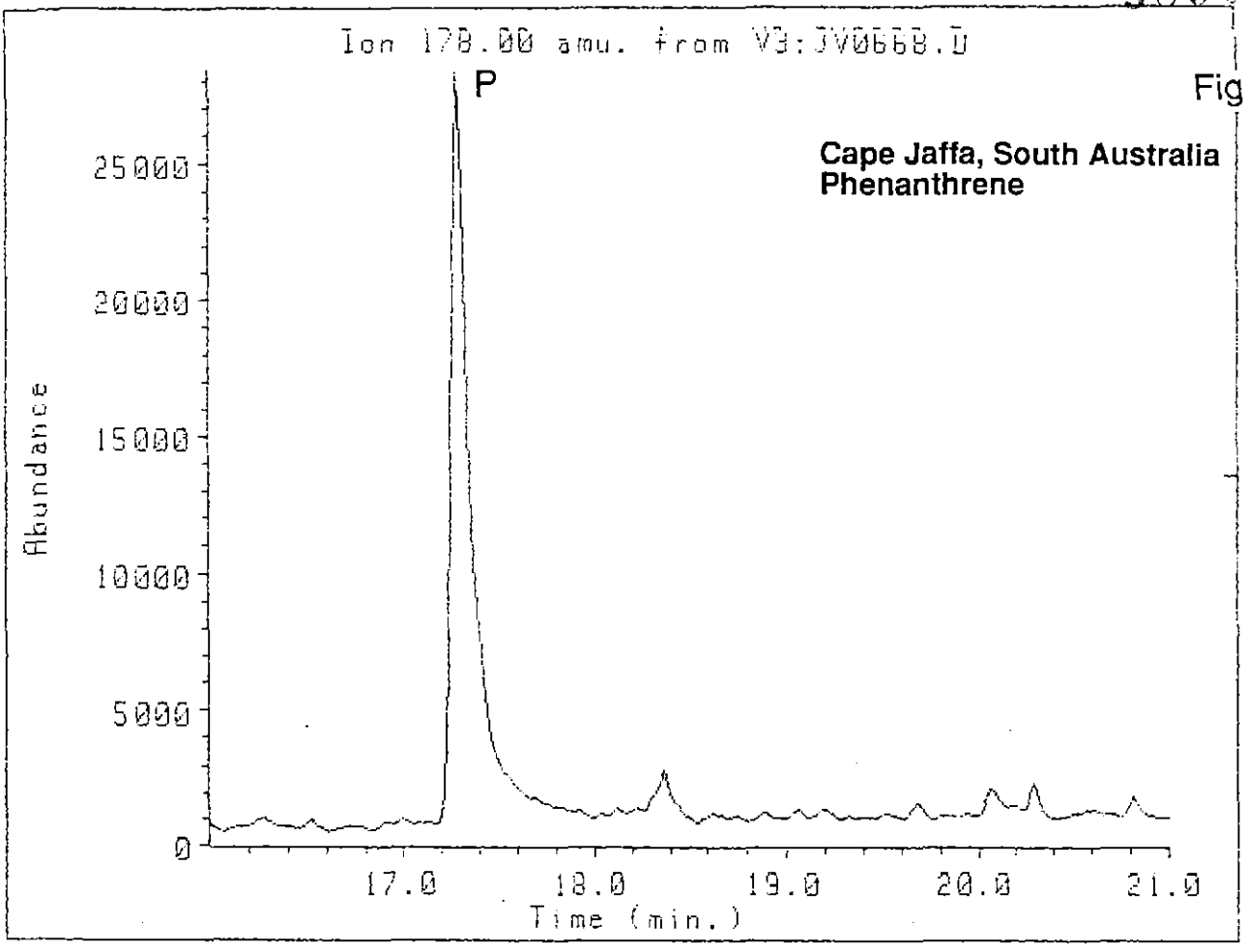
Ion 178.00 amu. from V3:JV0668.D
P
Cape Jaffa, South Australia
Phenanthrene
Abundance
25000
20000
15000
10000
5000
0
17.0
18.0
19.0
20.0
21.0
Time (min.)

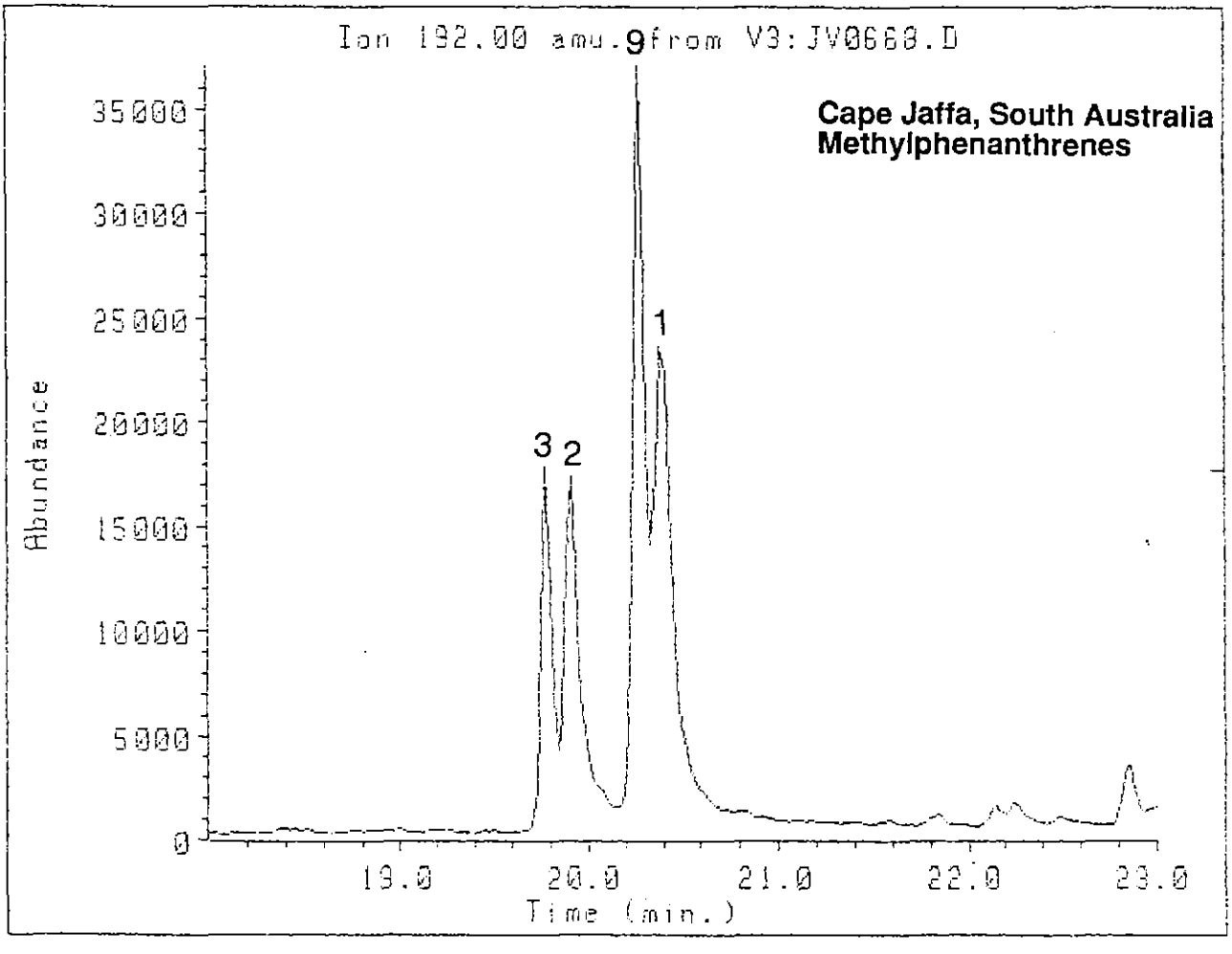
Ion 192.00 amu. from V3:JV0668.D
9
Cape Jaffa, South Australia
Methylphenanthrenes
1
2
3
Abundance
35000
30000
25000
20000
15000
10000
5000
0
19.0
20.0
21.0
22.0
23.0
Time (min.)

Fig. 9(i)

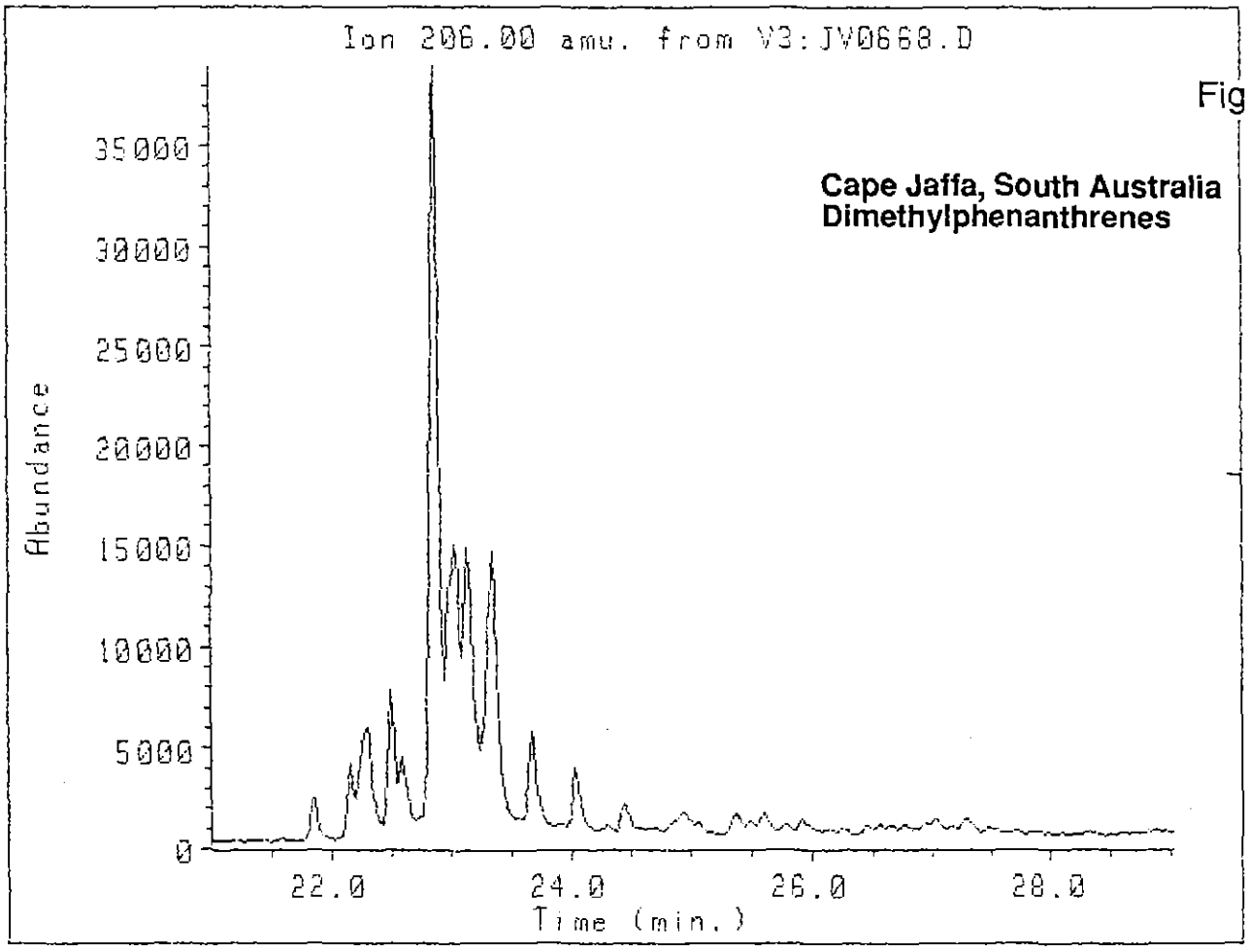
Ion 206.00 amu. from V3:JV0668.D
Cape Jaffa, South Australia
Dimethylphenanthrenes
Abundance
35000
30000
25000
20000
15000
10000
5000
0
22.0
24.0
26.0
28.0
Time (min.)

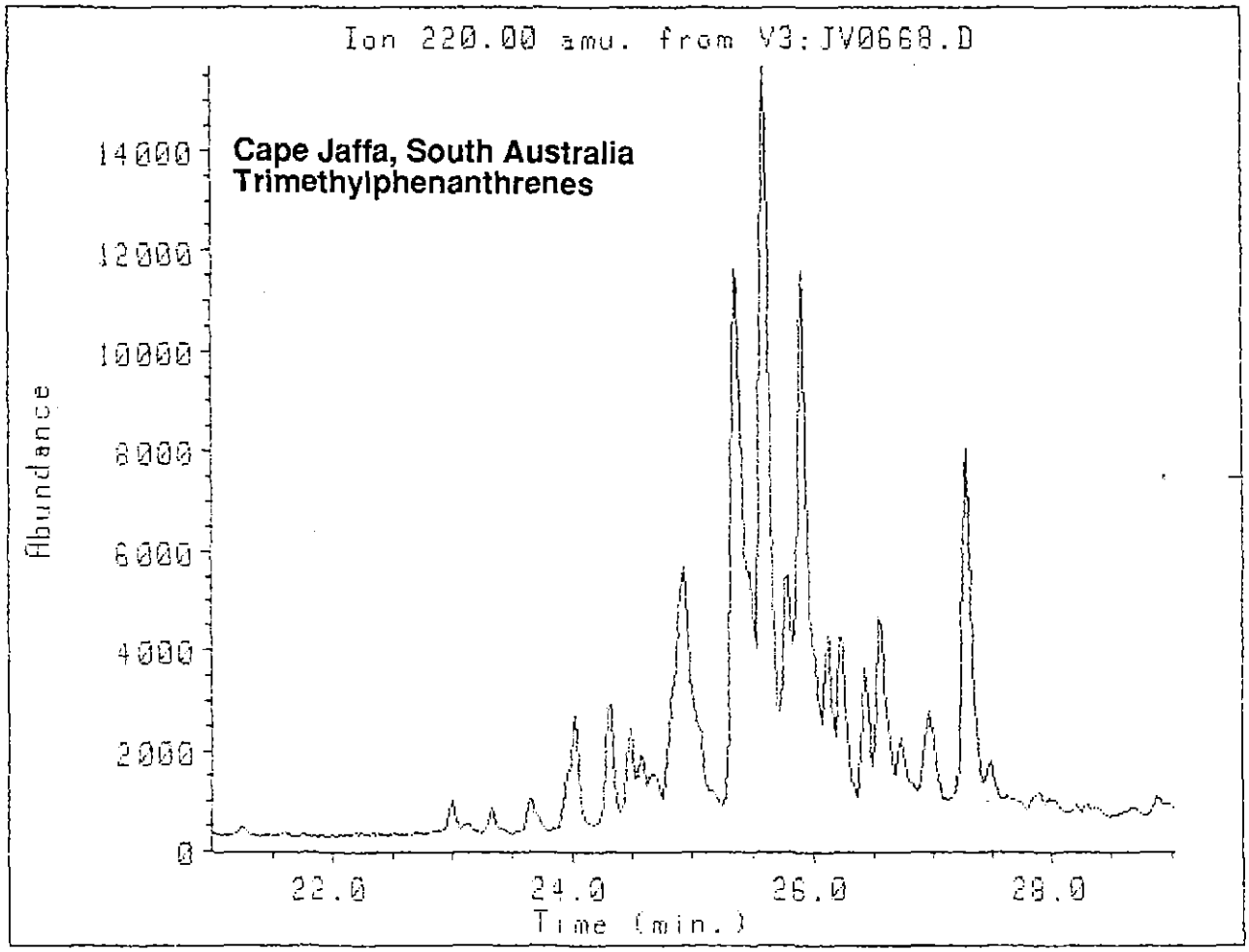
Ion 220.00 amu. from V3:JV0668.D
Cape Jaffa, South Australia
Trimethylphenanthrenes
Abundance
14000
12000
10000
8000
6000
4000
2000
0
22.0
24.0
26.0
28.0
Time (min.)

Fig. 9(j)

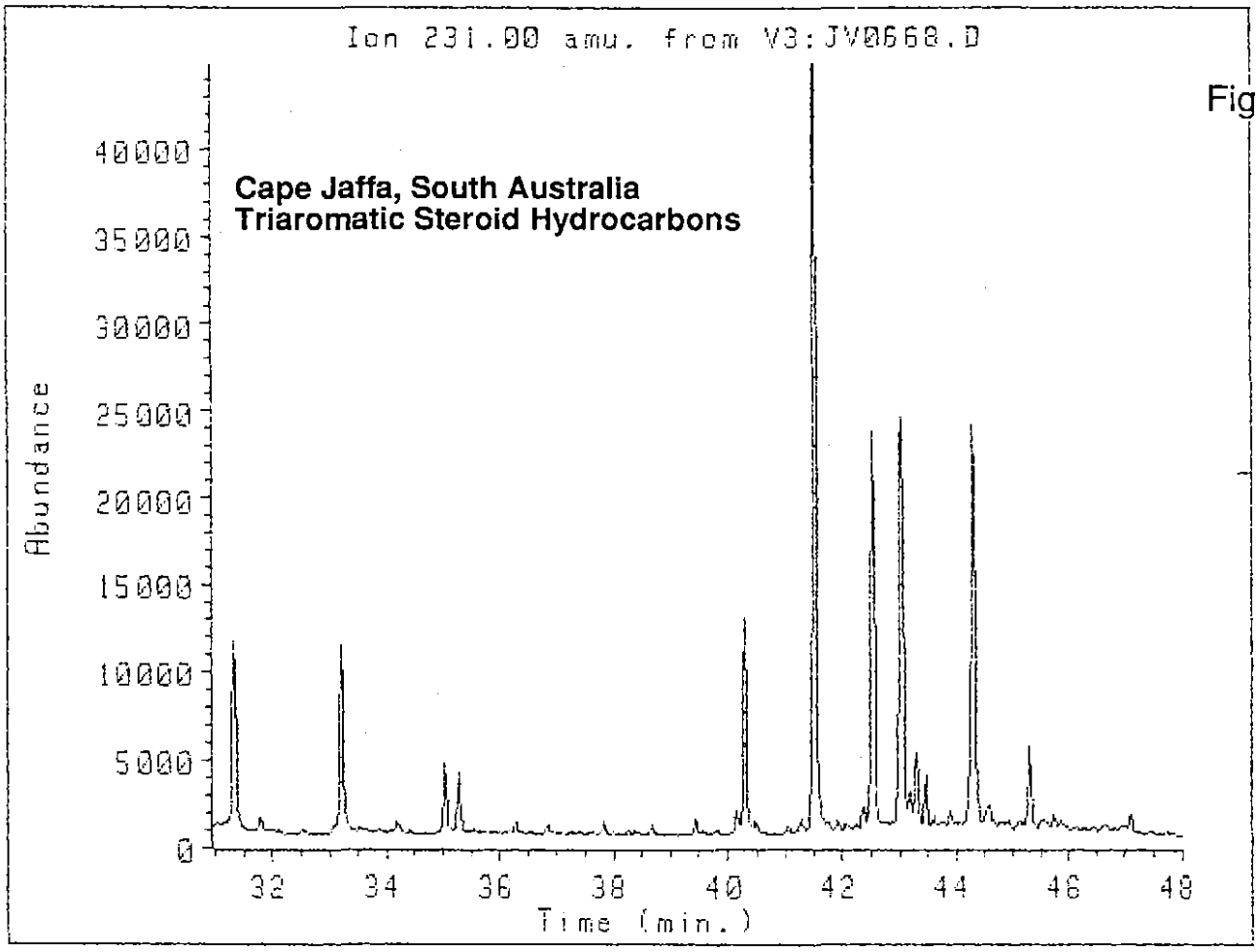
Ion 231.00 amu. from V3:JV0668.D
Cape Jaffa, South Australia
Triaromatic Steroid Hydrocarbons
Abundance
40000
35000
30000
25000
20000
15000
10000
5000
0
32
34
36
38
40
42
44
46
48
Time (min.)

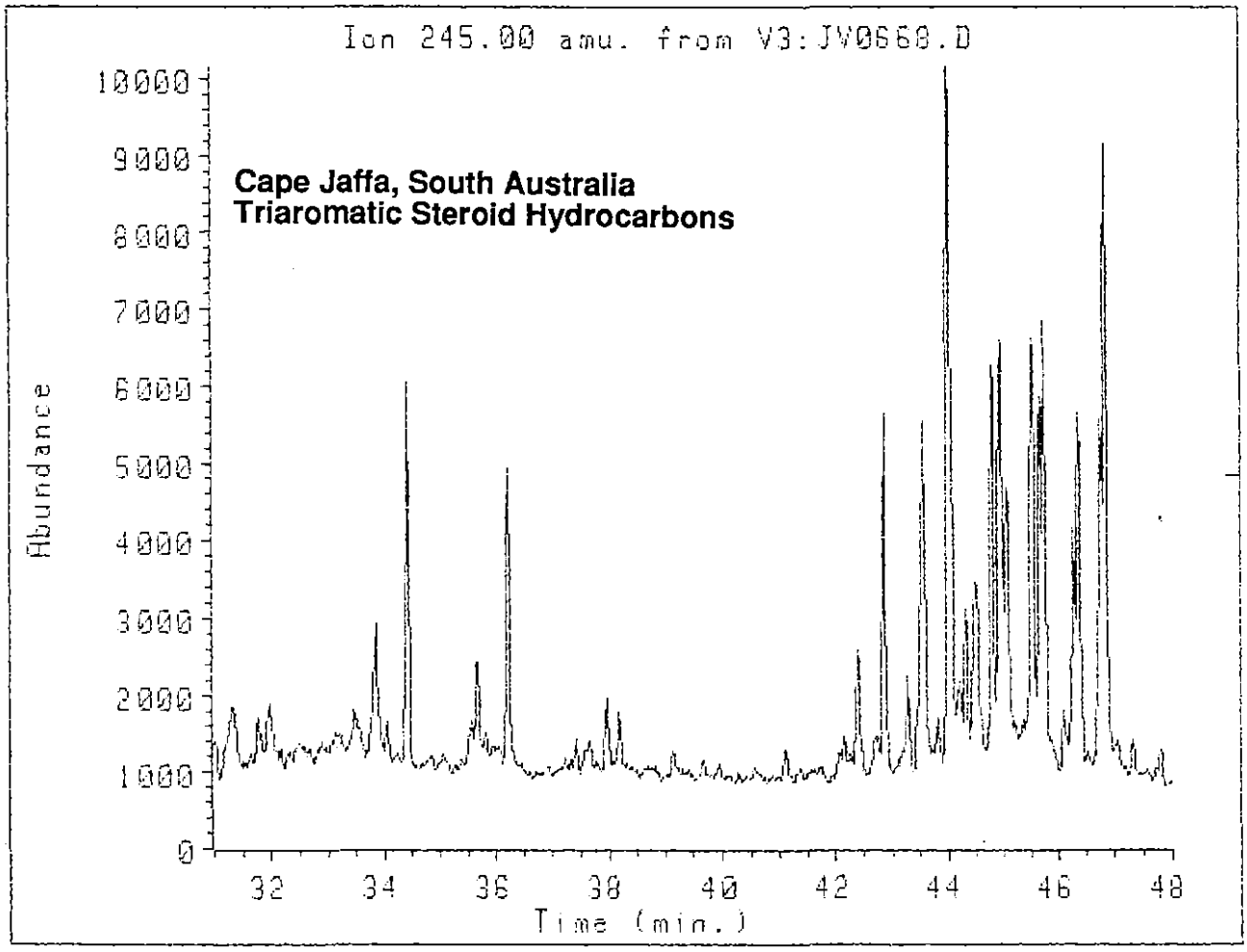
Ion 245.00 amu. from V3:JV0668.D
Cape Jaffa, South Australia
Triaromatic Steroid Hydrocarbons
Abundance
10000
9000
8000
7000
6000
5000
4000
3000
2000
1000
0
32
34
36
38
40
42
44
46
48
Time (min.)

Figure 10. GC and GC–MS data for the Western Australian bitumen.

(10a) Capillary gas chromatogram of the total aliphatic hydrocarbons in the Western Australian bitumen. Pr: pristane; Ph: phytane. n–Alkanes are denoted by n–C_X where "x" is the number of carbon atoms.

(10b). Mass fragmentograms for m/z 217 and 218 showing distribution of C_{26}–C_{30} steranes (labelled S) and diasteranes (labelled D) in the Western Australian bitumen. See Key 1 for peak identifications.

(10c) Mass fragmentograms for m/z 217 and 218 showing distribution of C_{21}–C_{23} steranes in the Western Australian bitumen.

(10d) Mass fragmentograms for m/z 259 showing distribution of C_{29}–C_{30} diasteranes (labelled D), and m/z 231 showing distribution of C_{28}–C_{30} 4–methyl steranes in the Western Australian bitumen.

(10e) Mass fragmentograms for m/z 191 showing distribution of C_{27}–C_{35} hopanes and m/z 205 showing distribution of methyl hopanes in the Western Australian bitumen. See Keys 2 and 3 for peak identifications.

(10f) Mass fragmentograms for m/z 191 showing distribution of C_{27}–C_{32} hopanes and m/z 177 showing distribution of demethylated hopanes (none detected) in the Western Australian bitumen.

(10g) Capillary gas chromatogram of the total aromatic hydrocarbons in the Western Australian bitumen.

(10h) Mass fragmentograms for m/z 178 and 192 showing the presence of phenanthrene and distribution of methylphenanthrenes respectively in the Western Australian bitumen.

(10i) Mass fragmentograms for m/z 206 and 220 showing the distribution of di– and trimethylphenanthrenes in the Western Australian bitumen.

(10j) Mass fragmentograms for m/z 231 and 245 showing the distribution of triaromatic steroidal hydrocarbons (with one and two methyl groups in the ABC ring system respectively) in the Western Australian bitumen.

Fig. 10(a)

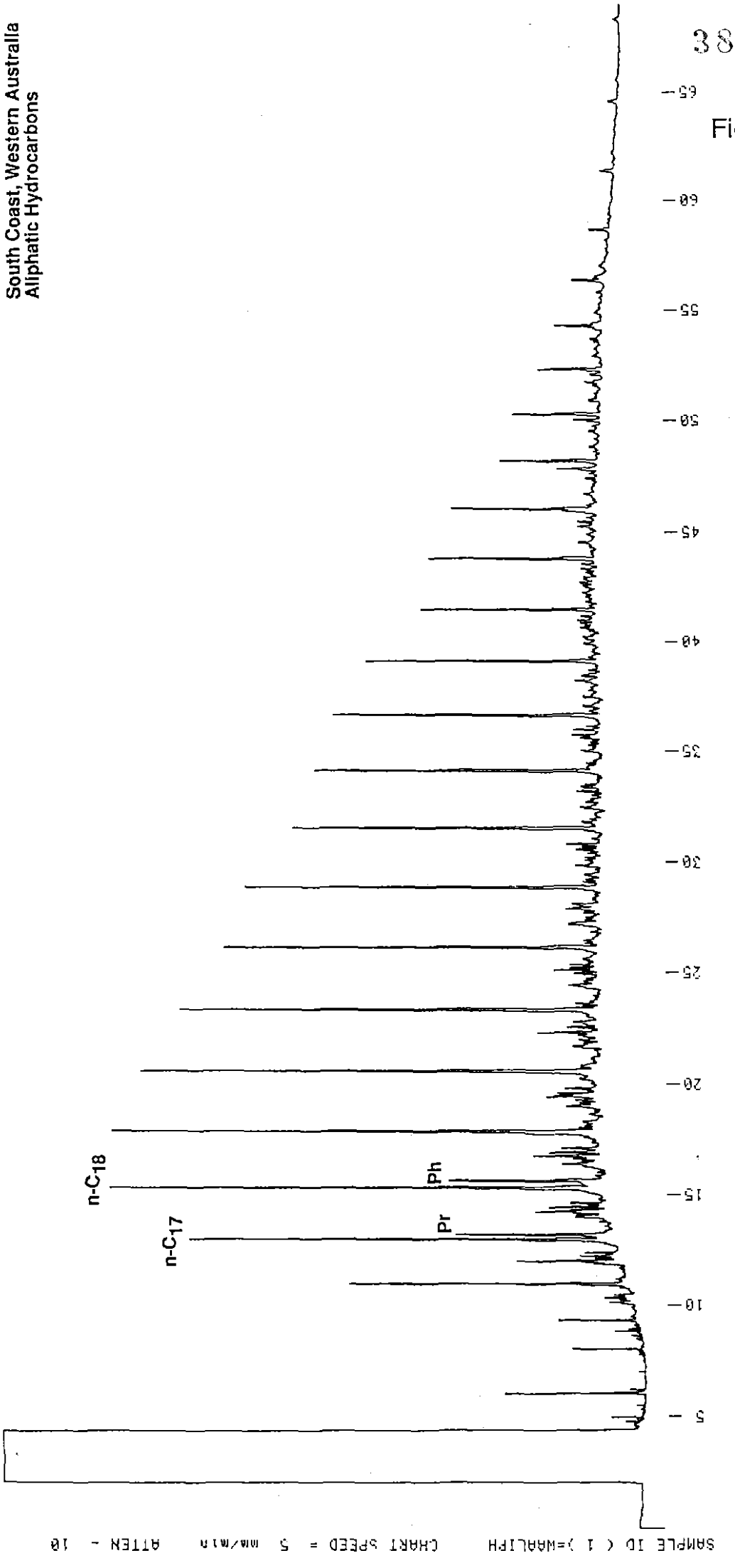
South Coast, Western Australia
Aliphatic Hydrocarbons
n-C18
Ph
n-C17
Pr
65
60
55
50
45
40
35
30
25
20
15
10
5
SAMPLE ID (1)=MAALIPH CHART SPEED = 5 mm/min ATTEN - 10

5 cm

Fig. 10(b)

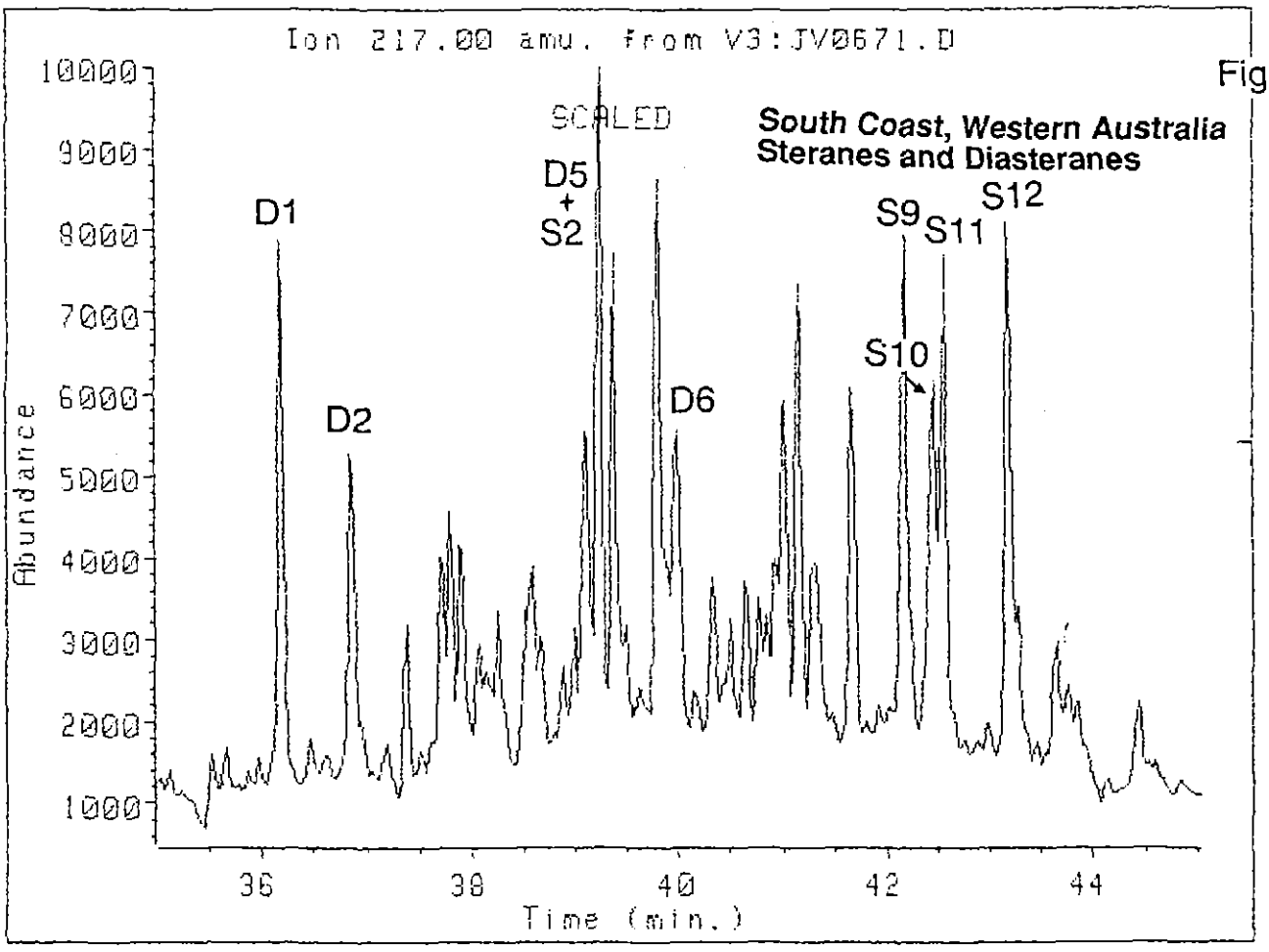
Ion 217.00 amu. from V3:JV0671.D
SCALED
South Coast, Western Australia
Steranes and Diasteranes
D1
D2
D5
+
S2
D6
S9
S11
S12
S10
Abundance
10000
9000
8000
7000
6000
5000
4000
3000
2000
1000
36
38
40
42
44
Time (min.)

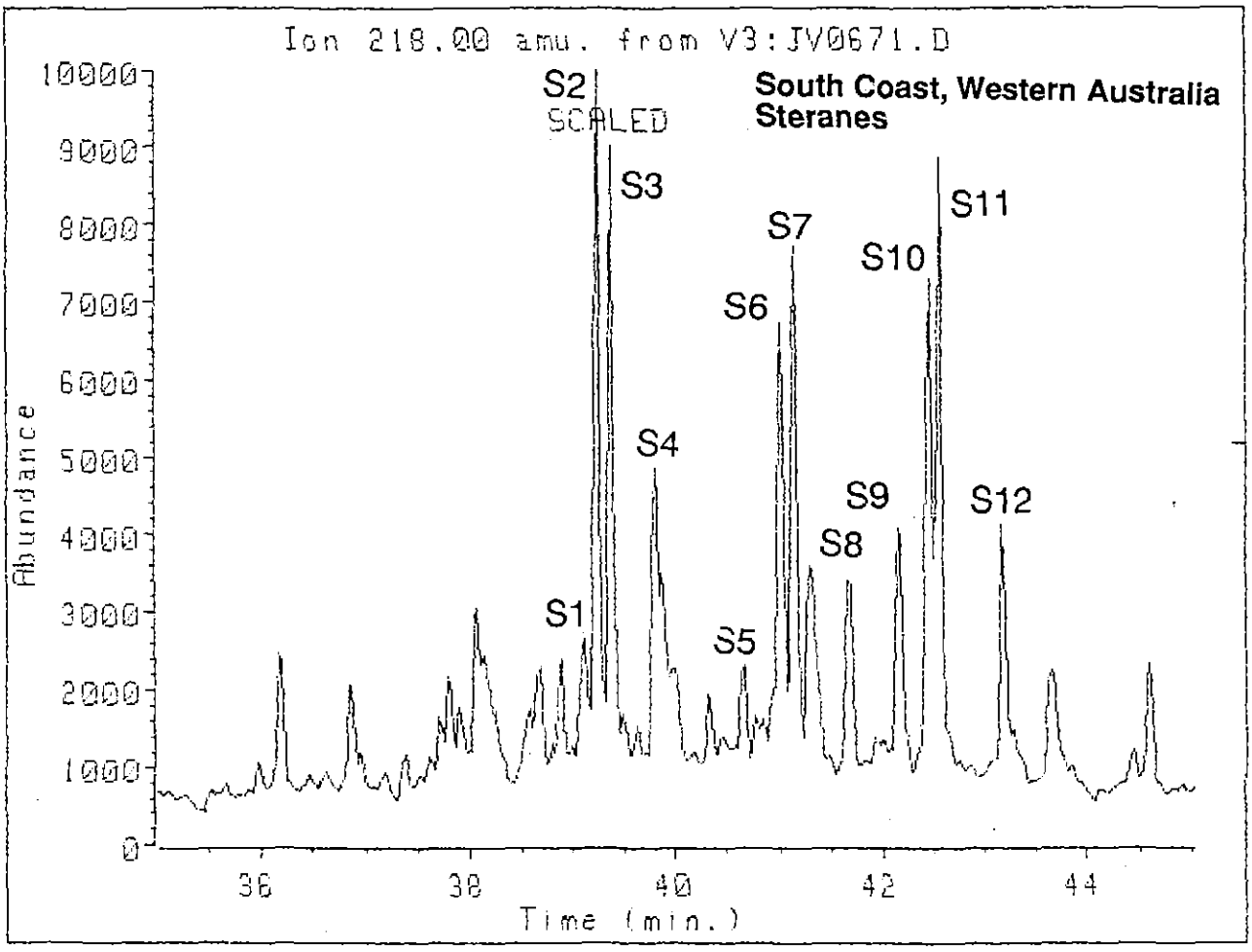
Ion 218.00 amu. from V3:JV0671.D
S2
SCALED
South Coast, Western Australia
Steranes
S3
S7
S11
S10
S6
S4
S9
S12
S8
S1
S5
Abundance
10000
9000
8000
7000
6000
5000
4000
3000
2000
1000
0
36
38
40
42
44
Time (min.)

5 cm

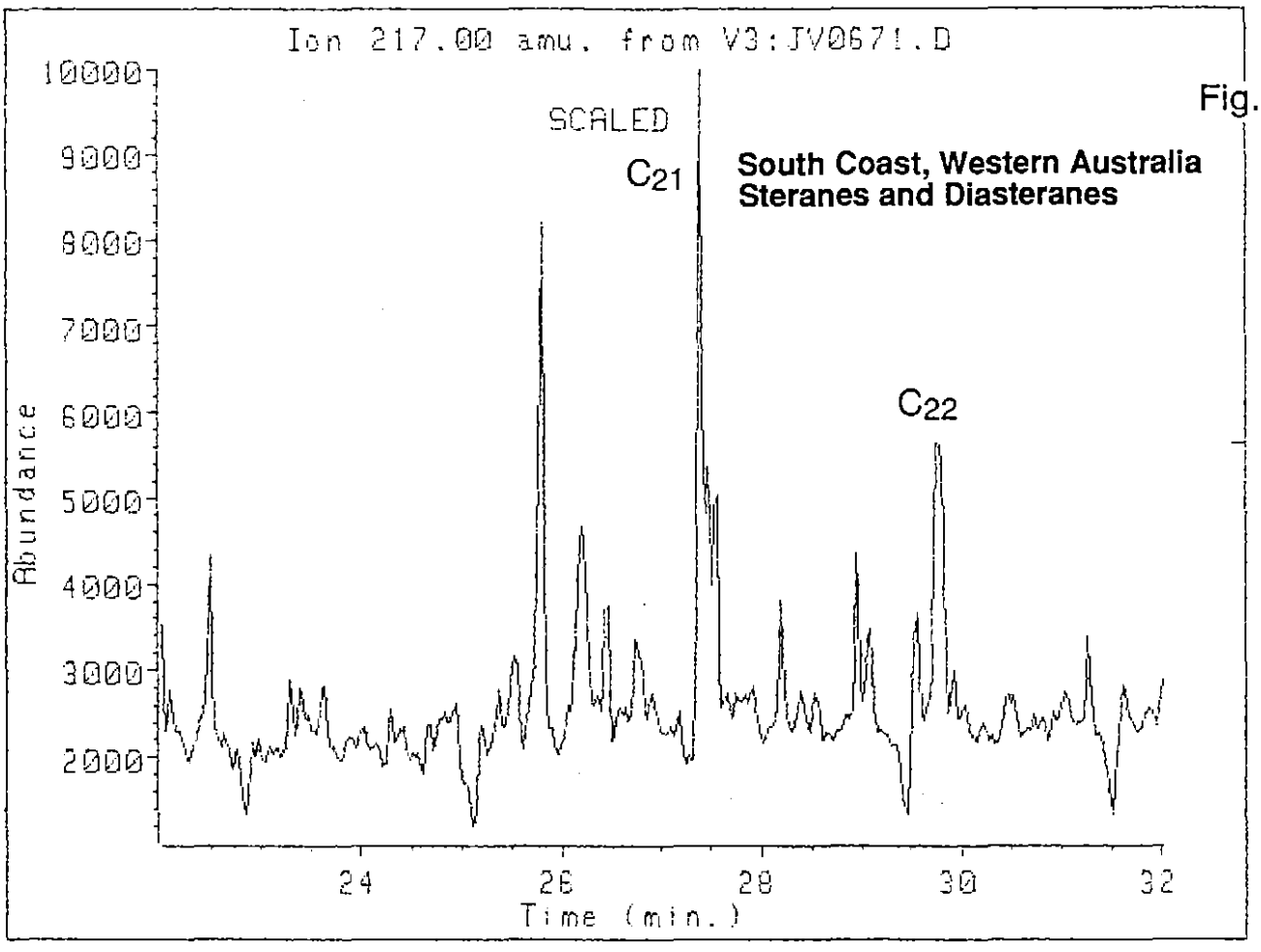
Ion 217.00 amu. from V3:JV0671.D
SCALED
C21
C22
South Coast, Western Australia
Steranes and Diasteranes
Abundance
Time (min.)

Fig. 10(c)

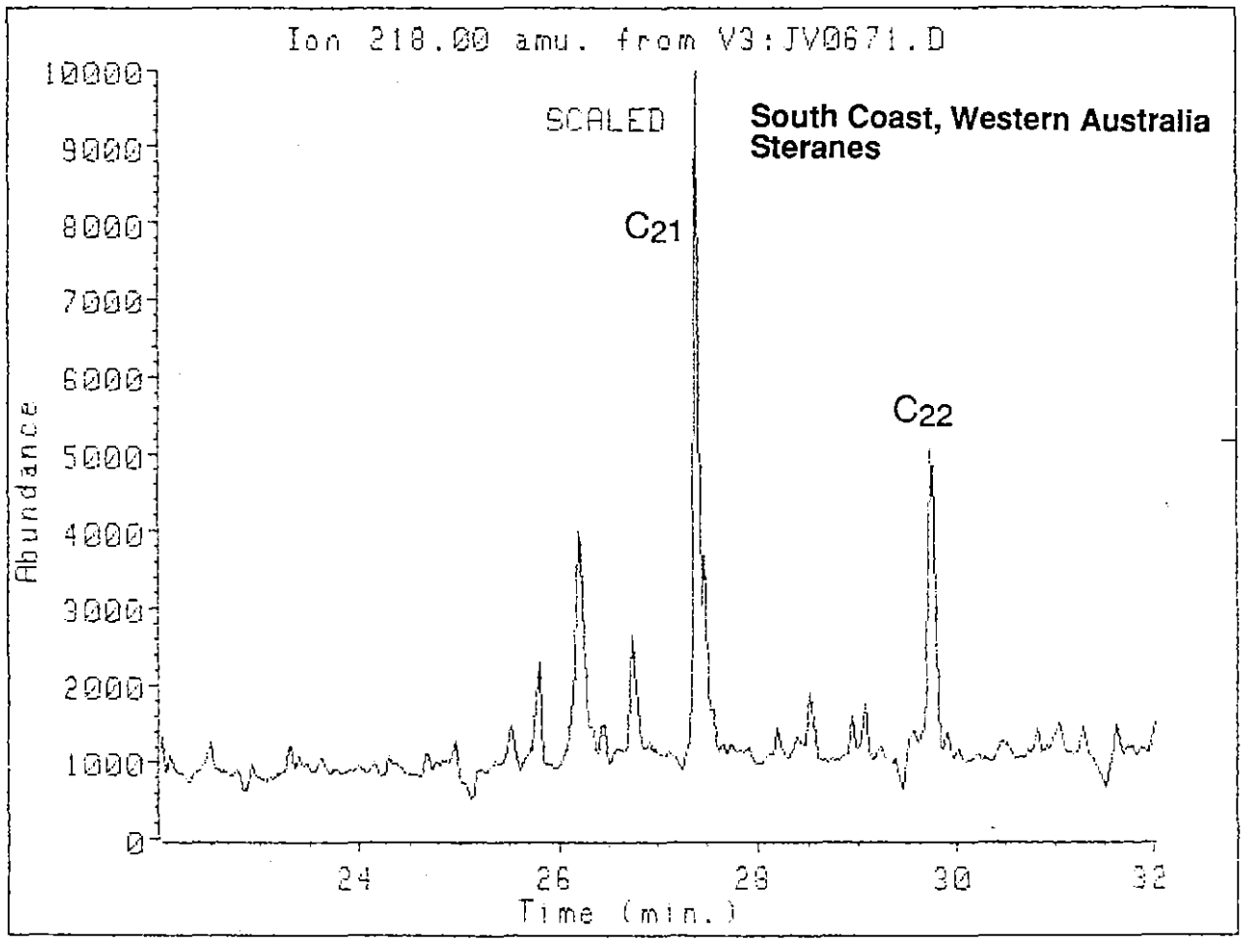
Ion 218.00 amu. from V3:JV0671.D
SCALED
C21
C22
South Coast, Western Australia
Steranes
Abundance
Time (min.)

5 cm

Fig. 10(d)

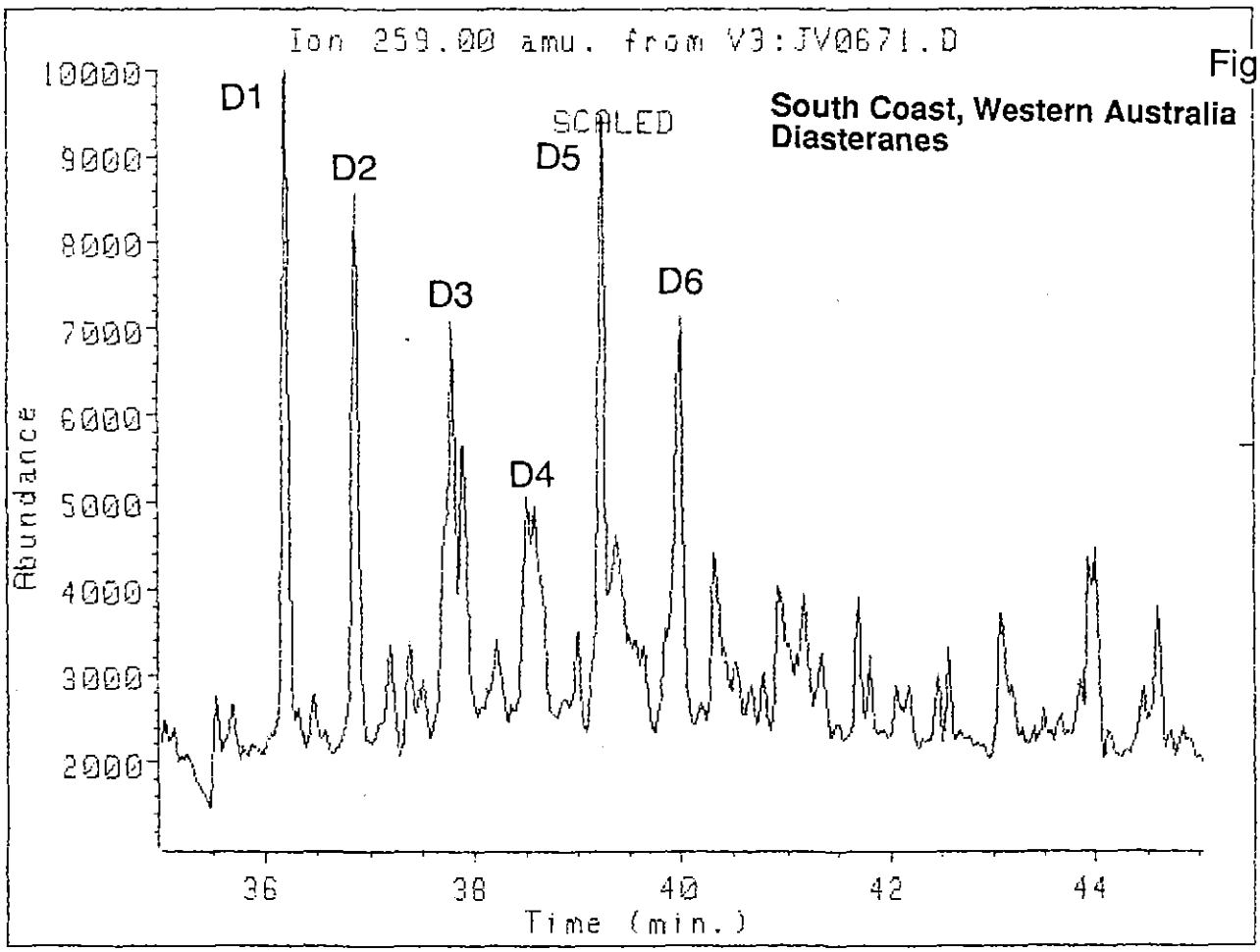
Ion 259.00 amu. from V3:JV0671.D
SCALED
South Coast, Western Australia
Diasteranes
D1
D2
D3
D4
D5
D6
Abundance
10000
9000
8000
7000
6000
5000
4000
3000
2000
36
38
40
42
44
Time (min.)

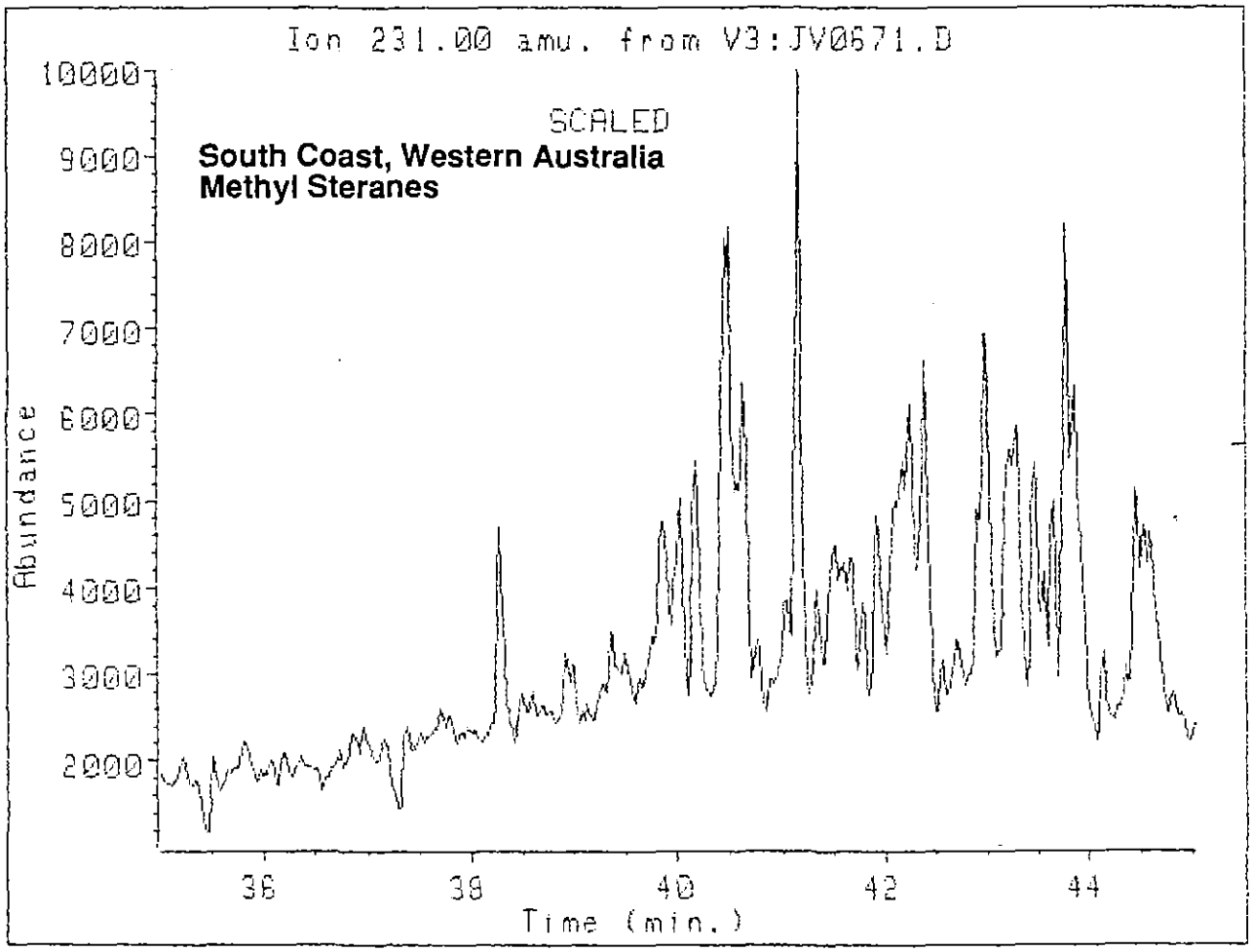
Ion 231.00 amu. from V3:JV0671.D
SCALED
South Coast, Western Australia
Methyl Steranes
Abundance
10000
9000
8000
7000
6000
5000
4000
3000
2000
36
38
40
42
44
Time (min.)

5 cm

Fig. 10(e)

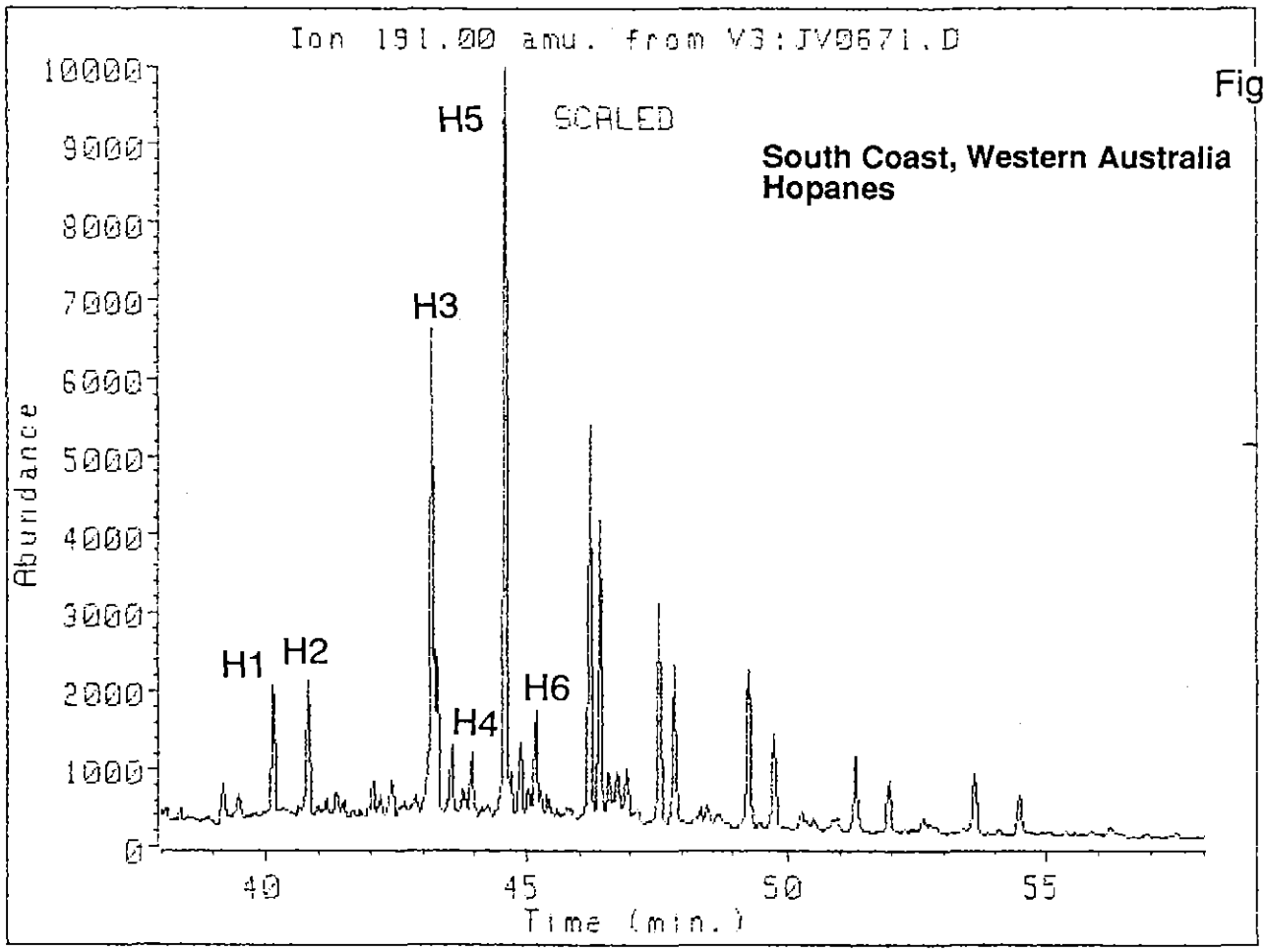
Ion 191.00 amu. from V3:JV0671.D
SCALED
South Coast, Western Australia
Hopanes
H1
H2
H3
H4
H5
H6
Abundance
Time (min.)

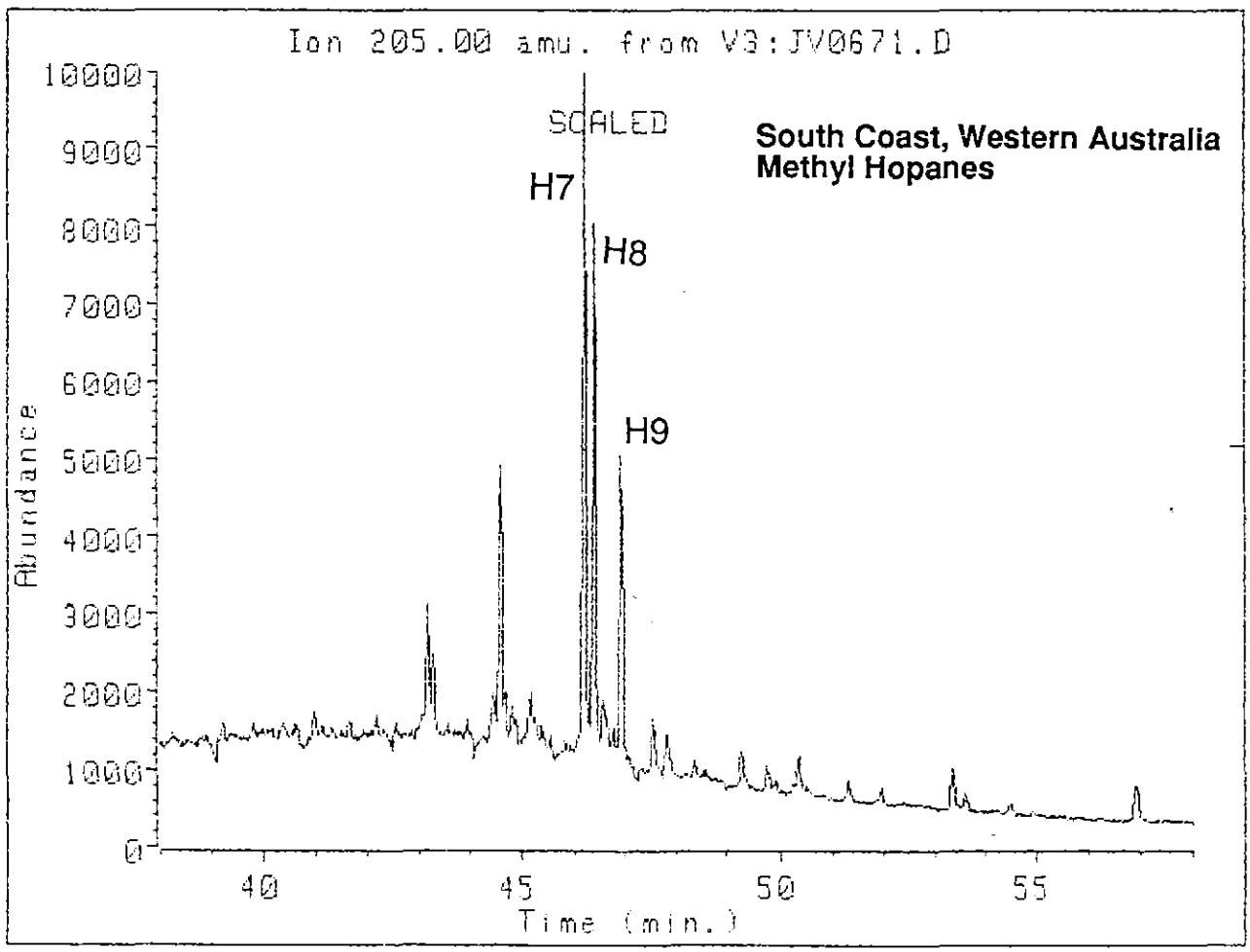
Ion 205.00 amu. from V3:JV0671.D
SCALED
South Coast, Western Australia
Methyl Hopanes
H7
H8
H9
Abundance
Time (min.)

5 cm

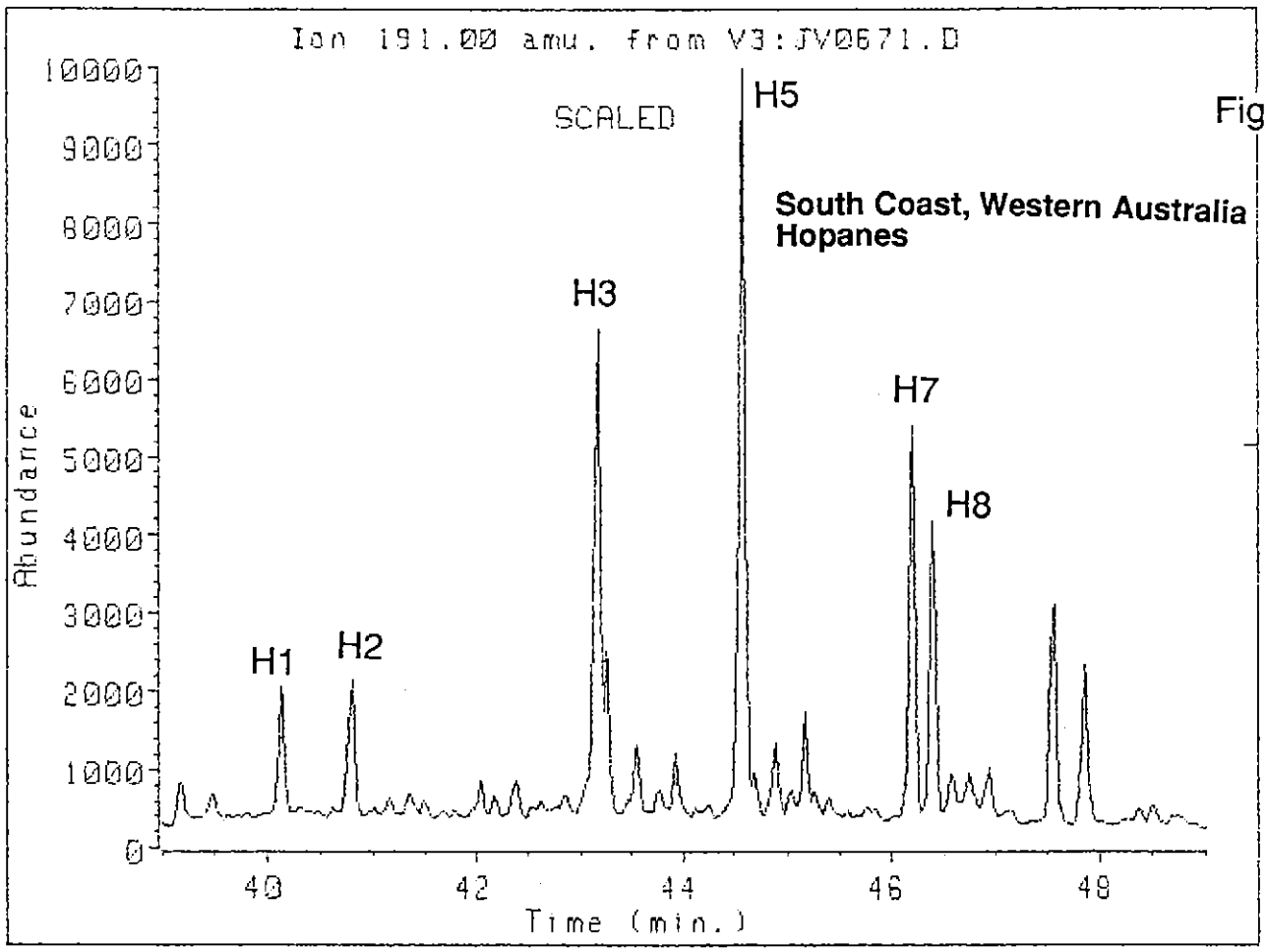
Ion 191.00 amu. from V3:JV0671.D
SCALED
H1
H2
H3
H5
H7
H8
South Coast, Western Australia
Hopanes
Abundance
Time (min.)

Fig. 10(f)

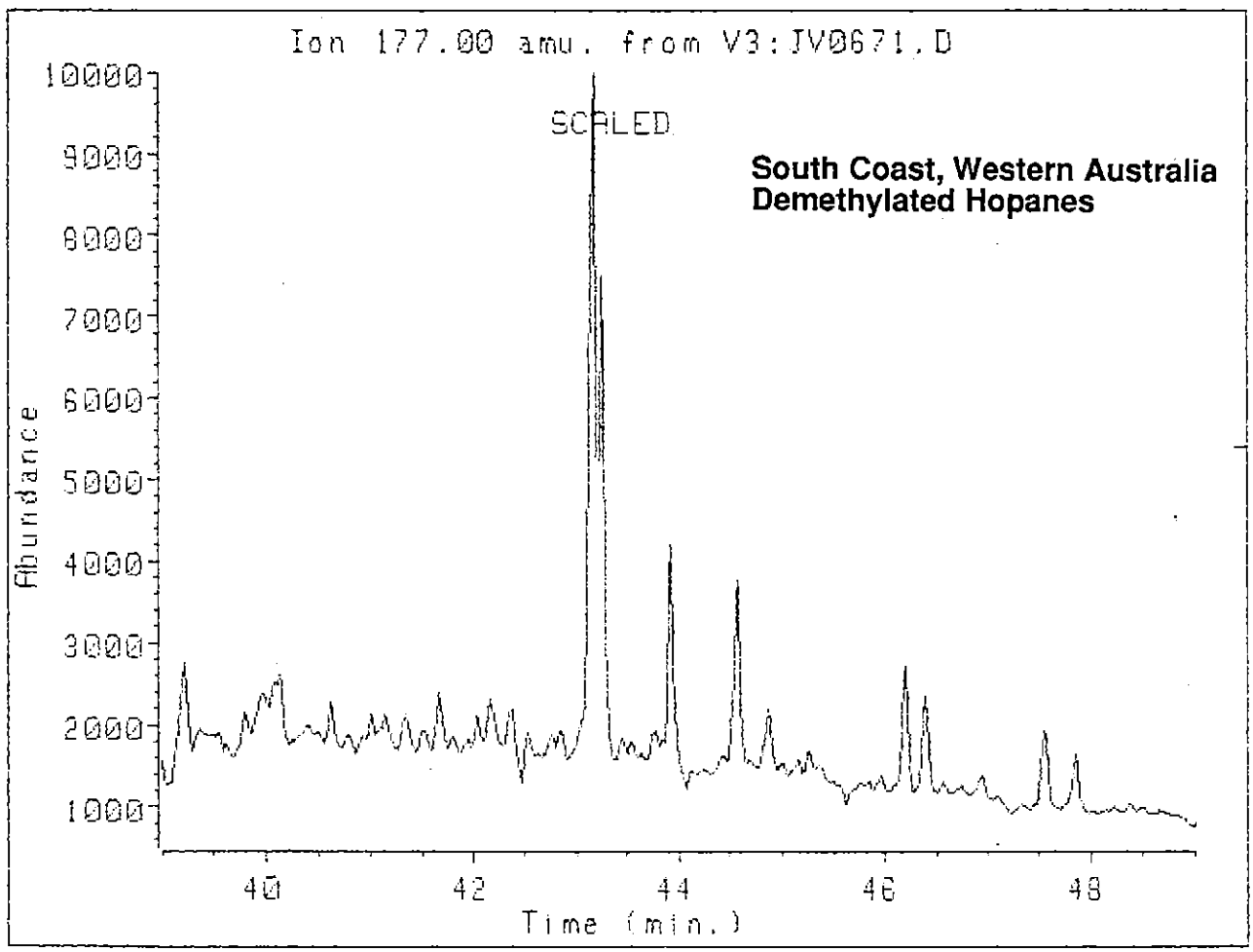
Ion 177.00 amu. from V3:JV0671.D
SCALED
South Coast, Western Australia
Demethylated Hopanes
Abundance
Time (min.)

South Coast, Western Australia
Aromatic Hydrocarbons

Fig. 10(g)

Fig. 10(h)

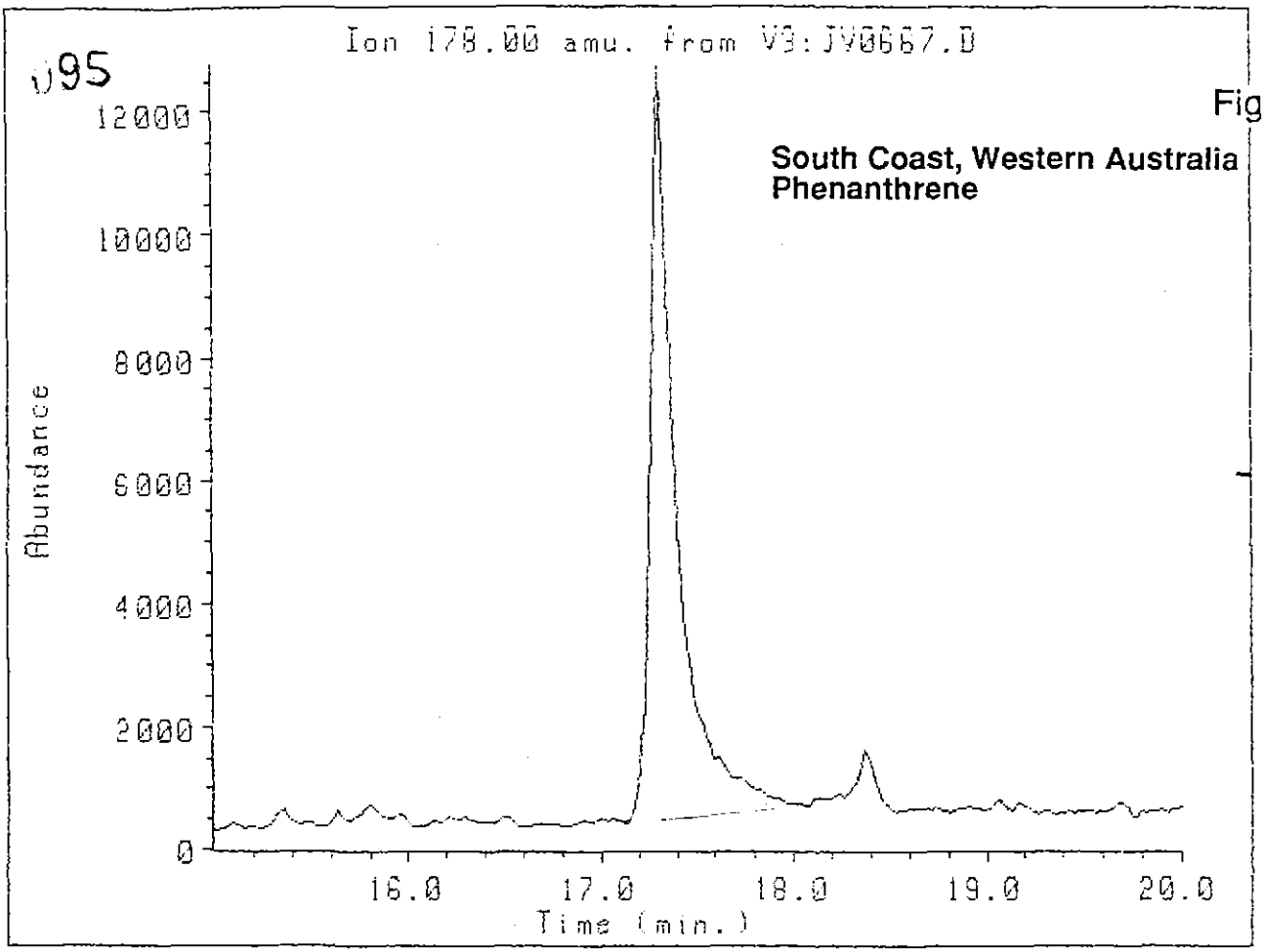
Ion 178.00 amu. from V3:JV0667.D
V95
12000
10000
8000
6000
4000
2000
0
Abundance
16.0
17.0
18.0
19.0
20.0
Time (min.)
South Coast, Western Australia
Phenanthrene

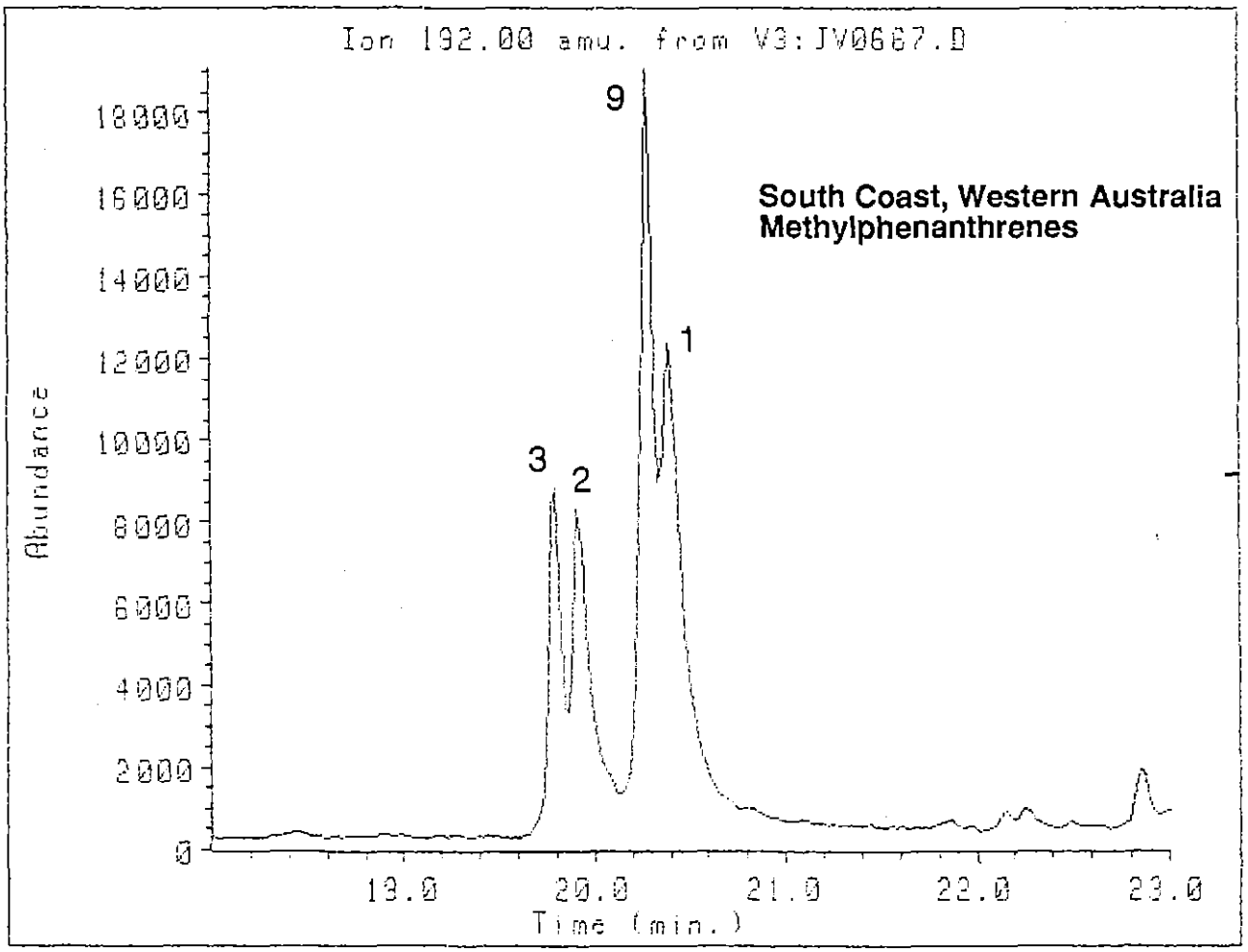
Ion 192.00 amu. from V3:JV0667.D
18000
16000
14000
12000
10000
8000
6000
4000
2000
0
Abundance
9
1
3
2
19.0
20.0
21.0
22.0
23.0
Time (min.)
South Coast, Western Australia
Methylphenanthrenes

Fig. 10(i)

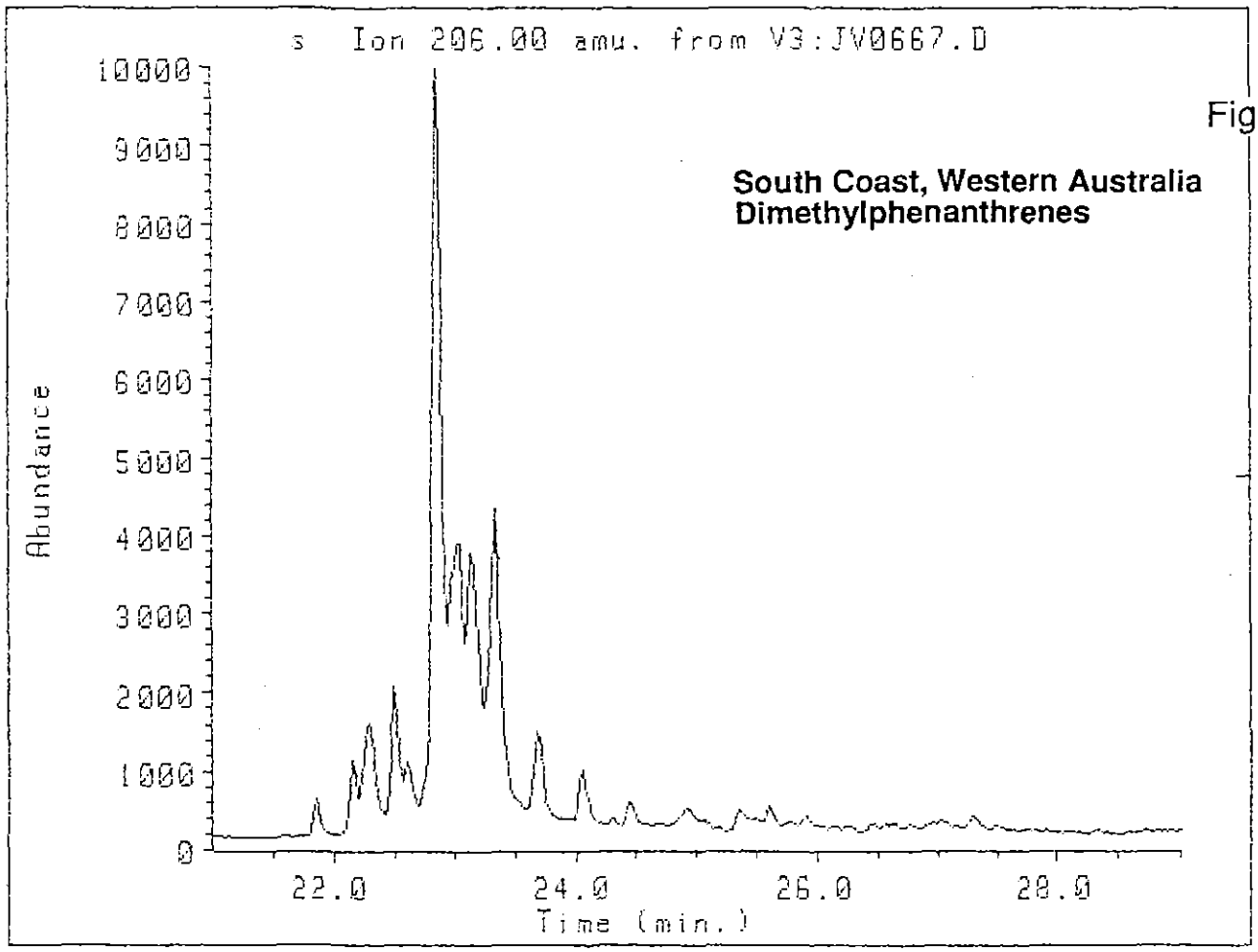
s Ion 206.00 amu. from V3:JV0667.D
South Coast, Western Australia
Dimethylphenanthrenes
Abundance
10000
9000
8000
7000
6000
5000
4000
3000
2000
1000
0
22.0
24.0
26.0
28.0
Time (min.)

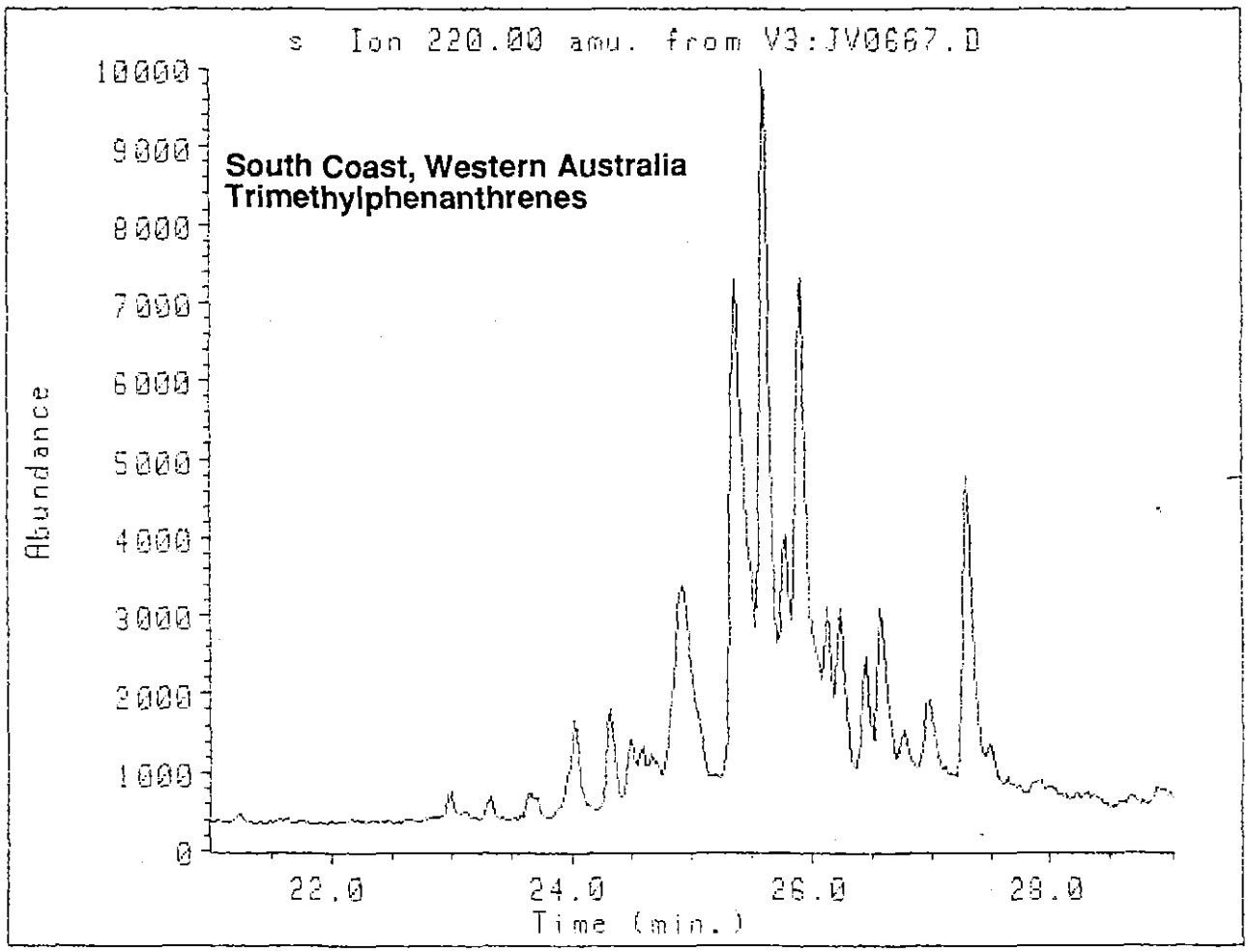
s Ion 220.00 amu. from V3:JV0667.D
South Coast, Western Australia
Trimethylphenanthrenes
Abundance
10000
9000
8000
7000
6000
5000
4000
3000
2000
1000
0
22.0
24.0
26.0
28.0
Time (min.)

Fig. 10(j)

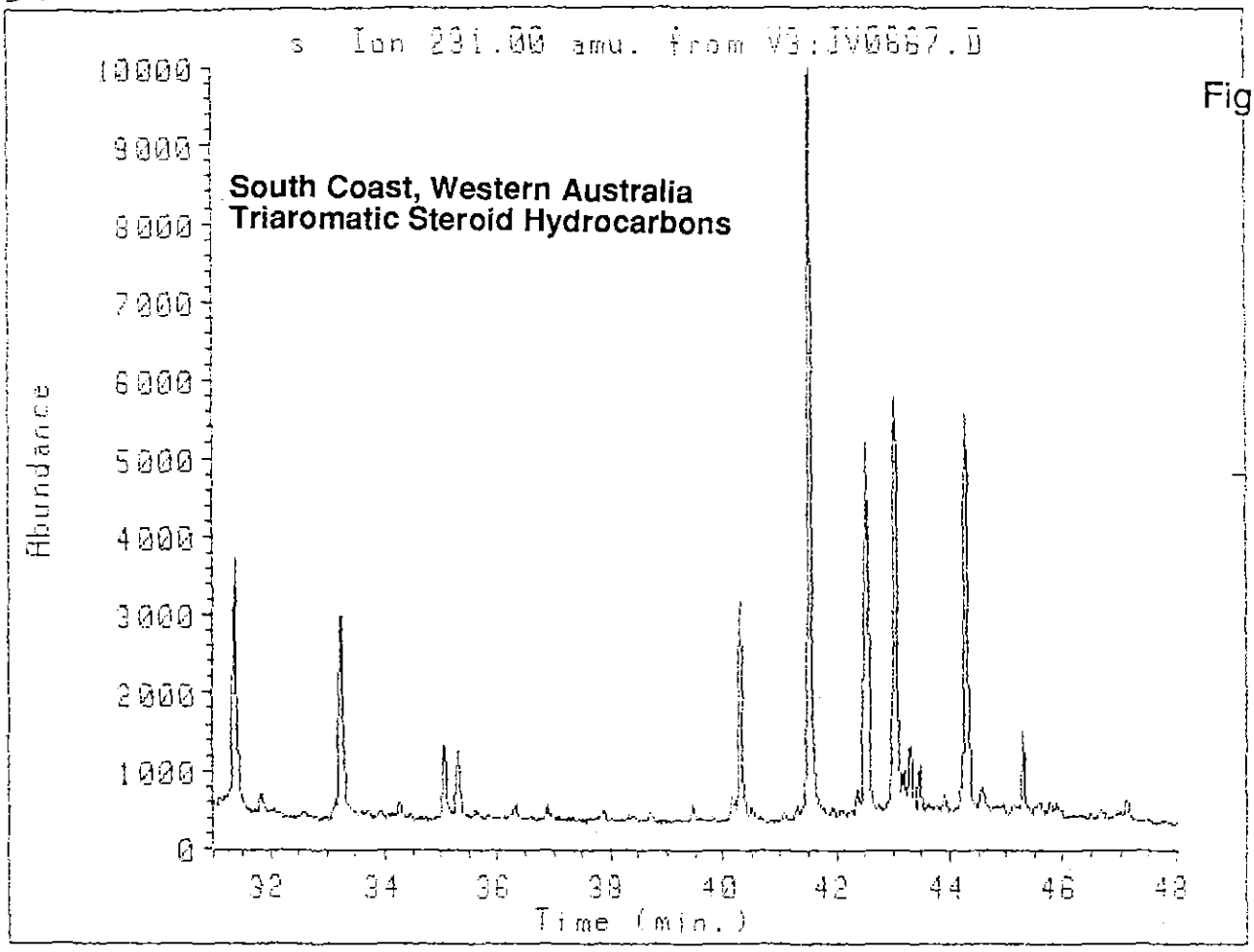
s Ion 231.00 amu. from V3:JV0667.D
South Coast, Western Australia
Triaromatic Steroid Hydrocarbons
Abundance
10000
9000
8000
7000
6000
5000
4000
3000
2000
1000
0
32
34
36
38
40
42
44
46
48
Time (min.)

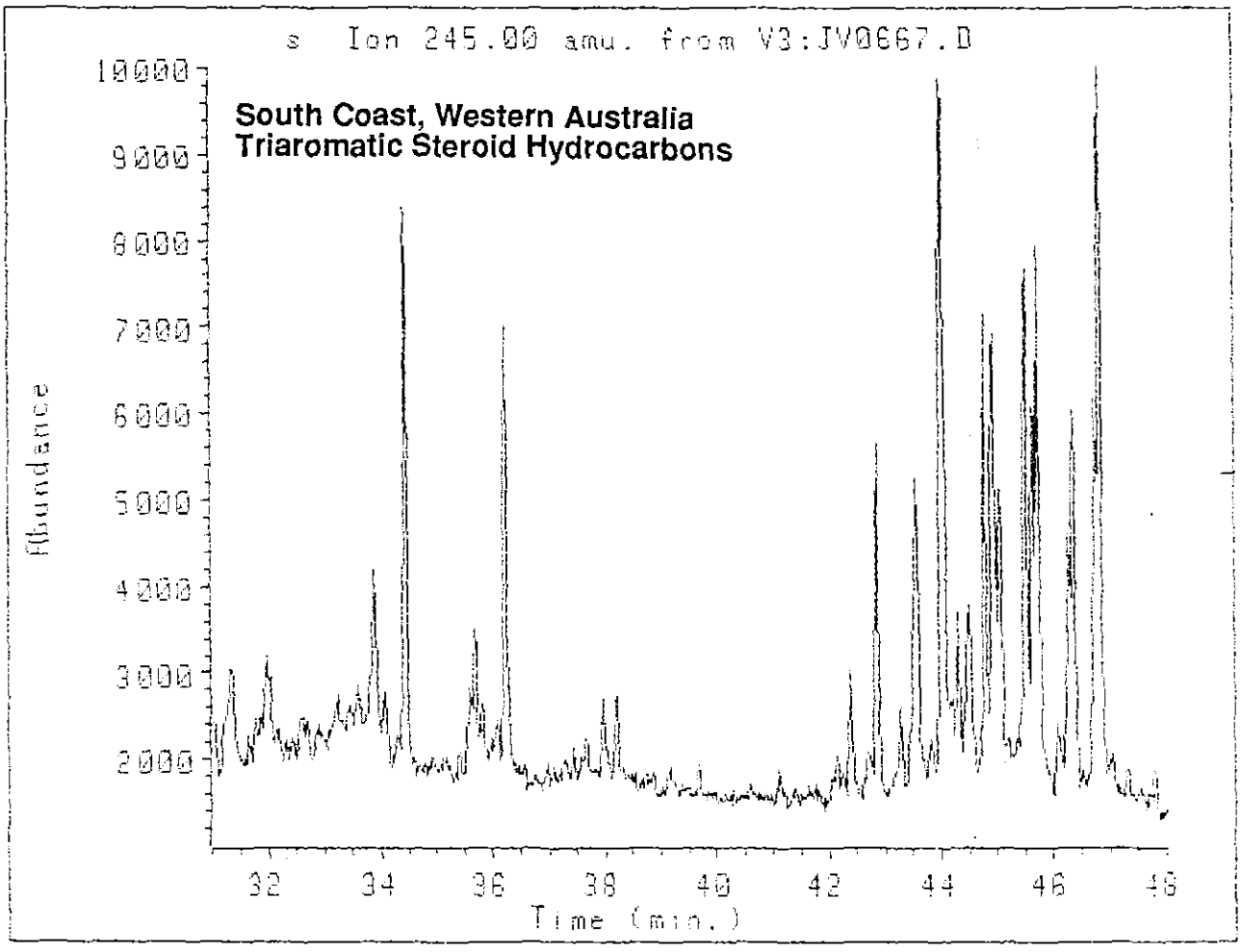
s Ion 245.00 amu. from V3:JV0667.D
South Coast, Western Australia
Triaromatic Steroid Hydrocarbons
Abundance
10000
9000
8000
7000
6000
5000
4000
3000
2000
32
34
36
38
40
42
44
46
48
Time (min.)

CONCLUSIONS

The carbonate from Benders Quarry has a very low content of hydrocarbons and it is obviously neither a source rock nor reservoir for petroleum hydrocarbons. The biomarker parameters are broadly similar to those of a carbonate previously analysed from Ida Bay, although some significant differences were noted.

Although the Florentine Valley mudstone contains comparatively small amounts of hydrocarbons, the biomarker patterns are remarkably similar to those previously determined for Ordovician carbonates from Ida Bay and Queenstown, Tasmania. Methyl hopanes are present in surprisingly high abundance for a mudstone.

The tars from South Bruny Island and Tunnack appear to have the same or very similar source. The extremely low abundance of aliphatic hydrocarbons is not typical of the composition expected for a crude oil. The presence of alkenes and polycyclic aromatic hydrocarbons suggest that these hydrocarbons were formed at high temperature, whereas the sterane and hopane maturity parameters indicate relatively immature organic matter. It is possible that these tars are derived from man-made petroleum products, but their wide distribution (Bruny Island, Tunnack and Bridgewater) is very difficult to explain unless they are in fact natural seeps. Their composition is quite different to modern bitumens used for road making in Tasmania that we have analysed. One might speculate that they could be products of dolerite heating of an organic-rich, but immature sediment.

The two tars from Cape Jaffa, South Australia and the south coast of Western Australia are clearly very similar in composition to samples of Tasmanian bitumens obtained from the Queen Victoria museum analysed by Volkman and O'Leary (1990a,b). This raises significant questions about the ultimate source of all these bitumens. If they have not been transported by sea over large distances, then one has to invoke similar source rocks occurring in Tasmania, South Australia and Western Australia. The petroleum must also

have been generated at similar levels of thermal maturity. If the bitumens had been at sea for different lengths of time, one might have expected to see greater differences in their composition of shorter–chain aliphatics and the more water soluble aromatics than is apparent. Note also that the prevailing surface currents are from west to east, so if the Tasmanian bitumens had been transported from Western or South Australian waters they should look more water washed and biodegraded than the tars from there, but this is not the case. Clearly, a number of questions remained unanswered and further work is needed, particularly to identify possible source rocks.

REFERENCES

AMDEL (1987) Maturity of five early Palaeozoic samples. Report F 6853/87.

Boreham, C. J., Crick, I. H. and Powell, T. G. (1988) Alternative calibration of the methylphenanthrene index against vitrinite reflectance: application to maturation measurement of oils and sediments. *Organic Geochemistry* **12**, 289–294.

Denwer, K. (1986) Geology and geochemistry of the Tasmanite oil shale. B. Sc (Hons) Thesis, Geology Department, University of Tasmania. 84 pp.

Radke, M. and Welte, D. H. (1983) The Methylphenanthrene Index (MPI): A maturity parameter based on aromatic hydrocarbons. In *Advances in Organic Geochemistry 1981* (eds M. Bjoroy *et al.*), pp. 504–512. John Wiley & Sons Ltd.

Radke, M., Leythaeuser, D. and Teichmüller, M. (1984) relationship between rank and composition of aromatic hydrocarbons for coals of different origins. *Org. Geochem.* **6**, 423–430.

Mackenzie, A. S., Hoffmann, C. F. and Maxwell, J. R. (1981) Molecular parameters of maturation in the Toarcian shales, Paris Basin, France—III. Changes in aromatic steroid hydrocarbons. *Geochim. Cosmochim. Acta* **45**, 1345–1355.

McKirdy, D. M., Cox, R. E., Volkman, J. K. and Howell, V. J. (1986) Botryococcane in a new class of Australian non-marine crude oils. *Nature* **320**, 57-59.

Simoneit, B. R. T., Grimalt, J. O., Wang, T. G., Cox, R. E., Hatcher, P. G. and Nissenbaum, A. (1986) Cyclic terpenoids of contemporary resinous plant detritus and of fossil woods, ambers and coals. *Organic Geochemistry* **10**, 877–889.

Volkman, J. K. (1988) Hydrocarbons in Ordovician limestones from Queenstown and Lune River, Tasmania. Report 88–HC1 to Conga Oil.

Volkman, J. K. and Holdsworth, D. (1989) Hydrocarbons in two tar samples from the Midlands, Tasmania. Unpublished Report 89–HC1 for Conga Oil Pty Ltd.

Volkman, J. K. and O'Leary, T. (1990a) Preliminary report on the organic geochemistry of some Tasmanian bitumens. Unpublished Report 90–HC1 for Conga Oil Pty Ltd.

Volkman, J. K. and O'Leary, T. (1990b) Aromatic hydrocarbons in some Tasmanian bitumens. Unpublished Report 90–HC2 for Conga Oil Pty Ltd.

Volkman, J.K., Everitt, D. A. and Allen, D. I. (1986) Some analyses of lipid classes in marine organisms, sediments and seawater using thin–layer chromatography–flame ionisation detection. *J. Chromatogr.* **356**, 147–162.

Volkman J. K., Alexander, R. , Kagi, R. I. and Woodhouse, G. W. (1983). Demethylated hopanes in crude oils and their applications in petroleum geochemistry. *Geochim. Cosmochim. Acta*. **47**, 785–794.